INFORMATION TO USERS

This manuscript has been reproduced from the microfilm master. UMI films the text directly from the original or copy submitted. Thus, some thesis and dissertation copies are in typewriter face, while others may be from any type of computer printer.

The quality of this reproduction is dependent upon the quality of the copy submitted. Broken or indistinct print, colored or poor quality illustrations and photographs, print bleedthrough, substandard margins, and improper alignment can adversely affect reproduction.

In the unlikely event that the author did not send UMI a complete manuscript and there are missing pages, these will be noted. Also, if unauthorized copyright material had to be removed, a note will indicate the deletion.

Oversize materials (e.g., maps, drawings, charts) are reproduced by sectioning the original, beginning at the upper left-hand corner and continuing from left to right in equal sections with small overlaps. Each original is also photographed in one exposure and is included in reduced form at the back of the book.

Photographs included in the original manuscript have been reproduced xerographically in this copy. Higher quality 6" x 9" black and white photographic prints are available for any photographs or illustrations appearing in this copy for an additional charge. Contact UMI directly to order.

UMI

A Bell & Howell Information Company
300 North Zeeb Road, Ann Arbor MI 48106-1346 USA
313/761-4700 800/521-0600

THE INFLUENCE OF DARK-ADAPTED RODS UPON COLOR VISION

by

ELIZABETH LEMBESSIS

A dissertation submitted to the Graduate Faculty in Psychology in partial fulfillment of the requirements for the degree of Doctor of Philosophy, The City University of New York.

1997

This manuscript has been read and accepted for the Graduate Faculty in Psychology in satisfaction of the dissertation requirement for the degree of Doctor of Philosophy.

3/27/97
Date

Thomas E. Frumkes
Chair of Examining Committee

3-27-97
Date

Executive Officer

Thomas E. Frumkes, PhD
Robert N. Lanson, PhD
Harold Schuckman, PhD
Israel Abramov, PhD
James Gordon, PhD

Supervisory Committee

THE CITY UNIVERSITY OF NEW YORK

Abstract

THE INFLUENCE OF DARK-ADAPTED RODS UPON COLOR VISION

by

Elizabeth Lembessis

Advisor: Professor Thomas E. Frumkes

Monocular changes in color vision were examined for 25 minutes following a substantial bleach of photopigment in the right, left, or both eye(s). A test flash of 3° diameter, 100 ms duration, and of 478, 511, 576, or 637 nm wavelength was presented 6° in the right eye temporal field. In some experiments, the observer adjusted retinal illuminance of the stimulus until its hue could be identified (i.e., the specific threshold); alternatively, stimulus illuminance was fixed at 5 tds. and the observer evaluated hue and saturation using "4 + 1" scaling (Gordon et al., 1994).

Following monocular bleaching, specific thresholds for all wavelengths increased during the rod recovery stage of dark adaptation, as reported by Lie (1963). The time courses and magnitudes of threshold change were similar for stimuli that appeared predominantly blue (478 nm) and yellow (576 nm) in hue. The magnitudes of threshold change

occurring with predominantly green (511 nm) and red (637 nm) hued stimuli were greater than the influences on 478 nm and 576 nm stimuli. In general, specific threshold changed more rapidly for 511 nm stimuli than for the other wavelengths.

After the first 5 minutes of dark adaptation following monocular bleaching, 5 td. stimuli became increasingly desaturated and shifted in hue; the shorter the wavelength, the greater the saturation change. In general, 637 nm stimuli appeared less red and more yellow. The appearances of the other stimuli changed in more varied ways.

The adapted state of the nonviewing eye exerted an influence upon color vision that varied with wavelength, response measure, and the observer. The most reliable interocular effect involved hue shifts for 637 nm stimuli, with similar time courses but smaller magnitudes than those observed monocularly.

Specific threshold and hue scaling data are most compatible with a chromatic suppressive rod-cone interaction model that posits a greater influence upon green/red than upon blue/yellow mechanisms. Saturation scaling data are most consistent with a luminosity channel summation model. The site(s) within the nervous system for rod-cone interaction remain ambiguous.

Acknowledgments

I would like to thank Dr. Tom Frumkes, Chairman of my committee, for his advice and assistance during this project. Thanks also to Drs. R. Lanson, H. Schuckman, J. Gordon, and I. Abramov, for their careful and thorough reading of my dissertation and their helpful suggestions and comments. The entire committee worked under severe time constraints and I am grateful to them all.

I am forever indebted to my experimental subjects, Ray Meaney, Aaron Dancygier, and Marily Trujillo, for the many, many months they spent as observers and, in Ray's case, as an experimenter as well. Thanks for making data collection enjoyable.

I am also very grateful to my other experimenters and pilot subjects, Jose Abarro, Malgorzata Knutelska, Colleen McMullen, George Pseudos, and Andre Ragnauth, who devoted much time and energy to these studies. It was a pleasure to work with them. Special mention must be made of Dina Moshe, who was instrumental in getting this research started.

I would like to thank Dina Moshe, Joe Vollaro, and Charles Zaroff for the many hours they spent as observers for an earlier project. Again, a pleasure. Thanks also to John Zhu, who wrote the software and provided technical support for the earlier projects, and to Drs. A. Genack and H. Gaffney for technical advice and assistance.

I am very grateful to Stan Sham, not only for providing technical assistance, but for his support and encouragement through the years. Live long and prosper!

Many thanks to Drs. Tina Moreau and Helen Cairns for their advice, encouragement, and many helpful suggestions on my first dissertation project. Special thanks to Dr. Cairns for helping me through an extremely painful period of grief.

Thanks to Mary Ann Schimatz, Mrs. Field, Helene Cinquemani, and Susan Wafferman for answering any and all requests with a smile. It was a pleasure to know you all.

Finally, thanks to my dear friend Dr. Jordon Hirshon, whose wise counsel, support, and helpfulness were invaluable over the years. Many thanks to Michael, Regina, and Lydia for their support.

I am grateful to my mother, brother, and aunt for always believing in me and to my maternal grandmother, who was denied a grade school education in her native country simply because she was a girl. She remained practically illiterate her entire life. In two generations . . .

To my wonderful husband, who makes it all worthwhile, thank you for your unfailing love and encouragement. "LA or another place, please." Many thanks to my feline typists, Nikkie and Amber, for helping me graph my data and prepare this manuscript.

Table of Contents

List of Tables

List of Figures

It ain't over till it's over

--Yogi Berra

I maintain, in truth
That with a smile we should instruct our youth
Be very gentle when we have to blame
And not put them in fear of virtue's name

--Moliere

Chapter 1

Introduction

An impressive body of evidence from several disciplines suggests that human color vision is processed in two stages or "zones": the trichromatic and the opponent-process zones. (For a modern review of evidence and theories, see Kaiser & Boynton, 1996.) Evidence from microspectrophotometric, molecular genetic, neurophysiological, and psychophysical studies shows that normal observers have three populations of cones that are maximally sensitive to different, but overlapping, portions of the visible spectrum (Gordon, 1989). Today, these populations are commonly referred to as the short-, middle-, and long-wavelength cone mechanisms, representing the wavelengths of light to which they are maximally sensitive (Smith & Pokorny, 1975). Even after further processing, all chromatic discriminations must reflect the initial differential activity of these separate populations of cones as posited by the Young-Helmholtz trichromatic theory. Although the actual neural locus of the trichromatic zone is rarely specified in modern zone theories, the implication is that this zone is quite distal in the visual system, perhaps involving only the photoreceptors and, possibly, several other types of neurons that have synapses within the retinal outerplexiform layer.

A wealth of neurophysiological and psychophysical evidence indicates that at more central zones within the visual system, signals from the three cone mechanisms combine to form very different signals that are similar to those suggested by the Hering opponent-process theory. Following Hurvich and Jameson (1957), modern zone theories posit that at the opponent-process zone, color vision is coded by separate blue/yellow and green/red chromatic channels and a third luminosity channel. Most zone theories posit that the activity level of the luminosity channel relates to brightness, that the relative polarities and activity levels of the color-opponent channels code hue, and that saturation involves a comparison between the relative activity levels of the luminosity and color-opponent channels (see Kaiser & Boynton, 1996). The actual neural locus of the opponent-process zone is quite vague (e.g., Abramov & Gordon, 1994) and depends upon the specific definition of "color-opponency"; however, it is quite clear that this zone must involve structures that are proximal to the retinal outerplexiform layer.

The duplicity theory of vision (Schultze, 1866) maintains that vision in higher vertebrates is mediated by two types of photoreceptors: rods and cones. According to common renditions in modern textbooks, the duplicity theory maintains that in humans, rods function at low light intensities and play no role in color vision, whereas cones

function at higher light intensities and are responsible for color sensations. Most modern zone theories adhere strictly to this form of the duplicity theory and fail to consider a role for rods in color vision. This probably reflects two methodological features common to most human color vision research: stimulation of the fovea and the use of extremely bright test stimuli and/or background fields. Given that the fovea is rod free (e.g., Polyak, 1941) and that rods saturate at relatively low levels of illumination (Aguilar & Stiles, 1954; Brill, 1990), the experimental data upon which theories are based are, by exclusion, "rod free." As reviewed below, however, a growing body of evidence suggests that under many viewing conditions, rods play some role in color vision. This should not be surprising, given that a large body of neurophysiological literature shows that the rods and cones of mammals, including old-world primates, interact at the photoreceptor level (Schneeweis & Schnapf, 1995) and at many more central levels of the visual system (Arden & Frumkes, 1986; Daw, Jensen, & Brunken, 1990; Gouras & Link, 1966; Merigan & Maunsell, 1993).

The present psychophysical study concerns the role of rods in color vision. My approach to this problem is to determine the influence of rod dark adaptation upon the perception of hue, an approach used first by Lie (1963). To put the problem in a broader perspective, I first

consider the problem of rod-cone interaction in general as well as a variety of previous approaches to the problem of the role of rods in color vision.

Achromatic Studies of Rod-Cone Interaction

Beginning with the work of von Kries and Nagel in 1896, a growing body of psychophysical research has provided compelling evidence that rod- and cone-related visual signals interact within the vertebrate visual system. Studies that directly investigated stimulus hue or saturation will be considered below; the majority of achromatic studies can be grouped into two categories (Denny, Frumkes, & Goldberg, 1990).

Studies suggesting rod-cone summation. The first type of study suggests that rod- and cone-related visual signals produce like-polarity responses at some locus within the visual system that sum together in a linear or quasilinear fashion. MacLeod (1972) first showed that rod- and cone-related flicker signals elicited by a middle-wavelength stimulus that appeared yellow under photopic conditions were likely to sum at some common locus and together determine flicker sensitivity. The rod signal, however, had a latency that was longer by approximately 75 ms than the cone signal. As a consequence and depending upon stimulus frequency, these signals would destructively interfere with each other, resulting in a small net signal, or sum together to produce an unusually large flicker

signal. MacLeod (1972), and more clearly, van den Berg and Spekreijse (1977) and Denny et al. (1990) predictably altered flicker sensitivity by manipulating the phase of separate stimuli that maximally affected rods (short wavelengths) or cones (long wavelengths). These psychophysical studies have been confirmed by means of ganglion cell recordings in cat (Rodieck & Rushton, 1976), suggesting that a summation of rod and cone signals can reflect a retinal mechanism.

Beginning with the work of Frumkes, Sekuler, Barris, Reiss, and Chalupa (1973), a large number of studies have shown that rod-stimulating backgrounds alter cone-mediated increment thresholds and that cone-stimulating backgrounds alter rod-mediated increment thresholds (e.g., Bauer, Frumkes, & Nygaard, 1983; Buck, Peeples, & Makous, 1979; Frumkes & Temme, 1977; Makous & Boothe, 1974). All of these increment threshold studies show that the influence of a "rod plus cone" background is similar to but greater in magnitude than the influence of a background that stimulates only one type of photoreceptor. In normal observers, these interactions always appear to be between rods and the long-wavelength cone mechanism, as indicated by field sensitivity spectra adhering to a Stiles π_5 mechanism, although comparable increment threshold data from a protanope produced a field sensitivity function with a Stiles π_4 spectrum (Frumkes, Naarendorp, & Goldberg,

1988).

Other measures of rod-cone summation have been provided by brightness-matching and threshold procedures. A number of investigators have found that both rods and cones contribute to the sensation of brightness (e.g., Drum, 1981; Palmer, 1976; Vienot & Chiron, 1992; Whittle & Challands, 1969). The meaning of these studies is far from clear because of the variety of results: although some data clearly suggest rod-cone summation (e.g., Palmer, 1976), others suggest some sort of inhibitory interaction (e.g., Drum, 1981). Beginning with the work of Ikeda and Urakubo (1969), some investigators have also tried to show that rod- and cone-related signals can sum together to produce a threshold sensation. Unequivocal evidence was provided by Frumkes et al. (1973). More recent data show that rod and cone signals from the short-wavelength (Naarendorp, Rice, & Sieving, 1996) as well as the middle-wavelength and long-wavelength (Buck & Knight, 1994) cone mechanisms can sum together to produce a threshold sensation.

Studies suggesting suppressive rod-cone interactions. Other psychophysical studies suggest highly nonlinear types of rod-cone interaction. Most of these studies show that as rods dark adapt, cone-mediated sensitivity to a variety of specific stimulus features tends to decrease. The oldest of these studies involved flicker sensitivity and showed that cone-mediated sensitivity to rapid flicker

decreases during the rod-recovery stage of dark adaptation; conversely, selective light adaptation of rods enhances cone-mediated flicker sensitivity (Alexander & Fishman, 1984; Coletta & Adams, 1984; Goldberg, Frumkes, & Nygaard, 1983; Lythgoe & Tansley, 1929). This type of rod-cone interaction is likely to specifically involve the long-wavelength cone mechanism, as suggested by action spectra resembling that of the Smith and Pokorny long-wavelength cone fundamental (Coletta & Adams, 1984). In addition, this type of rod-cone interaction is absent in protanopes (Frumkes, 1990). The underlying neurocircuitry is likely to be confined to the retinal outerplexiform layer, given that the interaction can be recorded intracellularly in most types of distal retinal neurons in cat and amphibian, including the cones themselves (Frumkes & Eysteinsson, 1988; Pflug, Nelson, & Ahnelt, 1990), and that it has been documented by ERG procedures in humans (Arden & Frumkes, 1986). Neurophysiological and neuropharmacological data from nonhuman animals and psychophysical data from humans with circumscribed retinal abnormalities suggest that these observations reflect an inhibitory influence of dark-adapted rods upon cone-mediated flicker perceptions, which is removed by rod light adaptation. For this reason, this flicker effect has often been referred to as suppressive rod-cone interaction (SRCI). However, because there are other SRCI-like effects that probably involve very

different mechanisms, I will refer to this phenomenon as flicker-SRCI (fSRCI) throughout the remainder of this thesis. Monocular flicker sensitivity is negligibly influenced by adapting the contralateral eye (Frumkes, Lange, Naarendorp, & Eysteinsson, 1995), a result consistent with the presumed distal retinal locus for fSRCI.

More recently, Frumkes and his colleagues (Lange, Denny, & Frumkes, 1997; Naarendorp, Denny, & Frumkes, 1988; Naarendorp & Frumkes, 1991) have shown an analogous influence of rod adaptation upon cone-mediated sensitivity to high spatial frequency gratings, an effect that is also absent in protanopes (Frumkes, 1990). However, the influence of monocular rod adaptation is virtually identical in both the viewing and nonviewing eye (Lange et al., 1997), suggesting that this effect must involve nonretinal structures. It is of interest that light adapting the rods or pressure blinding the nonviewing eye have similar influences upon grating sensitivity (Denny, Frumkes, Barris, & Eysteinsson, 1991), suggesting that this type of rod-cone interaction also reflects an inhibitory influence of dark-adapted eyes. It is probably another SRCI mechanism involving a vastly different neural pathway than the one involved in fSRCI effects. For this reason, I will refer to this effect throughout the remainder of this thesis as grating-SRCI (gSRCI). Although gSRCI has been

demonstrated by means of evoked potential procedures in humans (Eysteinsson, Barris, Denny, & Frumkes, 1993), there is no further evidence regarding the underlying neural circuitry.

Chromatic Studies of Rod-Cone Interaction

In 1896, von Kries and Nagel first noted that scotopic vision is very often "blueish." Since that time, a growing number of studies have suggested a variety of roles for rods in color vision. Certainly, it is well known that normal color vision is considerably different when rod participation is eliminated by using small, bright, foveal stimuli than when stimuli involve larger fields and are presented parafoveally (e.g., Nagy & Wolf, 1993; Pokorny, Smith, & Starr, 1976). Most modern investigations of rod participation in color vision fall into four categories.

Studies with "colorblind" observers. There is some evidence of a rod contribution to color vision from hereditary colorblind individuals who lack at least one of the normal cone photopigments. "Blue-cone monochromats," individuals who lack both the middle- and long-wavelength cone pigments, often show a rudimentary form of color vision that appears to involve a comparison of the signals mediated by the short-wavelength cone mechanism and rods (Kaiser & Boynton, 1996, p. 458). Furthermore, with large field stimulation, residual red-green color vision is often seen in protanopes and deuteranopes who lack the normal

long- or middle-wavelength cone pigment, respectively. Because only one cone photopigment exists that responds to the relevant stimulus wavelength, both Nagy (1980) and Smith and Pokorny (1977) argued that rod messages must interact with the single long- or middle-wavelength cone mechanism to provide this type of color discrimination (but see Montag, 1994). Unfortunately, this type of research yields few clues regarding the role of rods in normal color vision.

Studies of induced "scotopic hues." Presentation of a photopic stimulus can induce chromatic sensations in a purely scotopic stimulus (i.e., a stimulus with a luminance below that necessary for detection by cones). For example, Wilmer (1950) first showed that a red-appearing stimulus causes an adjacent, purely scotopic stimulus to appear blue. Since that time, researchers have reported a wide variety of demonstrations of such induced scotopic hues, most particularly since the early work by Stabell and Stabell (for a modern reference and a review of the earlier literature, see Buck, 1996, and Stabell & Stabell, 1994). A wide variety of scotopic hues have been induced, although there are many complex and poorly understood factors determining which specific hues are induced. For example, Buck (1996) insisted that successive (temporal) contrast seems to induce a much wider variety of hues than

simultaneous (spatial) contrast. He showed that regardless of the adjacent, photopic, inducing stimulus, the induced scotopic hue most commonly matched a photopic hue elicited by wavelengths < 520 nm. However, Stabell and Stabell (1994) reported a much wider variety of induced scotopic hues using simultaneous contrast. Indeed, using the framework of Land's retinex theory and Mondrian patterns, a rich variety of hues have been reported as a result of stimuli that can directly affect only rods and the long-wavelength cone mechanism (McKee, McCann, & Benton, 1977). The variety of these data and their lack of an obvious lawfulness limit their utility.

Studies of "tetrachromatic" color matching. In 1970, Trezona reviewed a large body of literature and more recently (1973, 1974) collected a great deal of her own data showing that classic trichromatic explanations could not account for colorimetric data involving large fields at mesopic luminance levels. She could account for these data, however, using a tetrachromatic, as opposed to the usual trichromatic, version of the Wright colorimeter, in which an extra, fourth set of controls adjusted rod-related luminance. Her data showed a rod contribution to color vision that disappeared as stimulus luminance increased. This rod contribution to color vision appeared to sum selectively with the short-wavelength cone signal. Trezona's results are supported in part by the summation

studies of Naarendorp et al. (1996) and are in qualitative agreement with the simultaneous contrast data of Buck (1996), which might suggest a selective interaction with the short-wavelength cone mechanism. However, because rods and the longer wavelength cones also summate their signals (Buck & Knight, 1994; Frumkes et al., 1973; Schneeweis & Schnapf, 1995), and because successive contrast induces a very wide spectrum of red and yellow scotopic hues, rod signals must additionally interact with the signals from the middle- and long-wavelength cone mechanisms.

Studies of rod-cone interaction during dark adaptation. Several researchers have examined cone vision during the rod recovery stage of dark adaptation. Lie (1963) measured the specific (hue identification) threshold function and its relation to the traditional detection threshold function during long-term dark adaptation. During the cone portion of the dark adaptation curve, the two thresholds are similar, but during the rod recovery phase, the specific threshold rises (throughout the remainder of this thesis, I refer to this general class of phenomenon as the "Lie effect"). Lie found qualitatively similar results using a wide variety of stimuli that varied in size, duration, retinal position, and wavelength. These results have been replicated and extended in a number of more recent studies. Unfortunately, in the published literature, the influence of stimulus wavelength has been

quite susceptible to interobserver variability and variability in the results from different laboratories, making it difficult to relate to modern color theory.

More recent experiments have indicated that the magnitude of the Lie effect is most consistent for wavelengths inducing sensations of green, often exceeding 1 log unit (Ambler, 1974; Spillmann & Conlon, 1972), but that the magnitude is less for other wavelengths. Long wavelength (red-appearing) stimuli prove particularly troublesome. For example, Ambler (1974) found that the Lie effect is neglible for a wavelength of 670 nm. However, this finding clearly reflects the observer's specific criteria for the sensation of red: depending upon the criteria used, the magnitude of the Lie effect obtained for sensations of red is at least as great as that obtained for other sensations induced by shorter wavelength stimuli (Peachey, Seiple, Auerbach, & Armington, 1987). Other more recent studies are particularly noteworthy. Alexander, Fishman, and Derlacki (1988) found that individuals with the Schubert-Bornschein type of stationary night blindness (who show a rod A wave in their ERG, indicating photoreceptor activity, but who fail to provide direct behavioral evidence of rod vision and fail to show a rod B wave in their ERG) show quite normal fSRCI, but do not show the Lie effect. Their data suggest that fSRCI reflects a rod influence mediated by horizontal cell feedback onto

cones, which is presumably unaffected by the disease (for a similar model based upon physiological data, see Frumkes & Eysteinsson, 1988; Pflug et al., 1990), whereas the Lie effect must be mediated more centrally. In addition, Prestrude, Watkins, and Watkins (1978) have shown that light adapting the nonviewing eye influences the time course of the Lie effect. This influence of extraretinal neural tissue is also consistent with a more proximal neural locus.

Models that Account for the Rod Contribution to Color Vision

Three models, none of which are mutually exclusive, might account for the rod contribution to color vision.

The summation of rod and short-wavelength cone signals model. Trezona (1970) suggested that light-evoked signals from rods sum with signals from the short-wavelength cone mechanism. Such a model accounts for her "tetrachromatic" colorimetry data, as well as a variety of evidence that associates "blueness" with scotopic vision. Regardless of how compelling these data might be, it should be noted that the short-wavelength cone mechanism also provides the signals for the red component of the hue elicited by short wavelengths. Moreover, the neurobiological and psychophysical evidence for rod-cone summation is not specific to the short-wavelength cone mechanism.

The luminosity/saturation model. Stabell and Stabell (1976a, 1976b) have collected a variety of data indicating

that stimuli become less saturated as rods dark adapt (but see Stabell & Stabell, 1975, 1979). Stating their conclusions in terms of modern zone theory, they imply that signals from photically stimulated rods sum with signals from cones to determine the magnitude of the signal provided by the luminosity channel; this signal, when compared with signals from the color-opponent channels, desaturates the appearance of the stimulus. At least in a qualitative manner, this model is consistent with evidence showing a rod contribution to brightness sensations. The Lie effect has also been similarly explained by Ambler (1974), Lie (1963), and Spillmann and Conlon (1972), although Ambler also suggested some specific rod involvement with the short-wavelength cone mechanism. If such a model accounts for the rod contribution to color vision, one would predict that changes in specific threshold and in apparent saturation would depend heavily upon stimulus wavelength. For example, an experiment could be conducted throughout the time course of dark adaptation, during which an observer compared the change in saturation of photopically matched, red-appearing (circa 650 nm) and blue-appearing (circa 470 nm) stimuli. Due to the difference in relative photopic and scotopic spectral sensitivity, the 470 nm stimulus would have a much greater influence upon rods; therefore, the blue-appearing stimulus should become more desaturated than the red-appearing

stimulus during dark adaptation. I am unaware of data directly supporting this possibility.

The chromatic-SRCI model. This type of model suggests that dark-adapted rods suppress some type of color-related signal during dark adaptation. That is, the major influence of dark-adapted rods upon color vision is a type of SRCI. This mechanism could have many forms. On the one hand, dark-adapted rods might selectively inhibit signals from some type of cone in the trichromatic zone. This is unlikely, because the results of Alexander et al. (1988) suggest that the neural locus for the Lie effect is proximal to the retinal outerplexiform layer. On the other hand, dark-adapted rods might suppress various channels at later stages of color processing. Such a suppression is not likely to involve the luminosity channel, because rod dark adaptation increases rather than decreases apparent brightness (Vienot & Chiron, 1992; Whittle & Challands, 1969). However, dark-adapted rods could suppress the activity of the blue/yellow and/or green/red chromatic channels. Although never considered previously, this type of model is quite attractive, because there is a good deal of similarity between the time course of the Lie effect and the time courses of fSRCI (Goldberg et al., 1983) and gSRCI (Naarendorp et al., 1988) during dark adaptation. Throughout the remainder of this thesis, I will refer to this model as the chromatic-SRCI (cSRCI) model.

Rationale

The present thesis was designed to directly test the luminosity/saturation and cSRCI models of rod involvement in color vision. I examined the change in color perception evoked by a small, parafoveally presented flash of light during the time course of dark adaptation. Stimulus wavelengths of 478, 511, 576, and 637 nm were chosen to approximate the unique hues of blue, green, yellow, and red, respectively. In the first experiment, I measured specific and detection thresholds (i.e., the procedure of Lie, 1963). Although the general nature of my results was similar to that of Lie's results, the influence of stimulus wavelength was sufficiently reliable across all observers to permit a comparison of the three models listed above that may account for the rod contribution to color vision.

Two shortcomings of the first experiment are that specific threshold is a one-dimensional index, subject to a great deal of subjective interpretation. In addition, the luminosity/saturation model invites the use of separate measures of hue and saturation during dark adaptation. While collecting data for the first experiment, I became aware of the "4 + 1 categories" hue and saturation scaling procedure used by Gordon, Abramov, and Chan (1994). In brief, an observer evaluates the appearance of a stimulus in terms of its percentage of blue, green, yellow, and red (totalling 100%) and its percentage of saturation (from 0%

to 100%).

Hue and saturation scaling is essentially a type of magnitude estimation procedure (e.g., Stevens, 1956, 1958), wherein observers assign numbers to their impressions of a stimulus. These numerical descriptions are then averaged. Graham and Ratoosh (1962) objected to such a procedure because it treats learned verbal responses, that is, the numerical responses, as numerical data. The observer's numerical responses are added and averaged as if they were quantified outcomes of independent measuring operations, which have not been carried out (Graham & Ratoosh). Although one can determine the average luminance associated with a number response, one cannot determine the average number response associated with that luminance.

Hue and saturation scaling, however, involves a ratio scale of measurement. Such a scale implies a true zero point, which allows for an assumption of an equality of ratios. The determination of equal ratios may be accomplished by determining successive equal intervals beginning at the scale's zero value (Stevens, 1951). The procedure of Gordon et al. (1994) allows for true zero points for both hue and saturation. Observers' reports can be "0% blue" or "0% saturation," indicating a total absence of that hue or of any chromatic component in their sensations of the stimulus, respectively. To ensure equal intervals and to allow for comparisons of sensations and of

experimental effects, Gordon et al. addressed the problem of unequal variances that is generated by the use of bounded percentage scales. They applied an arcsine transform to each data point before averaging. This procedure reduced the variances and resulted in a more rectangular distribution of variances when plotted against their respective means.

Although this procedure might seem even more subjective than the specific threshold measure, it has proved to be far more reliable both within and across observers. Moreover, the size and duration of stimuli most commonly used by Gordon et al. (1994) were similar to those used in Experiment 1, and the stimulus illuminance levels often used (6 trolands) were very similar to the specific threshold values obtained in the totally dark-adapted eye. Therefore, in the second experiment, I recorded the hue and saturation perceived by the observer throughout the time course of dark adaptation using the scaling procedure of Gordon et al. (1994).

Finally, different types of SRCI reflect different neural processes that are monocular, binocular, or interocular in nature. In addition, previous research has suggested that the Lie effect is mediated by a neural mechanism proximal to that accounting for fSRCI and may involve some binocular interaction (Prestrude et al., 1978). However, no researcher has directly investigated

the possibility that the change in color vision induced by rod adaptation can be obtained by means of interocular adaptation, as is the case for gSRCI. Therefore, in both experiments of this study, I compared the influence of monocular, interocular, and binocular rod adaptation upon color vision.

Chapter 2

Method

Observers

Four observers participated in the present study. EL, the author, was a 41-year old female and an experienced psychophysical observer. The other three observers (RM, a 22-year old male; AD, a 21-year old male; and MT, a 21-year old female) had no prior experience with visual psychophysics, but became sufficiently reliable after several preliminary training sessions. EL, the author, was totally aware of the purpose of all aspects of experimentation, as was RM, an author on one preliminary communication (Lembessis, Meaney, Moshe, & Frumkes, 1996). Observers AD and MT, Queens College undergraduate students, remained totally naive about the purpose of the present study and the nature of their results throughout the entire period of experimentation. As indicated below, RM was an observer in the first experiment, MT was an observer in the second experiment, EL was an observer in both experiments, and AD participated in most of the first experiment and all of the second experiment.

AD was slightly myopic (20/30) in his viewing eye, but wore no correcting spectacles. The other three observers wore spectacles to correct their vision while collecting all data. The color vision and color discrimination of all four observers was normal as assessed by their responses on

the Farnsworth Dichotomous Test for Color Blindness-Panel D-15 (Psychological Corporation) and the Farnsworth-Munsell 100 Hue Test (Psychological Corporation). In addition, the binocular vision of all four observers was normal as assessed by their sensitivity to random-dot stereograms.

Apparatus

Conceptually, the two experiments were quite similar. First, the photopigment of the viewing eye, the nonviewing eye, or both eyes of the observer was bleached by exposure to an intense preadapting field. After this preadapting field was extinguished and for the next 25 minutes, the observer's response to a spectrally narrow-band stimulus was continually tracked. Two pieces of apparatus were used.

Preadapting (bleaching) stimulator. This was a specially constructed, binocular, 1-channel Maxwellian view system with a 12 V, 75 W, tungsten halogen source. The light presented to the observer was a circular, foveally centered, 40^{o}, white light field of 1.3×10^{5} td (see Calibration section below). The interpupillary distance of the apparatus could be varied easily by means of a geared arrangement that adjusted the position of two rhomboid prisms and the distance between the two final eye lenses. Furthermore, the image of the source in the plane of the pupil was < 2 mm, small enough to insure that the observer's pupil would not serve as an optical stop. With

careful alignment and appropriate placement of a baffle, it was possible to bleach photopigment in only the viewing eye, the nonviewing eye, or both eyes of the observer. The illuminances provided by these two channels were within 0.1 log units, as judged by the subjective influence of an interposed 0.1 log unit filter on relative brightness and as measured with an illuminometer.

The main optical stimulator. All stimuli used directly for data collection were presented to one of the observer's eyes (generally the right) by means of a 5-channel Maxwellian view optical system built by Nygaard and Frumkes (1985) and described by Goldberg (1983). As indicated in Figure 1 (adapted from Goldberg, 1983), there was a separate source for each channel. Four of the sources were LEDs: S1 was "green" (LEDtronics L200CWG500), S2 was "red" (Hewlett Packard 45cd), S3 was "blue" (LEDtronics L200CWGBG/150), and S4 was "yellow" (LEDtronics L200CWLY5), with peak wavelengths of 565, 660, 490, and 585 nm, respectively, and half bandwidths of about 40 nm. One source, S4, was filtered by a Wratten 29 filter (F4) that passed wavelengths of 610 nm or more; this source provided a red fixation target. S5 was a tungsten source used only to ensure proper alignment of the observer with the optical system.

As illustrated in Figure 1, the output of S1 was first collimated by L1. The collimated beam then passed through

Figure 1. Schematic representation of the main optical stimulator. A1 and A2 are apertures. B1 to B4 are beamsplitters. F1 to F5 are filters. L1 to L10 are lenses. NP is the nodal plane of the observer's eye. P1 and P2 are prisms. S1 to S5 are light sources. W1 and W2 are neutral density wedges. (Adapted from Goldberg, 1983).

Figure 1. Schematic Representation of the Main Optical Stimulator

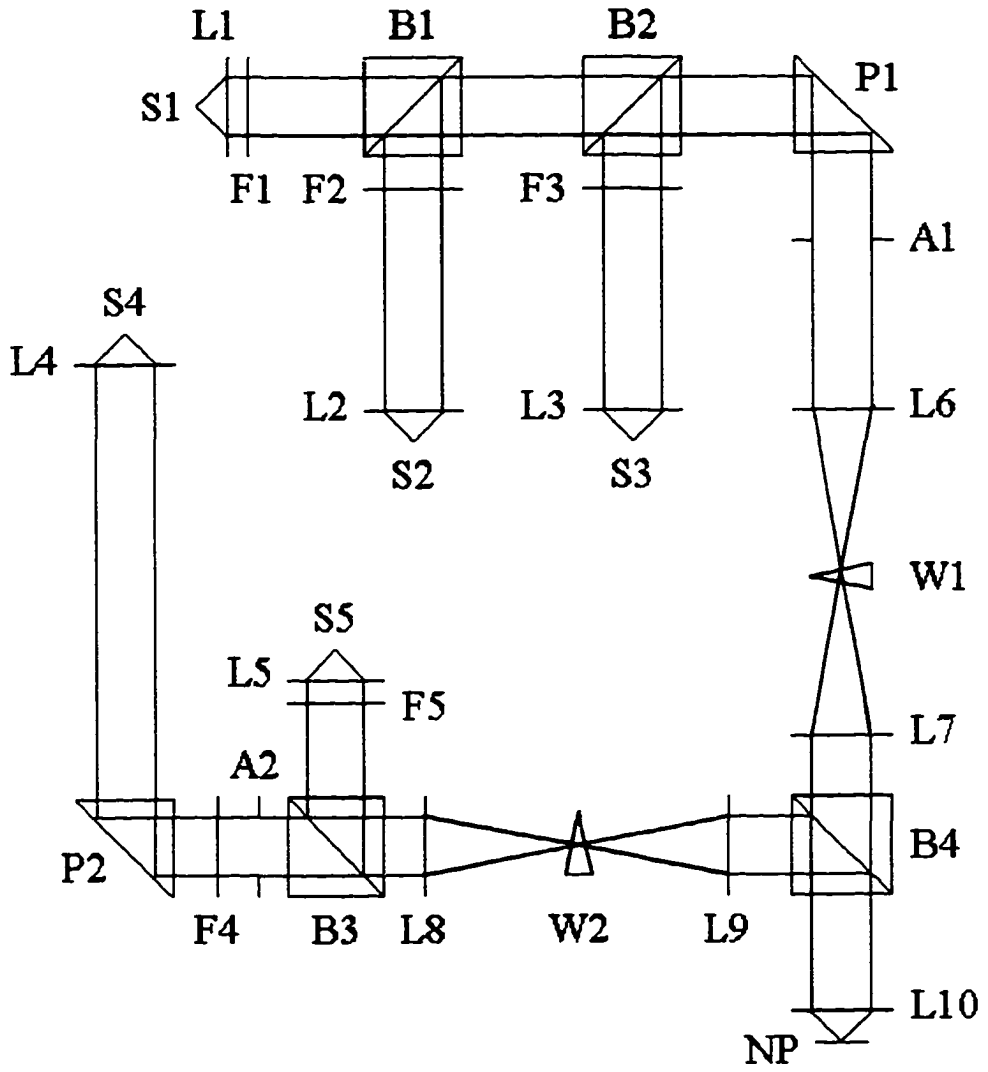

two beam splitters (B1 and B2), was deflected 90° by a reflecting prism (P1), and was truncated by an aperture stop (A1). The collimated beam was then refocused by L6 onto the plane of absorbance of a Kodak 4-log unit circular neutral density wedge (W1) and recollimated by L7. The recollimated beam then passed through another beamsplitter (B4) and was refocused by L10 onto the nodal plane of the observer's eye.

Outputs of the other sources (S2 to S4) followed similar paths. By means of a series of beam splitters and reflecting prisms, these ray paths were superimposed in the nodal plane of the observer's eye. If both apertures were removed, the paths completely filled L10, producing a 28° diameter, circular visual field in Maxwellian view. The focused, superimposed images of all four sources, measured at the position of the observer's nodal plane, was under 3 mm in diameter, considerably smaller than the observer's pupil in the low illuminance conditions of this study. The observer's head was stabilized with a full mouth bite bar, whose position could be adjusted in three planes. At the beginning of every experimental sitting, the observer adjusted the position of the bite bar and, therefore, his or her visual alignment by moving the bite bar to the left or right and up or down until the stimulus appeared at its subjective brightest. When the observer was correctly aligned, the Maxwellian image was placed in the center of,

and passed entirely through, the observer's pupil. To ensure correct alignment, the observer manipulated the position of the bite bar until the stimulus appeared at its brightest.

Apertures A1 and A2, whose positions were controlled by two-dimensional micromanipulators, determined the spatial configuration and visual field loci of all of the stimuli presented to the observer's retina. Using a projection technique, it was determined that a 1.6 mm diameter aperture produced a retinal image of about 2^{o} diameter. Using this information, the exact size of stimuli produced by each source could be specified. Aperture-stopped stimuli were made by precision drilling into 1/10 inch aluminum.

The final 28^{o} field of view produced by this apparatus is indicated schematically in Figure 2. The fixation target was a continually exposed red stimulus consisting of four small circles. The test stimuli were 3^{o} diameter circles, which, with respect to the center of the fixation target, were presented along the horizontal meridian and 6^{o} to the right. Thus, if the right eye was used for viewing, this stimulus appeared in the temporal field; on the rare occasions when the left eye was used for viewing, the test stimulus was presented in the nasal field. The duration of the test stimuli (100 ms in both experiments) was determined by the duration of a 15 V pulse delivered by a

Figure 2. Schematic representation of the stimulus field. The observer fixated on the center of an imaginary square formed by four small, red circles. The 3^{o} circular test stimulus appeared 6^{o} to the right of fixation, in the observer's right eye temporal field. For one experiment, the stimulus appeared 6^{o} to the right of fixation, in the observer's left eye nasal field.

Figure 2. Schematic Representation of the Stimulus Field

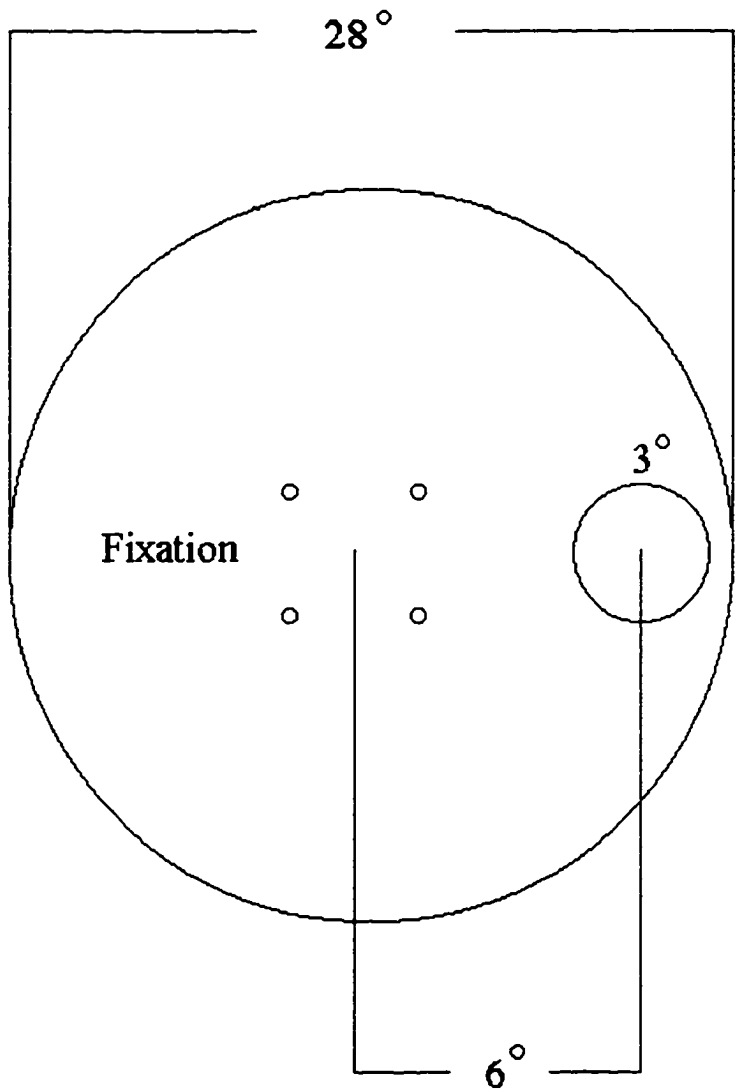

4710 Ortek stimulator. As determined by a series resistor of 470 ohms, the current that drove the LED source was less than 35 mA, the maximal value suggested by the manunfacturer's specifications. A three position rotary switch determined which LED was used as a source.

The illuminances of all test stimuli were controlled by a circular neutral density wedge, whose position was controlled by a 40-turn, calibrated dial. Further neutral density filtering was accomplished as needed with fixed filters placed at F3.

The spectral properties of all test stimuli reflected both the LED source used and the specific interference filter interposed in the path of the relevant light beams. In all cases, Baird Atomic or Ditric Optics narrow-band interference filters were used. The "blue" and "green" stimuli were produced by placing either a 472 nm or 512 nm filter, respectively, at F3, in the path of the "blue" LED light source (S3). The "yellow" stimulus was produced by placing a 577 nm filter at F1, in the path of the "green" LED light source (S1), and the "red" stimulus was produced by placing a 632 nm filter at F2, in the path of the "red" LED light source (S2). The four resulting "monochromatic stimuli" had the spectral properties indicated in Figure 3. Thus, the prototypical "blue, green, yellow, and red" stimuli had peak outputs at 478 nm, 511 nm, 576 nm, and 637 nm, respectively (see Calibration section below).

Figure 3. Spectral properties of the four stimuli. The actual spectral outputs of the stimuli were determined by multiplying the percent relative intensities of the LED light sources by the percent transmission rates of the filters and then determining peak wavelengths.

Figure 3. Spectral Properties of the Four Stimuli

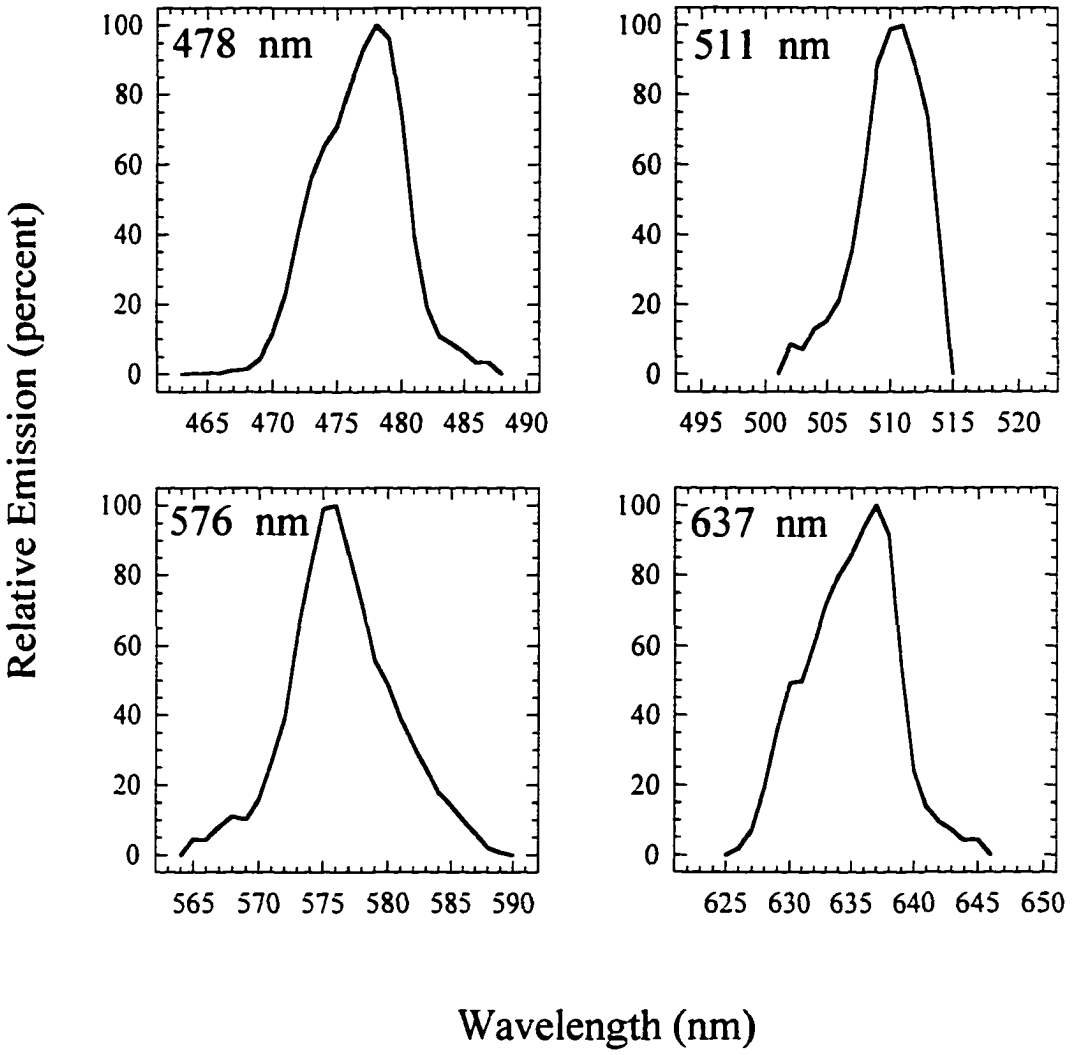

Calibration

The actual wavelengths of the test stimuli were determined by first multiplying the percent relative intensities of the LEDs (based on typical spectral distribution functions such as those reported by Watanabe, Mori, & Nakamura, 1992) by the transmission spectra of the filters (as determined by an AVIV Associates UV-VIS-IR model 14DS spectrophotometer), and then determining peak wavelengths. The actual spectral outputs of these four stimuli are shown in Figure 3.

The retinal illuminance of each source, with no neutral density filtering in the beam path, was determined by a procedure proposed by Nygaard and Frumkes (1982). For their technique to be valid, the source image must be smaller than the observer's pupil, the plane of reference of the measuring device must be filled with light, and the device must be placed at a distance at least 10 times the radius of the source image. The detector head of a United Detector Power Meter (model 351), with a photometric filter in place, was placed 70 mm from the Maxwellian image, on a plane normal to the optical axis of the final eye lens. Photopic retinal illuminance, expressed in photopic trolands, was provided by the equation

$$E_R = 10^6 Ed$$

(Nygaard & Frumkes, 1982), where E is the illuminance falling on the detector head, and d is the distance from

the detector head to the source image. The procedure was repeated for each light source. At maximum intensity, the 478 nm test stimulus provided approximately 5, the 511 nm stimulus approximately 15, the 576 nm stimulus approximately 12, and the 637 nm stimulus approximately 25 photopic trolands retinal illuminance.

General Procedure

A typical experimental session proceeded in the following manner. After insuring that the position of the observer's bite bar was adjusted to produce correct alignment, the observer first dark adapted for 25 minutes. (In cases where the first dark adaptation function of the experimental period followed binocular preadaptation bleaching, this preliminary dark adaptation was not used.) Then, the observer's viewing eye (generally the right eye), nonviewing eye, or both eyes were exposed to the bleaching field(s) for 30 seconds. As rapidly as possible, the observer then moved to the main optical stimulator and for the following 25 minutes, continually "tracked" sensitivity with the type of response(s) indicated below.

The following restraints were used in data collection. In any one experimental sitting lasting generally 1 to 4 hours, data were collected in a maximum of 4 dark adaptation sessions. Rest periods of at least 10 minutes between sessions were provided to "refresh" the observer. The observer rested in the dark.

Experiment 1: Specific (hue identification) and detection thresholds. After bleaching the viewing, nonviewing, or both eyes, the observer dark adapted for 25 minutes. During that time, the observer tracked either the specific or detection threshold of the presented stimulus by turning the dial that adjusted the wedge of the apparatus, thereby adjusting the intensity of the stimulus. When tracking specific threshold, the observer tracked the threshold for a specified hue (e.g., "blue") rather than hue in general. The stimulus was presented for 100 ms every 3 s (0.33 Hz). Threshold readings were taken by the experimenter every 30 s by noting the position of the calibrated dial that controlled stimulus illumination. The experimenter gave the observer verbal warning signals several seconds before the reading was due. The observer had 15 s after the 30 s mark to indicate that he or she had determined the threshold. If the threshold had not been determined by then, the reading was skipped. Between each scheduled reading, the dial was turned by the experimenter or the observer a random number of turns below the last threshold reading. Thus, all readings reflected ascending threshold determinations. The sole exception was the first reading, for which the dial was set at maximum intensity.

All specific thresholds were determined before detection thresholds. For each of these two threshold categories, the four wavelengths were presented in separate

blocks. For each wavelength block, there was a minimum of three dark adaptation sessions for each of the three preadaptation conditions. For each observer, then, there was a total of 24 conditions and a minimum of 72 dark adaptation sessions. The precise number of dark adaptation sessions depended on the consistency of the threshold curves. That is, the observer dark adapted under each condition until a minimum of three consistent threshold curves was obtained. When feasible, three dark adaptation sessions, one for each of the three preadaptation conditions, occurred on each day of testing. The order of the preadaptation conditions was randomized.

Experiment 2: Hue and saturation scaling. During dark adaptation, the retinal illuminances of the four test stimuli were held constant at 5 photopic trolands. This value was the maximal achievable with the dimmest of the four wavelengths used.

Subsequent to preadaptation bleaching, the observer dark adapted for 25 minutes. During that time, the stimulus was presented for 100 ms every 5 s (0.20 Hz). Every 30 s, the experimenter prompted the observer to report the hue and saturation of the stimulus. The report of hue was restricted to the four choices blue, green, yellow, and red, either singly or in any combination. The report was in the form of a percentage of each hue seen; all percentages added up to 100. For example, a report of

hue might have been, "60% blue, 40% green." The report of saturation was the percentage of the stimulus that was chromatic (as opposed to achromatic). The report of saturation was a single percentage ranging from 0 to 100. The experimenter gave the observer verbal warning signals several seconds before the report was due. The observer had 15 s after the 30 s mark to make his or her report. If the observer could not do so, the report was skipped.

The four stimulus wavelengths were presented in separate blocks. For each wavelength block, there was a minimum of four dark adaptation sessions for each of the three preadaptation conditions. For each subject, then, there was a total of 12 conditions and a minimum of 48 dark adaptation sessions. The precise number of dark adaptation sessions depended on the consistency of the obtained data. The observer dark adapted under each condition until a minimum of four consistent sets of data was obtained. When feasible, three dark adaptation sessions, one for each of the three preadaptation conditions, occurred on each day of testing. The order of the preadaptation conditions was randomized.

Chapter 3

The Influence of Dark-Adapted Rods Upon Specific Thresholds

General Observations

Figure 4 shows for observer EL, change in specific (on the left) and detection (on the right) threshold, for a 511 nm flash as a function of the time following the extinction of the preadapting bleaching field. The three sets of functions were obtained when the bleaching stimulus was presented to the viewing eye (monocular), to both eyes (binocular), or to the nonviewing eye (interocular). As indicated in Figure 4, interocular preadaptation had relatively little effect upon specific or detection thresholds, although both monocular and binocular preadaptation produced relatively normal dark adaptation curves such as presented in the classical literature (e.g., Hecht, 1937). Also, Figure 4 shows that the influence of monocular and binocular adaptation upon specific threshold is considerably different than the influence upon detection threshold. However, other types of conclusions are relatively difficult to make from this sort of plot. For this reason, I rely quite heavily on various types of derived plots throughout the remainder of this thesis.

A compilation of specific and detection thresholds in a "raw format" such as Figure 4 is presented in Appendix A as Figures 41 to 52 for all three observers and with all four test stimuli. The remainder of this section concerns

Figure 4. Specific (hue identification) and detection thresholds for observer EL for a 511 nm stimulus as a function of time in the dark following monocular, binocular, and interocular preadaptation. The test stimulus was a 3^{o} circle presented for 100 ms every 3 s at 6^{o} in the right eye temporal field.

Figure 4. Specific (Hue Identification) and Detection Thresholds
EL 511 nm

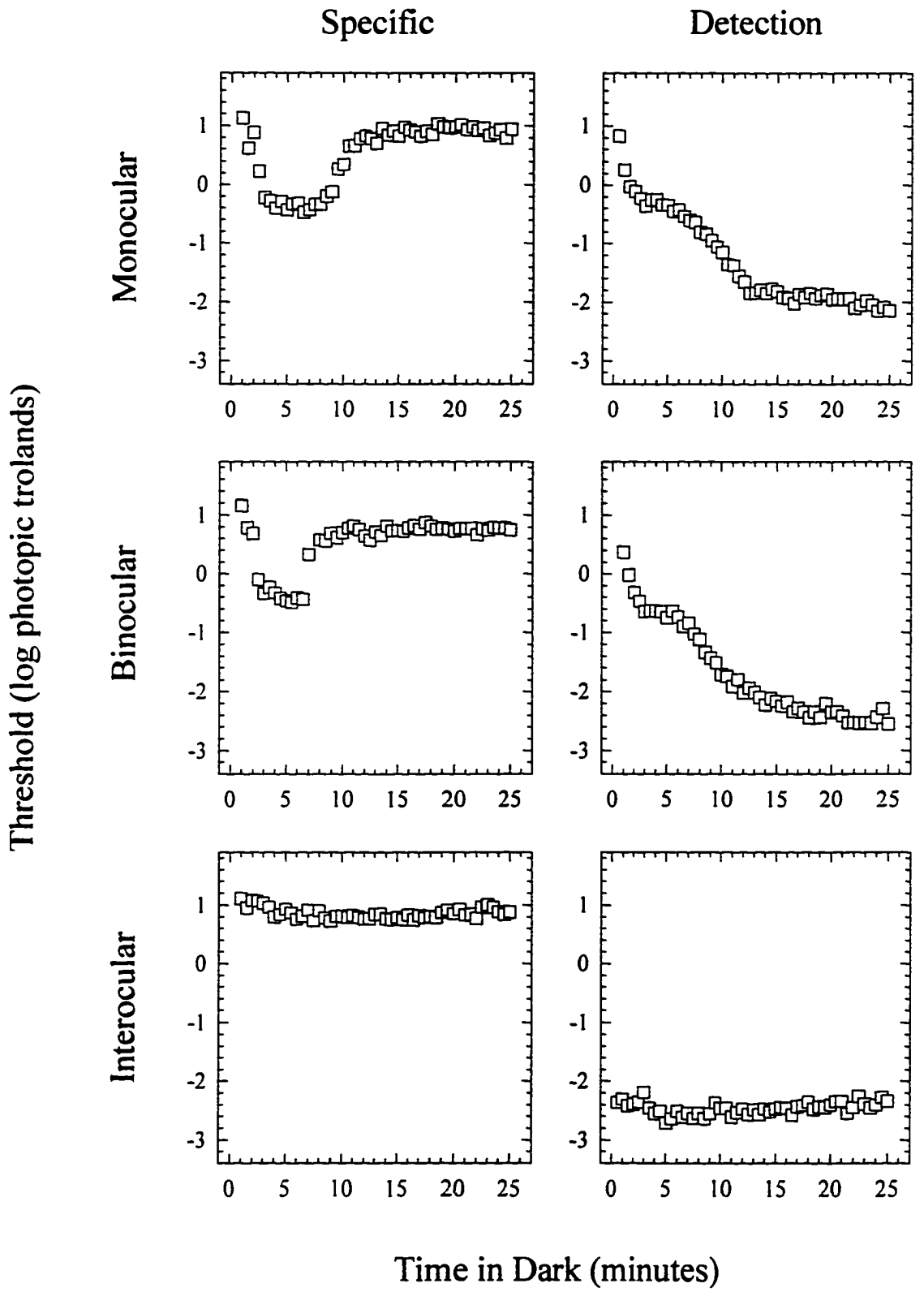

the influence of stimulus wavelength upon the changes in threshold during the rod recovery stage of adaptation, concentrating on data obtained following a monocular bleach of photopigment. The influence of the adapted state of the nonviewing eye upon threshold is considered in Chapter 6 below.

The Relationship Between Specific and Detection Threshold During Dark Adaptation

Figure 5 directly compares the influence of monocular preadaptation upon specific and detection thresholds (the open and closed symbols, respectively) for the four wavelength test stimuli used. Data obtained with the 478 and 511 nm stimuli replicated the general findings of Lie (1963) and other investigators (e.g., Prestrude et al., 1978; Spillmann & Conlon, 1972). That is, during the first minutes of dark adaptation, both specific and detection thresholds adhere quite closely to each other. However, during the rod recovery phase of adaptation, when detection threshold continues to decline, specific threshold increases. Similar results were obtained with longer wavelength test stimuli except that detection and specific thresholds rarely correspond. Very similar overall findings are apparent in the results for observer EL following binocular bleaching of photopigment as plotted in Figure 6; although not illustrated, similar conclusions can be made from the data of the other observer so examined

Figure 5. Specific (hue identification) and detection thresholds for observer EL for all four stimulus wavelengths as a function of time in the dark following monocular preadaptation. The test stimulus was a 3^{o} circle presented for 100 ms every 3 s at 6^{o} in the right eye temporal field.

Figure 5. Specific (Hue Identification) and Detection Thresholds EL Monocular

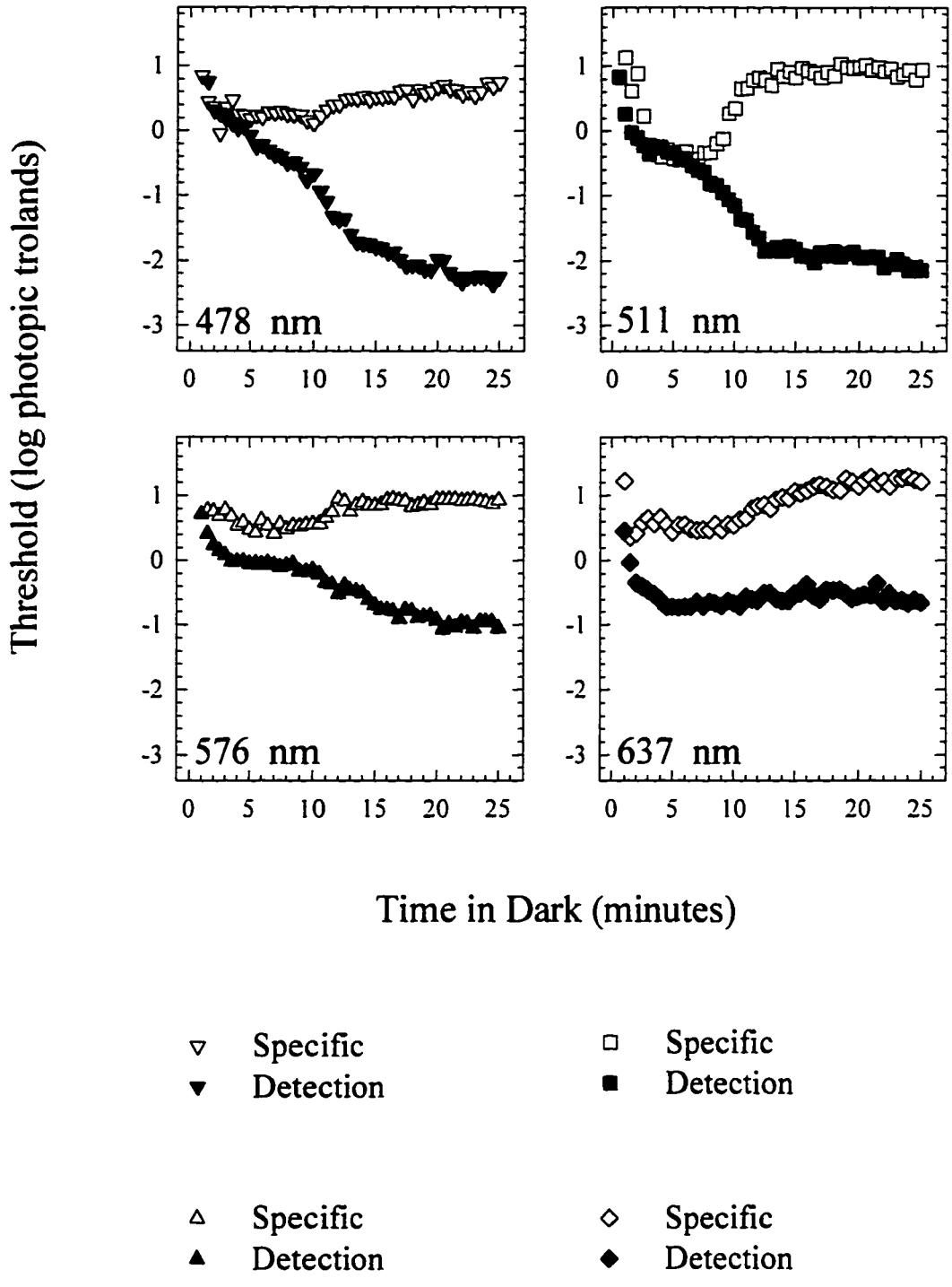

Figure 6. Specific (hue identification) and detection thresholds for observer EL for all four stimulus wavelengths as a function of time in the dark following binocular preadaptation. The test stimulus was a 3^{o} circle presented for 100 ms every 3 s at 6^{o} in the right eye temporal field.

Figure 6. Specific (Hue Identification) and Detection Thresholds EL Binocular

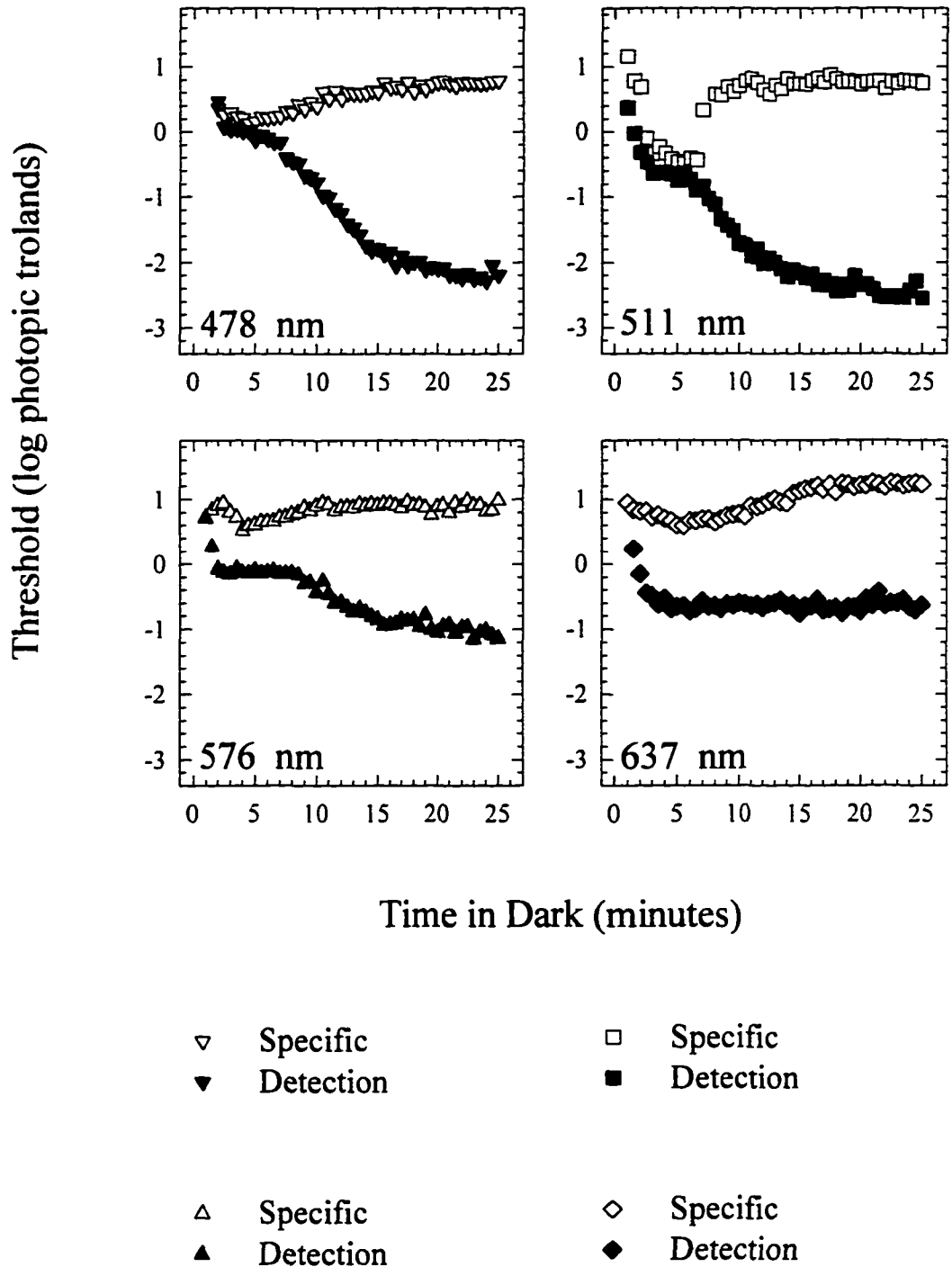

(see Appendix A, Figures 45 to 48).

From data such as shown in Figure 5, Lie (1963), Spillmann and Conlon (1972), and other investigators concluded that the rise in specific threshold during the later stages of dark adaptation is attributable to rod dark adaptation. As pointed out by previous investigators, this is the most likely conclusion if the cone plateau stage of detection threshold dark adaptation functions indicates the completion of cone photopigment regeneration.

The Influence of Test Stimulus Hue and Wavelength Upon the Magnitude of the Lie Effect

Figure 7 shows the change in specific threshold during dark adaptation following a monocular bleach of photopigment for observer EL; the different shaped symbols indicate the wavelength of the test stimulus as well as its perceived hue at specific threshold. For purpose of comparison, these functions were shifted along the ordinate to superimpose the blue and yellow functions and to superimpose the red and green functions during the time period from 20 to 25 minutes in the dark. Notice that the blue (478 nm) and yellow (576 nm) functions are quite similar: specific threshold decreases during the first few minutes of dark adaptation and then remains at an interim plateau value till approximately 10 minutes in the dark. Then from approximately 10 to 18 minutes in the dark, specific threshold increases about 0.5 log units. Although

Figure 7. Specific (hue identification) thresholds for observer EL for all four stimulus wavelengths as a function of time in the dark following monocular preadaptation. The test stimulus was a 3° circle presented for 100 ms every 3 s at 6° in the right eye temporal field.

Figure 7. Specific (Hue Identification) Thresholds
EL Monocular

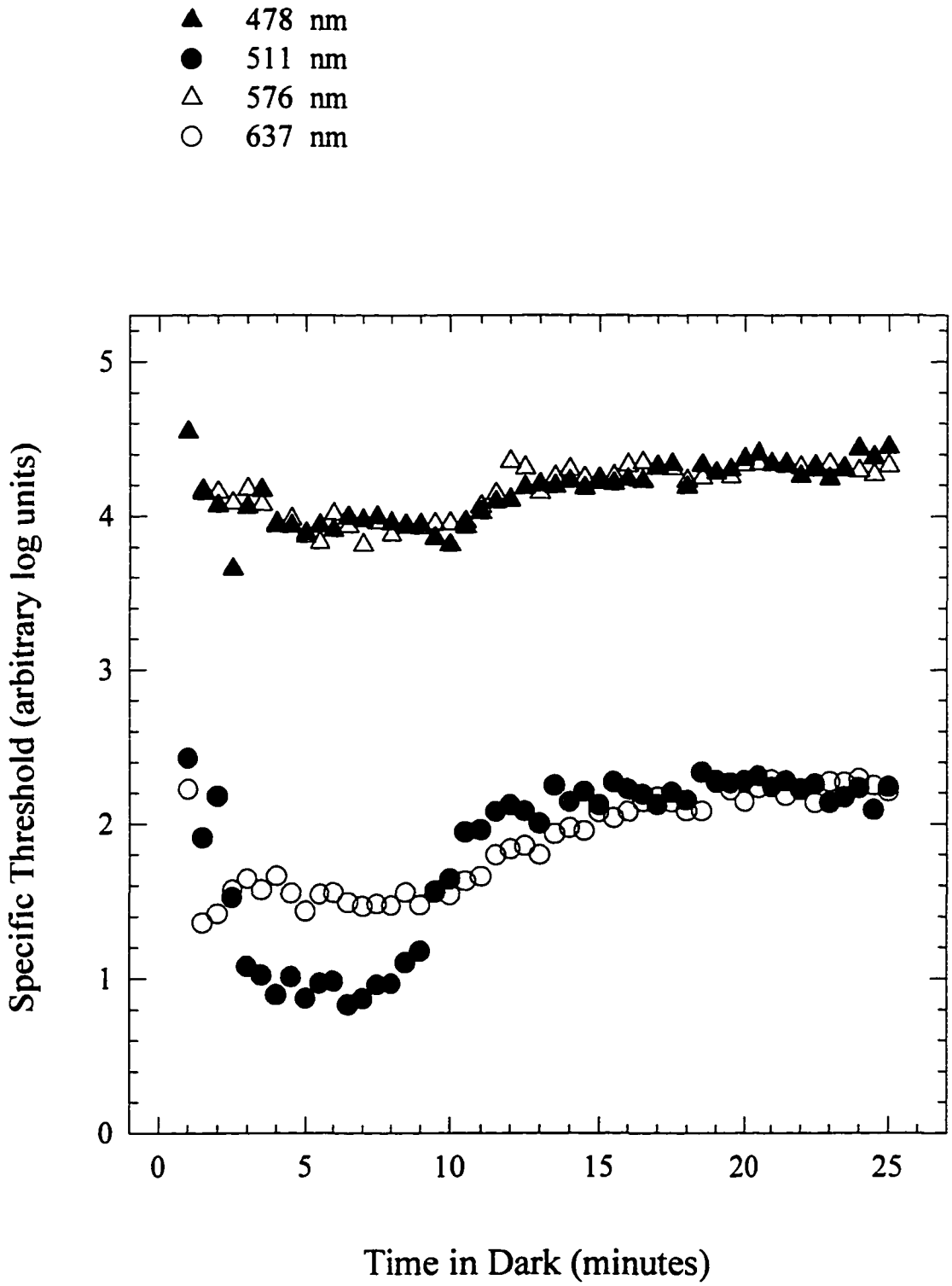

the red (637 nm) data describe a time course quite similar to the blue/yellow function, the increase in specific threshold is considerably larger, about 0.8 log units. For green (511 nm) stimuli, the magnitude of the specific threshold increase is larger still (1.3 log units) and follows a considerably faster time course.

Results from comparable experiments with two other observers are shown in Figures 8 and 9. The results from observer RM shown in Figure 8 are very similar to those described above for EL. Results from AD, shown in Figure 9, are less similar to EL in that the blue and yellow functions differ somewhat from each other; also, although the magnitude of the green and red functions are almost identical, they differ strikingly in time course. Nevertheless, in spite of some interobserver variability, the results from all three observers in Figures 7 to 9 are consistent in showing that the rod adaptation influence on specific threshold is similar in magnitude for blue and yellow and that the influence on red and green is greater than the influence on blue and yellow. Although not plotted here, similar conclusions were obtained from analyzing the results of equivalent experiments following a binocular bleach of photopigment.

While I was collecting the data illustrated in Figures 7 to 9, Vollaro, Lembessis, McMullen, and Frumkes (1997) performed a comparable monocular study in our laboratory

Figure 8. Specific (hue identification) thresholds for observer RM for all four stimulus wavelengths as a function of time in the dark following monocular preadaptation. The test stimulus was a 3^{o} circle presented for 100 ms every 3 s at 6^{o} in the right eye temporal field.

Figure 8. Specific (Hue Identification) Thresholds
RM Monocular

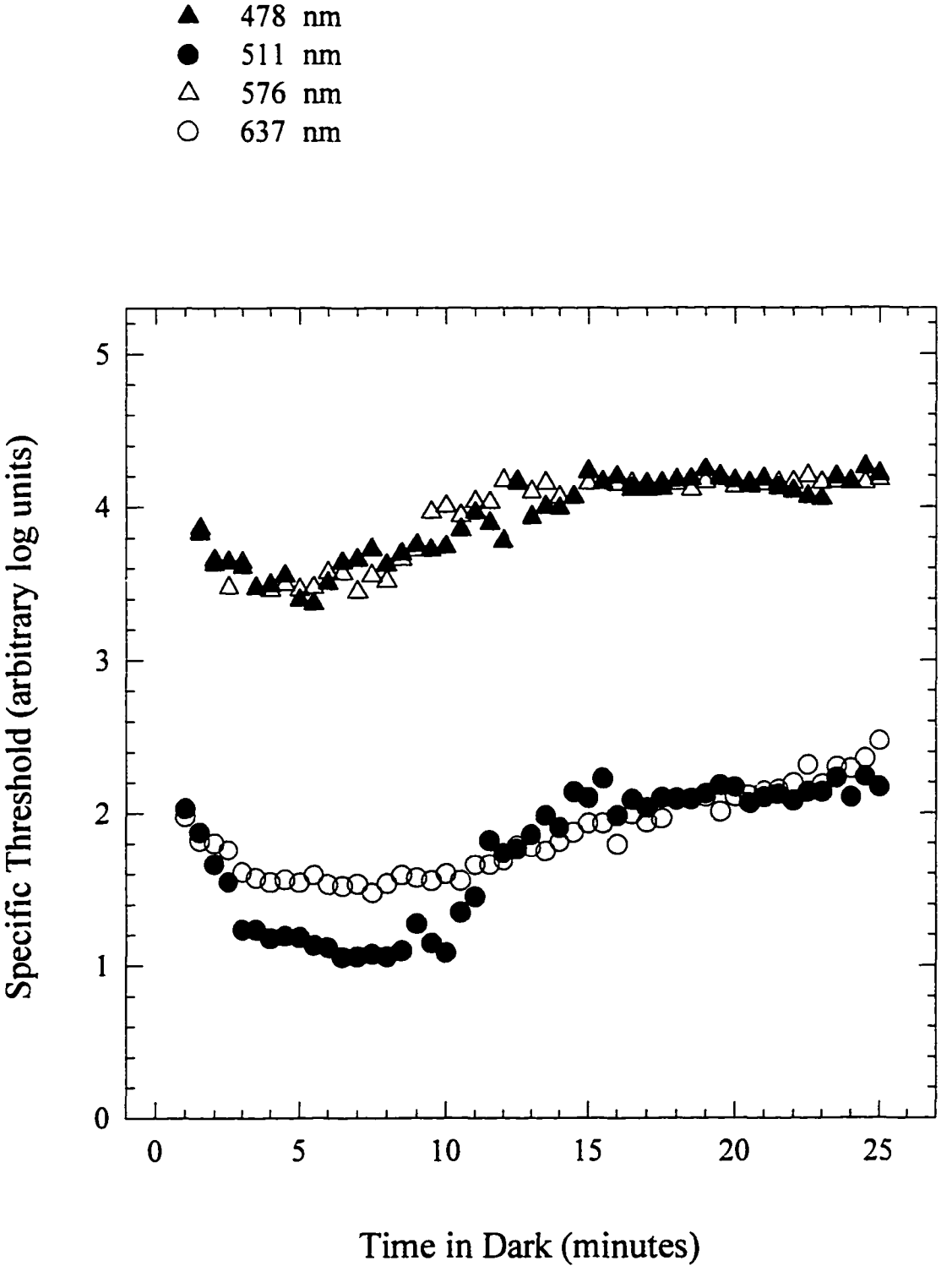

Figure 9. Specific (hue identification) thresholds for observer AD for all four stimulus wavelengths as a function of time in the dark following monocular preadaptation. The test stimulus was a 3^{o} circle presented for 100 ms every 3 s at 6^{o} in the right eye temporal field.

Figure 9. Specific (Hue Identification) Thresholds
AD Monocular

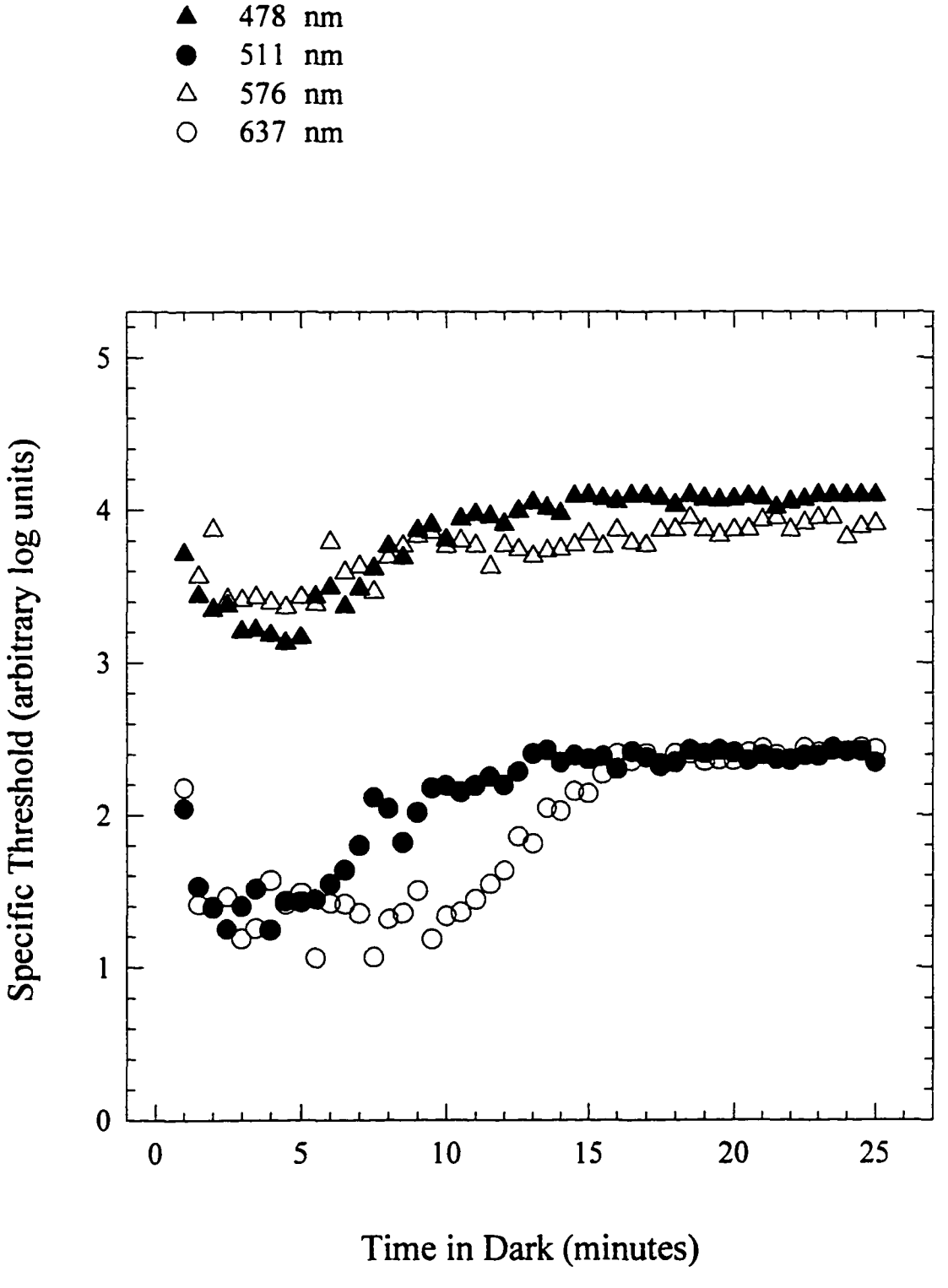

with the same apparatus using a light adaptation procedure. That is, they examined specific threshold as a function of the luminance of a continually exposed background field of 500 nm. Results from two of their observers are shown in Figures 10 and 11. For both of their observers, increasing background field illuminance up to about 1 scotopic td., the approximate threshold illuminance for directly influencing cones, decreased specific threshold. Also notice that the changes in specific threshold seem to adhere to a blue/yellow and to a green/red function; the magnitude of the green/red effect is much larger. Collectively then, the results in Figures 7 to 11 for all five observers show that rod adaptation has similar influences upon the detection of blue and yellow hues and greater influences upon green and red hues.

Most previous reports of the Lie effect were explained by the luminosity/saturation model outlined in the Introduction. In brief, this hypothesis assumes that light-evoked rod signals sum selectively with the cone luminosity signal, and that rod light adaptation reduces and rod dark adaptation enhances the magnitude of this light-evoked rod signal. Such a version of the luminosity/saturation model can explain why selective rod dark adaptation should desaturate, and selective rod light adaptation should increase saturation of any given wavelength test stimulus. However, it is incapable of

Figure 10. Specific thresholds for observer JV for 460 nm, 512 nm, 577 nm, and 632 nm stimuli as a function of the luminance of a continually exposed 500 nm background field. (From Vollaro, Lembessis, McMullen, and Frumkes, 1997.)

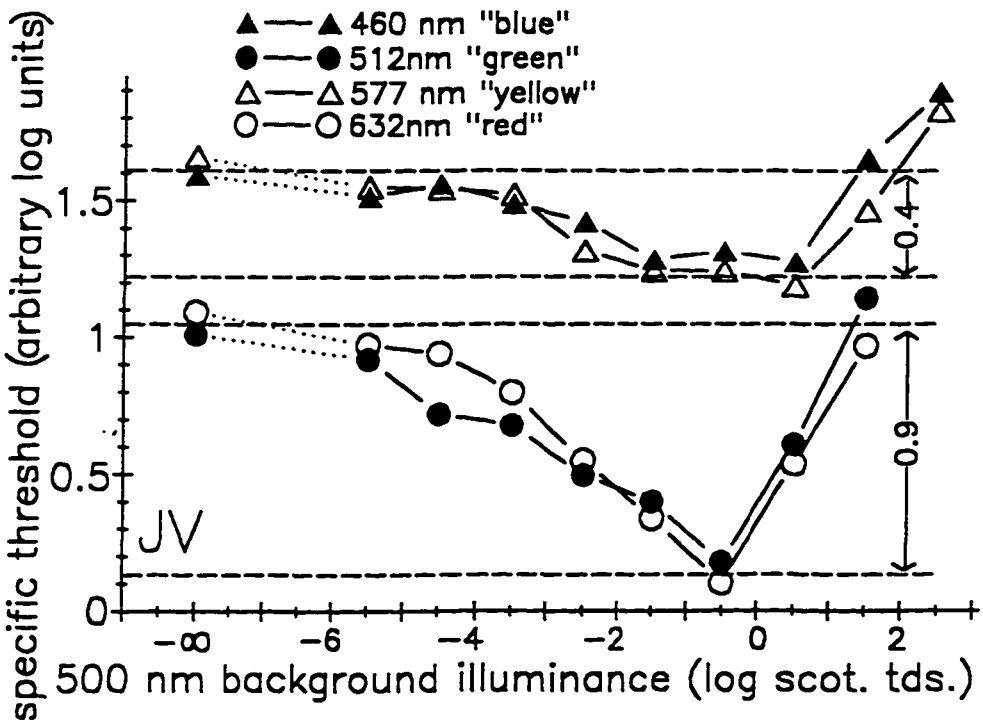

Figure 11. Specific thresholds for observer CM for 460 nm, 512 nm, 577 nm, and 632 nm stimuli as a function of the luminance of a continually exposed 500 nm background field. (From Vollaro, Lembessis, McMullen, and Frumkes, 1997.)

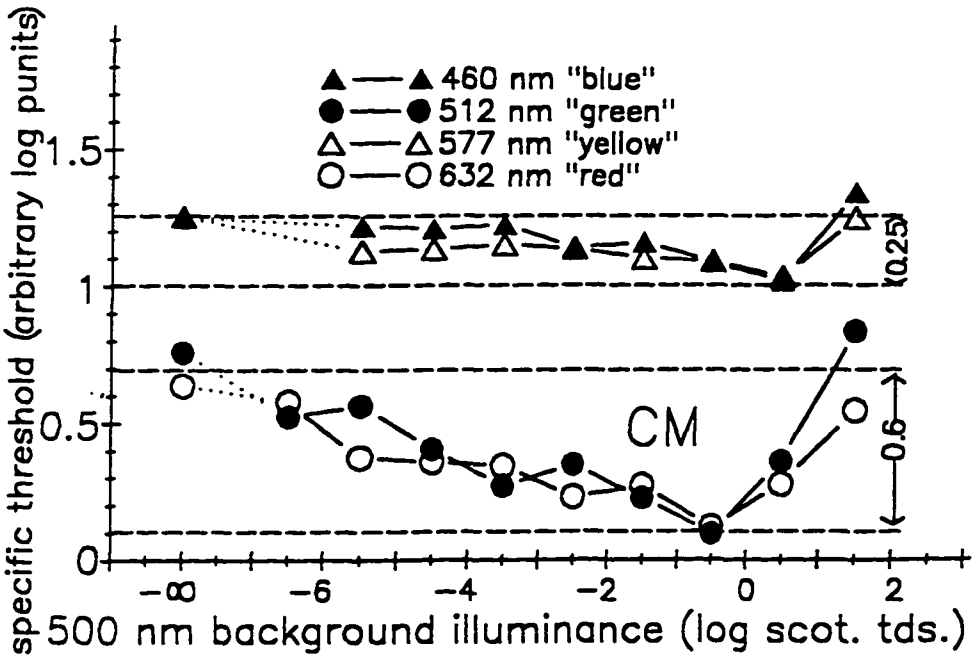

explaining the influence of stimulus wavelength upon the relative magnitude of the Lie effect. In the dark-adapted eye and at illuminance values approximating specific threshold, it is reasonable to assume that the ratio of scotopic to photopic illuminance provides an index monotonically related to the magnitude of the rod signal evoked by a test stimulus when it is at specific threshold luminance. According to the formula provided by Wyszecki and Stiles (1967, p. 226), this ratio is 6.01 (for 478 nm), 1.90 (for 511 nm), 0.17 (for 576 nm), and 0.01 (for 637 nm). For the range of test wavelengths I used in obtaining the data of Figures 7 to 9 (between 478 and 637 nm), this index consistently increases as wavelength decreases. For this reason, the luminosity/saturation model would predict that the shorter the wavelength of the test stimulus, the greater the magnitude of Lie effect. Such a prediction is totally at odds with the observed data, which, in fact, indicate a greater magnitude Lie effect for red-appearing (the longest wavelength) than blue-appearing (the shortest wavelength) stimuli.

Obviously, neither the short-wavelength cone summation model nor the luminosity/saturation model would predict a pairing of blue and yellow versus green and red functional relationships. This pairing suggests the possibility that the influence of rod adaptation upon hue is related instead to an influence upon color-opponent mechanisms. In the

experiments described below, I also examined the validity of the short-wavelength cone summation and luminosity/ saturation models.

Chapter 4

The Influence of Dark Adaptation Upon Saturation

General Observations

Figure 12 shows for observer EL, change in perceived saturation or in percent blueness, greeness, yellowness, or redness of a 511 nm flash as a function of the time following the extinction of a monocular, preadapting bleaching field. All data were obtained according to the "4 + 1" hue and saturation scaling procedure originally proposed by Gordon et al. (1994), as modified by the procedures specified in the Methods section. As plotted, it is easy to see in the lowest set of coordinates that bleaching had a very large influence upon the saturation of the stimulus. Saturation increased for the first few minutes of dark adaptation, decreased slowly from about 2.5 till 10 minutes in the dark, then decreased more rapidly. The upper right graph shows that the apparent greenness of the stimulus decreased from about 10 to 15 minutes in the dark, and the lower right graph shows that the stimulus never appeared at all red in hue. However, other conclusions are difficult to make when the data are examined in this manner. For this reason, I rely quite heavily on various types of derived plots while presenting the results of hue and saturation scaling data in this thesis. A compilation of hue and saturation scaling in a raw format such as Figure 12 is presented in Appendix B as

Figure 12. Hue and saturation scaling for observer EL for a 511 nm stimulus as a function of time in the dark following monocular preadaptation. The test stimulus was a 3^{o} circle presented for 100 ms every 5 s at 6^{o} in the right eye temporal field.

Figure 12. Hue and Saturation Scaling
EL 511 nm Monocular

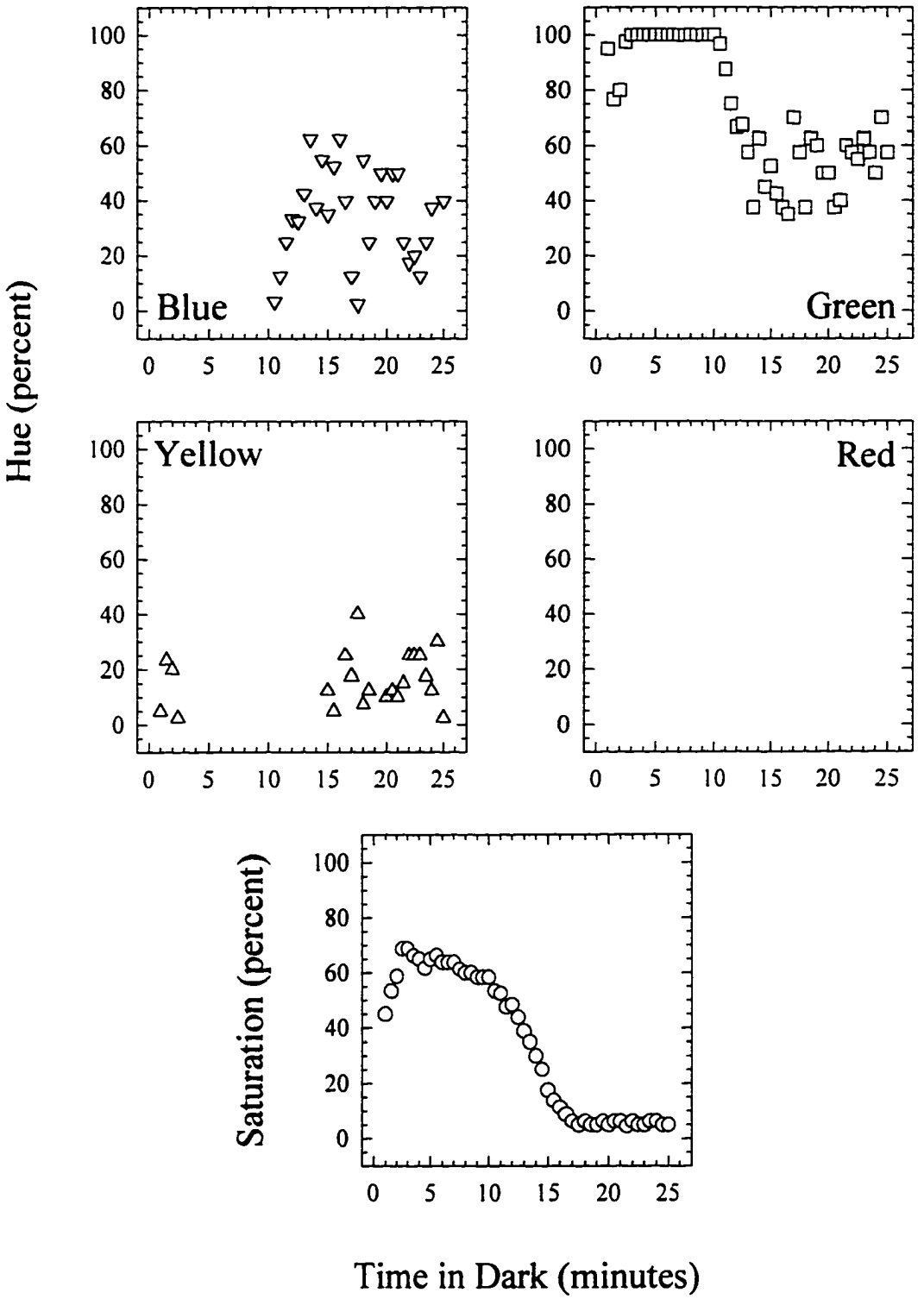

Figures 53 through 88 for all three observers, for all four wavelength test stimuli, and following either monocular, binocular, or interocular bleach of photopigment. The remainder of this chapter concerns the influence of stimulus wavelength upon saturation following a monocular bleach of photopigment. The following chapter concerns changes in hue, while the last chapter is concerned with the influence of the adapted state of the nonviewing eye upon saturation, hue, and specific threshold.

The Relationship Between Detection Threshold and Saturation During Dark Adaptation

For observer EL, Figures 13 and 14 show detection threshold (left functions) and change in saturation (right functions) for the four wavelength stimuli used in this study as a function of the time following the extinction of the monocular bleaching stimulus. As is well established in the classical literature (e.g., Hecht, 1937), the decrease in threshold occurring after the cone plateau stage of adaptation depends quite heavily upon stimulus wavelength. For observer EL and using a plot similar to Figures 13 and 14, I estimated the size of the photochromatic interval by drawing horizontal lines through the rod and cone plateau stages of long-term adaptation. For example, for a 511 nm stimulus, the cone plateau value was -0.3 log tds., the rod plateau value -2.2 log tds. The

Figure 13. Detection thresholds and saturation scaling for observer EL for 478 nm and 511 nm stimuli as a function of time in the dark following monocular preadaptation. The test stimulus was a 3^{o} circle presented for 100 ms every 3 s (detection threshold) or 5 s (saturation scaling) at 6^{o} in the right eye temporal field.

Figure 13. Detection Thresholds
Saturation Scaling
EL Monocular

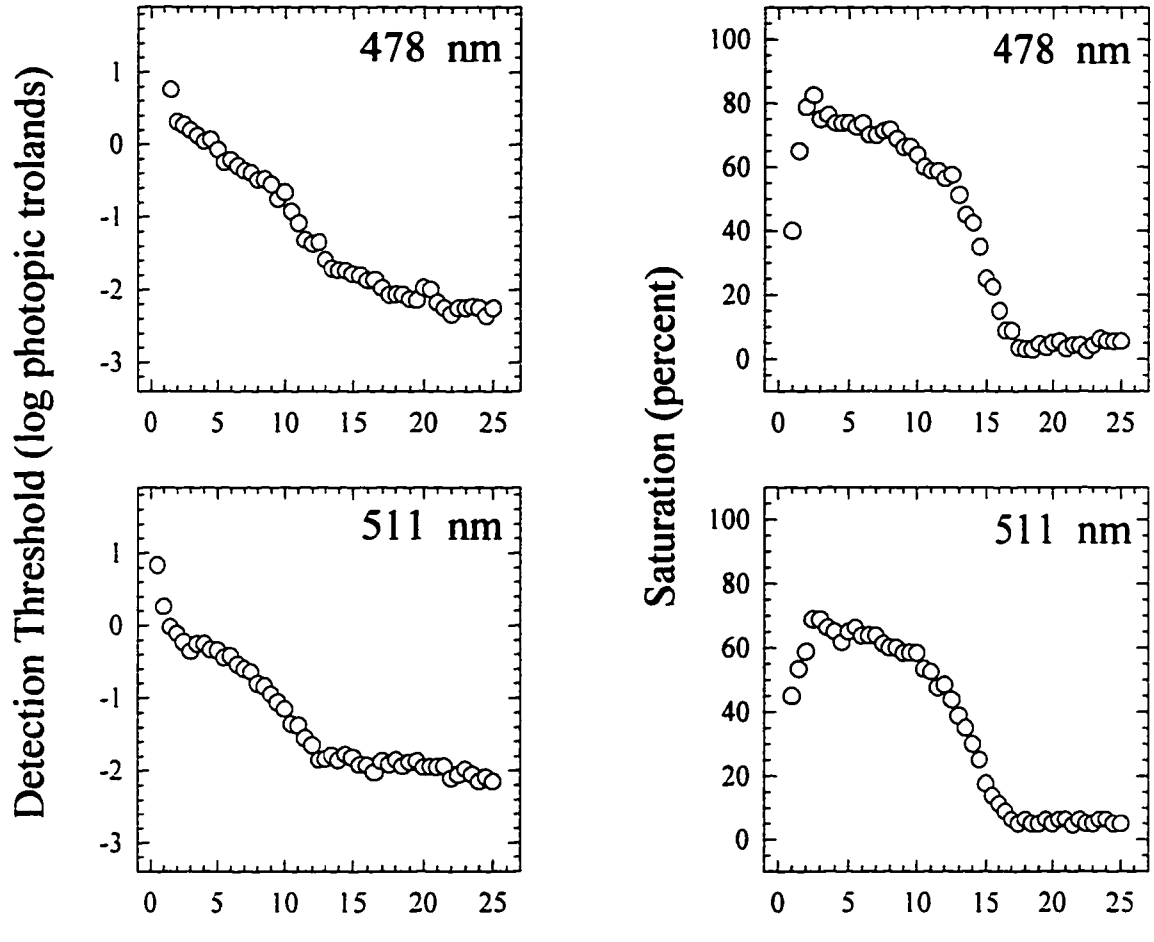

Figure 14. Detection thresholds and saturation scaling for observer EL for 576 nm and 637 nm stimuli as a function of time in the dark following monocular preadaptation. The test stimulus was a 3^{o} circle presented for 100 ms every 3 s (detection threshold) or 5 s (saturation scaling) at 6^{o} in the right eye temporal field.

Figure 14. Detection Thresholds
Saturation Scaling
EL Monocular

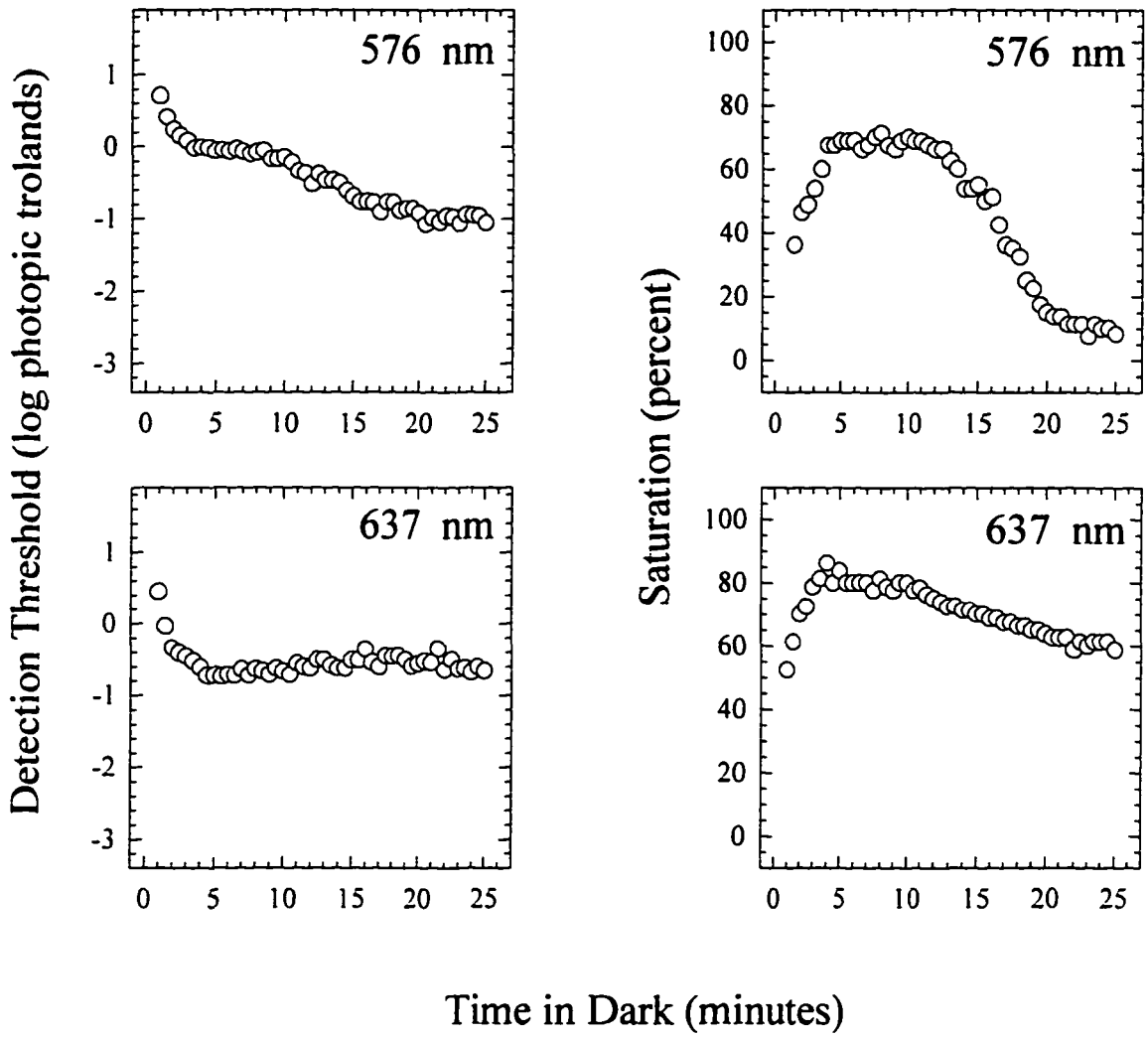

difference between these values serves as an estimate of the size of the photochromatic intervals. For observer EL, the differences were, in $\log_{10}$ units, 2.4 (for 478 nm), 1.9 (for 511 nm), 1.0 (for 576 nm), and 0.0 (for 637 nm). Alternatively, one could consider the scotopic illuminances corresponding to 5 photopic trolands, which are 77 scotopic trolands (for 478 nm), 24 scotopic trolands (for 511 nm), 2 scotopic trolands (for 576 nm), and 0.12 scotopic trolands (for 637 nm). The important consideration here is that the shorter the wavelength of the test flash, the larger the size of the photochromatic interval. Although no similar detection threshold data were obtained from the other two observers who gave saturation estimates, similar detection threshold results were obtained from observer RM (see Appendix A, Figures 45 to 48) and in data reported in the classical literature (e.g., Hecht, 1937). Thus, the photochromatic interval decreases from a maximum value with 478 nm stimuli to a minimum value with 637 nm wavelength stimuli.

In an overall sense, there appears to be a degree of similarity between the change in detection threshold (plotted in log units) and the change in saturation (plotted in linear units) shown in Figures 13 and 14 for observer EL. That is, the change in both measures occurring during the rod recovery stage of adaptation decreases as stimulus wavelength increases. However, there

is no apparent systematic relationship. For example, for observer EL, although saturation of a 637 nm stimulus decreases continually from 10 to 25 minutes in the dark, detection threshold is quite stable during this time period. In contrast, although the change in detection threshold for a 511 nm stimulus during this time period is quite gradual, saturation changes only up until about 17 minutes in the dark. Although not illustrated, a similar lack of correspondence is observed when changes in detection threshold and saturation following a binocular bleach are compared. Thus, although it is likely that these two sets of data relate to each other, I have not been able to specify any exact relationship.

Although no other observer in the present study provided the same two sets of data, the detection threshold data for EL are quite similar to those for RM and to published data, and there appears to be some similarity in the saturation data from the other two observers (see below). For these reasons, the lack of an exact relationship between detection threshold and saturation changes is probably not idiosyncratic to observer EL.

The Influence of Test Stimulus Wavelength Upon Changes in Saturation During Dark Adaptation

For all three observers, Figures 15 to 17 plot saturation scaling values as a function of time in the dark following the extinction of a monocular bleach of

Figure 15. Saturation scaling for observer EL for all four stimuli as a function of time in the dark following monocular preadaptation. The test stimulus was a 3^{o} circle presented for 100 ms every 5 s at 6^{o} in the right eye temporal field.

Figure 15. Saturation Scaling
EL Monocular

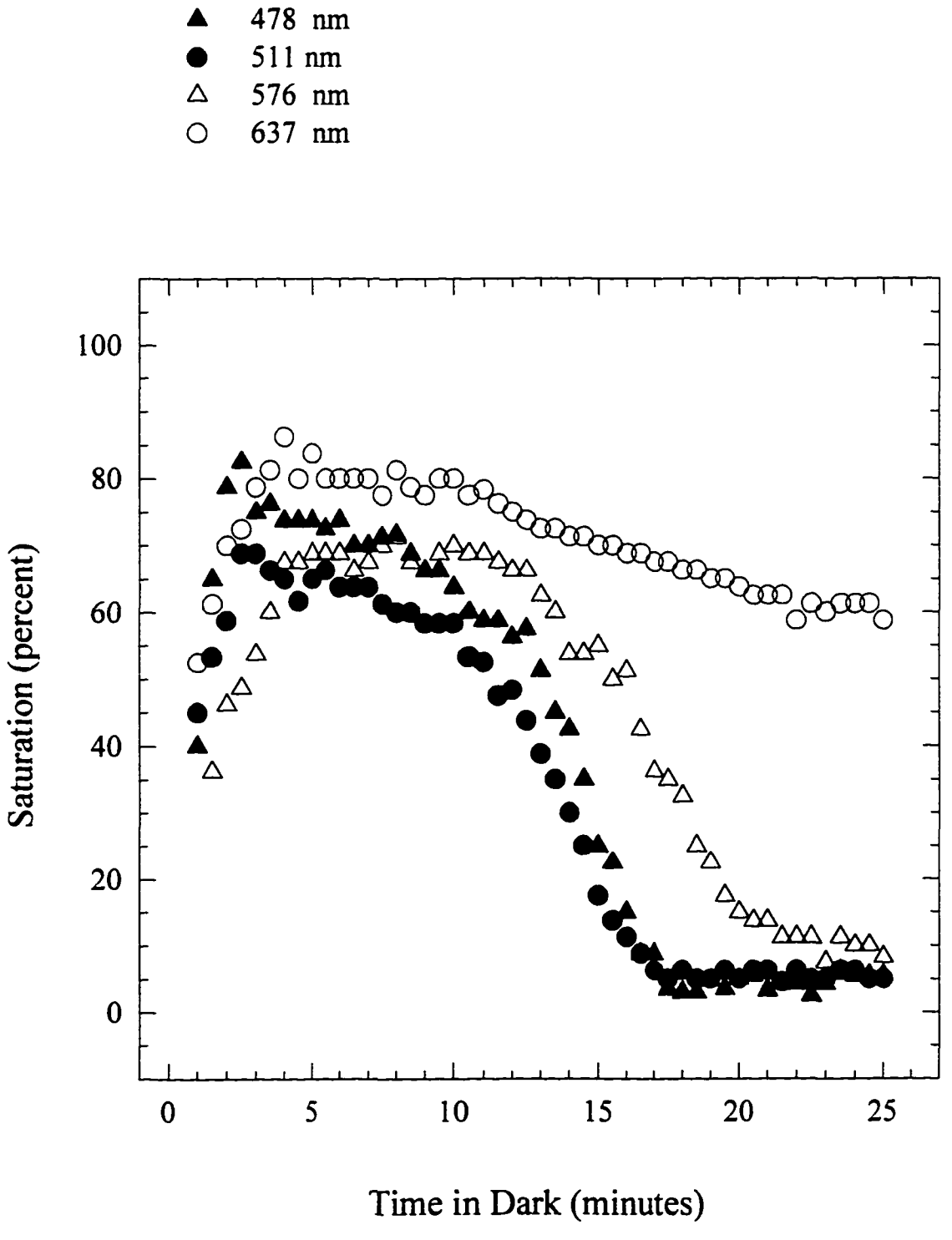

Figure 16. Saturation scaling for observer AD for all four stimuli as a function of time in the dark following monocular preadaptation. The test stimulus was a 3^{o} circle presented for 100 ms every 5 s at 6^{o} in the right eye temporal field.

Figure 16. Saturation Scaling
AD Monocular

▲ 478 nm
● 511 nm
△ 576 nm
○ 637 nm

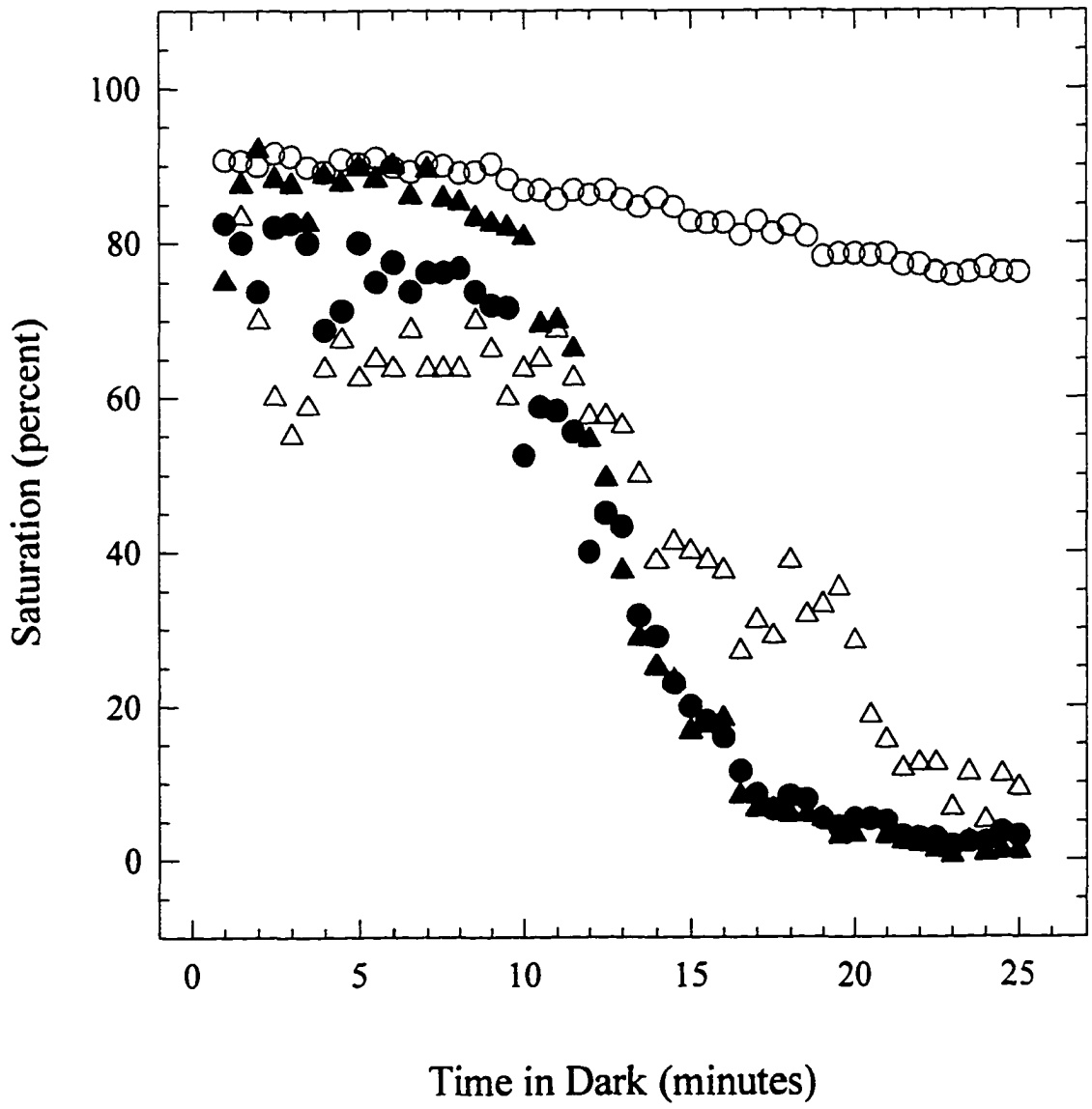

Figure 17. Saturation scaling for observer MT for all four stimuli as a function of time in the dark following monocular preadaptation. The test stimulus was a 3^{o} circle presented for 100 ms every 5 s at 6^{o} in the right eye temporal field.

Figure 17. Saturation Scaling
MT Monocular

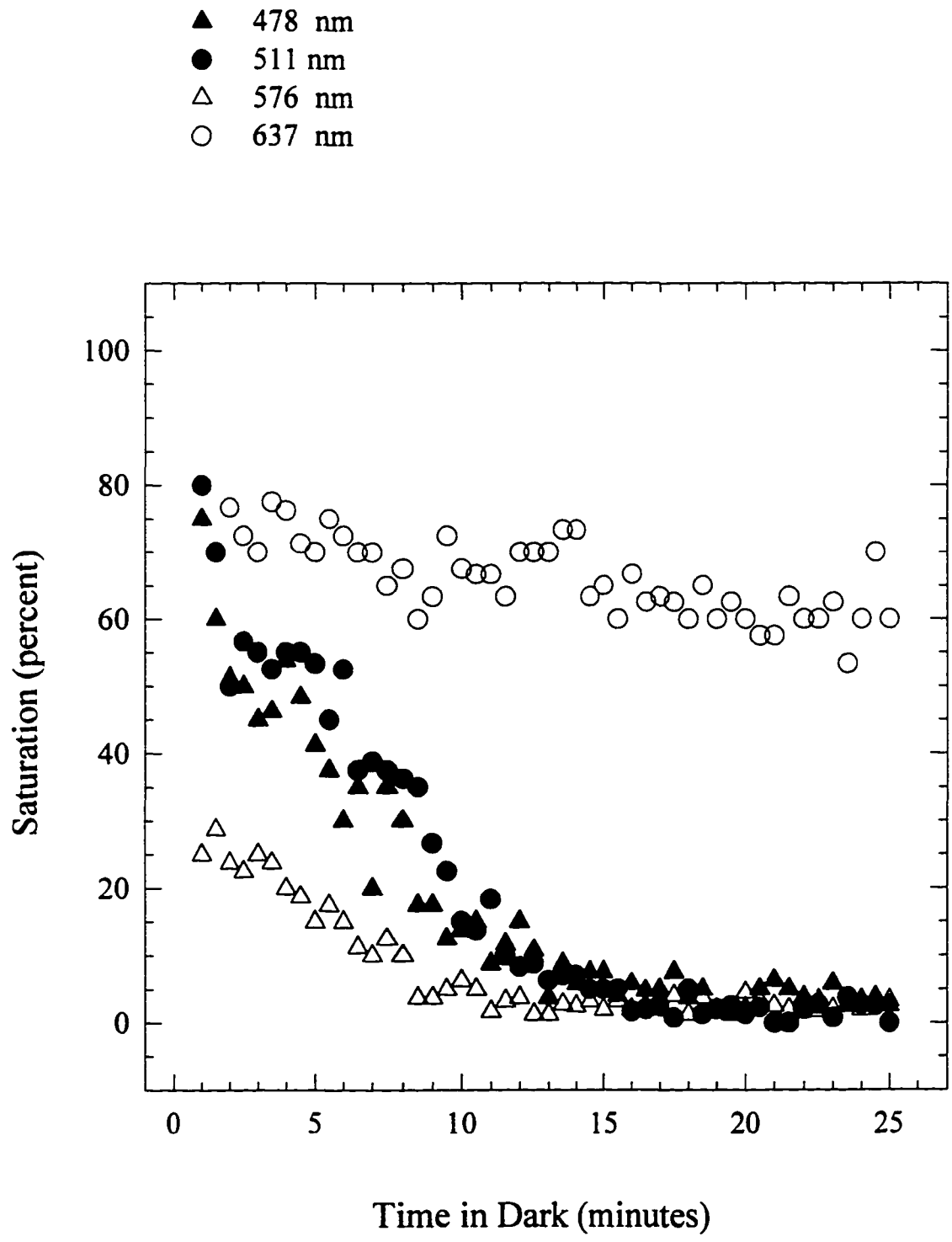

photopigment for all four wavelength test flashes. (Although not illustrated, analagous plots of saturation changes following binocular bleaches of photopigment are quite similar.) Changes in saturation during the first five minutes of adaptation are quite variable. For example, for observer EL, saturation increases for the two longer wavelengths, although for observer MT, it decreases for the two shorter wavelengths. The overall change in saturation during the cone recovery stage of adaptation is quite variable and is not discussed further here.

In contrast to the variability found during the first five minutes, there are important similarities in the saturation data from all three observers after 5 minutes in the dark. First, all observers evaluated the 637 nm stimulus as the most saturated throughout the rod recovery stage of adaptation. Second, and as noted in Figures 13 and 14 above for observer EL, all observers found all four wavelengths to decrease in saturation throughout the rod recovery stage of adaptation. This change in saturation is smallest and slowest for 637 nm stimuli. For observers EL and AD, but not for MT, it is slower for 576 nm stimuli than for shorter wavelengths.

In order to quantify the foregoing saturation data, I drew horizontal lines through the saturation data obtained during the cone plateau stages of adaptation and the rod plateau stages of adaptation (see Figure 18, which is

Figure 18. Saturation scaling for observer AD for all four stimuli as a function of time in the dark following monocular preadaptation. The test stimulus was a 3^{o} circle presented for 100 ms every 5 s at 6^{o} in the right eye temporal field.

This is Figure 16 replotted as follows: For each of the four stimuli, horizontal lines have been drawn through the cone and rod plateau stages of dark adaptation.

Figure 18. Saturation Scaling
AD Monocular

▲ 478 nm
● 511 nm
△ 576 nm
○ 637 nm

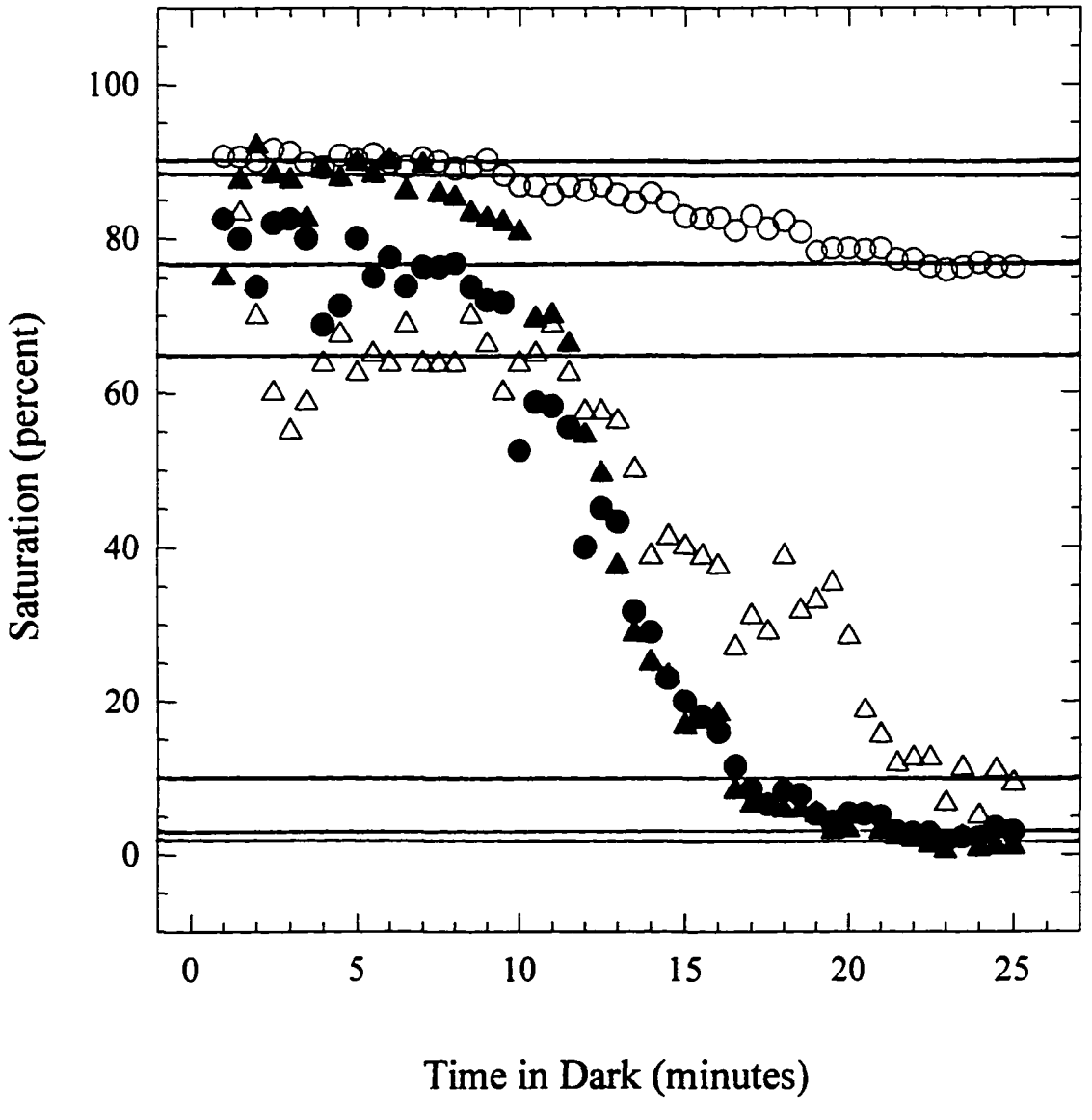

Table 1

Change in Stimulus Saturation Following Monocular Bleaching

Observer	Wavelength	Cone Plateau (% saturation)	20-25 minutes (% saturation)	Change
EL	478 nm	70	5	65
	511	64	5	59
	576	67	10	57
	637	80	60	20
AD	478 nm	88	2	86
	511	77	3	74
	576	65	10	55
	637	90	77	13
MT	478 nm	59	2	57
	511	55	2	53
	576	21	2	19
	637	73	60	13

Figure 16 replotted as described). These results are summarized numerically in Table 1 for all three observers. Change in saturation is greatest for the shortest wavelength stimulus (478 nm) and decreases monotonically to a much smaller value for the shortest wavelength (637 nm).

In interpreting the results in Figures 15 to 17 and Table 1, I assume that regardless of the mechanism by which rods influence color perception, the size of any light-evoked rod signal in the totally dark-adapted eye increases in magnitude with the size of the photochromatic interval. Based upon my analysis of Figures 13 and 14 and similar data from RM, it follows that the magnitude of the rod signal evoked by a 5 photopic td. test stimulus decreases as stimulus wavelength increases. Based on this assumption, the data in Figures 15 to 17 and Table 1 have two important implications. First, for different wavelength test flashes, the change in saturation resulting from rod dark adaptation is likely to be related to the size of the light-evoked rod signal. For this reason, these data are apparently compatible with the luminosity/saturation model summarized in the Introduction section. Because of individual differences and the inability to quantitatively predict the time course of saturation changes, this support is limited. I cannot discern any relationship between the short-wavelength cone summation or cSRCI models and these same data.

Second, there is little obvious relationship between the changes in saturation observed in Figures 15 to 17 and the changes in specific threshold reported in the previous chapter. The changes in specific threshold during dark adaptation were greatest for the 511 nm and 637 nm stimuli and least for the 478 nm and 576 nm stimuli. In contrast, Figures 15 to 17 suggest a monotonic relationship between wavelength and saturation. For this reason, it seems unlikely that specific threshold depends too heavily on saturation and seems more likely to relate to stimulus hue.

In summary, the results reported in this chapter lead to two conclusions. First, it seems that as posited by the luminosity/saturation model, light-evoked rod signals are likely to affect luminosity, presumably by summing their input with the luminosity cone signal. Second, there is little apparent relationship between this influence upon luminosity and change in specific threshold. For this reason, it seems likely that rods might contribute to color vision by means of two different mechanisms.

Chapter 5

The Influence of Dark Adaptation Upon Hue

General Observations

Figure 19 shows for observer EL the changes in perceived saturation and in percent blueness, greeness, yellowness, or redness of a 511 nm stimulus as a function of the time following the extinction of a monocular, preadapting bleaching field. These data were also presented as Figure 12 in Chapter 4 above and were obtained according to the "4 + 1" hue and saturation scaling procedure originally proposed by Gordon et al. (1994), as modified by the procedures specified in the Methods section. The upper right graph shows that the apparent greenness of the stimulus decreased from about 10 to 15 minutes in the dark, and the lower right graph shows that the stimulus never appeared at all red in hue. A compilation of hue and saturation scaling in a raw format such as Figure 19 is presented in Appendix B as Figures 53 through 88 for all three observers, for all four wavelength test stimuli, and following either monocular, binocular, or interocular bleach of photopigment.

Figure 20 shows for all three observers the changes in percent redness and yellowness of a 637 nm stimulus following the extinction of a monocular preadaptation bleach of photopigment. Of all the four wavelength stimuli, the data for the 637 nm stimulus are the most

Figure 19. Hue and saturation scaling for observer EL for a 511 nm stimulus as a function of time in the dark following monocular preadaptation. The test stimulus was a 3^{o} circle presented for 100 ms every 5 s at 6^{o} in the right eye temporal field.

Figure 19. Hue and Saturation Scaling
EL 511 nm Monocular

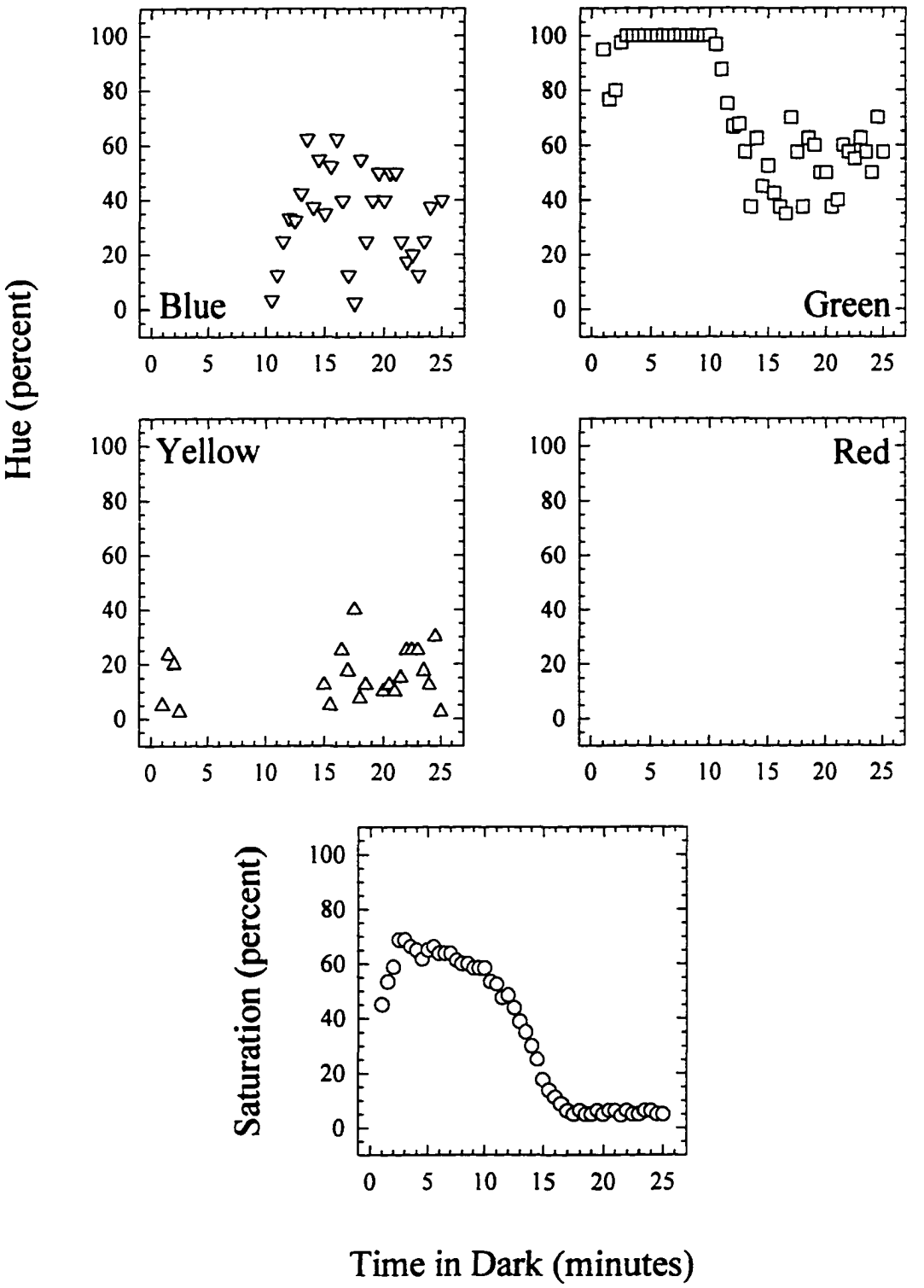

Figure 20. Hue scaling for observers AD, EL, and MT for a 637 nm stimulus as a function of time in the dark following monocular preadaptation. The test stimulus was a 3^{o} circle presented for 100 ms every 5 s at 6^{o} in the right eye temporal field.

Figure 20. Hue Scaling
637 nm Monocular

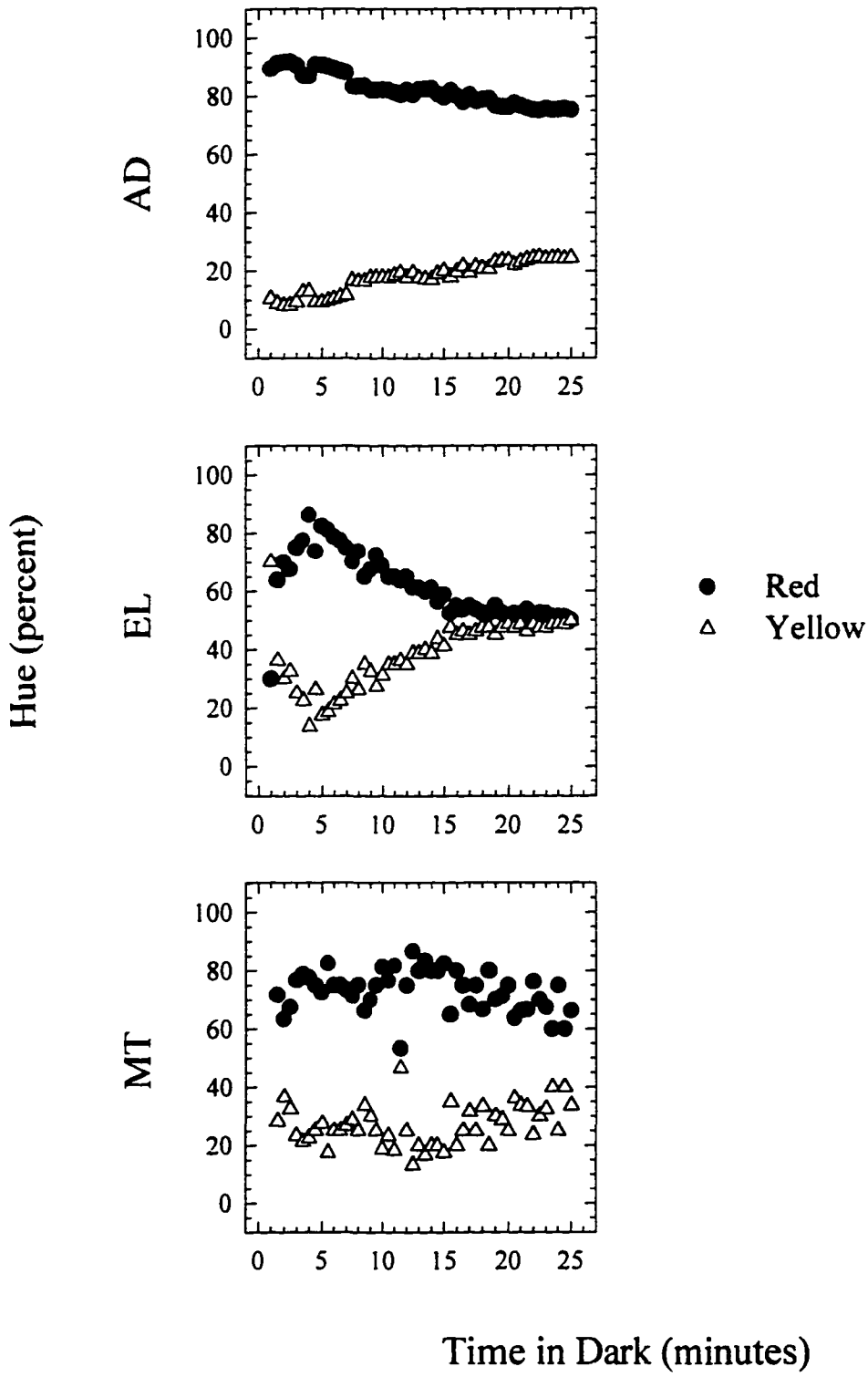

consistent and involve the most dramatic shift in hue. First, this stimulus always appears more red than any other hue, but even at 1 minute in the dark, appears somewhat yellow. More importantly, after about 5 minutes in the dark, this stimulus becomes progressively less red and progressively more yellow. In fact, when totally dark adapted, observer EL assigned almost equal values to red and yellow hues.

To summarize EL's data in Figure 20, rod dark adaptation apparently causes a photopically red-hued stimulus to become more of a yellow/red mix (orange). Although not as dramatic as EL's data, the data from the other two observers show the same trend toward less redness and more yellowness.

Results for the other wavelength stimuli are more variable across observers. For example, Figures 21 and 22 show for observers EL and AD, respectively, the changes in perceived saturation and in percent blueness, greeness, and yellowness of a 511 nm stimulus following the extinction of a monocular preadaptation bleach of photopigment. Following a small initial increase to 100% greeness by 2.5 minutes, EL's reports of greeness remain at 100% until 10 minutes in the dark, when they start to decrease to half that. This lowered greeness was accompanied by a shift toward more blueness or yellowness. For AD, an opposite trend is seen. His reports of greeness do not reach 100%

Figure 21. Hue and saturation scaling for observer EL for a 511 nm stimulus as a function of time in the dark following monocular preadaptation. The test stimulus was a 3^{o} circle presented for 100 ms every 5 s at 6^{o} in the right eye temporal field.

Figure 21. Hue and Saturation Scaling
EL 511 nm Monocular

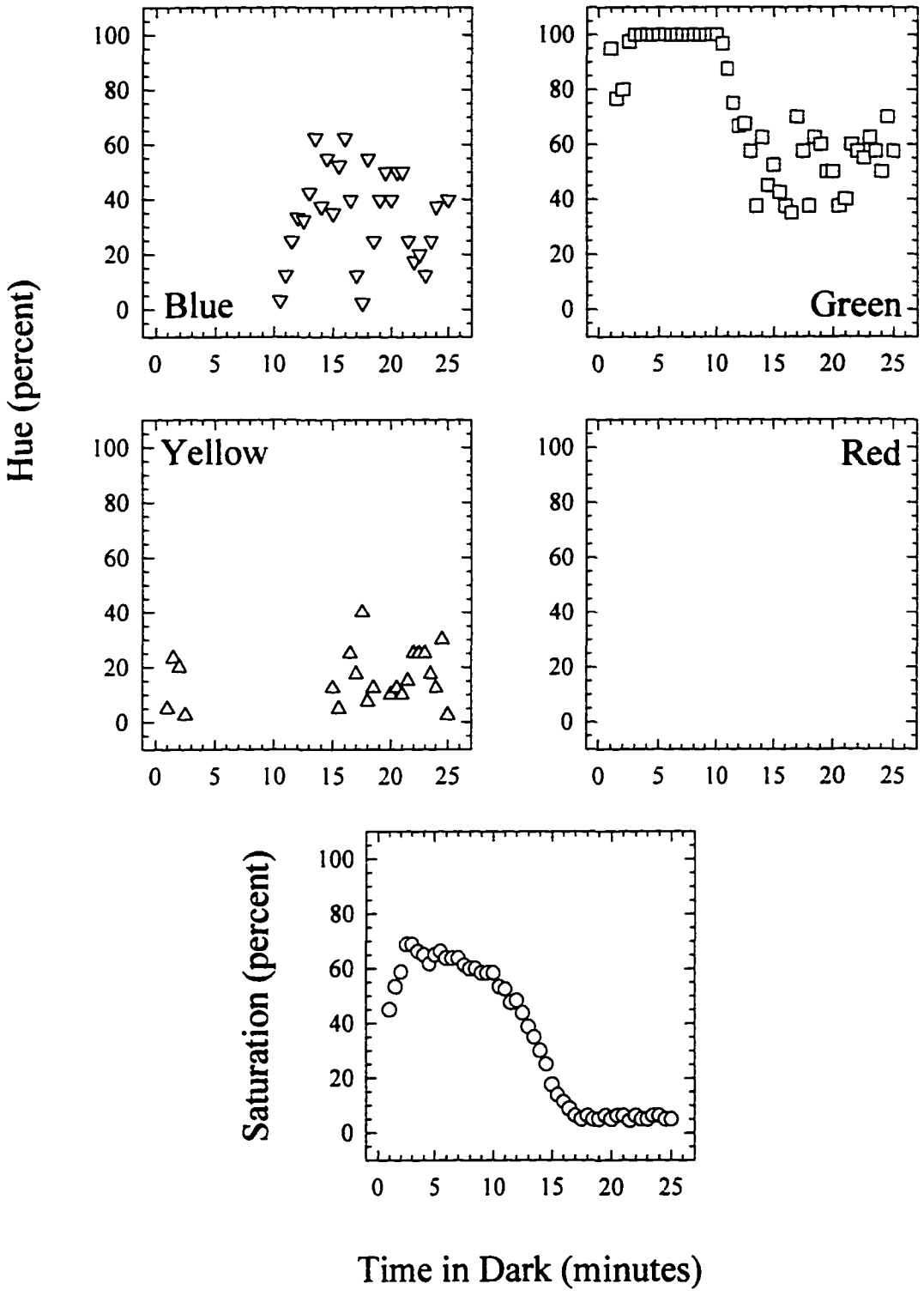

Figure 22. Hue and saturation scaling for observer AD for a 511 nm stimulus as a function of time in the dark following monocular preadaptation. The test stimulus was a 3^{o} circle presented for 100 ms every 5 s at 6^{o} in the right eye temporal field.

Figure 22. Hue and Saturation Scaling
AD 511 nm Monocular

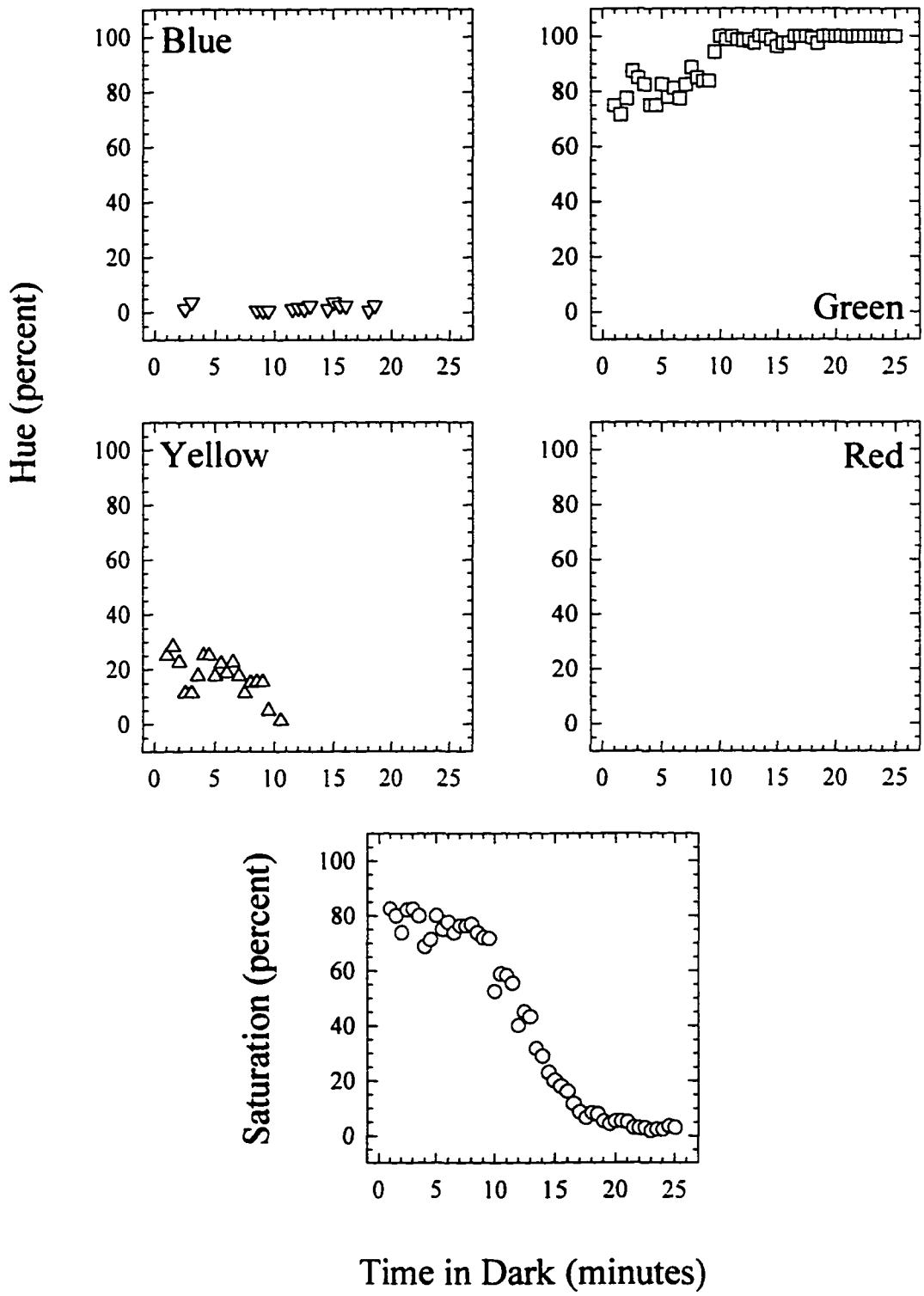

until 10 minutes in the dark. Unlike EL, AD shows no real change in perceived greeness for the remainder of the dark adaptation session. A small but consistent report of yellowness in the first few minutes disappears after 11 minutes in the dark, and a very small report of blueness is no longer made after 19 minutes in the dark. In summary, for EL, a green-appearing stimulus becomes less green and more blue or yellow, whereas for AD, a yellowish-green-appearing stimulus becomes more green and less yellow.

Two aspects of these results should be noted. First, the data points in this and other hue and saturation scaling figures represent means of several sessions. During an experimental session, three hues would not usually be reported together for one stimulus presentation. That is, a single hue would be reported, or the hues would be reported in pairs of green and yellow or green and blue, for example. On a few occasions, three hues would be reported together, something not predicted by opponent-process theories. In these situations, the stimulus would appear mottled, would look as though lines of different hues were running through it, or would have separate hue sections. In this way, blue and yellow could be seen together in one stimulus presentation. Second, in the last 8 minutes of the dark adaptation sessions presented in Figure 19, EL evaluated the stimulus as being extremely unsaturated. That evaluation must be kept in mind when

examining the hue data for the same time period. That is, EL was perceiving only hints of hue that were predominantly green. Even though reports of green above 60% appear at about 12 and 23 minutes, the stimulus looked very different at those times, not only because yellow hadn't reappeared by 12 minutes.

Table 2 summarizes the results presented in Figures 53 to 88 in Appendix B. Because no baseline hue scaling was done before preadaptation, Table 2 compares the reported hues at the cone and rod plateaus. There is a marked variability in the observers' reports of changes in hue. The most consistent changes were seen with the 637 nm stimulus. Its appearance changed from a yellowish red to one that was less red and more yellow. The changes for the blue-appearing 478 nm stimulus were less consistent, with EL reporting a shift toward green or yellow, whereas AD and MT reported a shift toward only green. The changes reported for the 511 and 576 nm stimuli were quite variable.

Three different models were suggested in the Introduction to account for the influence of rods on color vision. In interpreting these data in terms of those three hypotheses, I assume that rod dark adaptation would increase the size of any rod signal, whether evoked by test stimulus presentation or whether due to a tonic influence from unstimulated rods. The only finding that is

Table 2

Description of Change in Hue Induced by Rod Adaptation

Obs	Wavlgth	Changes in Stimulus Appearance
EL	478 nm	blue becomes less blue, more green or yellow
	511	green becomes less green, more blue or yellow
	576	yellow becomes less yellow, more green
	637	yellowish-red becomes equally yellow and red
AD	478	blue becomes less blue, more green
	511	yellowish-green becomes less yellow, more green
	576	reddish-yellow becomes less red, more yellow
	637	yellowish-red becomes less red, more yellow.
MT	478	blue becomes less blue, more green
	511	yellowish-green stays the same
	576	yellow-green stays the same
	637	yellowish-red becomes slightly less red, slightly more yellow

consistent with a short-wavelength cone summation model is the increased blueness of the 511 nm stimulus for observer EL; none of the other 11 sets of functions show any special relationship between rod adaptation and any aspect of vision easily related to blueness or short wavelength cones. However, many color models posit that both short- and middle-wavelength cones contribute to blueness (Kaiser & Boynton, 1996); therefore, EL's report of increased blueness for a 511 nm stimulus is consistent with both short- and middle-wavelength cone and rod signal summation.

According to the luminosity/saturation model, the change in apparent color with rod dark adaptation is attributable to an increase in the magnitude of the light-evoked rod signal that sums with the cone luminosity signal. Certainly, my analysis of the saturation data in the foregoing chapter of this thesis provides some evidence for this. However, such a model could not predict the adaptation-induced shifts in hue that are evident in the results of all three observers. Thus, some other mechanism must additionally account for adaptation-induced changes in color.

According to the cSRCI model, the rod contribution to color vision is attributable to separate suppressive influences upon the green/red and blue/yellow opponent mechanisms. Based upon my analysis of specific threshold data, there is good reason to believe that the influence is

much greater upon the green/red than blue/yellow mechanism. If this is the case, one would predict that stimuli would appear not only less saturated with dark adaptation, but would also appear reduced in redness and greeness more than in blueness and yellowness. In other words, from a relativistic viewpoint, stimuli should become more blue and more yellow with adaptation. In fact, data obtained for the 637 nm stimulus for all three observers are in accord with this prediction: for all observers, this stimulus becomes less red and more yellow. The data for the other stimuli differed across observers; however, given that the spectral properties of "unique hues" are subject to considerable individual variability (e.g. Kaiser & Boynton, 1996), the obtained differences between observers are not unexpected.

As described above, EL and AD differed in their responses to the 511 nm stimulus. EL reported that the stimulus appeared considerably less green and more blue or yellow during dark adaptation, whereas AD reported that the same stimulus appeared less yellow and more green. Figures 23 and 24 show changes in hue and saturation for EL and AD, respectively, for the 478 nm stimulus following the extinction of a monocular preadaptation bleach of photopigment. Although both observers report that this stimulus appears less blue during dark adaptation, the decrease in blueness and increase in greeness is much more

Figure 23. Hue and saturation scaling for observer EL for a 478 nm stimulus as a function of time in the dark following monocular preadaptation. The test stimulus was a 3^{o} circle presented for 100 ms every 5 s at 6^{o} in the right eye temporal field.

Figure 23. Hue and Saturation Scaling
EL 478 nm Monocular

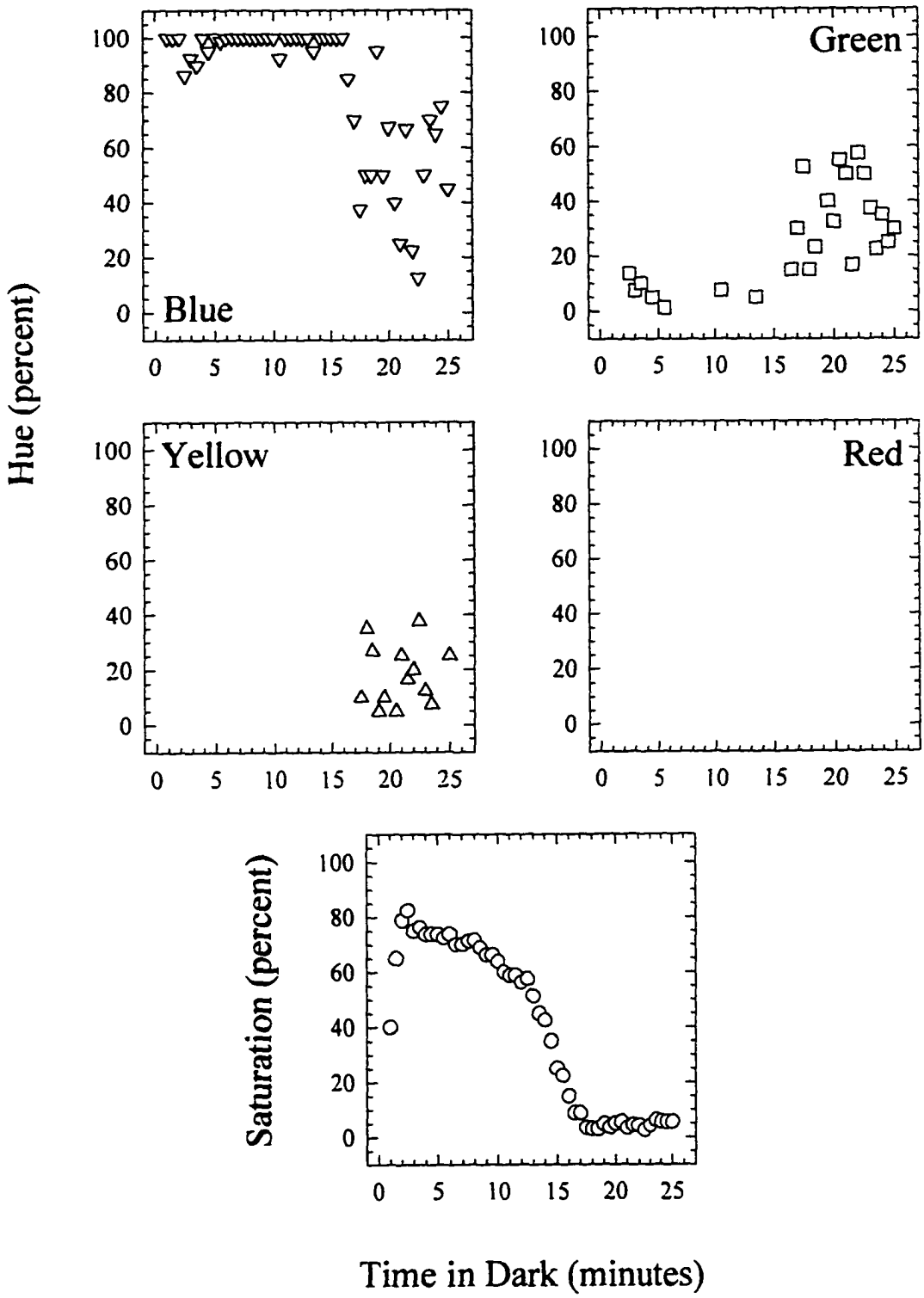

Figure 24. Hue and saturation scaling for observer AD for a 478 nm stimulus as a function of time in the dark following monocular preadaptation. The test stimulus was a 3^{o} circle presented for 100 ms every 5 s at 6^{o} in the right eye temporal field.

Figure 24. Hue and Saturation Scaling
AD 478 nm Monocular

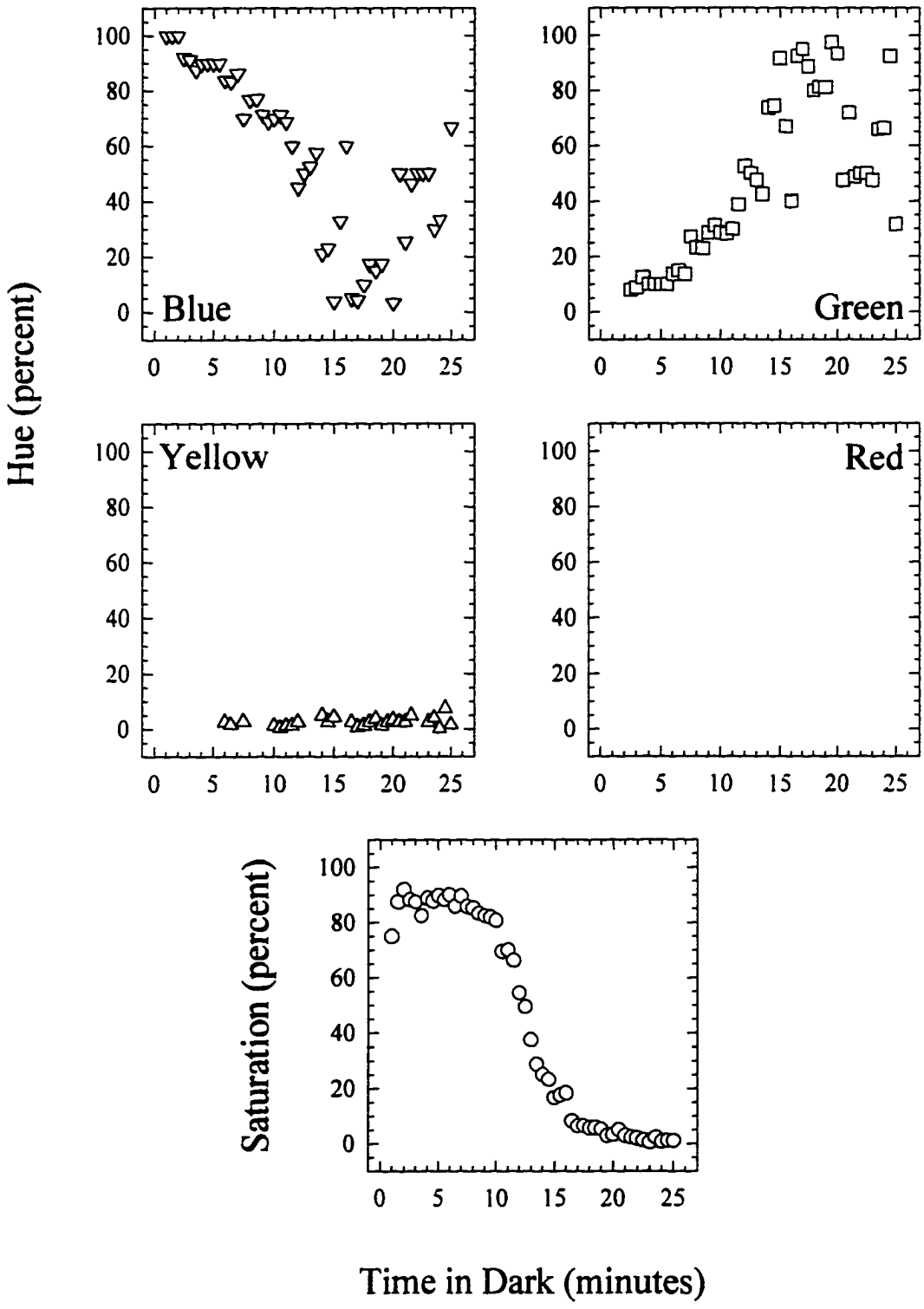

pronounced for AD than for EL. It is also interesting that AD showed a more pronounced Lie effect (see Figure 9) for the 478 and 576 nm stimuli than did EL (see Figure 7). Were it not for AD's report that the 576 nm stimulus became more yellow and less red during dark adaptation, it would appear that for this observer, the blue/yellow opponent mechanism is suppessed more than the green/red opponent mechanism.

In general, the present saturation and hue scaling data lead to the following conclusions. First, rod dark adaptation causes a marked desaturation of all hues examined. It is likely that this adaptation-induced change is at least partially attributable to a summation of the light-evoked rod signal and the cone luminosity signal. Second, rod dark adaptation induces hue shifts such that photopically red-appearing stimuli consistently become more yellow and less red for all observers. This result is consistent with a cSRCI model that suggests that dark-adapted rods predominantly suppress the activity of red/green color opponency.

Chapter 6

The Influence of the Adapted State of the Nonviewing Eye Upon Color Perception

The foregoing three chapters documented the influence of monocular rod dark adaptation upon sensitivity to color. As indicated in the Method section, I also obtained comparable data following binocular and interocular bleach of photopigment. This chapter specifically addresses these results.

Detection (achromatic) Thresholds

Although the major thrust of this thesis involves a consideration of rod influence upon color vision, I did obtain a good deal of detection threshold data as control measures. Figure 25 shows detection thresholds for observer EL following both monocular and binocular bleach of photopigment. It is quite clear that there is no consistent difference between these two sets of data. Although not illustrated, essentially the same conclusion can be drawn from similar data collected from observer RM.

The influence of an interocular bleach of photopigment upon detection threshold is summarized for all three observers in Figures 26 to 28. In these graphs, the ordinate is greatly expanded in comparison with the scale used in Figure 25, and the four sets of functions are shifted with respect to each other to further comparison.

For the first few minutes of nonviewing eye dark

Figure 25. Detection thresholds for observer EL for all four stimuli as a function of time in the dark following monocular and binocular preadaptation. The test stimulus was a 3^{o} circle presented for 100 ms every 3 s at 6^{o} in the right eye temporal field. For the sake of comparison, the threshold functions for the 511 nm stimulus have been shifted on the ordinate.

Figure 25. Detection Thresholds
EL

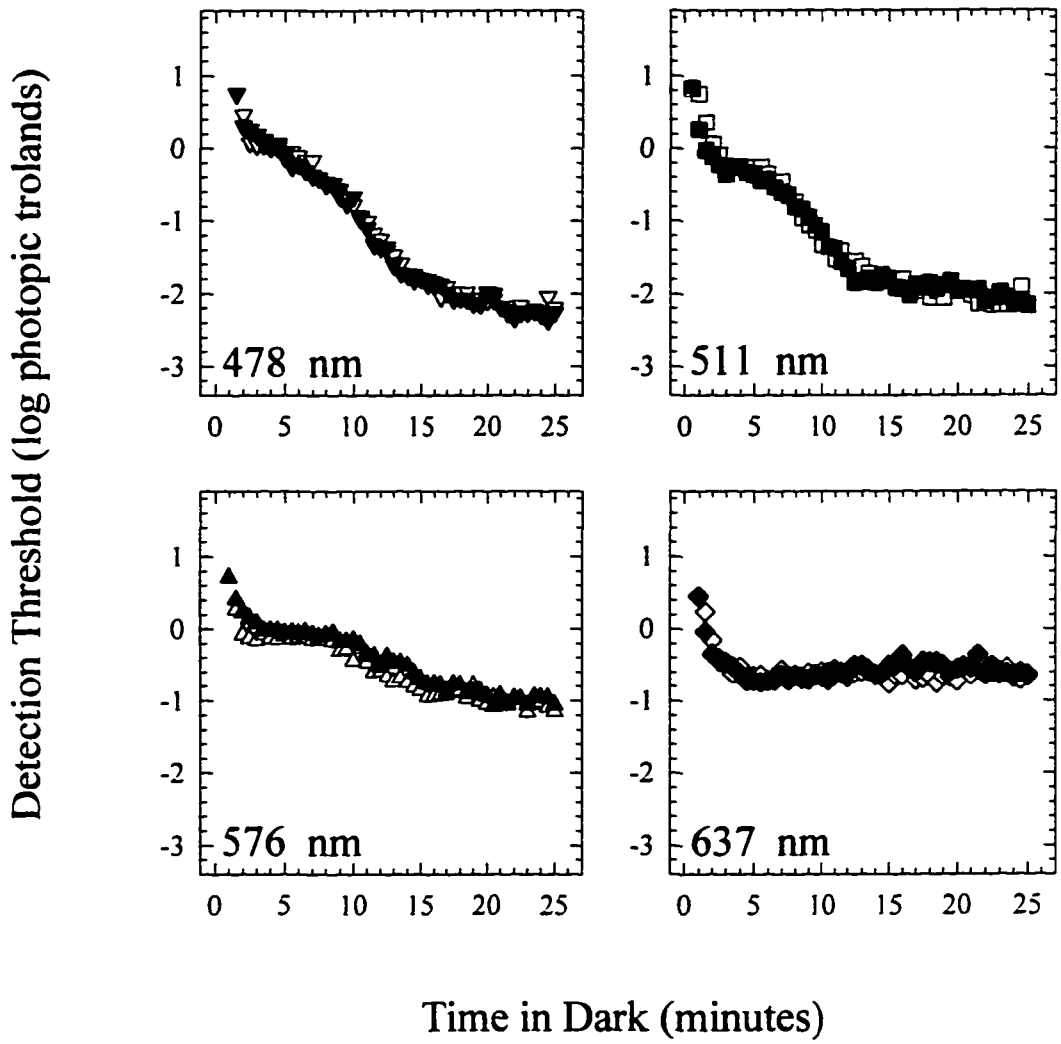

Figure 26. Detection thresholds for observer EL for all four stimuli as a function of time in the dark following interocular preadaptation. The test stimulus was a 3^{o} circle presented for 100 ms every 3 s at 6^{o} in the right eye temporal field.

Figure 26. Detection Thresholds
EL Interocular

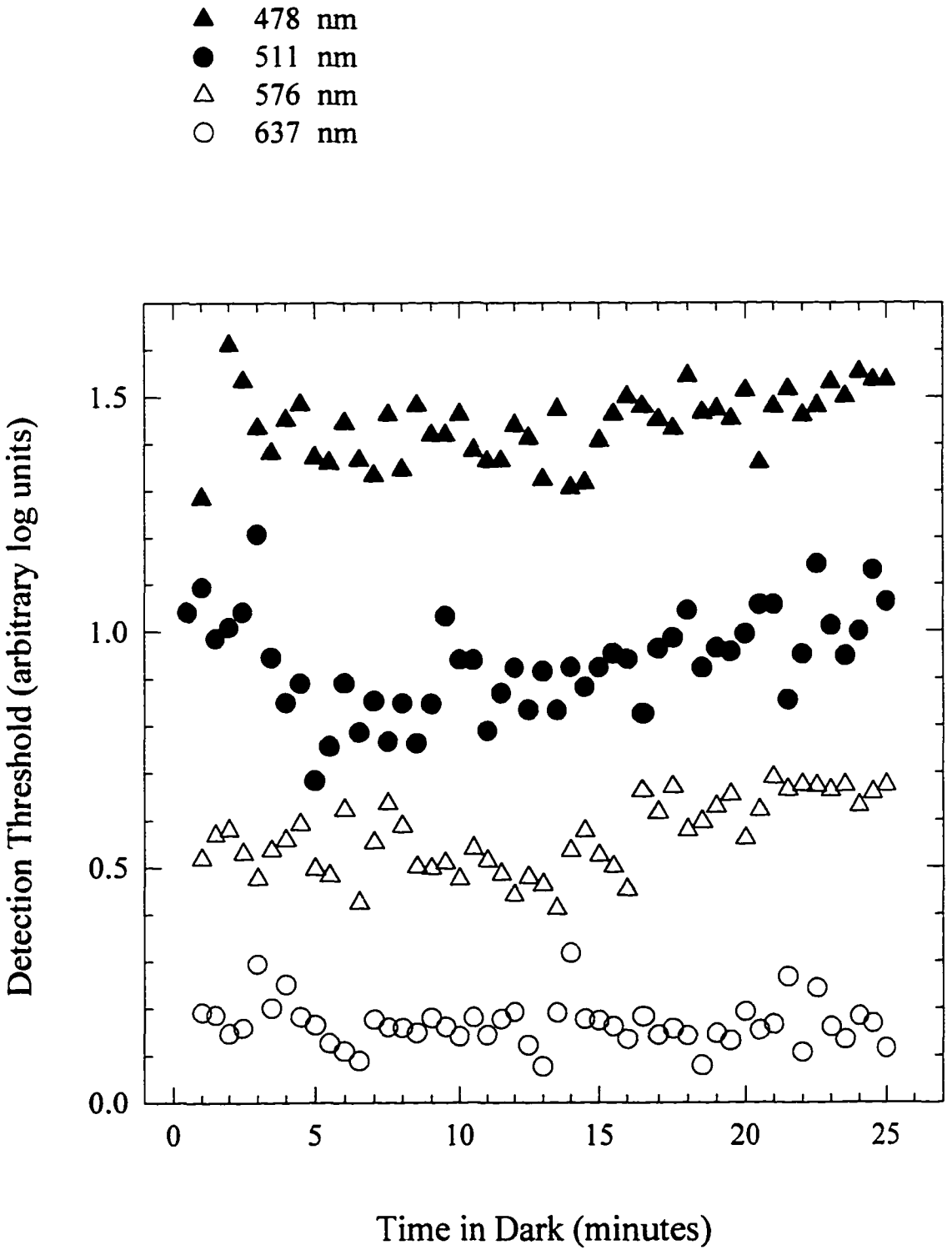

Figure 27. Detection thresholds for observer RM for all four stimuli as a function of time in the dark following interocular preadaptation. The test stimulus was a 3^{o} circle presented for 100 ms every 3 s at 6^{o} in the right eye temporal field.

Figure 27. Detection Thresholds
RM Interocular

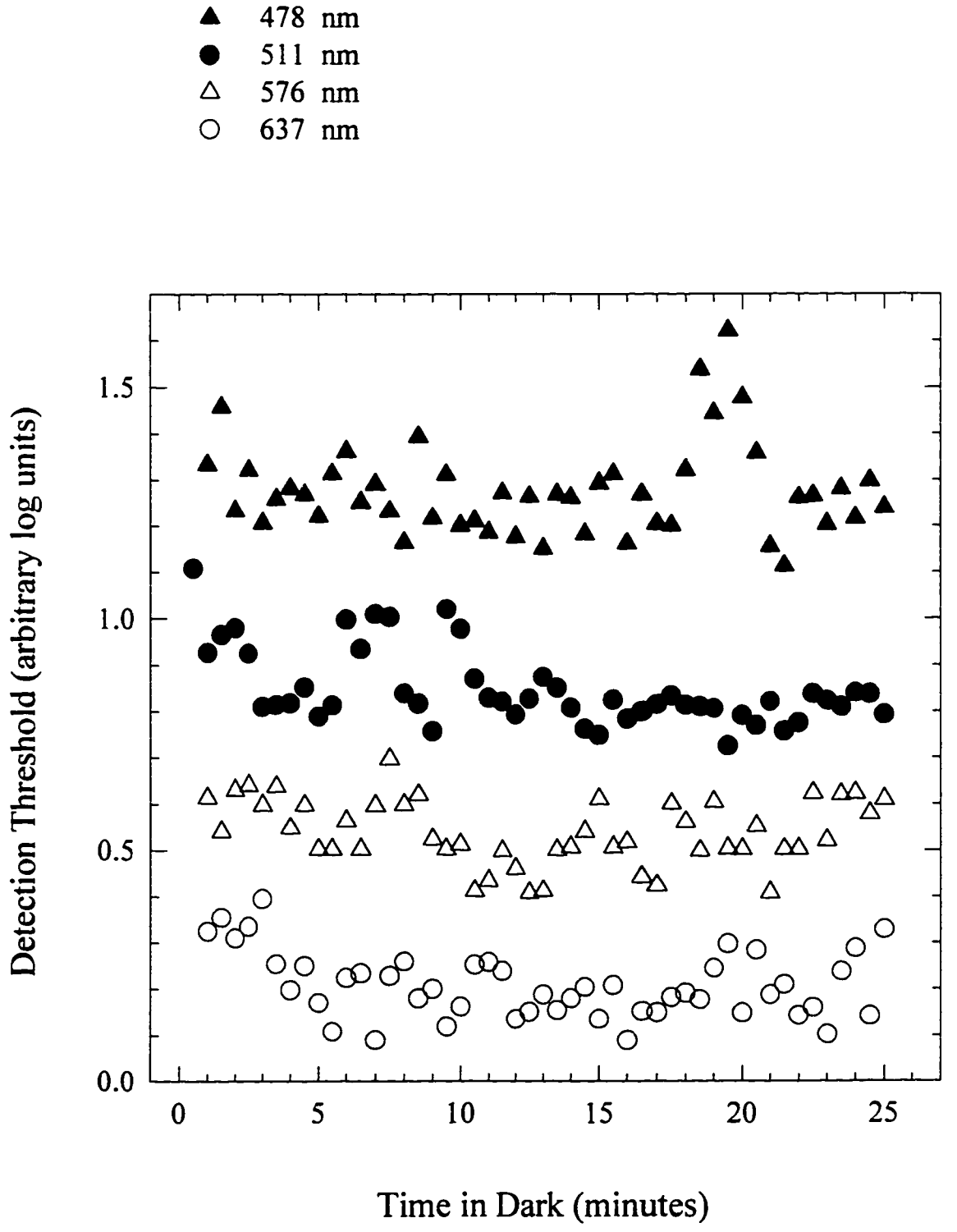

Figure 28. Detection thresholds for observer AD for all four stimuli as a function of time in the dark following interocular preadaptation. The test stimulus was a 3° circle presented for 100 ms every 3 s at 6° in the right eye temporal field.

Figure 28. Detection Thresholds
AD Interocular

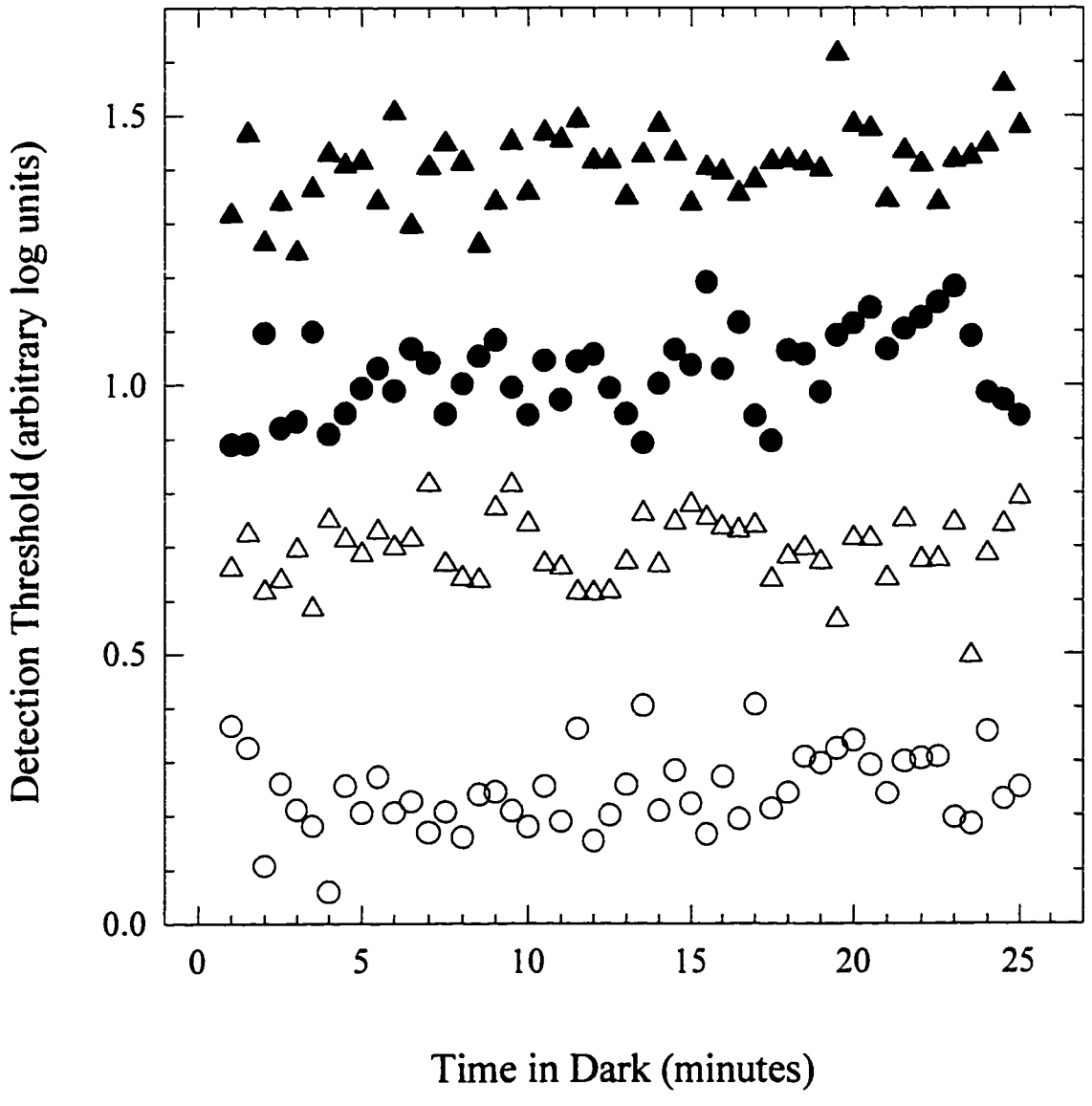

adaptation, thresholds for the 478 and 511 nm stimuli for EL (Figure 26) decrease, but not for the two longer wavelengths. Such an early decrease in threshold is also seen in some of the data from the other two observers but for different wavelengths (for the 511 and 637 nm stimuli for RM in Figure 27, for only the 637 nm stimulus for AD in Figure 28). From about 5 to 15 minutes in the dark and for the three shorter wavelength stimuli, EL also shows a detection threshold that appears to be appreciably lower than after 25 minutes in the dark. This effect is maximally 0.2 to 0.25 log units, and it cannot be seen with the 637 nm stimulus. In contrast, observers RM and AD show little consistent change in detection threshold after 5 to 10 minutes in the dark.

Collectively then, the present results suggest that the adapted state of the nonviewing eye exerts at most a small influence upon monocular detection thresholds: whatever influences are observed are largely obscured by marked individual differences.

A number of prior studies have suggested an influence of the adapted state of the nonviewing eye upon the time course of dark adaptation (e.g., Auerbach, Dorrenhaus, & Cavonius, 1992; Lansford & Baker, 1969; Makous, Teller, & Boothe, 1976; Paris & Prestrude, 1975; Prestrude, 1976; Prestrude et al., 1978). It is difficult to totally reconcile the present negative findings with these prior

findings. However, two noteworthy methodological differences should be mentioned. First, most of the above cited investigators studied the influence of a continually presented adapting field to the nonviewing eye, and they did not examine the effect of a bleach of photopigment. Second, the influence of this adapting field depended quite heavily upon the retinal position of the test stimulus (see particularly Auerbach et al. and Prestrude, 1976) and the degree of overlap between the visual fields in the two eyes (see Makous et al.). Such variables were not manipulated because my detection threshold data were collected as controls for the color vision data.

Comparison of the Influence of the Nonviewing Eye Upon Specific Threshold and Saturation Measures

Binocular-monocular comparisons. Figures 29 to 31 directly compare the changes in specific threshold following a monocular and binocular bleach of photopigment by plotting the data obtained with one observer and one test stimulus wavelength on the same sets of coordinates. In all cases, monocular data are plotted with closed symbols, binocular data are plotted with open symbols. For all four wavelengths and all three observers, the initial decrease in specific threshold during the cone recovery phase of adaptation does not differ with these two procedures, nor does the magnitude of the later increase in specific threshold. In others words, the adapted state of

Figure 29. Specific (hue identification) thresholds for observer EL for all four stimuli as a function of time in the dark following monocular and binocular preadaptation. The test stimulus was a 3^{o} circle presented for 100 ms every 3 s at 6^{o} in the right eye temporal field.

Figure 29. Specific (Hue Identification) Thresholds
EL

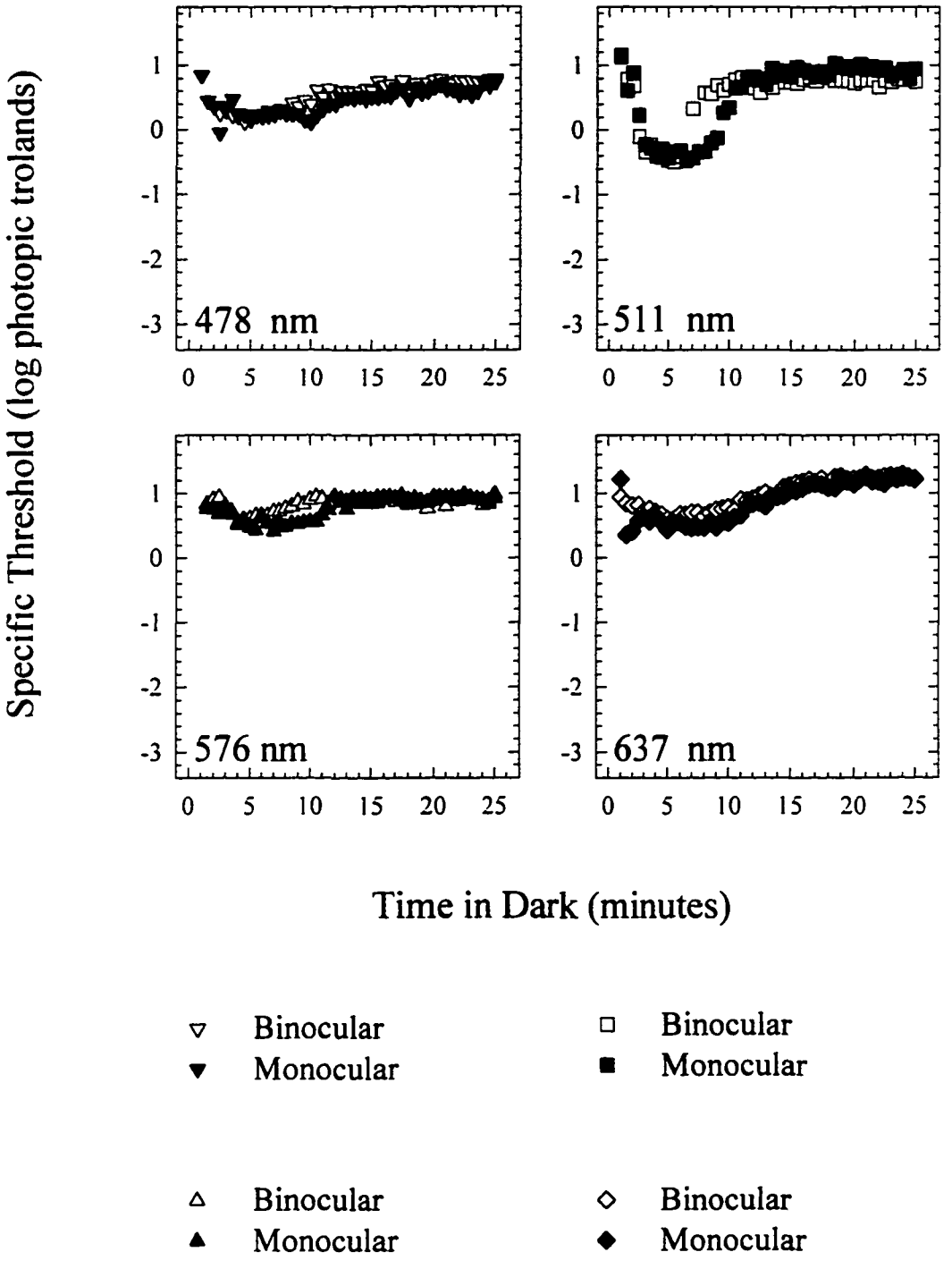

Figure 30. Specific (hue identification) thresholds for observer RM for all four stimuli as a function of time in the dark following monocular and binocular preadaptation. The test stimulus was a 3^{o} circle presented for 100 ms every 3 s at 6^{o} in the right eye temporal field.

Figure 30. Specific (Hue Identification) Thresholds
RM

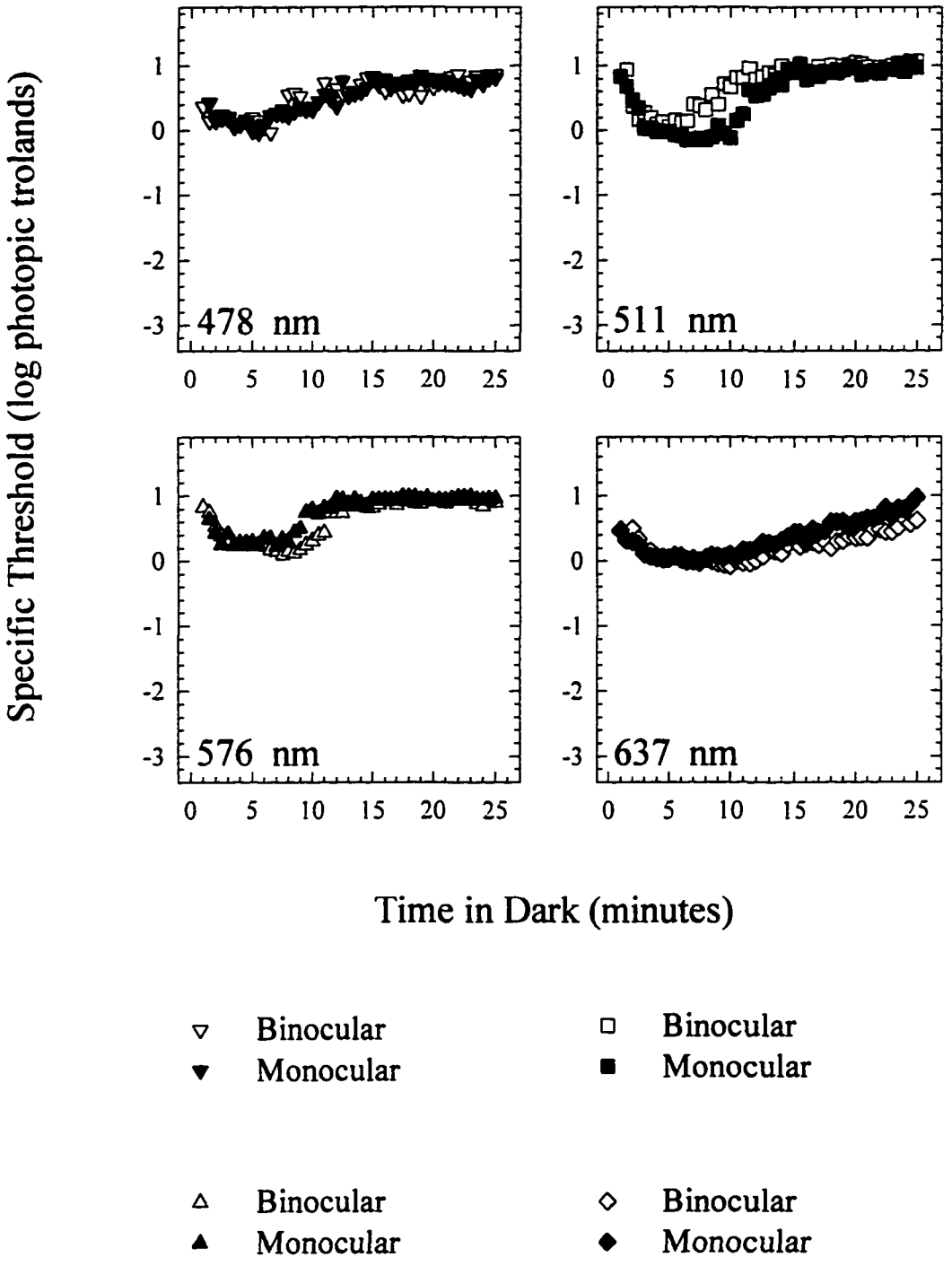

Figure 31. Specific (hue identification) thresholds for observer AD for all four stimuli as a function of time in the dark following monocular and binocular preadaptation. The test stimulus was a 3^{o} circle presented for 100 ms every 3 s at 6^{o} in the right eye temporal field.

Figure 31. Specific (Hue Identification) Thresholds AD

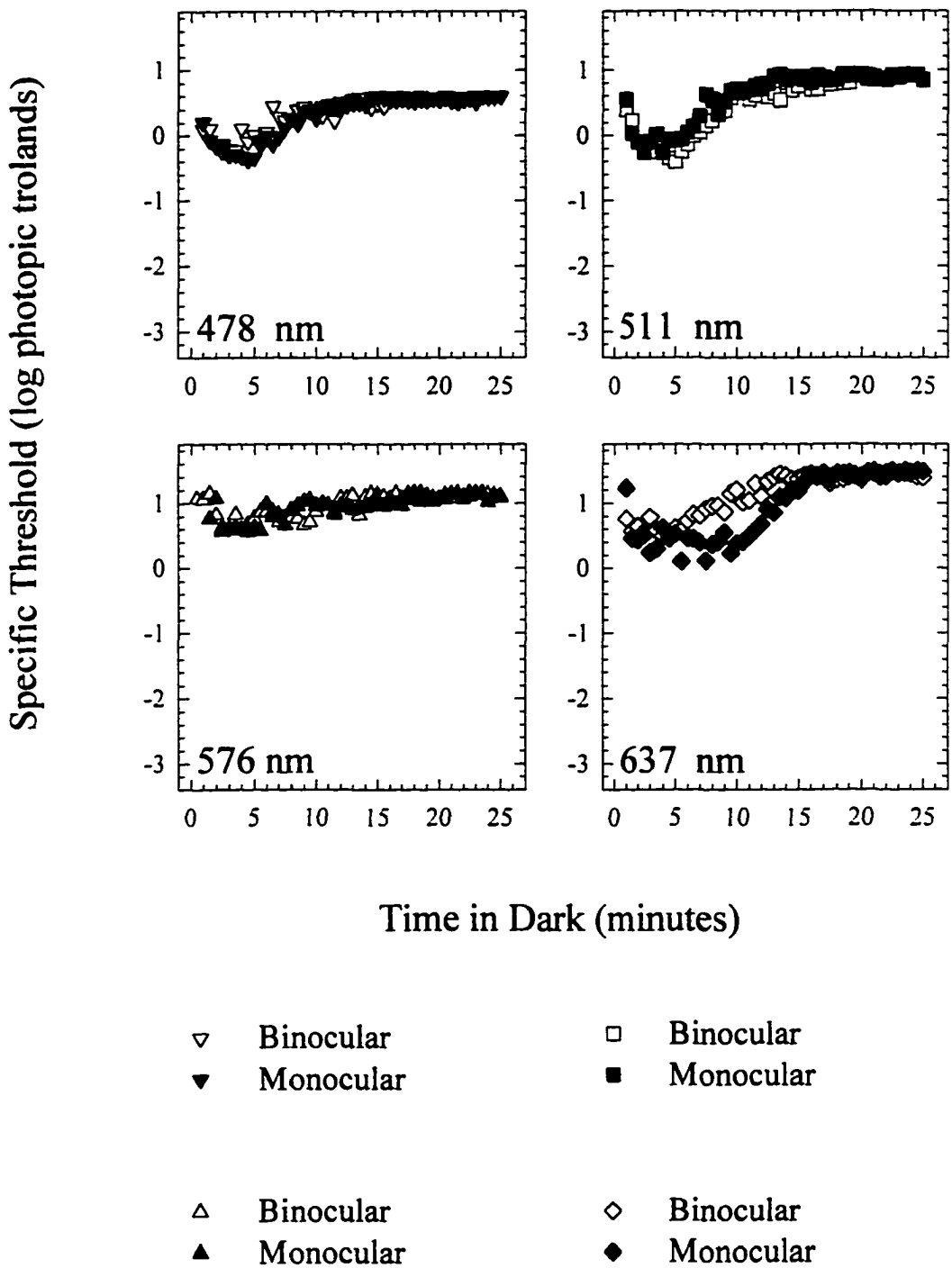

the nonviewing eye does not obviously influence the magnitude of the Lie effect. However, the adapted state of the nonviewing eye often influences the time course of the increase in threshold occurring during the later stages of dark adaptation. For example, examine the data of EL (Figure 29). With a 511 nm stimulus, the later increase in specific threshold occurs several minutes earlier following binocular bleaching. These results were consistent with one report (Prestrude et al., 1978) showing that an adapting field in the nonviewing eye caused a similar acceleration of this increase in specific threshold. For observer EL, a similar effect is seen with the other three wavelengths, but is less marked, particularly for the 637 nm stimulus. Results for observer RM (Figure 30) with 478 and 511 nm stimuli are comparable to those from EL. However, with the two longer wavelengths, binocular bleaching causes a slower increase in specific threshold than monocular bleaching, just the opposite effect seen with EL. Observer AD (Figure 31) shows yet another pattern of differences. In particular, with a 511 nm stimulus, binocular bleaching leads to a slowing rather than the acceleration of the time course of specific threshold changes obtained with the other two observers.

Throughout most of the present study all subjects observed the test stimulus with their right (dominant) eye. I wondered whether the results shown in Figures 29 to 31

would be at all affected by this. With the same three observers and using a 511 nm stimulus, I compared the influence of monocular versus binocular bleaching upon specific thresholds in the left and right eyes. Results for all observers are shown in Figure 32. Except for AD, these data were collected about a year or more after the data in Figures 29 to 31; therefore, they assessed the reliability of the aforementioned findings. Notice that for all observers, the effects of monocular and binocular bleaching on specific threshold in the left eye (left sets of coordinates) are quite similar. In contrast, results for the right eye again show that the increase in specific threshold occurs earlier following binocular bleaching for observers EL and RM, and later for observer AD.

In a comparable fashion, Figures 33 to 35 compared the influence of monocular versus binocular bleaching upon changes in saturation. For observer EL (Figure 33), binocular bleaching always leads to a faster change in saturation, particularly after 5 mninutes in the dark. This finding is consistent with her specific threshold data shown in Figure 29. Observer AD (Figure 34) also shows a faster change in saturation following binocular bleaching, except perhaps in the case of the 637 nm stimulus. However, observer MT (Figure 35; for whom no specific threshold data were collected) showed no difference in the influence of monocular versus binocular adaptation upon

Figure 32. Specific (hue identification) thresholds for observers AD, EL, and RM for a 511 nm stimulus as a function of time in the dark following monocular and binocular preadaptation. The test stimulus was a 3^{o} circle presented for 100 ms every 3 s at 6^{o} in the right eye temporal field and the left eye nasal field.

Figure 32. Specific (Hue Identification) Thresholds
511 nm

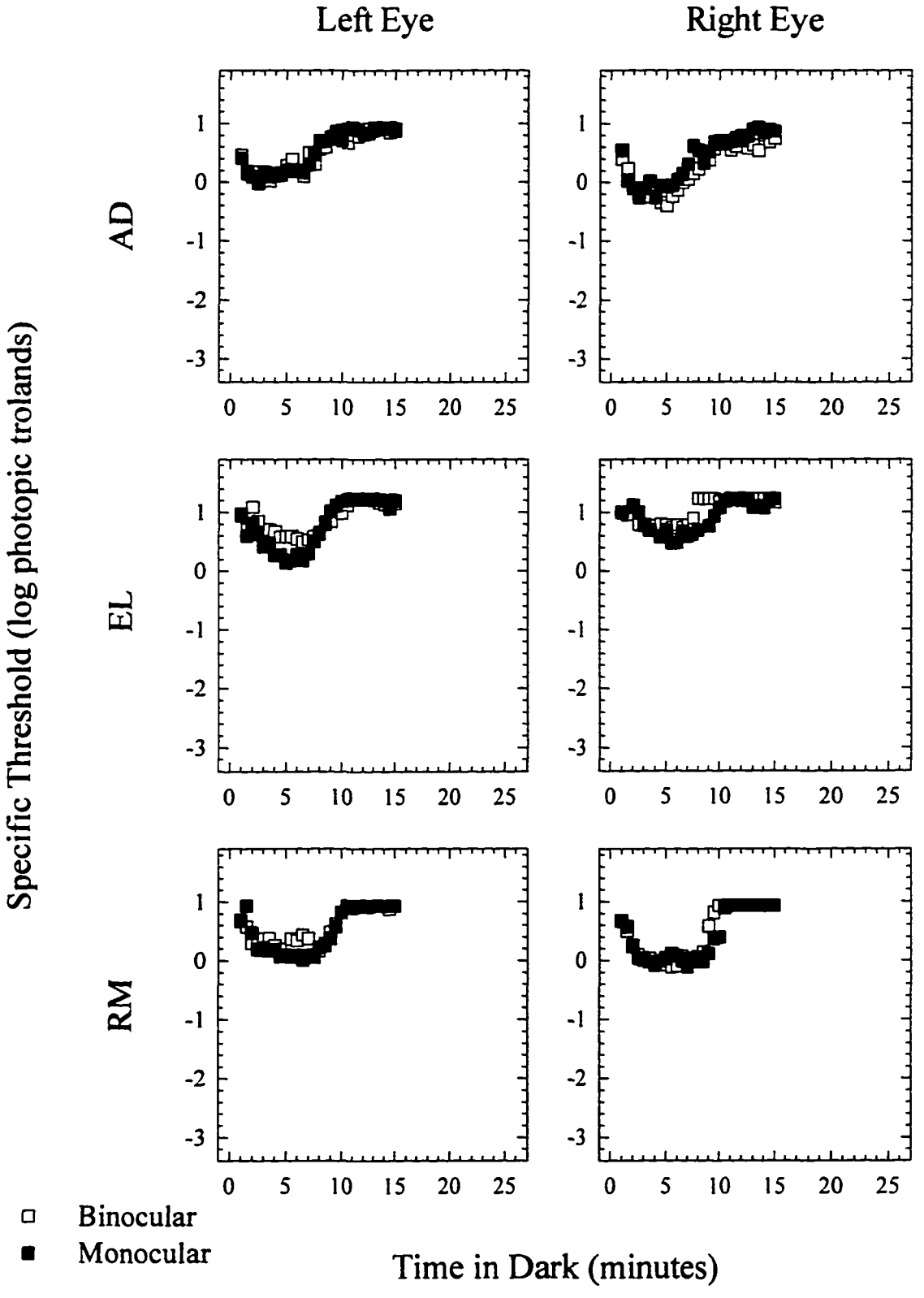

Figure 33. Saturation scaling for observer EL for all four stimuli as a function of time in the dark following monocular and binocular preadaptation. The test stimulus was a 3^{o} circle presented for 100 ms every 5 s at 6^{o} in the right eye temporal field.

Figure 33. Saturation Scaling
EL

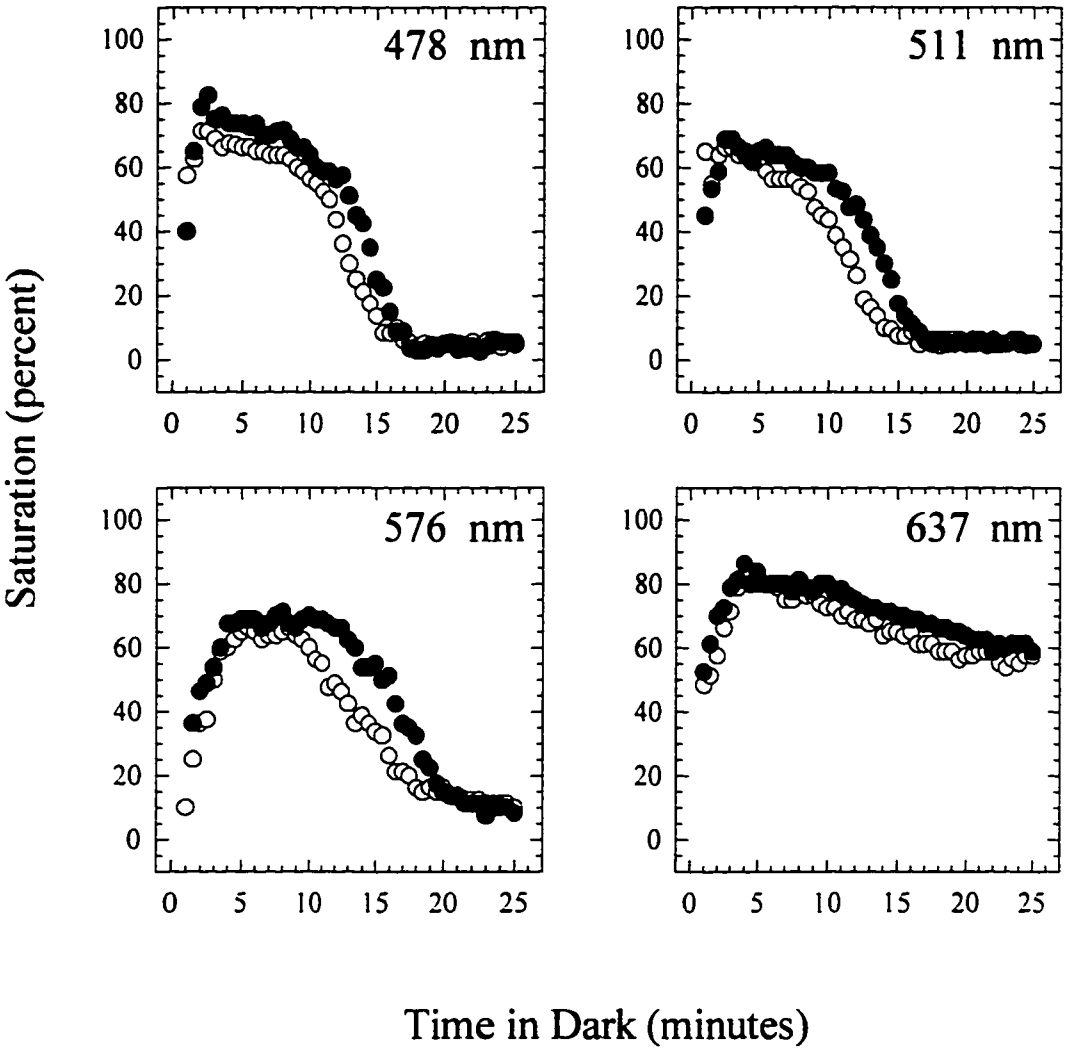

Figure 34. Saturation scaling for observer AD for all four stimuli as a function of time in the dark following monocular and binocular preadaptation. The test stimulus was a 3° circle presented for 100 ms every 5 s at 6° in the right eye temporal field.

Figure 34. Saturation Scaling
AD

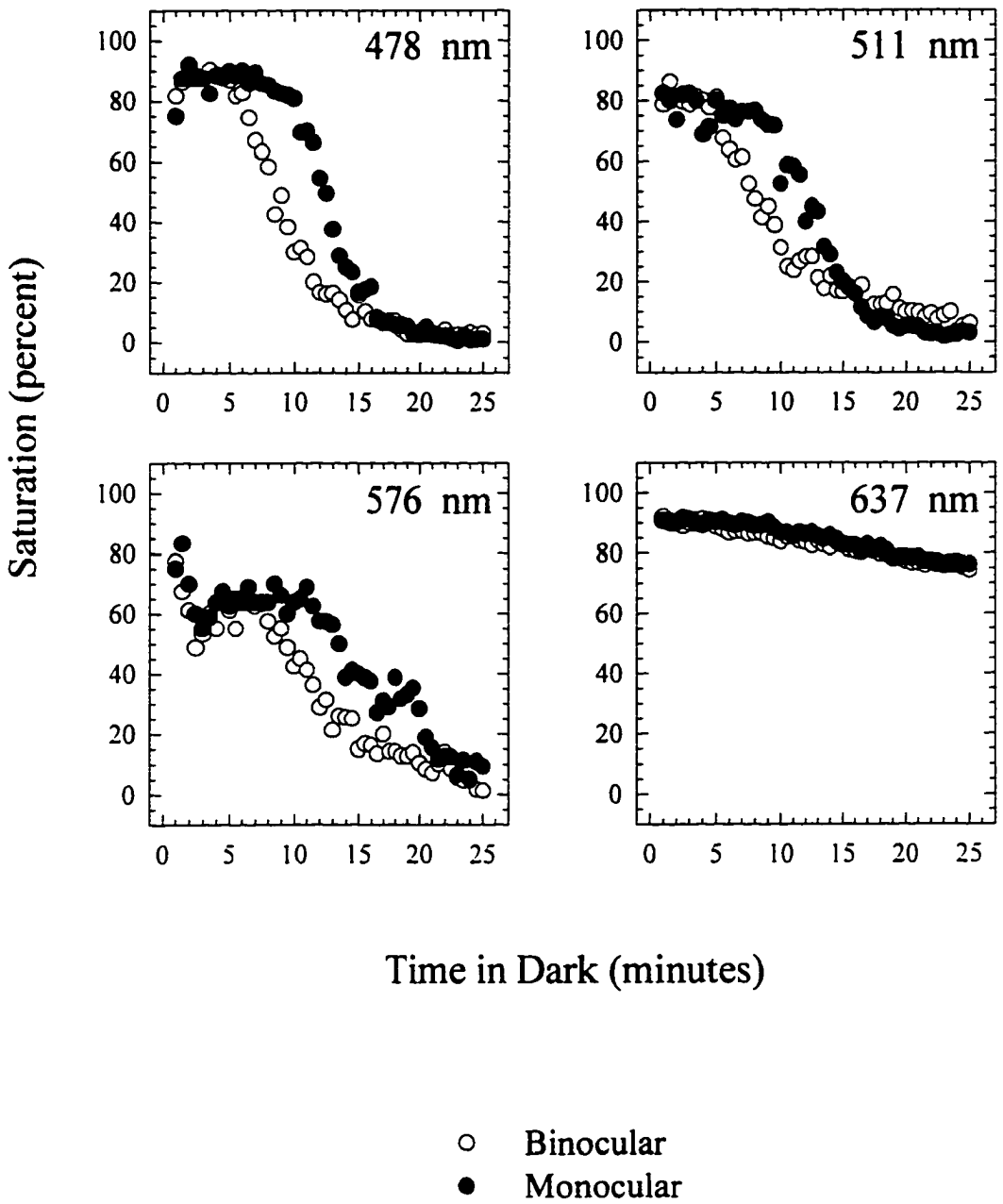

Figure 35. Saturation scaling for observer MT for all four stimuli as a function of time in the dark following monocular and binocular preadaptation. The test stimulus was a 3^{o} circle presented for 100 ms every 5 s at 6^{o} in the right eye temporal field.

Figure 35. Saturation Scaling
MT

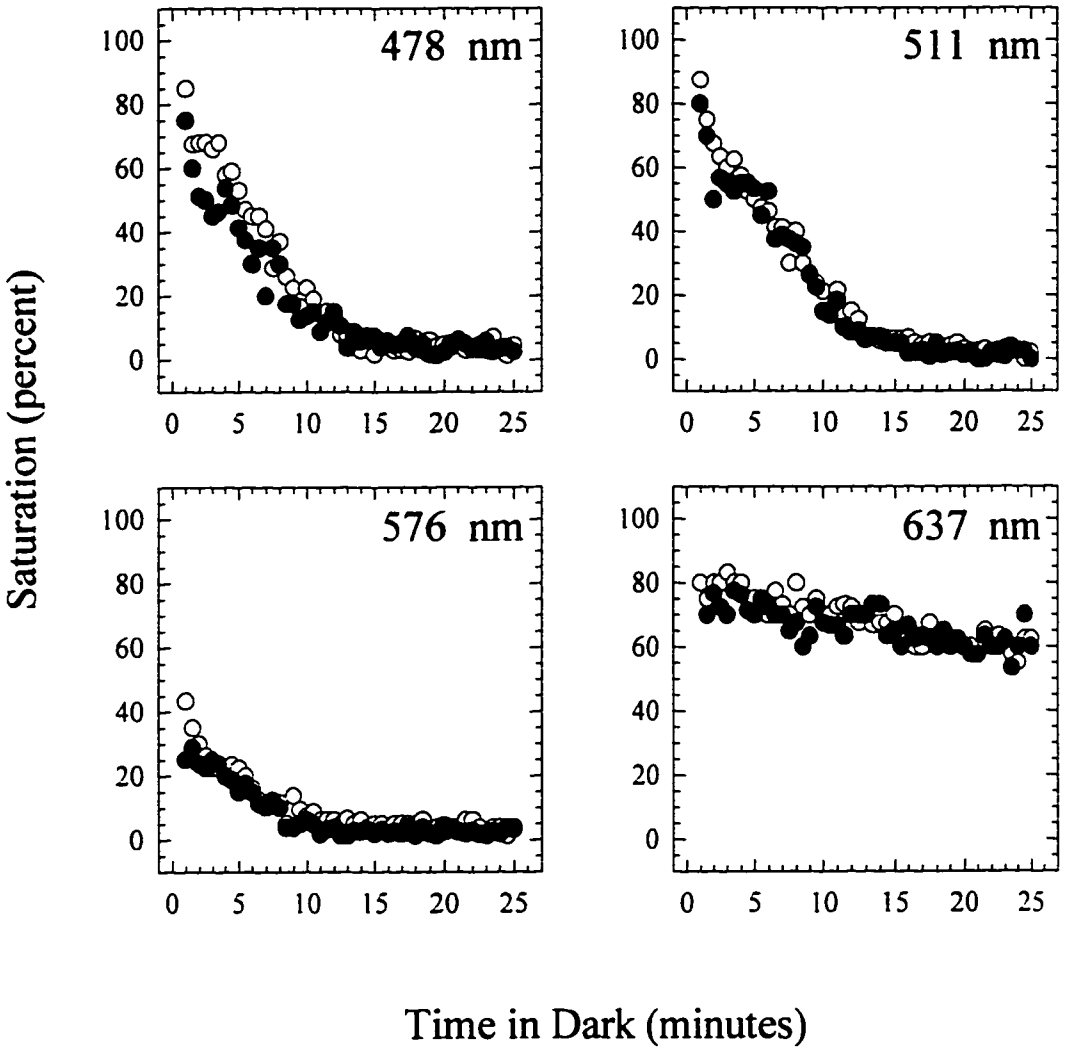

saturation.

Collectively, the results in Figures 29 to 35 indicate that the adapted state of the nonviewing eye can clearly influence the time course of changes in specific threshold and saturation induced by monocular adaptation, but does not influence the magnitude of these changes. This influence depends on wavelength, the test eye examined, the response measure used, and on the specific observer used for data collection.

Influence of Interocular Adaptation Figures 36 to 38 show changes in specific threshold for all four wavelength stimuli following an interocular bleach of photopigment. Overall, the influence of an interocular bleach of photopigment is quite small and variable. For the first few minutes of adaptation, observers EL (Figure 36) and RM (Figure 37) show a decrease in specific threshold for 478 nm and 511 nm stimuli, whereas AD (Figure 38) does not. In some cases (i.e., for observer EL with 478 and 511 nm stimuli and for observer RM with 478 and 637 nm stimuli), there is a consistent increase in specific threshold from about 10-20 minutes in the dark, which resembles at least superficially, the monocular Lie effect described in the Introduction. I do not consider this effect too seriously for two reasons. First, these findings are much too subject to variability among subjects. Second, this effect, which is at most 0.2 to 0.3 log units, does not

Figure 36. Specific (hue identification) thresholds for observer EL for all four stimuli as a function of time in the dark following interocular preadaptation. The test stimulus was a 3^{o} circle presented for 100 ms every 3 s at 6^{o} in the right eye temporal field.

Figure 36. Specific (Hue Identification) Thresholds
EL Interocular

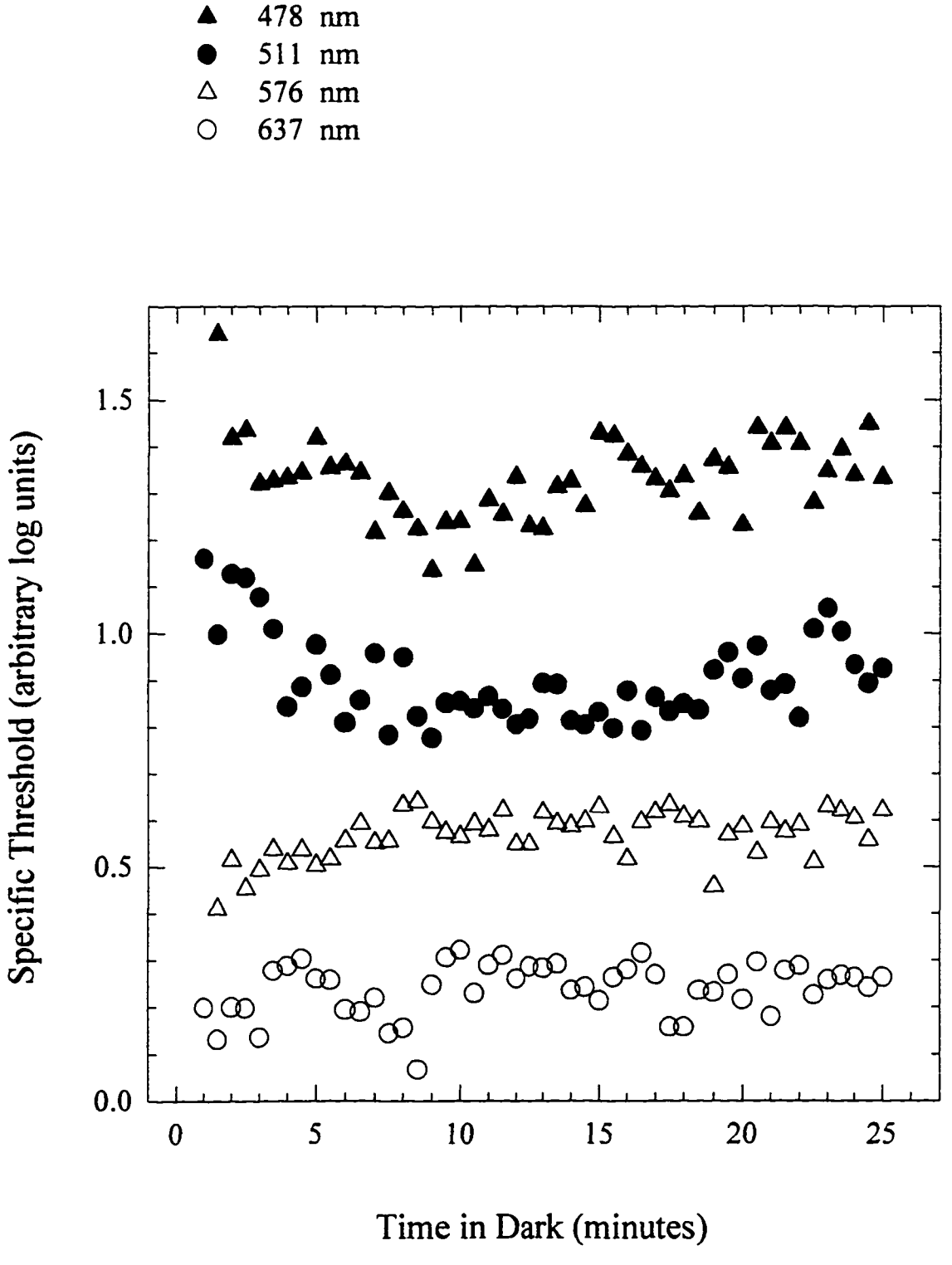

Figure 37. Specific (hue identification) thresholds for observer RM for all four stimuli as a function of time in the dark following interocular preadaptation. The test stimulus was a 3^{o} circle presented for 100 ms every 3 s at 6^{o} in the right eye temporal field.

Figure 37. Specific (Hue Identification) Thresholds
RM Interocular

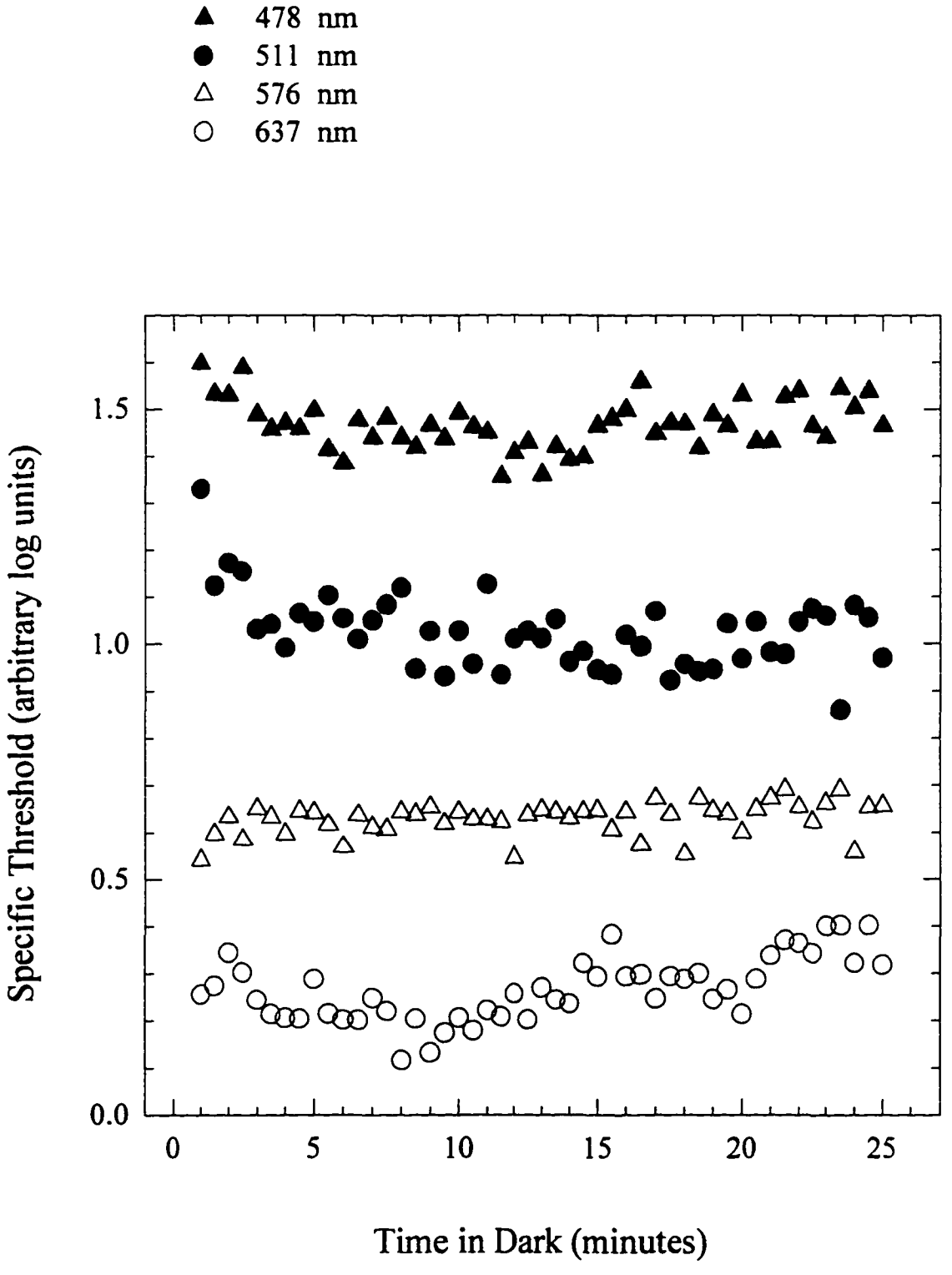

Figure 38 Specific (hue identification) thresholds for observer AD for all four stimuli as a function of time in the dark following interocular preadaptation. The test stimulus was a 3^{o} circle presented for 100 ms every 3 s at 6^{o} in the right eye temporal field.

Figure 38. Specific (Hue Identification) Thresholds
AD Interocular

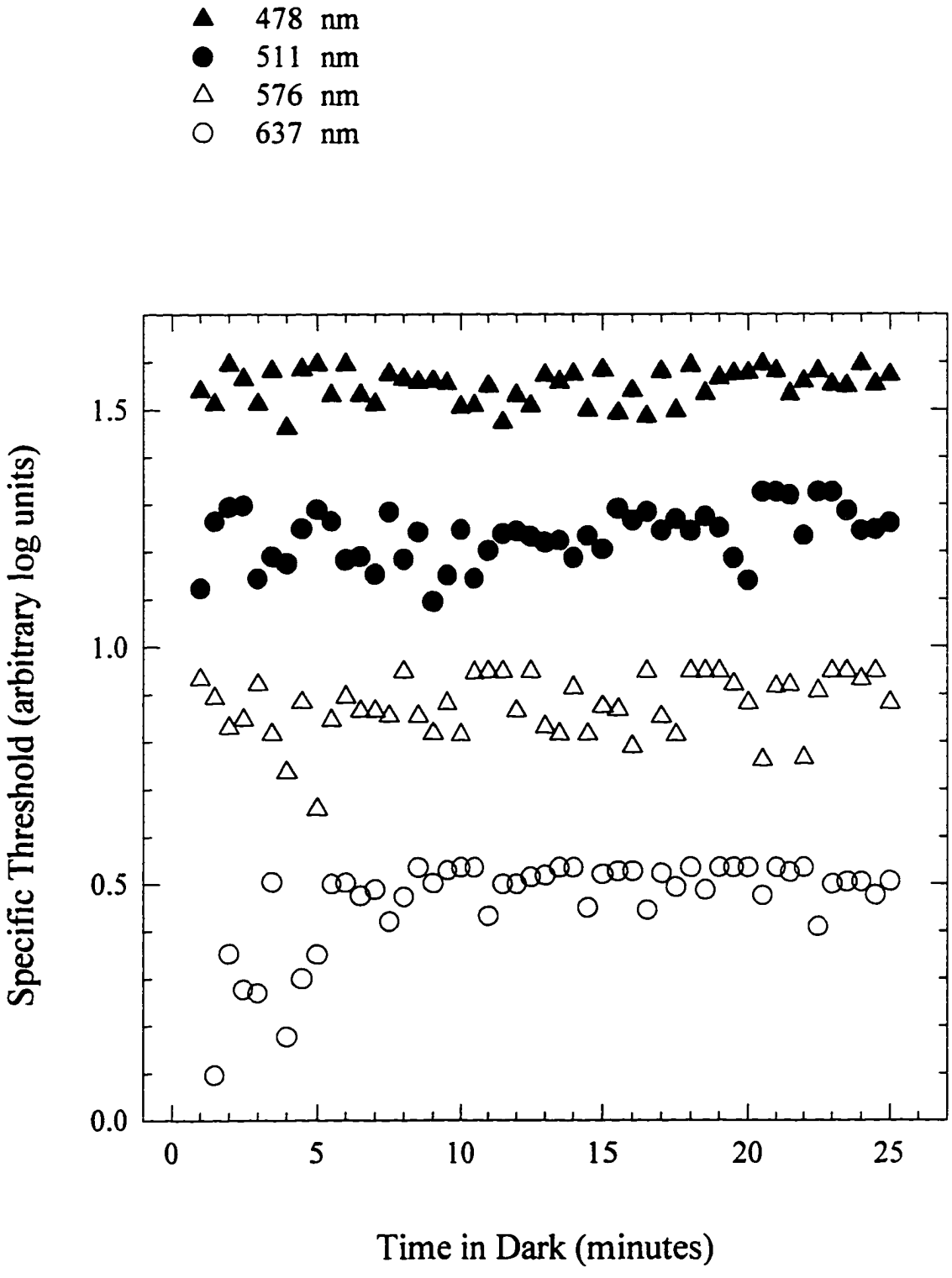

resemble closely enough the monocular Lie effect. For example, in Figure 39, I replot the 511 nm monocular Lie effect for observer EL (i.e., from Appendix A, Figure 42) and the 511 nm interocular data for observer EL in Figure 36. Arbitrarily, I expanded the vertical scaling of the ordinate to foster a comparison of the time courses of these two functions. This plot clearly shows that the monocular Lie effect has a much different time course than the slow, interocular influence.

Although not replotted here, analysis of the data contained within Appendix B shows that the influence of an interocular bleach of photopigment upon saturation is also quite small and inconsistent among the three observers used. Observer EL showed no consistent influence of interocular bleaching; MT showed a decrease in saturation for the first 10 minutes of adaptation with 511 and 576 nm stimuli, whereas AD showed small decreases in saturation after 10 minutes in the dark for all wavelengths except the 576 nm stimulus.

Influence of the Adapted State of the Nonviewing Eye Upon Hue

With the exception of data obtained with a 637 nm stimulus, there are no obvious, consistent influences of the adapted state of the nonviewing eye upon hue. The overall influence of binocular and monocular bleaching are quite similar, and I could discern no obvious differences

Figure 39. Specific (hue identification) thresholds for observer EL for a 511 nm stimulus as a function of time in the dark following monocular and interocular preadaptation. The test stimulus was a 3^{o} circle presented for 100 ms every 3 s at 6^{o} in the right eye temporal field. For the sake of comparison, the vertical scaling of the ordinate has been expanded.

Figure 39. Specific (Hue Identification) Thresholds
EL 511 nm

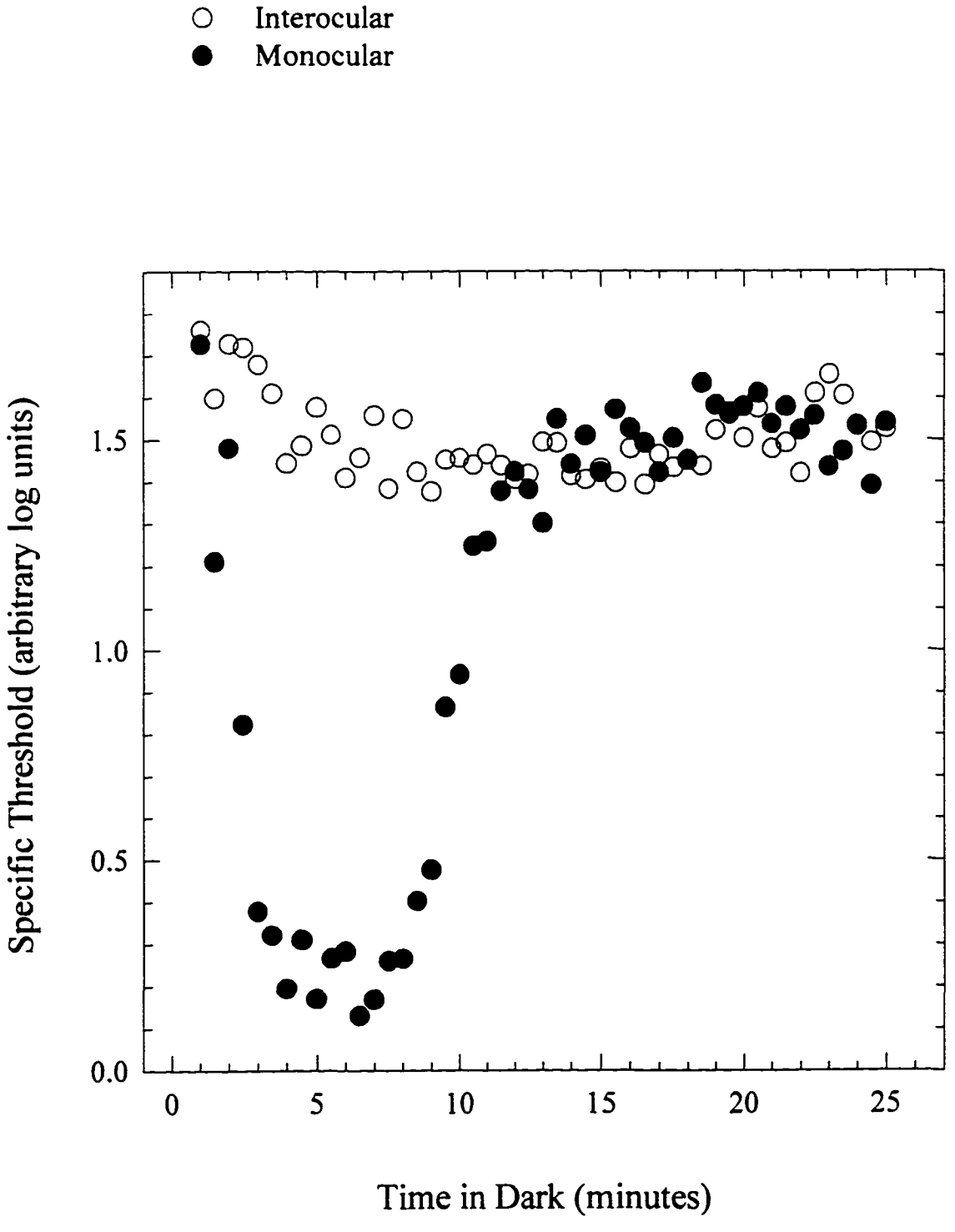

in time course. Interocular effects were generally quite small and inconsistant.

However, the results with a 637 nm test stimulus show some consistency. Figure 40 shows for all three observers, the change in redness and yellowness of a 637 nm stimulus as a function of the time period following a monocular, interocular, and binocular bleach of photopigments. For all three observers and for all three bleaching procedures, the stimuli become progressively less red and progressively more yellow. It is of interest that for observers MT and EL, binocular changes in redness and yellowness were noticeably larger than those obtained following monocular bleaching, suggesting that the binocular influence might reflect a sum of the monocular and interocular influences. This tendency, however, is not as apparent in the results for observer AD.

With the exception of hue data obtained with a 637 nm stimulus, the results of the experiments summarized in this chapter were disappointing. In general, these data show that the adapted state of the nonviewing eye can influence monocular color sensitivity, but these influences are generally small and inconsistent across observers.

Figure 40. Hue scaling for observers AD, EL, and MT for a 637 nm stimulus as a function of time in the dark following monocular, binocular, and interocular preadaptation. The test stimulus was a 3^{o} circle presented for 100 ms every 5 s at 6^{o} in the right eye temporal field.

Figure 40. Hue Scaling
637 nm

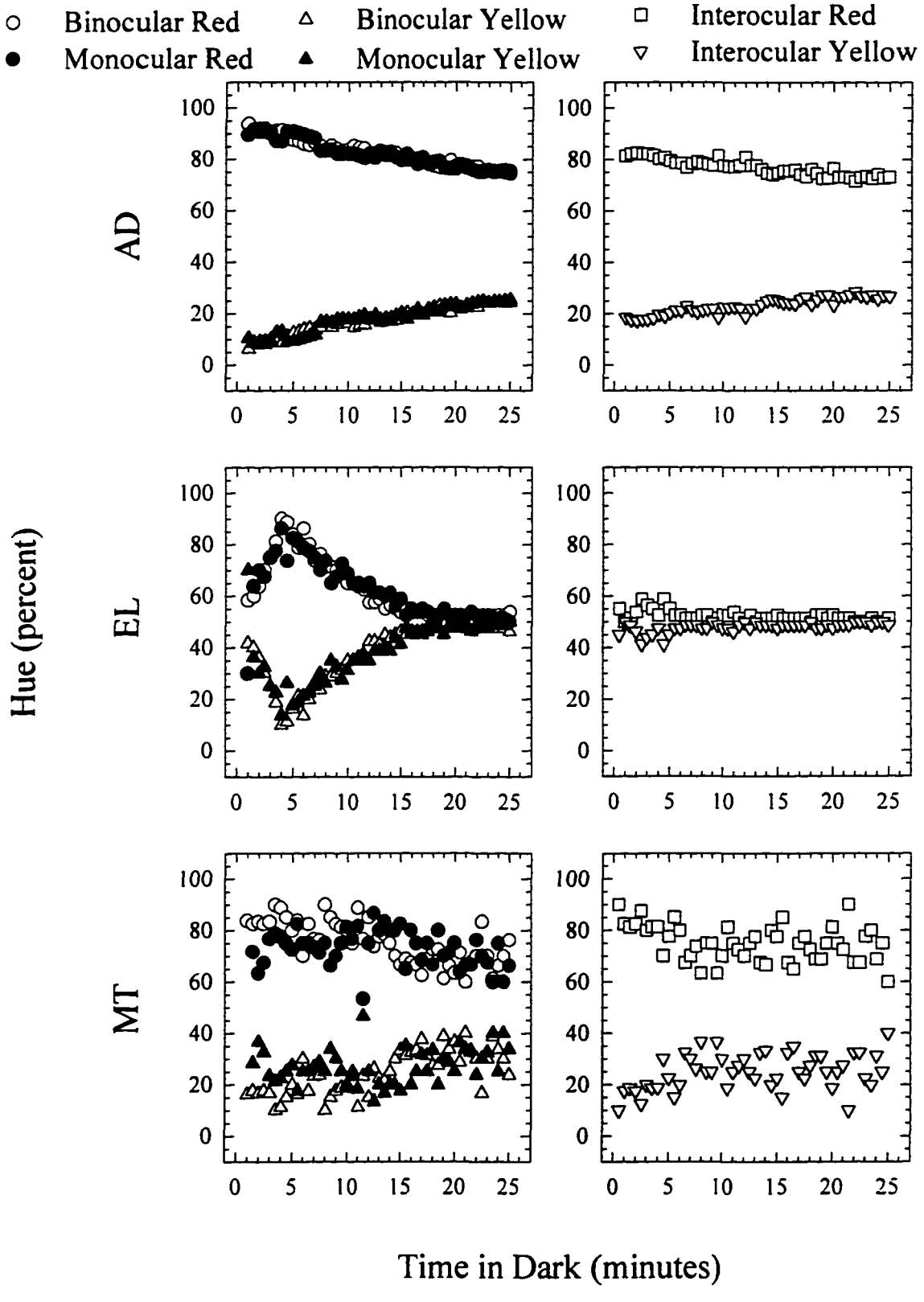

Chapter 7

General Discussion

The foregoing results show that color vision changes dramatically during the rod recovery stage of dark adaptation. The present study shows that monocular specific thresholds increase, stimulus saturation decreases, and in some cases stimuli markedly change in hue. The adapted state of the nonviewing eye influenced color vision, but this influence was small and varied according to the eye viewing the test stimulus, the wavelength of the test stimulus, the response measure used to assess sensitivity to color, and the observer providing the data.

General Mechanism for Rod Influence on Color Vision

Three models were proposed in the Introduction that might explain the role of rods in color vision: the short-wavelength cone summation model, the luminosity/saturation model, and the cSRCI model.

The specific threshold data are largely consistent with the cSRCI model. Specifically, the time course and magnitude of threshold changes were similar for stimuli that appeared predominantly blue (478 nm) and yellow (576 nm) in hue. In addition, the magnitude of threshold change occurring with predominantly green- (511 nm) and red-appearing (637 nm) stimuli were similar and greater than the influence upon 478 and 576 nm stimuli. Although not

part of this thesis, very similar findings were obtained using a light adaptation procedure (Vollaro et al., 1997). These results from five observers (three in the present study, two in the study of Vollaro et al.) are consistent with a model that proposes that rod dark adaptation is associated with reduced activity in the blue/yellow opponent-process mechanism and a separate, larger reduction of activity within the green/red opponent mechanism.

A priori, this influence could involve a facilitatory influence of dark-adapted rods or a suppressive (presumably inhibitory) influence of dark-adapted rods upon color opponent mechanisms. The present series of experiments provides no direct means to decide between these two alternatives, but I favor the latter possibility for two reasons. First, there is clinical evidence suggesting that color vision remains relatively unaffected by a variety of conditions characterized by a lack of normal rod function (Deutman, 1977), which is inconsistent with a facilitative role for rods in color vision. Second, there are two types of SRCI mechanism known to influence cone-mediated vision pertaining to high temporal frequency and high spatial frequency (Frumkes & Eysteinsson, 1988; Lange et al., 1997). I suggest that these specific threshold findings reflect similar SRCI mechanisms, that is, chromatic-SRCI (cSRCI). The observed wavelength specificity is incompatible with models positing a summation of light-

evoked rod signals with signals from short-wavelength cones or with the cone luminosity signal.

The present scaling data show that all of the wavelength test stimuli used in the present study desaturate during rod dark adaptation. For all three observers, the greater the wavelength, the smaller this desaturating effect. As argued in Chapter 4, this monotonic relationship is consistent with a summation of light-evoked rod signals with the cone luminosity channel signal. Because this wavelength dependency differs from that observed with the specific threshold measures, a desaturation (or luminosity channel summation) model cannot entirely explain the Lie effect. Certainly, the saturation scaling data in no way support a short-wavelength cone summmation model. Unfortunately, stimulus size and retinal position were not varied in these studies. These factors might have effected a different profile of results.

Changes in hue scaling are also noted during the time period when the aforementioned desaturation occurs. In particular, the hue of the 637 nm stimulus becomes less red and more yellow; hue shifts obtained with the other wavelengths differ considerably among the results of the three observers used, making interpretation somewhat difficult. Nevertheless, the 637 nm data are consistent with a model that posits an inhibitory influence of dark-adapted rods upon mechanisms that specifically suppress the

coding of red. It is also compatible with a cSRCI model such as that suggested to account for specific threshold data that involve a greater magnitude of influence upon green/red than upon blue/yellow opponent mechanisms.

Collectively, the hue, saturation, and specific threshold data can be explained by assuming that the role of rods in color vision involves: 1) a summation of light-evoked rod signals with the light-evoked cone luminosity channel signal, and 2) a cSRCI mechanism acting separately on green/red and blue/yellow opponency. If dark adaptation has a stonger suppressive influence upon red and green hues, then by default a stimulus must appear more blue and yellow. Such an explanation can qualitatively account for the association between blue and scotopic vision noted by previous researchers. Thus, I suggest that scotopic vision involves a selective suppression of red and green rather than a rod contribution to the short-wavelength cone channel.

Possible Mechanisms for and Neural Sites of Rod Contribution to Color Vision

There are many sites within the nervous system for rod-cone interaction, including electrical coupling between rods and cones, synaptic input from the rod-driven AII amacrine cell to cone bipolar cells, a convergence of rod and cone pathways on the same ganglion cells, and extraretinal interactions.

Rod-cone electrical coupling. This is well established in all vertebrate classes, including primates (Schneeweis & Schnapf, 1995). Two considerations make this electrical coupling between photoreceptors an unlikely source of a predominant influence upon color vision. First, if this were the source of influence, one would expect to find high levels of rod input to both the magnocellular and parvocellular pathways, a finding at odds with a considerable amount of electrophysiological data (Lee, 1996). In particular, the parvocellular pathway, which presumably mediates color opponency, has relatively little rod input in comparison with the magnocellular pathway (Purpura, Kaplan, & Shapley, 1988). Second, the coupling that is found between rods and cones appears to occur indiscriminately with all cone types (Schneeweis & Schnapf, 1995), and there is no evidence for color opponency in either the photoreceptors or horizontal cells of any primate (e.g., Dacey, Lee, Stafford, Pokorny, & Smith, 1996). To the extent that the present findings involve color opponency, they argue against this distal retinal site for rod influence.

The AII rod amacrine cell input to cone pathways. In all mammals, including humans, the best understood rod input to cone pathways involves the AII amacrine cell (e.g., Daw et al., 1990; Kolb, 1994). This on-amacrine cell is electrically coupled to on-cone bipolar cells and

supplies inhibitory input to off-center ganglion cells. Unfortunately, the color specificity of this pathway in primates has not been determined. However, the importance of this pathway in all studied species as well as its on-excitatory-off-inhibitory characteristic make it a strong candidate for an influence upon color opponency.

Convergence of rod and cone inputs to magnocellular pathways. The work of Barry Lee and his colleagues (see Lee, 1996, for a review) suggests that the parasol-retinal-magnocellular-geniculate pathway is the neural analog of the luminosity channel, whereas the midget-retinal-parvocellular-geniculate pathway is the analog of color opponency: the former receives a considerable amount of rod input, the latter relatively little. To the extent that light-evoked rod signals are enhanced during the later stages of dark adaptation, this might well account for a light-evoked rod contribution to the luminosity channel. Because this convergence site is monocular, it is consistent with the relatively small influence of the adapted state of the nonviewing eye upon saturation.

Cerebral sites of interaction. The blob cells in striate cortex, which are monocular, are often the source of spectral opponency within cortex (Livingstone & Hubel, 1984; Tootell, Silverman, Hamilton, De Valois, & Switkes, 1988; Ts'o & Gilbert, 1988; but see Sato, Katsuyama, Tamura, Hata, & Tsumoto, 1994). Edwards, Purpura, and

Kaplan (1995) proposed that the superficial layers of striate cortex receive both an indirect magnocellular input that is focused on the blobs and an indirect parvocellular input that is spread evenly throughout these layers. Given that rods probably contribute more to the magnocellular pathway than to the parvocellular pathway (Purpura et al., 1988), the model of Edwards et al. allows for a possible influence of rods on blob cells. Such rod input might involve a multitude of interactions between magnocellular and parvocellular pathways in extrastriate visual cortex.

Importance of the adapted state of the nonviewing eye. The influence of the adapted state of the nonviewing eye has been carefully studied for nonchromatic types of SRCI. The SRCI influence upon sensitivity to rapid flicker, which is known to involve distal retinal processing (Frumkes & Eysteinsson, 1988), is purely monocular (Lange et al., 1997). In contrast, the influence upon sensitivity to high spatial frequencies is completely binocular: virtually identical influences are observed from adapting either the viewing or the nonviewing eye (Lange et al.). Although there are other possibilities, this binocular characteristic suggests a cerebral site for rod-cone interaction. The present chromatic findings (a slight, variable influence of the adapted state of the nonviewing eye) are not comparable to either flicker- or grating-SRCI.

This "partial binocularity" is reminiscent of various

studies of visual masking from the 1950s and 1960s. For example, presentation of a brief adapting field to the viewing eye can reduce sensitivity to a monocular test flash by several log units (Crawford, 1947). In contrast, contralateral adapting flash stimulation only slightly alters senstivity that is mediated by the nonviewing eye, unless the two stimuli are very similar in spatial configuration (e.g., Battersby & Wagman, 1962). Today, "Crawford masking" is largely attributed to changes within the photoreceptor cells themselves (e.g., Adelson, 1982; Kleinschmidt & Dowling, 1975) and the importance of this retinochiasmal influence remains obscure.

Most of the present chromatic data are also likely to involve a site where the visual system is likely to be organized in a monocular fashion. The small, variable interocular influences upon specific threshold and saturation have a different time course than the monocular effects (Figure 39 in the previous chapter). The small differences between monocular and binocular specific threshold data, which are inconsistently seen, suggest that the interaction between rods and cones is accomplished at a monocular (relatively distal) portion of the visual pathway and is only slightly modified at a subsequent binocular (more proximal) site. The only possible exception to this involves the influence of adaptation upon the hue evoked by the 637 nm stimulus. In this case, monocular, binocular,

and interocular rod adaptation exerted similar influences upon hue. In two observers, the binocular influence was noticeably larger than the monocular influence, suggesting a summation of monocular and interocular influences.

Collectively, the foregoing results might be explained by a model in which saturation changes reflect convergence of rod and cone inputs into the magnocellular (luminosity) pathway, and specific thresholds are mediated at an unknown monocular site, such as the AII amacrine cell. In contrast, rod adaptational influences upon hue might involve an extrastriate cortical site where vision is coded binocularly.

Possible Future Experiments

Although not as clear as desired, the present results have a considerable amount of heuristic value. While I was collecting my data, Vollaro et al. (1997) examined a comparable influence of rod light adaptation upon specific thresholds. Some of these data were reported above (Figures 10 and 11 in Chapter 3). It is noteworthy that these data showed much greater, consistent similarity between blue- and yellow-appearing stimuli and between green- and red-appearing stimuli than was found with the present dark adaptation procedure. In a detailed spectral analysis, Vollaro et al. also found that the rod influence upon many different wavelength test stimuli was a tetramodal function that closely resembled the four hue

scaling functions observed by Gordon et al. (1994). Perhaps the present hue and saturation scaling data would have shown greater interobserver reliability had a similar light adaptation procedure been employed.

More generally, a cSRCI model might have great predictive validity for other techniques used to study the rod contribution to color vision. For example, color matching studies could be done with mixtures of primaries in a dark-adapted portion of the visual field, with the mixture superimposed on an adapting field. If there is a stronger cSRCI influence upon green/red than upon blue/yellow mechanisms, adaptation should have a predictable influence. Such a technique could also determine whether rod adaptation suppresses a truly color opponent mechanism, or affects separately blue, green, yellow, and red mechanisms. Finally, the AII amacrine cell provides a particularly strong rod inhibitory input to off-cone pathways. This suggests a very different rod influence upon cones at the onset versus offset of illumination, which could be assessed by psychophysical studies involving transient adapting flashes rather than bleaching or background adaptation procedures.

In conclusion, the present study uniquely shows that the major role of rods in color vision is a suppression of color-opponent channels.

Appendix A

Appendix A is a compilation of figures showing specific (hue identification) and detection thresholds for observers EL, RM, and AD for all four test stimuli following monocular, binocular, and interocular preadaptation.

Figure 41. Specific (hue identification) and detection thresholds for observer EL for a 478 nm stimulus as a function of time in the dark following monocular, binocular, and interocular preadaptation. The test stimulus was a 3^{o} circle presented for 100 ms every 3 s at 6^{o} in the right eye temporal field.

Figure 41. Specific (Hue Identification) and Detection Thresholds
EL 478 nm

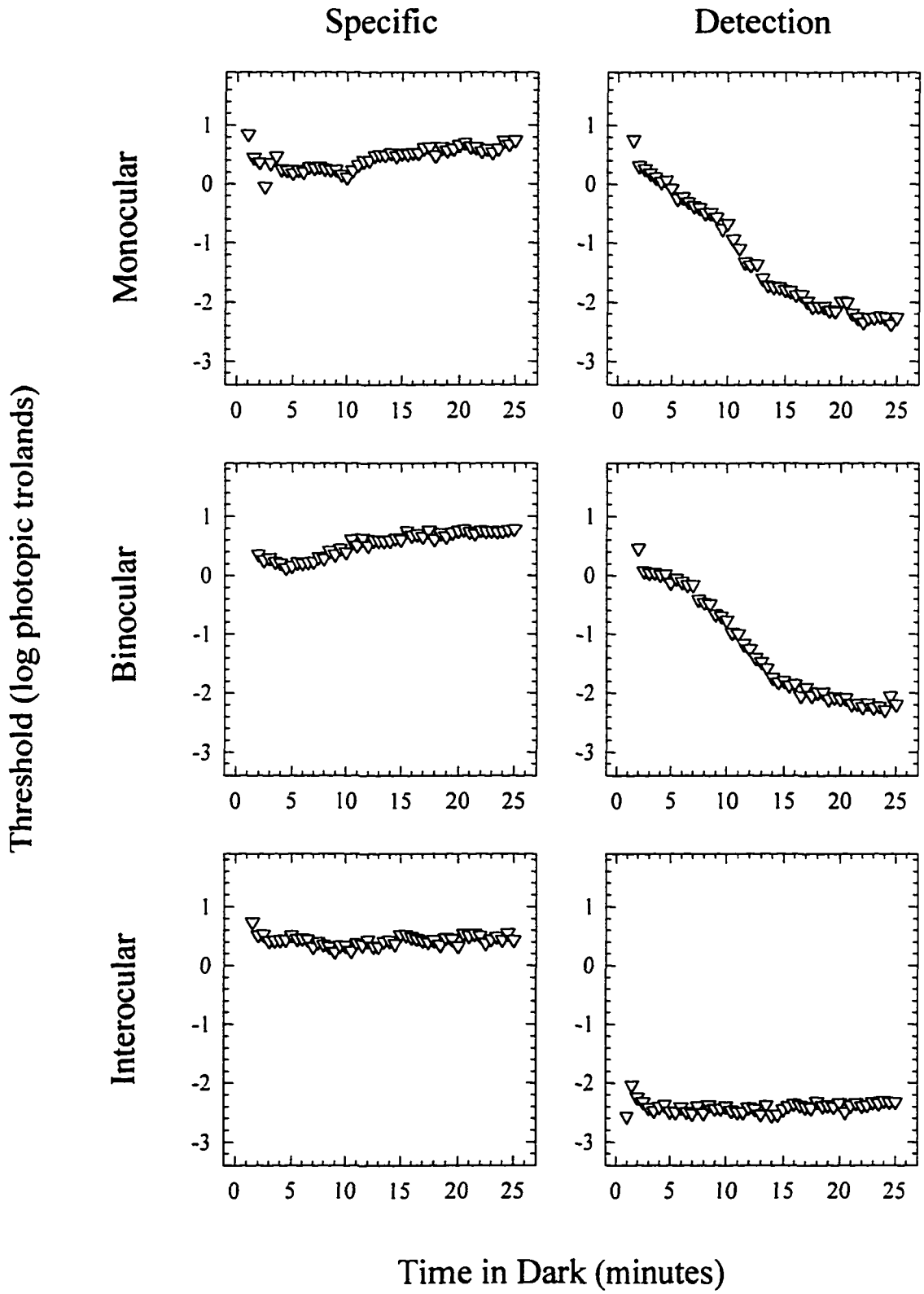

Figure 42. Specific (hue identification) and detection thresholds for observer EL for a 511 nm stimulus as a function of time in the dark following monocular, binocular, and interocular preadaptation. The test stimulus was a 3^{o} circle presented for 100 ms every 3 s at 6^{o} in the right eye temporal field.

Figure 42. Specific (Hue Identification) and Detection Thresholds
EL 511 nm

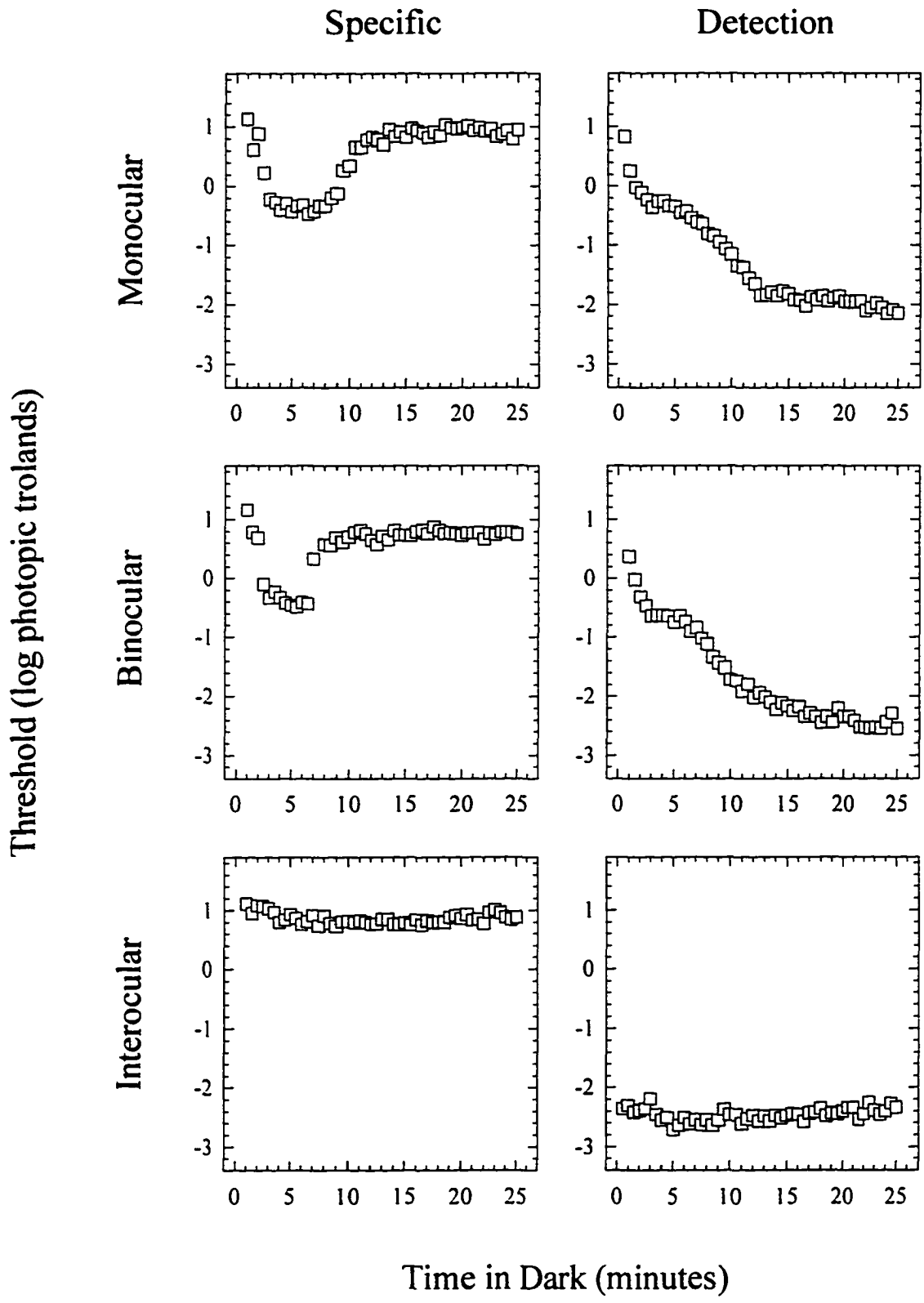

Figure 43. Specific (hue identification) and detection thresholds for observer EL for a 576 nm stimulus as a function of time in the dark following monocular, binocular, and interocular preadaptation. The test stimulus was a 3^{o} circle presented for 100 ms every 3 s at 6^{o} in the right eye temporal field.

Figure 43. Specific (Hue Identification) and Detection Thresholds
EL 576 nm

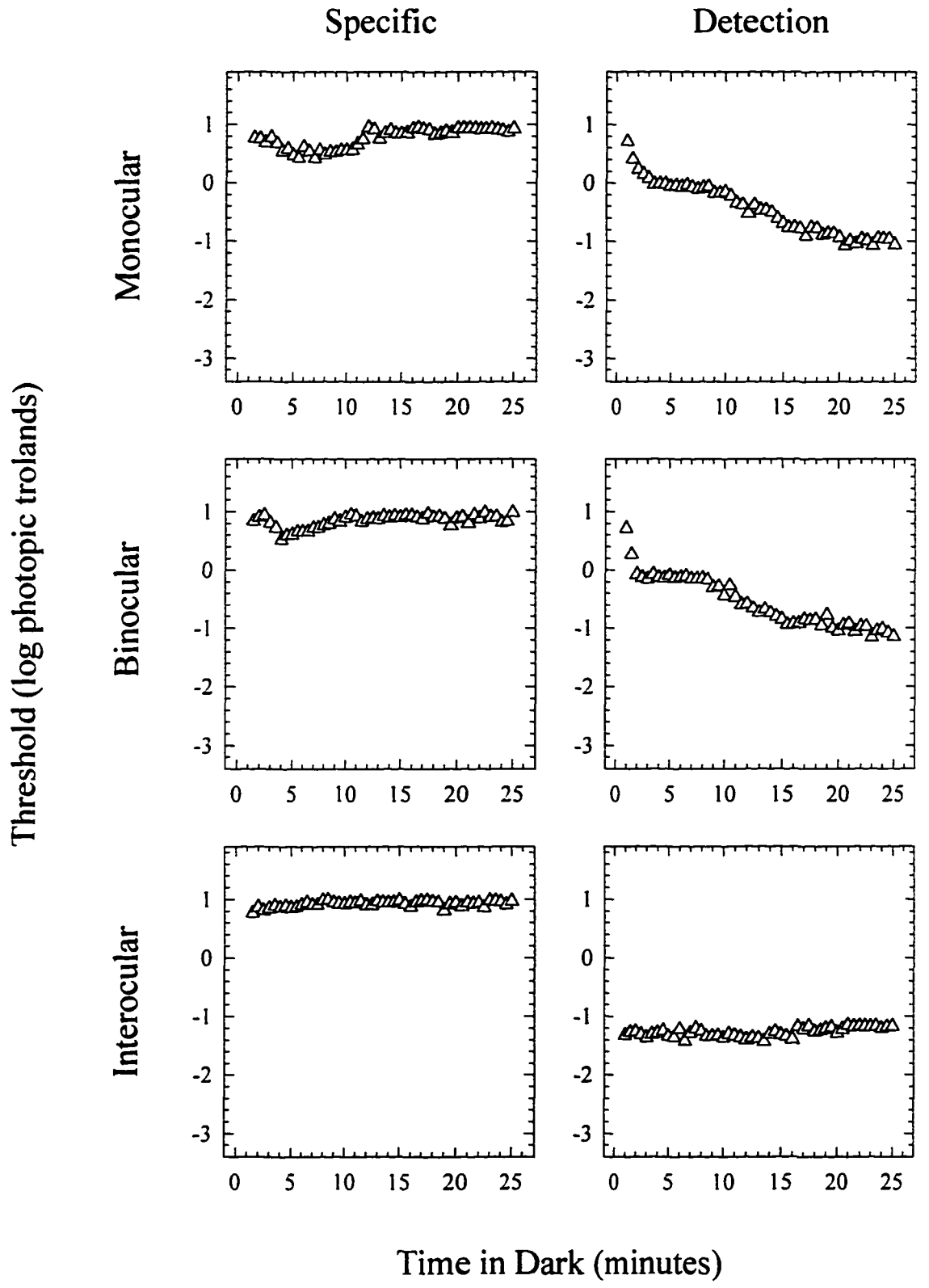

Figure 44. Specific (hue identification) and detection thresholds for observer EL for a 637 nm stimulus as a function of time in the dark following monocular, binocular, and interocular preadaptation. The test stimulus was a 3^{o} circle presented for 100 ms every 3 s at 6^{o} in the right eye temporal field.

Figure 44. Specific (Hue Identification) and Detection Thresholds
EL 637 nm

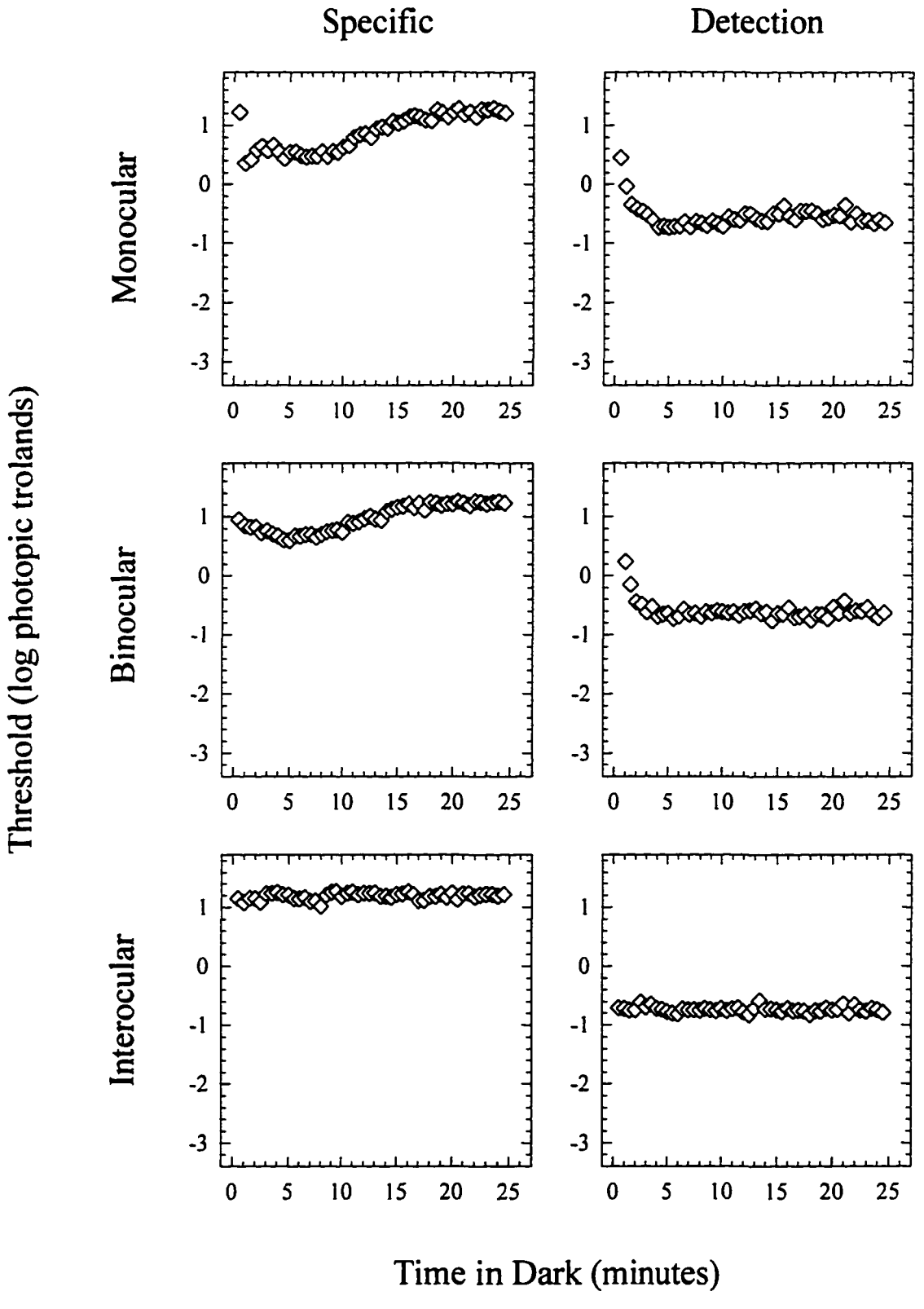

Figure 45. Specific (hue identification) and detection thresholds for observer RM for a 478 nm stimulus as a function of time in the dark following monocular, binocular, and interocular preadaptation. The test stimulus was a 3^{o} circle presented for 100 ms every 3 s at 6^{o} in the right eye temporal field.

Figure 45. Specific (Hue Identification) and Detection Thresholds
RM 478 nm

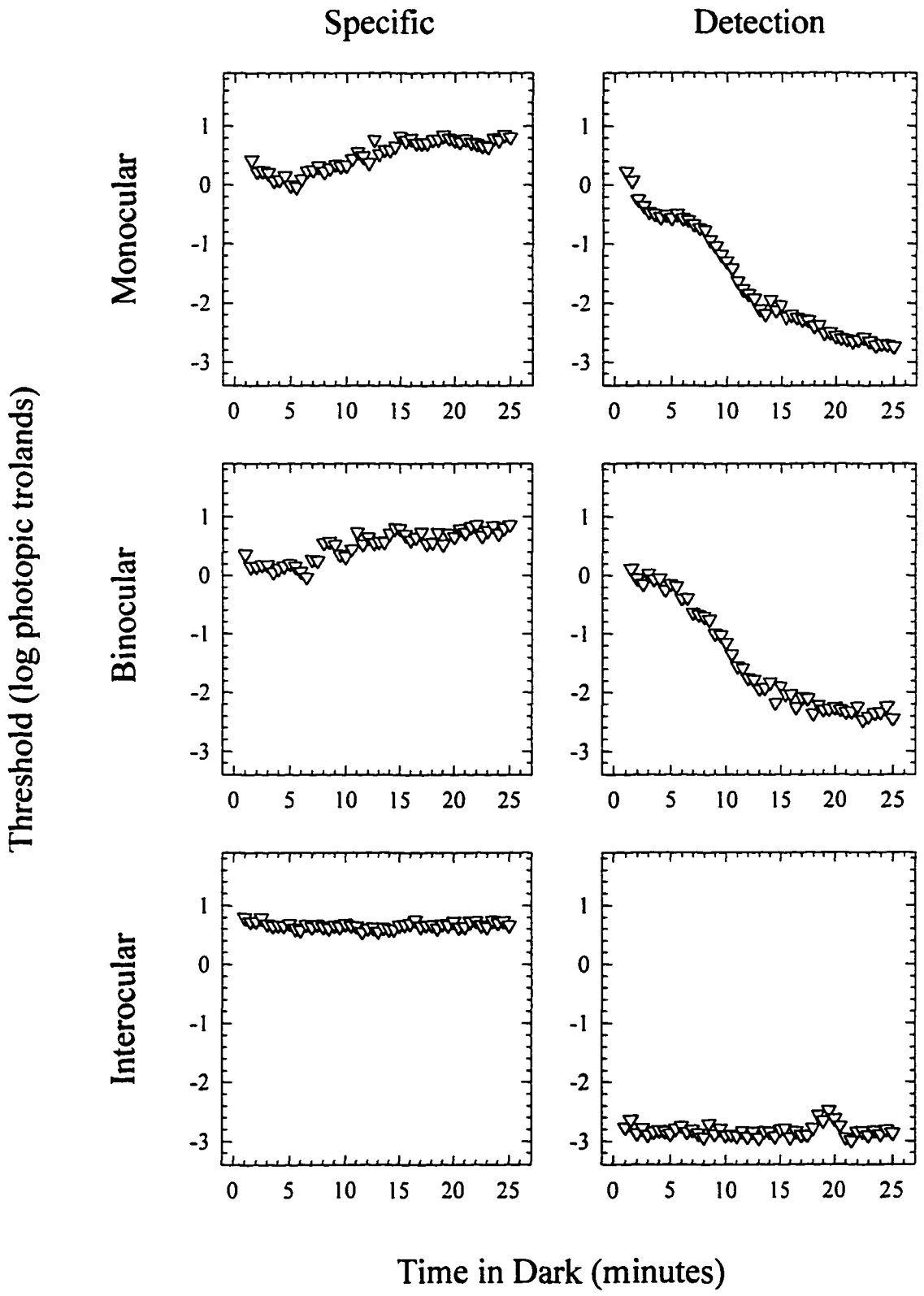

Figure 46. Specific (hue identification) and detection thresholds for observer RM for a 511 nm stimulus as a function of time in the dark following monocular, binocular, and interocular preadaptation. The test stimulus was a 3^{o} circle presented for 100 ms every 3 s at 6^{o} in the right eye temporal field.

Figure 46. Specific (Hue Identification) and Detection Thresholds
RM 511 nm

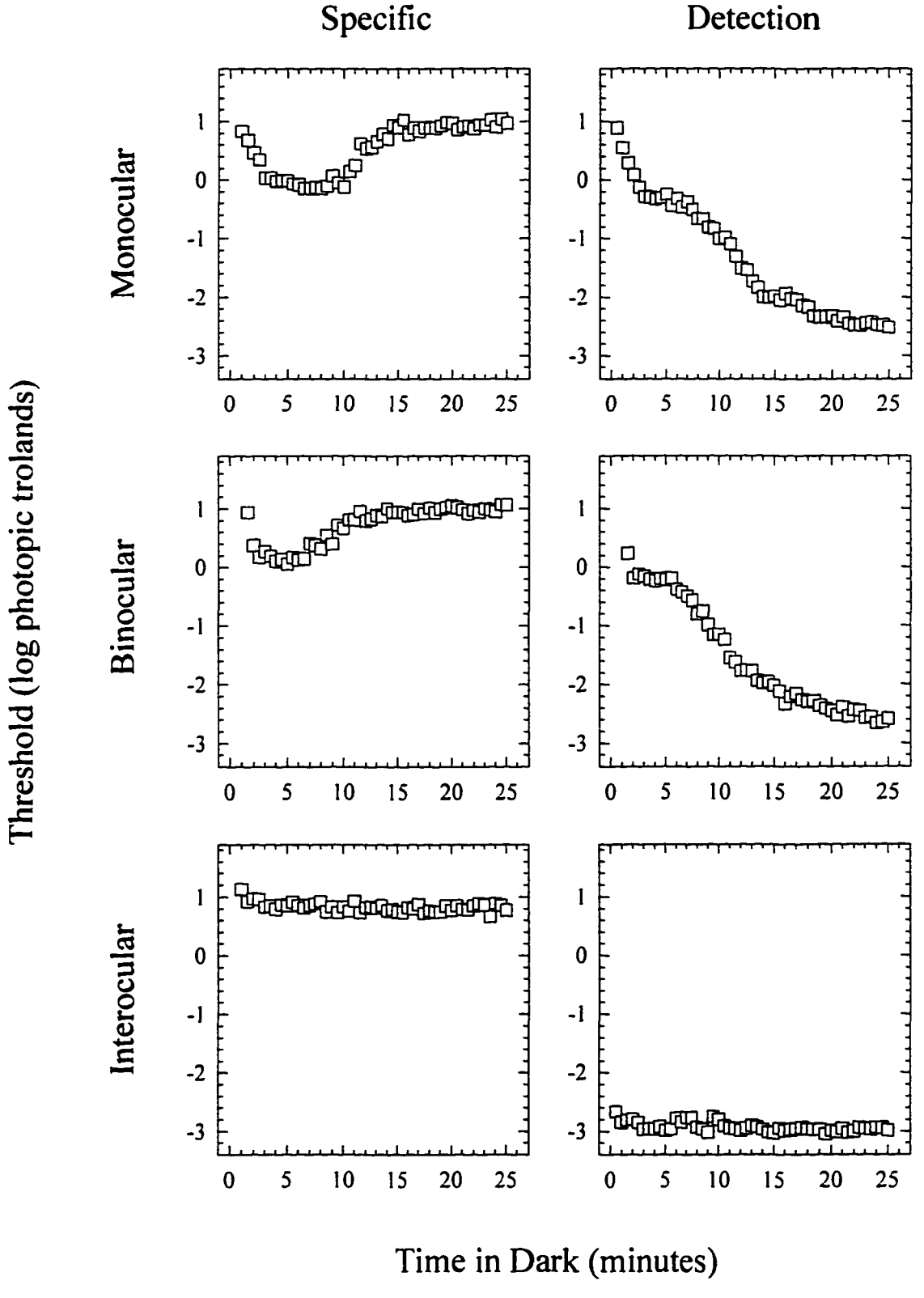

Figure 47. Specific (hue identification) and detection thresholds for observer RM for a 576 nm stimulus as a function of time in the dark following monocular, binocular, and interocular preadaptation. The test stimulus was a 3^{o} circle presented for 100 ms every 3 s at 6^{o} in the right eye temporal field.

Figure 47. Specific (Hue Identification) and Detection Thresholds RM 576 nm

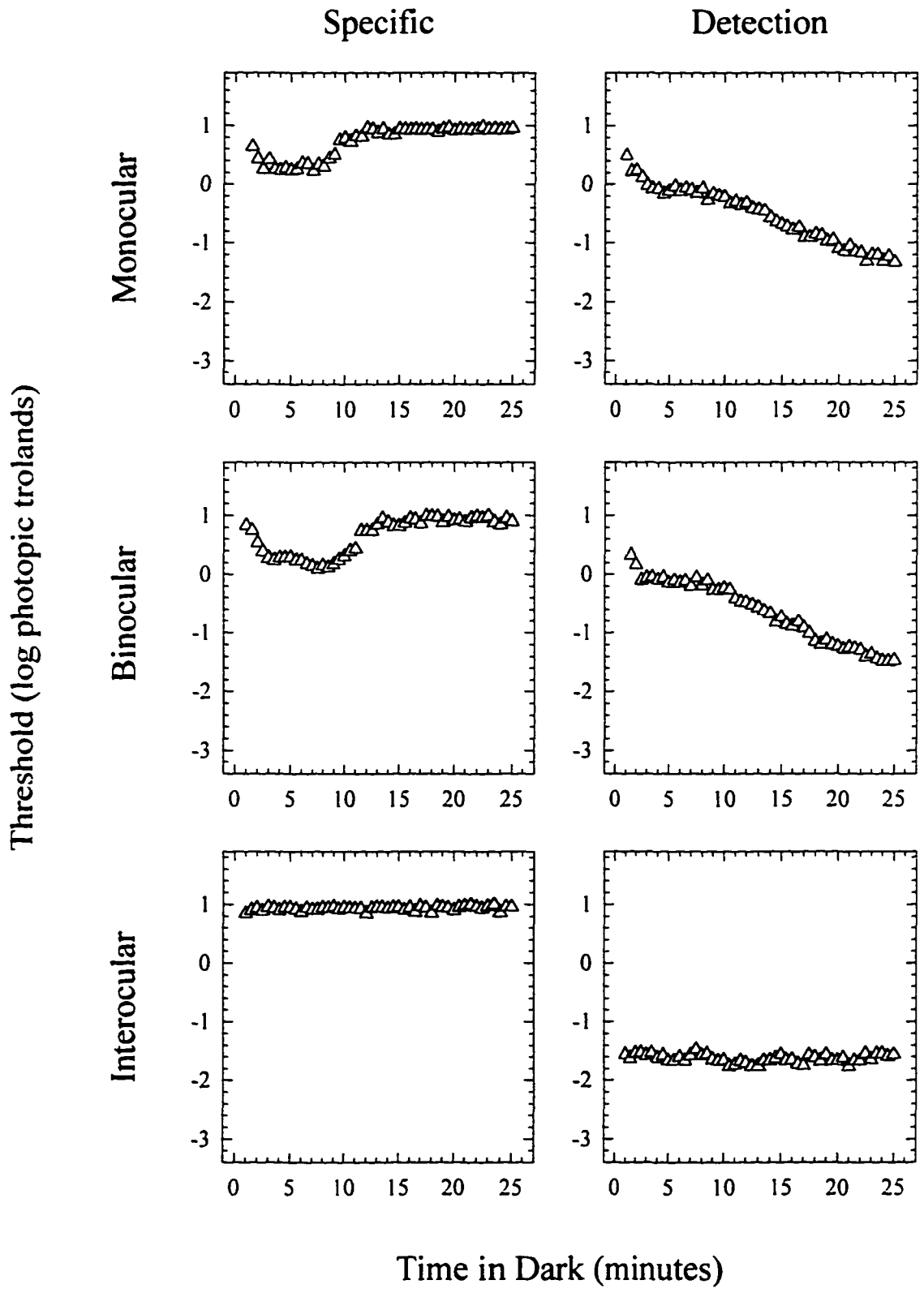

Figure 48. Specific (hue identification) and detection thresholds for observer RM for a 637 nm stimulus as a function of time in the dark following monocular, binocular, and interocular preadaptation. The test stimulus was a 3^{o} circle presented for 100 ms every 3 s at 6^{o} in the right eye temporal field.

Figure 48. Specific (Hue Identification) and Detection Thresholds
RM 637 nm

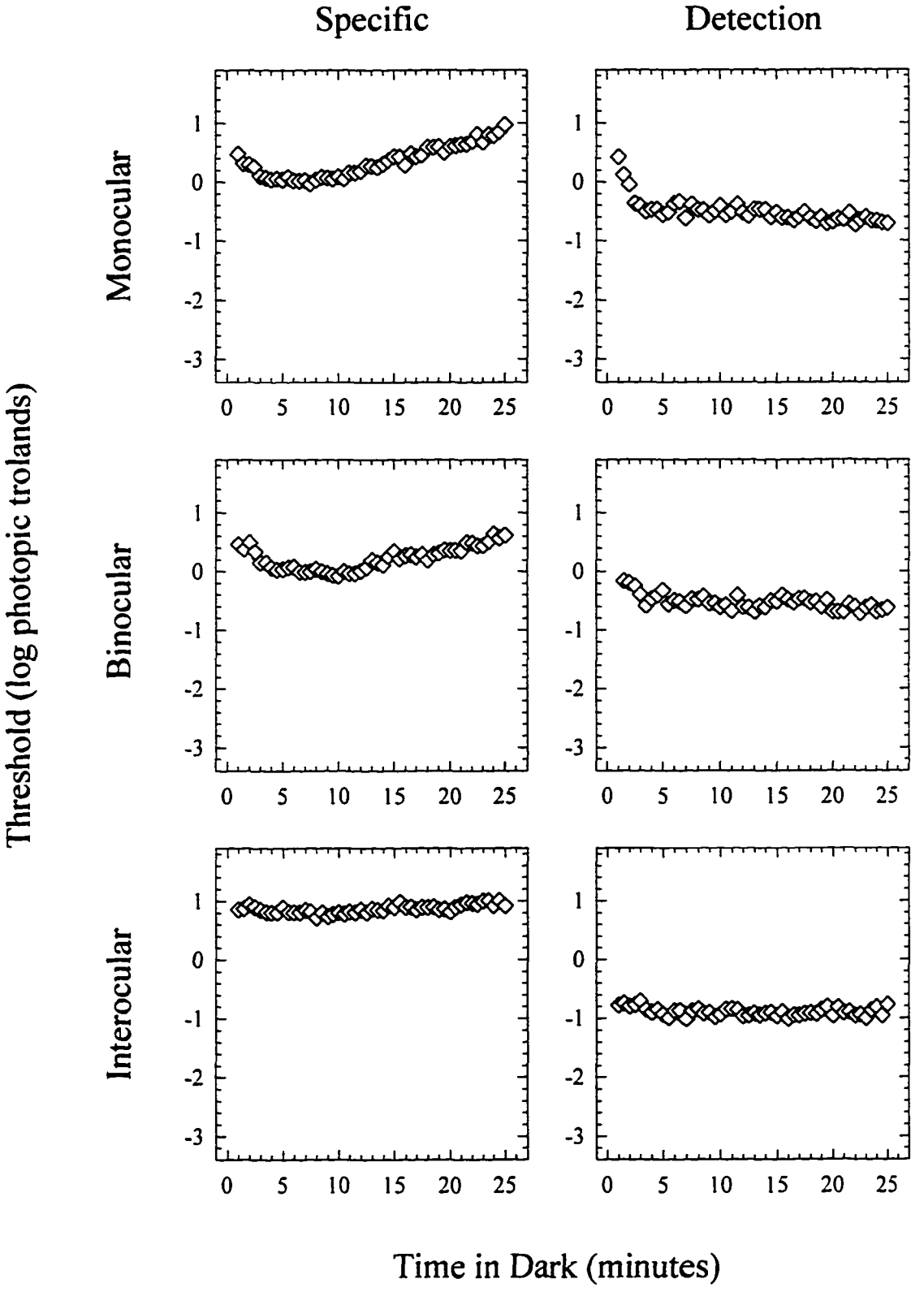

Figure 49. Specific (hue identification) and detection thresholds for observer AD for a 478 nm stimulus as a function of time in the dark following monocular, binocular, and interocular preadaptation. The test stimulus was a 3^{o} circle presented for 100 ms every 3 s at 6^{o} in the right eye temporal field.

Figure 49. Specific (Hue Identification) and Detection Thresholds AD 478 nm

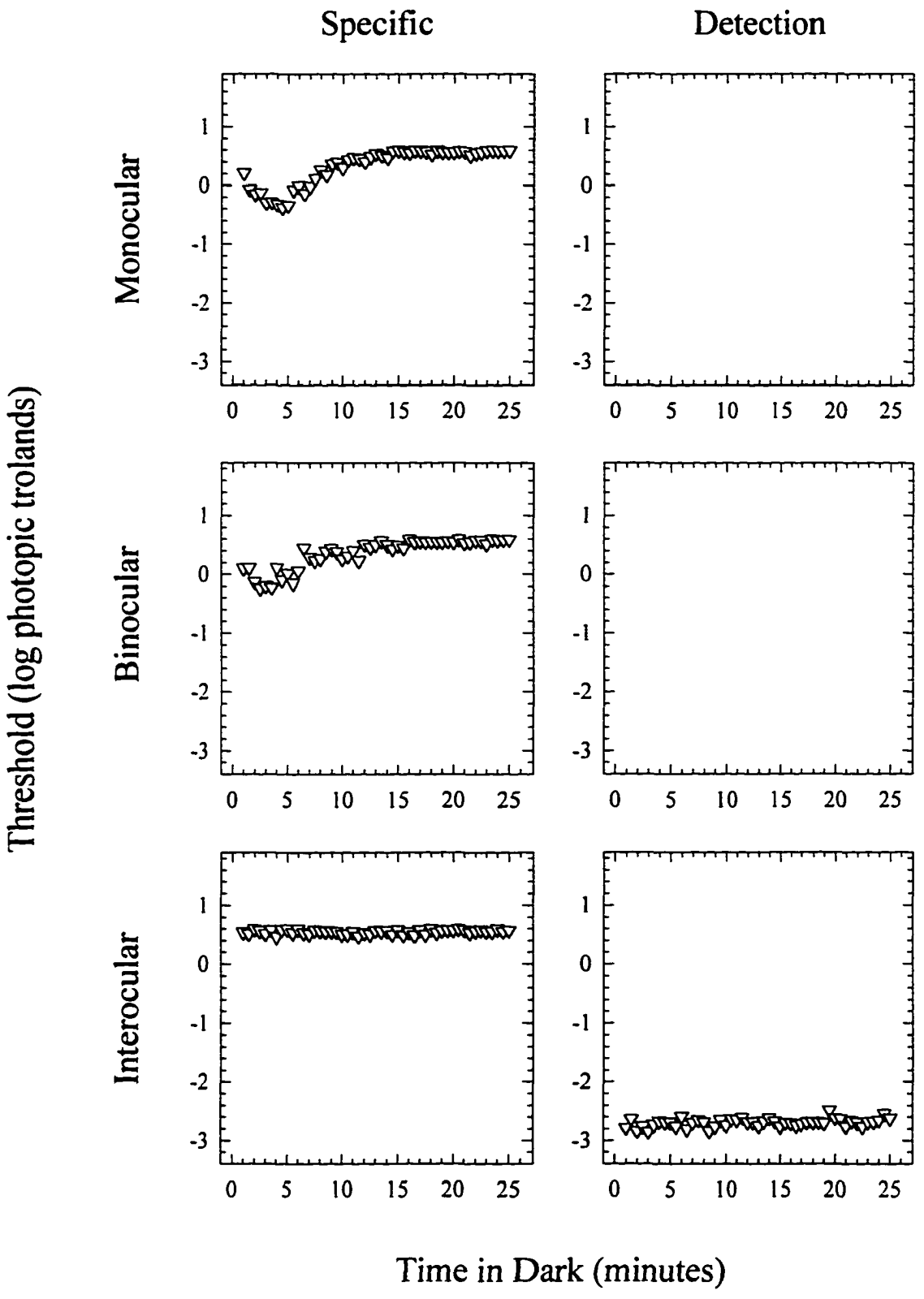

Figure 50. Specific (hue identification) and detection thresholds for observer AD for a 511 nm stimulus as a function of time in the dark following monocular, binocular, and interocular preadaptation. The test stimulus was a 3^{o} circle presented for 100 ms every 3 s at 6^{o} in the right eye temporal field.

Figure 50. Specific (Hue Identification) and Detection Thresholds AD 511 nm

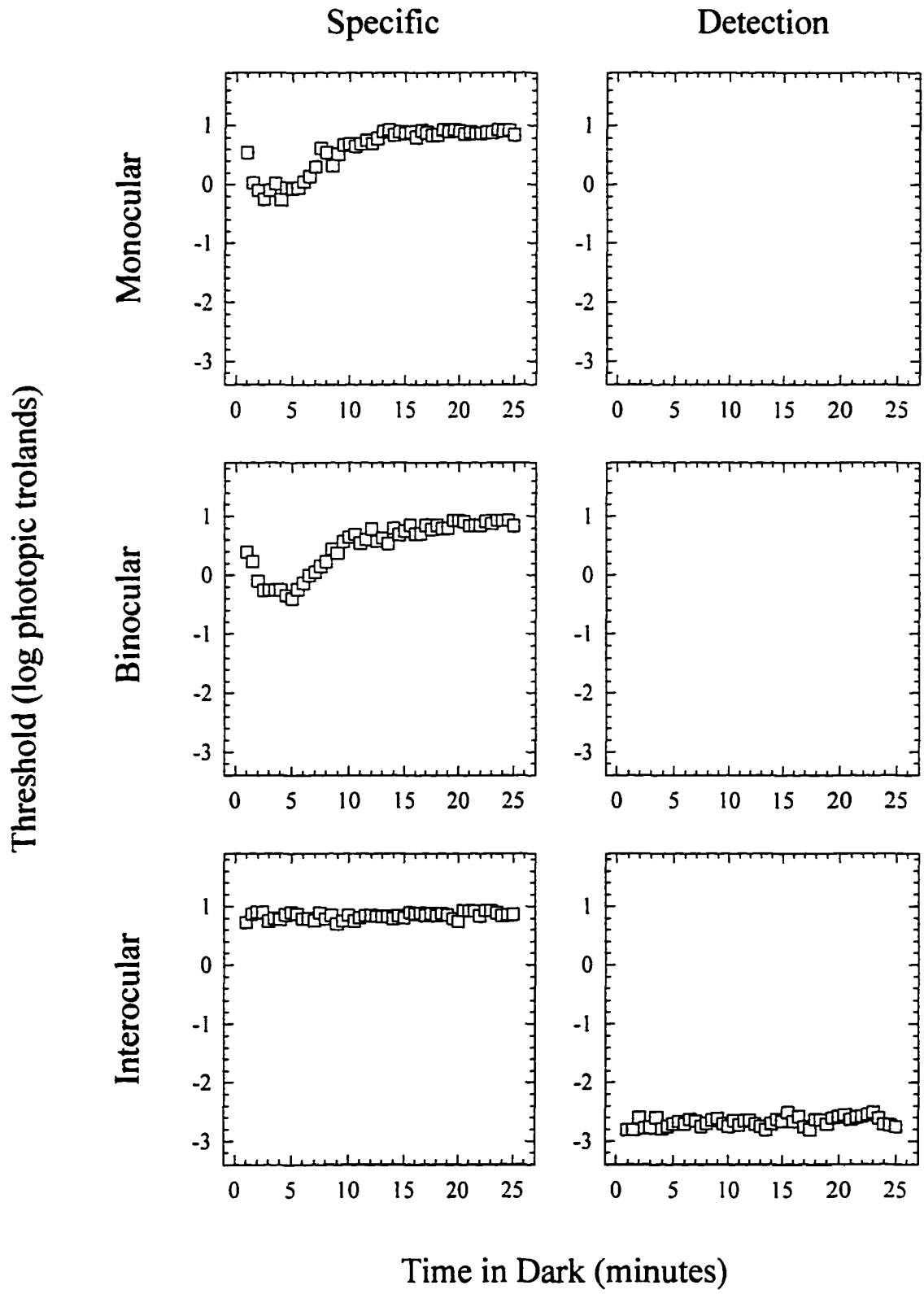

Figure 51. Specific (hue identification) and detection thresholds for observer AD for a 576 nm stimulus as a function of time in the dark following monocular, binocular, and interocular preadaptation. The test stimulus was a 3^{o} circle presented for 100 ms every 3 s at 6^{o} in the right eye temporal field.

Figure 51. Specific (Hue Identification) and Detection Thresholds AD 576 nm

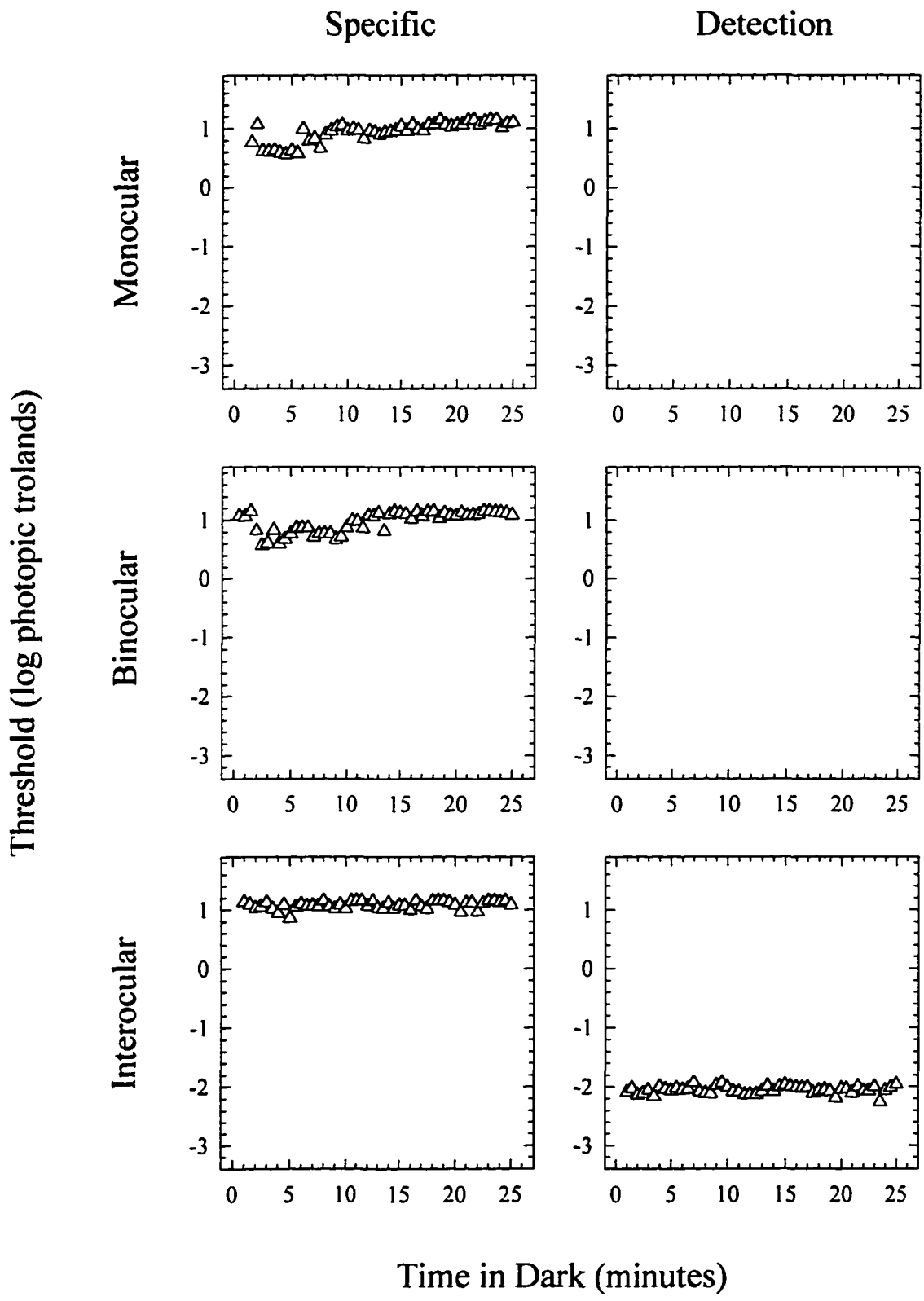

Figure 52. Specific (hue identification) and detection thresholds for observer AD for a 637 nm stimulus as a function of time in the dark following monocular, binocular, and interocular preadaptation. The test stimulus was a 3^{o} circle presented for 100 ms every 3 s at 6^{o} in the right eye temporal field.

Figure 52. Specific (Hue Identification) and Detection Thresholds AD 637 nm

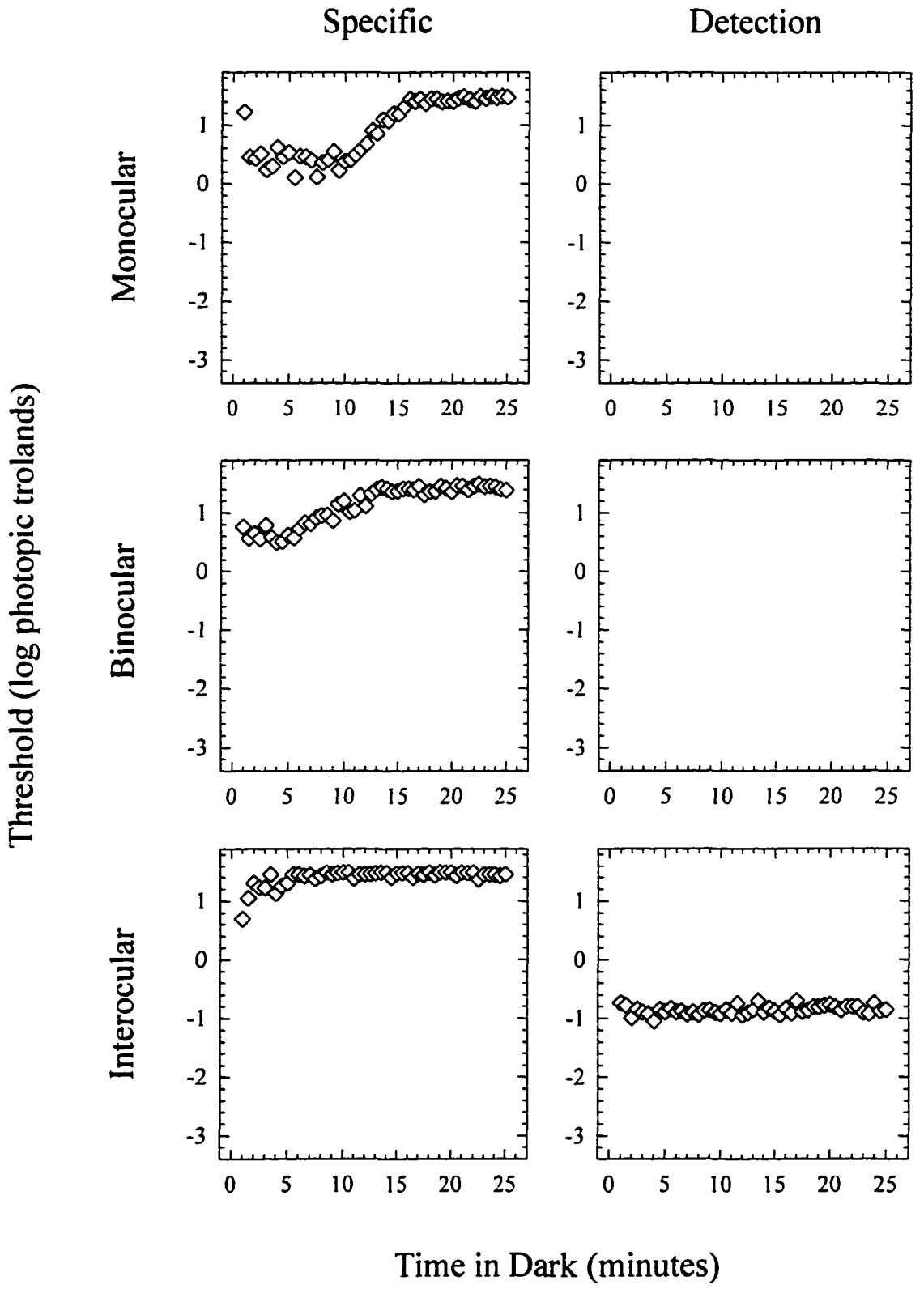

Appendix B

Appendix B is a compilation of figures showing hue and saturation scaling for observers EL, MT, and AD for all four test stimuli following monocular, binocular, and interocular preadaptation.

Figure 53. Hue and saturation scaling for observer EL for a 478 nm stimulus as a function of time in the dark following monocular preadaptation. The test stimulus was a 3^{o} circle presented for 100 ms every 5 s at 6^{o} in the right eye temporal field.

Figure 53. Hue and Saturation Scaling
EL 478 nm Monocular

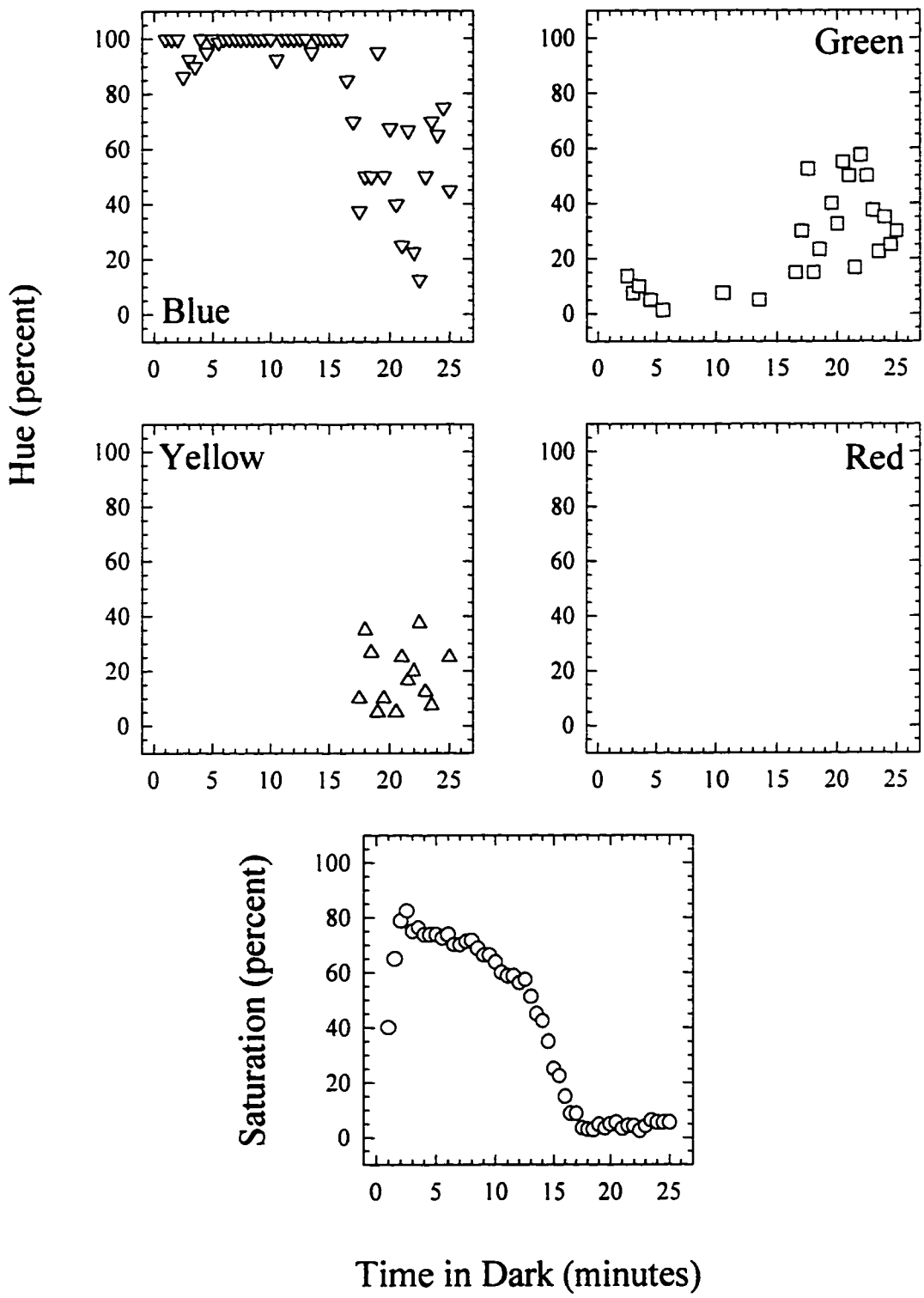

Figure 54. Hue and saturation scaling for observer EL for a 478 nm stimulus as a function of time in the dark following binocular preadaptation. The test stimulus was a 3^{o} circle presented for 100 ms every 5 s at 6^{o} in the right eye temporal field.

Figure 54. Hue and Saturation Scaling
EL 478 nm Binocular

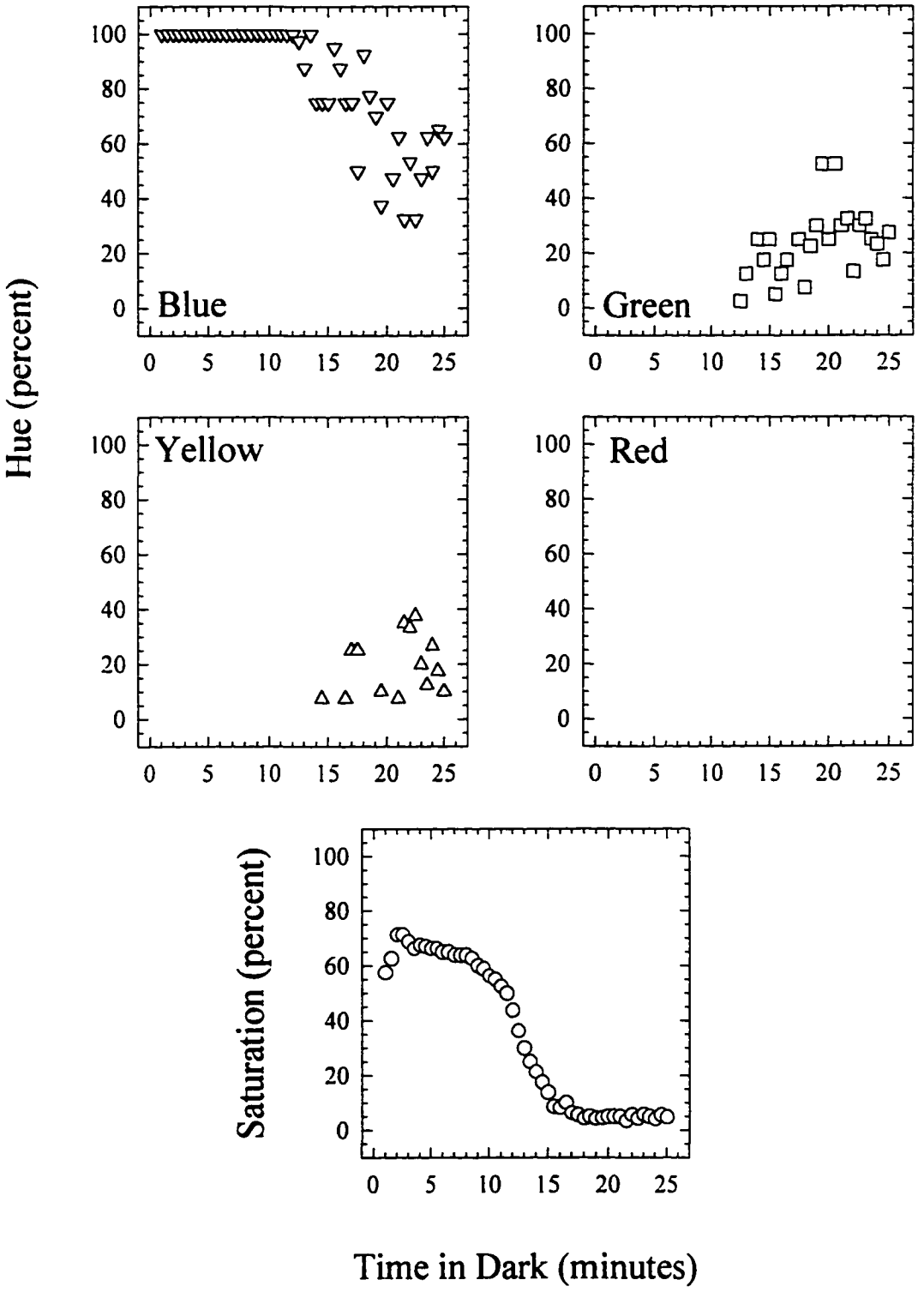

Figure 55. Hue and saturation scaling for observer EL for a 478 nm stimulus as a function of time in the dark following interocular preadaptation. The test stimulus was a 3^{o} circle presented for 100 ms every 5 s at 6^{o} in the right eye temporal field.

Figure 55. Hue and Saturation Scaling
EL 478 nm Interocular

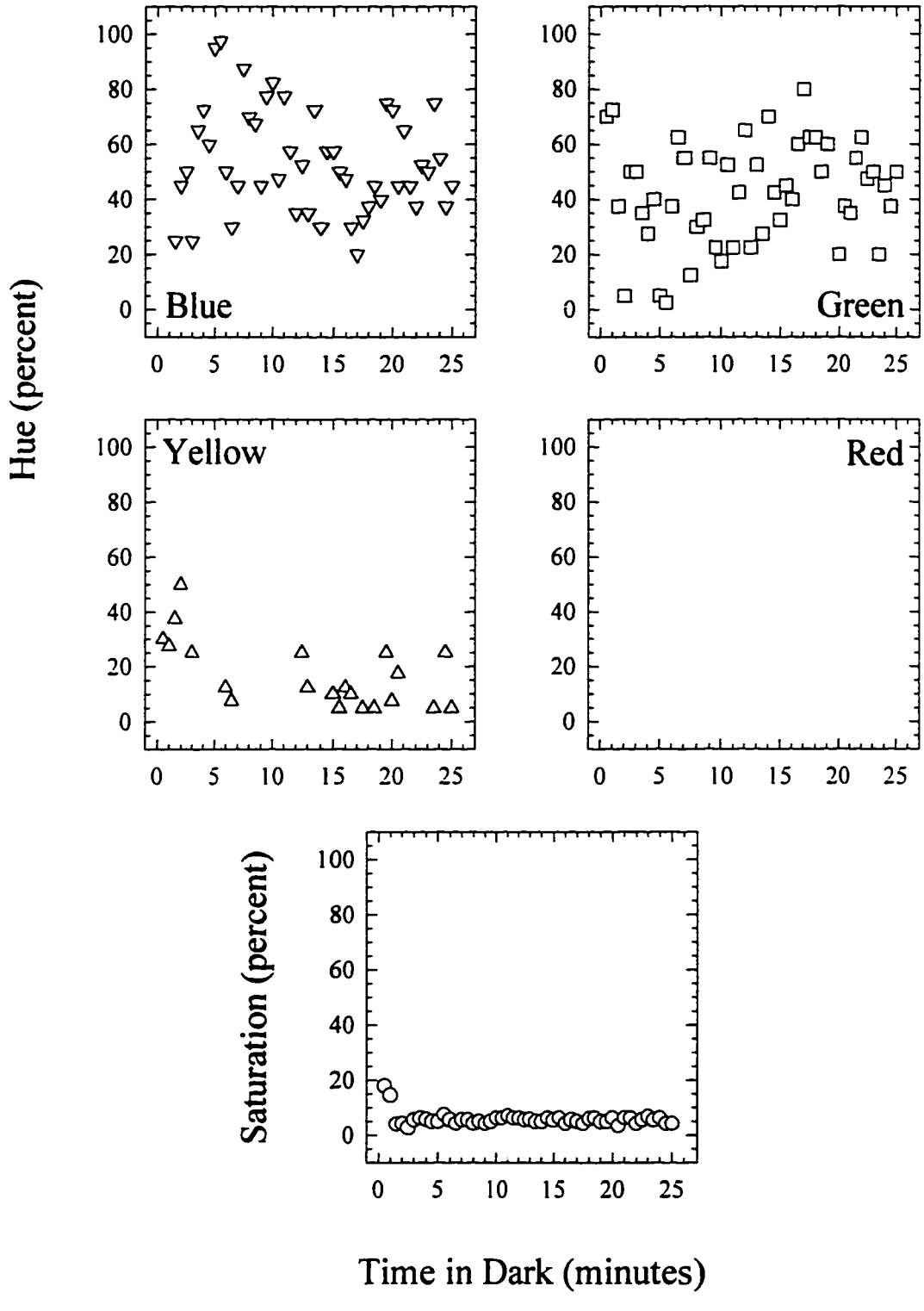

Figure 56. Hue and saturation scaling for observer EL for a 511 nm stimulus as a function of time in the dark following monocular preadaptation. The test stimulus was a 3^{o} circle presented for 100 ms every 5 s at 6^{o} in the right eye temporal field.

Figure 56. Hue and Saturation Scaling
EL 511 nm Monocular

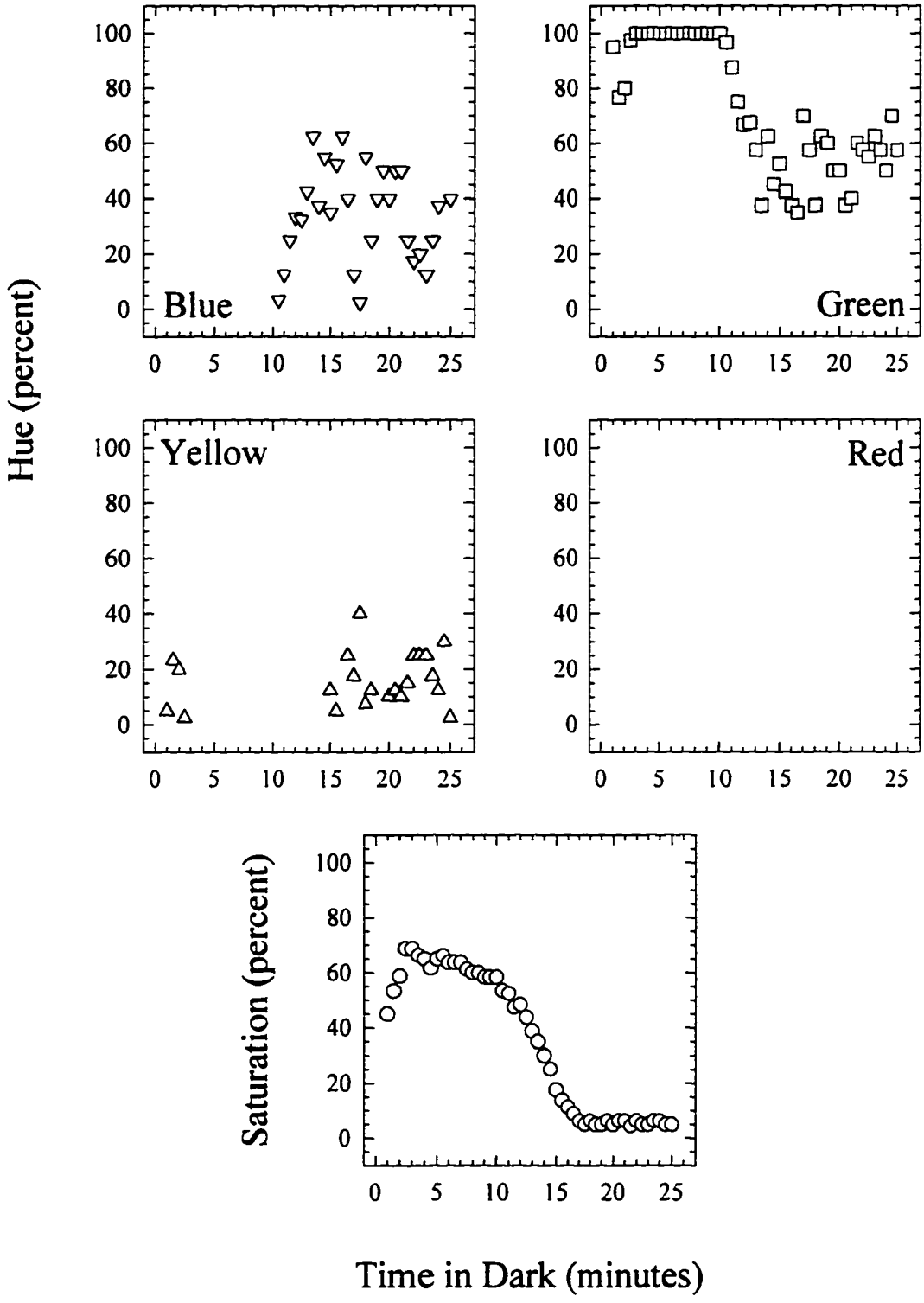

Figure 57. Hue and saturation scaling for observer EL for a 511 nm stimulus as a function of time in the dark following binocular preadaptation. The test stimulus was a 3^{o} circle presented for 100 ms every 5 s at 6^{o} in the right eye temporal field.

Figure 57. Hue and Saturation Scaling
EL 511 nm Binocular

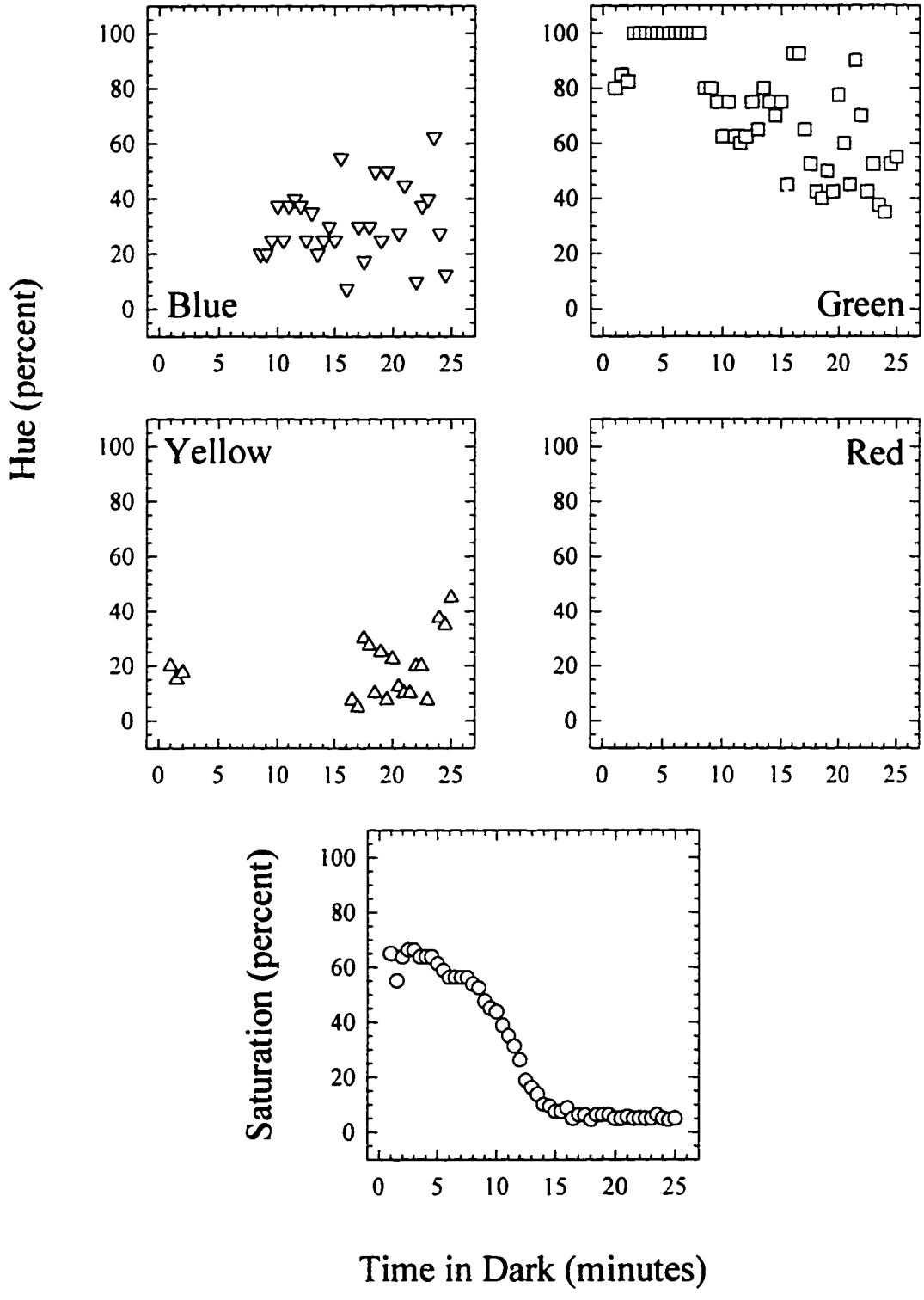

Figure 58. Hue and saturation scaling for observer EL for a 511 nm stimulus as a function of time in the dark following interocular preadaptation. The test stimulus was a 3^{o} circle presented for 100 ms every 5 s at 6^{o} in the right eye temporal field.

Figure 58. Hue and Saturation Scaling
EL 511 nm Interocular

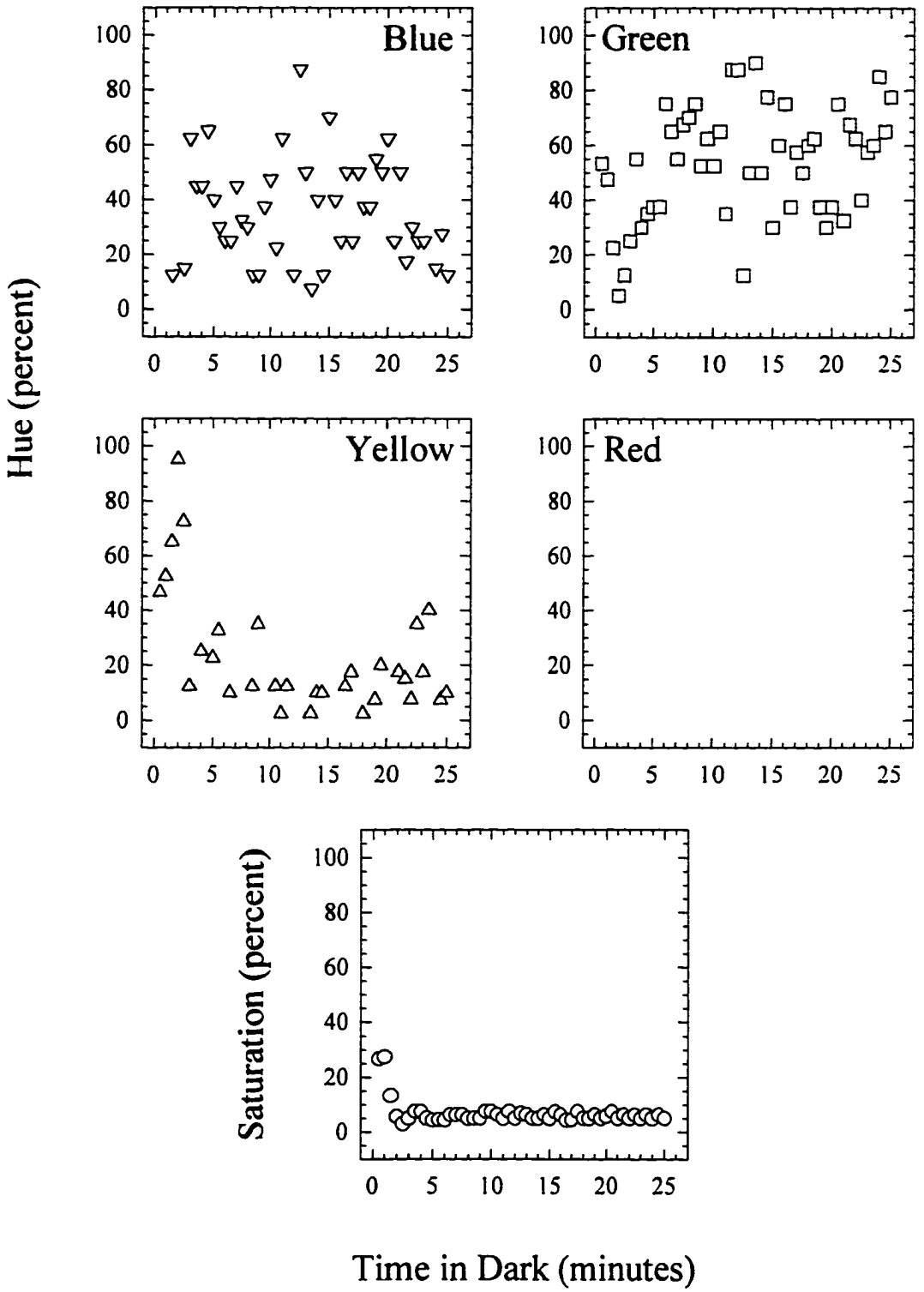

Figure 59. Hue and saturation scaling for observer EL for a 576 nm stimulus as a function of time in the dark following monocular preadaptation. The test stimulus was a 3^{o} circle presented for 100 ms every 5 s at 6^{o} in the right eye temporal field.

Figure 59. Hue and Saturation Scaling
EL 576 nm Monocular

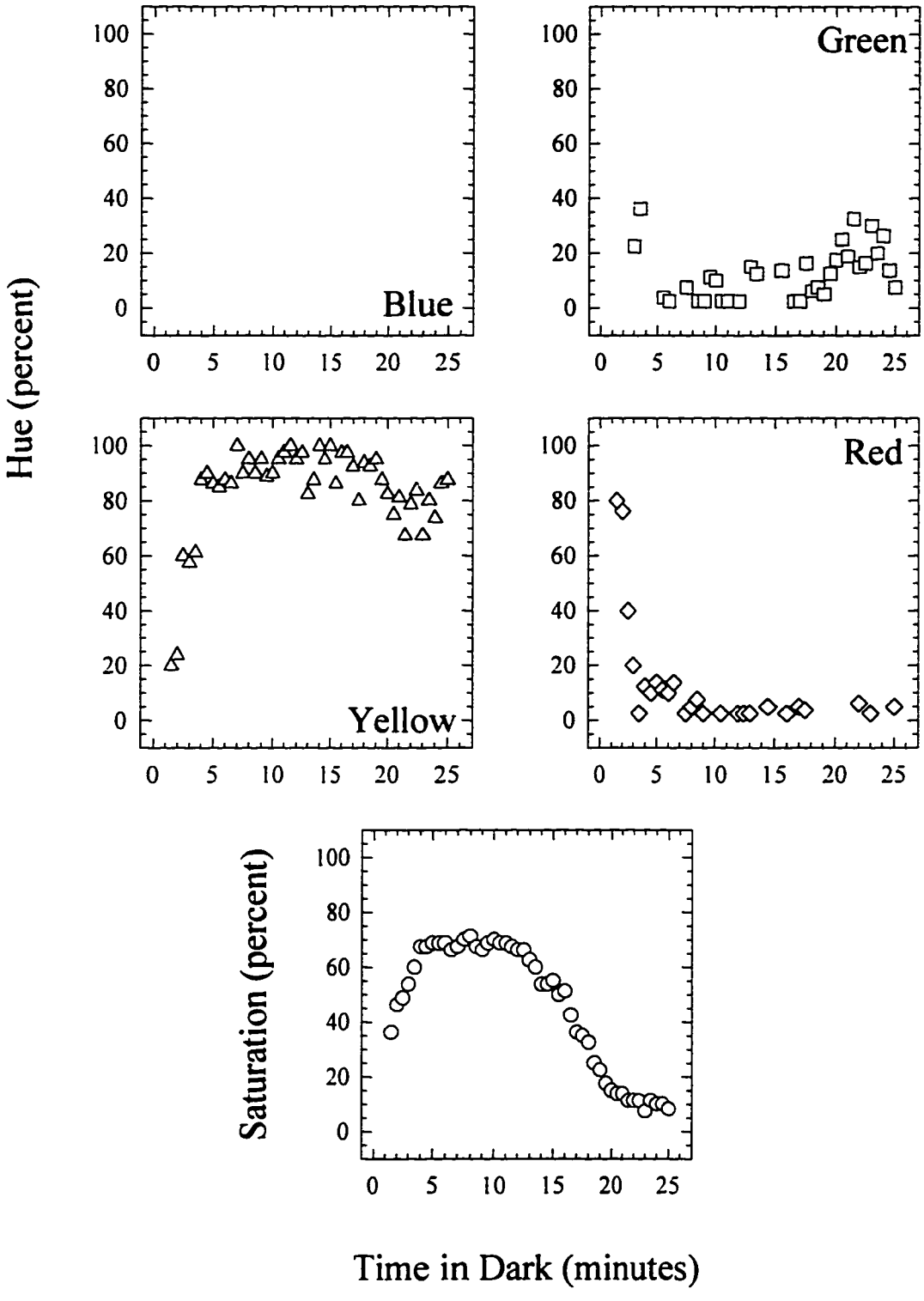

Figure 60. Hue and saturation scaling for observer EL for a 576 nm stimulus as a function of time in the dark following binocular preadaptation. The test stimulus was a 3^{o} circle presented for 100 ms every 5 s at 6^{o} in the right eye temporal field.

Figure 60. Hue and Saturation Scaling
EL 576 nm Binocular

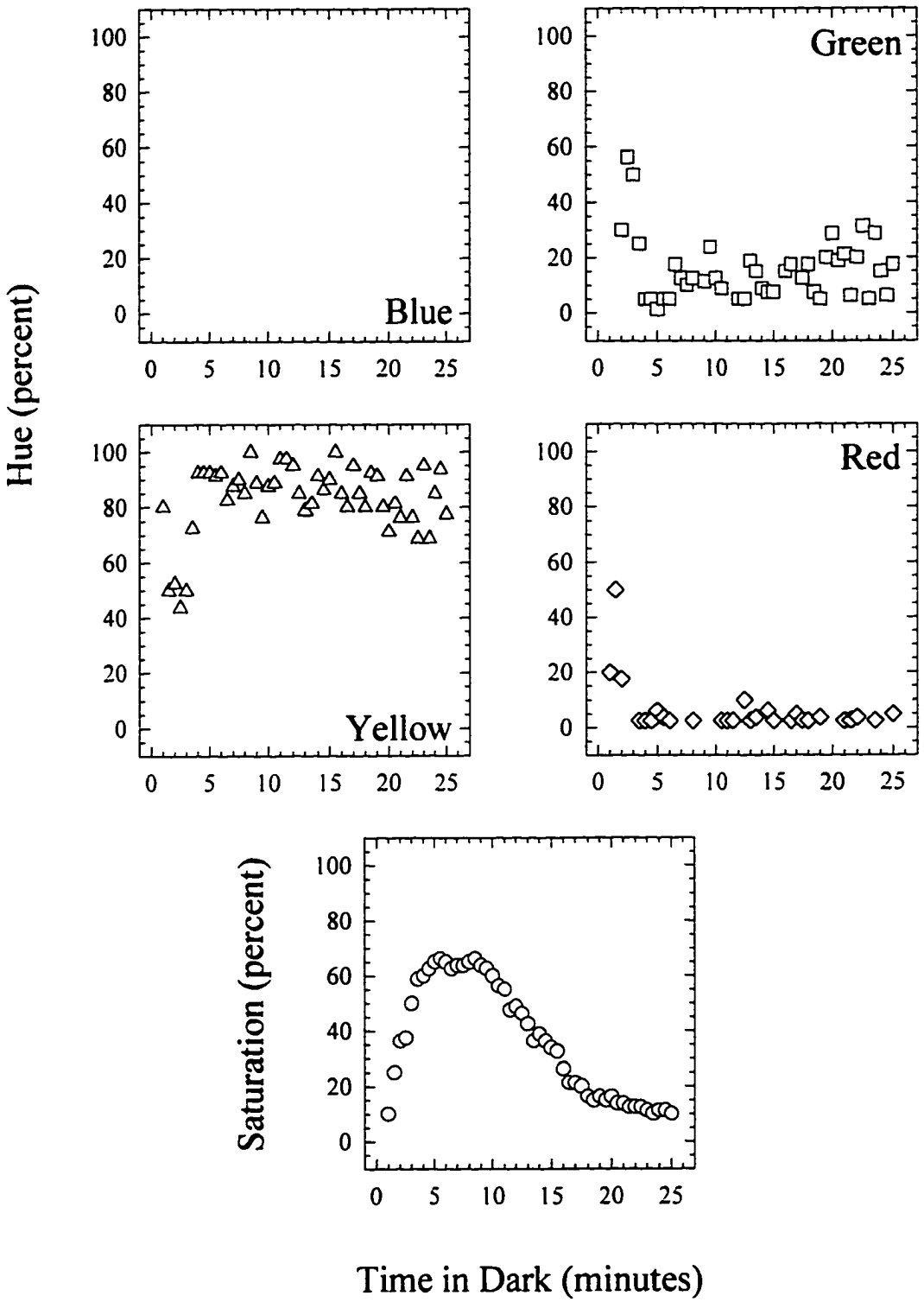

Figure 61. Hue and saturation scaling for observer EL for a 576 nm stimulus as a function of time in the dark following interocular preadaptation. The test stimulus was a 3^{o} circle presented for 100 ms every 5 s at 6^{o} in the right eye temporal field.

Figure 61. Hue and Saturation Scaling
EL 576 nm Interocular

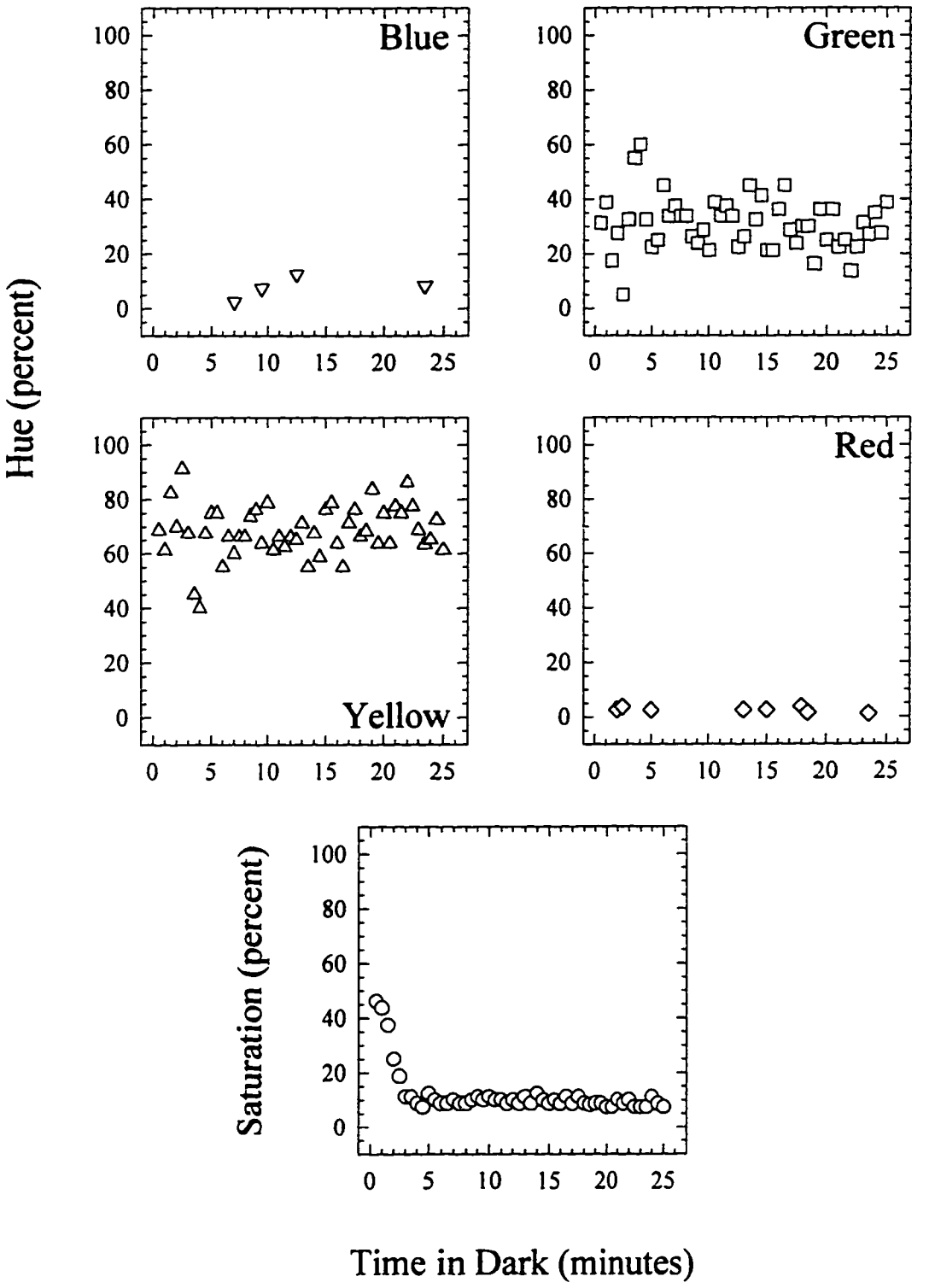

Figure 62. Hue and saturation scaling for observer EL for a 637 nm stimulus as a function of time in the dark following monocular preadaptation. The test stimulus was a 3^{o} circle presented for 100 ms every 5 s at 6^{o} in the right eye temporal field.

Figure 62. Hue and Saturation Scaling
EL 637 nm Monocular

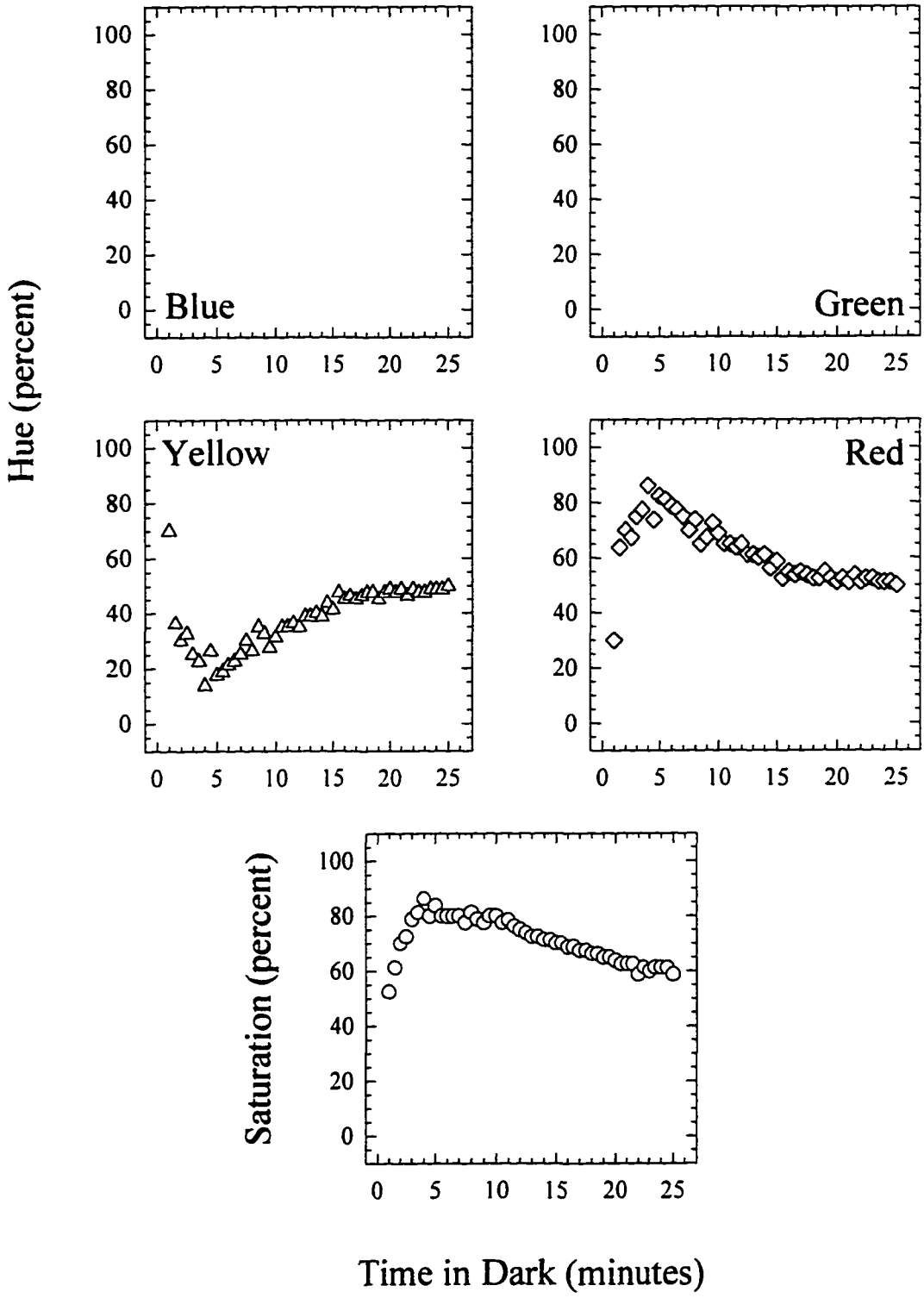

Figure 63. Hue and saturation scaling for observer EL for a 637 nm stimulus as a function of time in the dark following binocular preadaptation. The test stimulus was a 3^{o} circle presented for 100 ms every 5 s at 6^{o} in the right eye temporal field.

Figure 63. Hue and Saturation Scaling
EL 637 nm Binocular

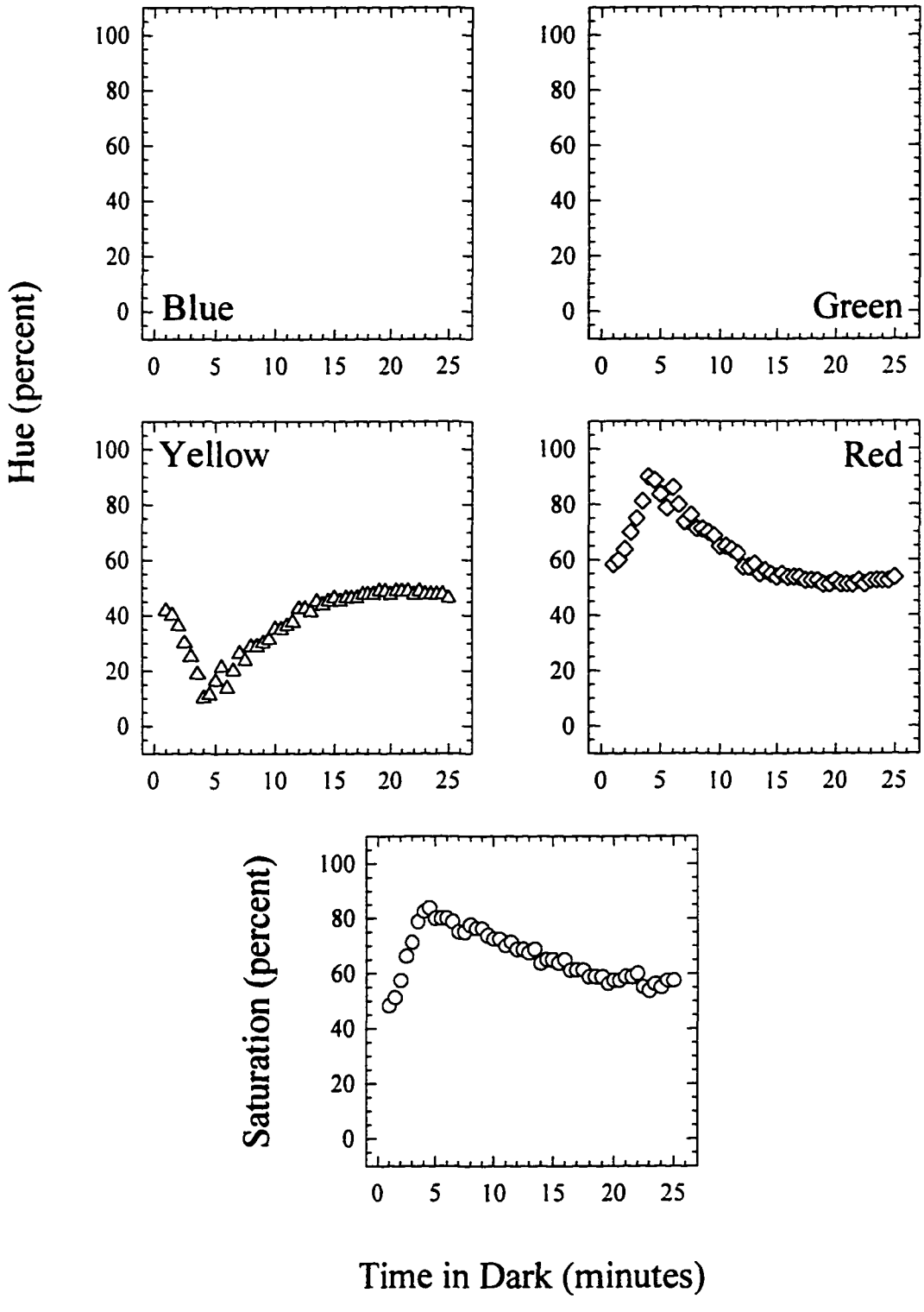

Figure 64. Hue and saturation scaling for observer EL for a 637 nm stimulus as a function of time in the dark following interocular preadaptation. The test stimulus was a 3^{o} circle presented for 100 ms every 5 s at 6^{o} in the right eye temporal field.

Figure 64. Hue and Saturation Scaling
EL 637 nm Interocular

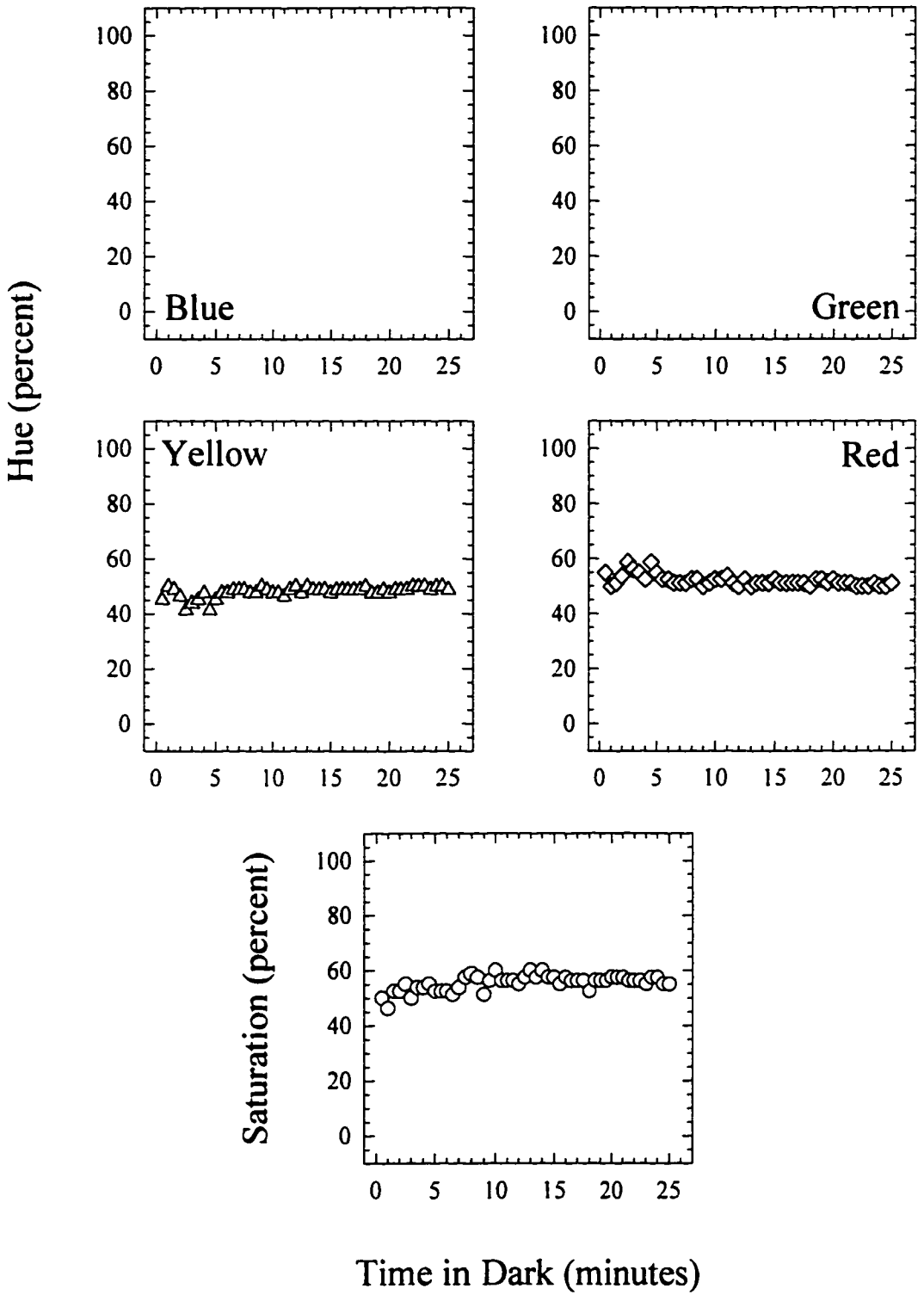

Figure 65. Hue and saturation scaling for observer MT for a 478 nm stimulus as a function of time in the dark following monocular preadaptation. The test stimulus was a 3^{o} circle presented for 100 ms every 5 s at 6^{o} in the right eye temporal field.

Figure 65. Hue and Saturation Scaling
MT 478 nm Monocular

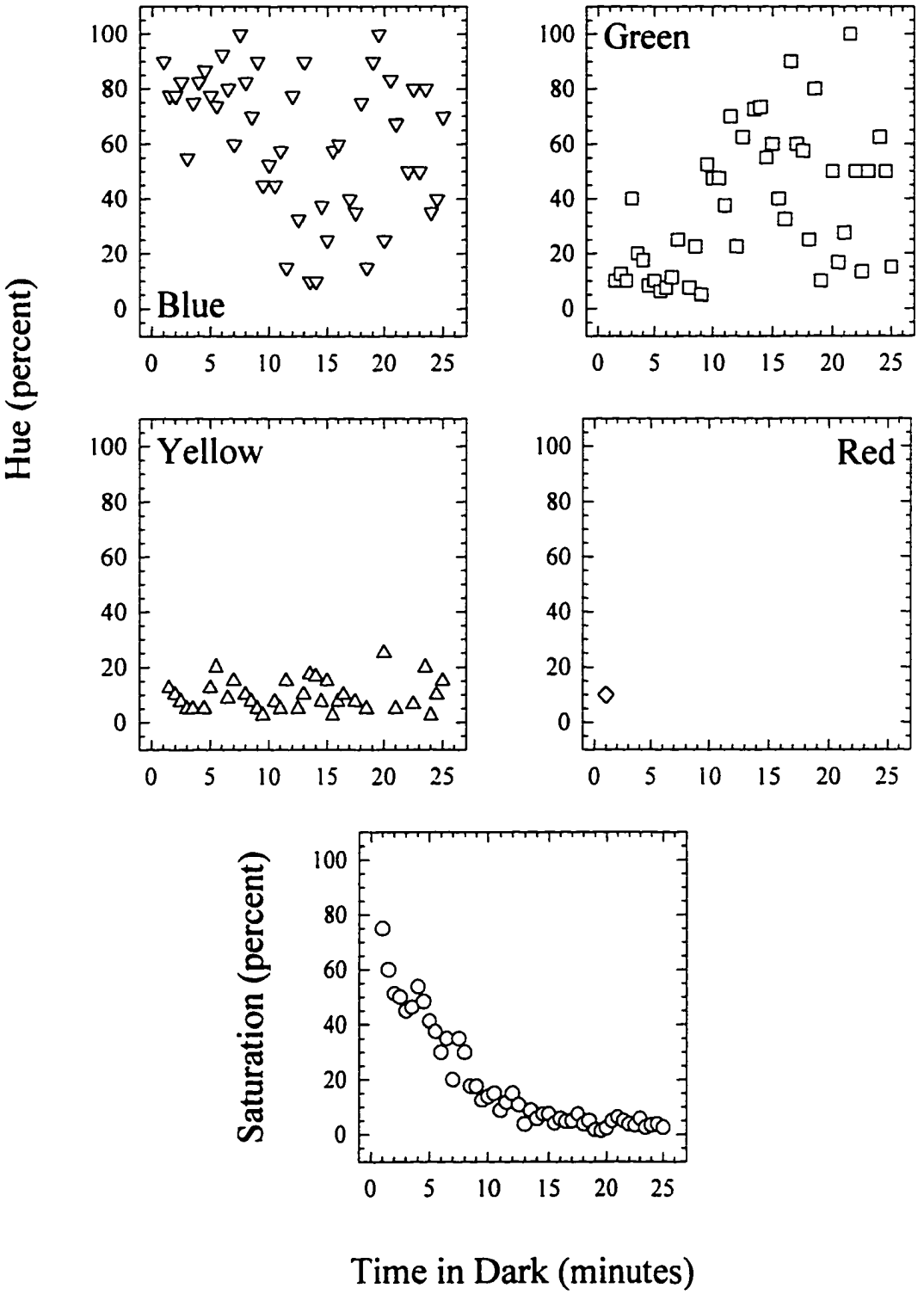

Figure 66. Hue and saturation scaling for observer MT for a 478 nm stimulus as a function of time in the dark following binocular preadaptation. The test stimulus was a 3^{o} circle presented for 100 ms every 5 s at 6^{o} in the right eye temporal field.

Figure 66. Hue and Saturation Scaling
MT 478 nm Binocular

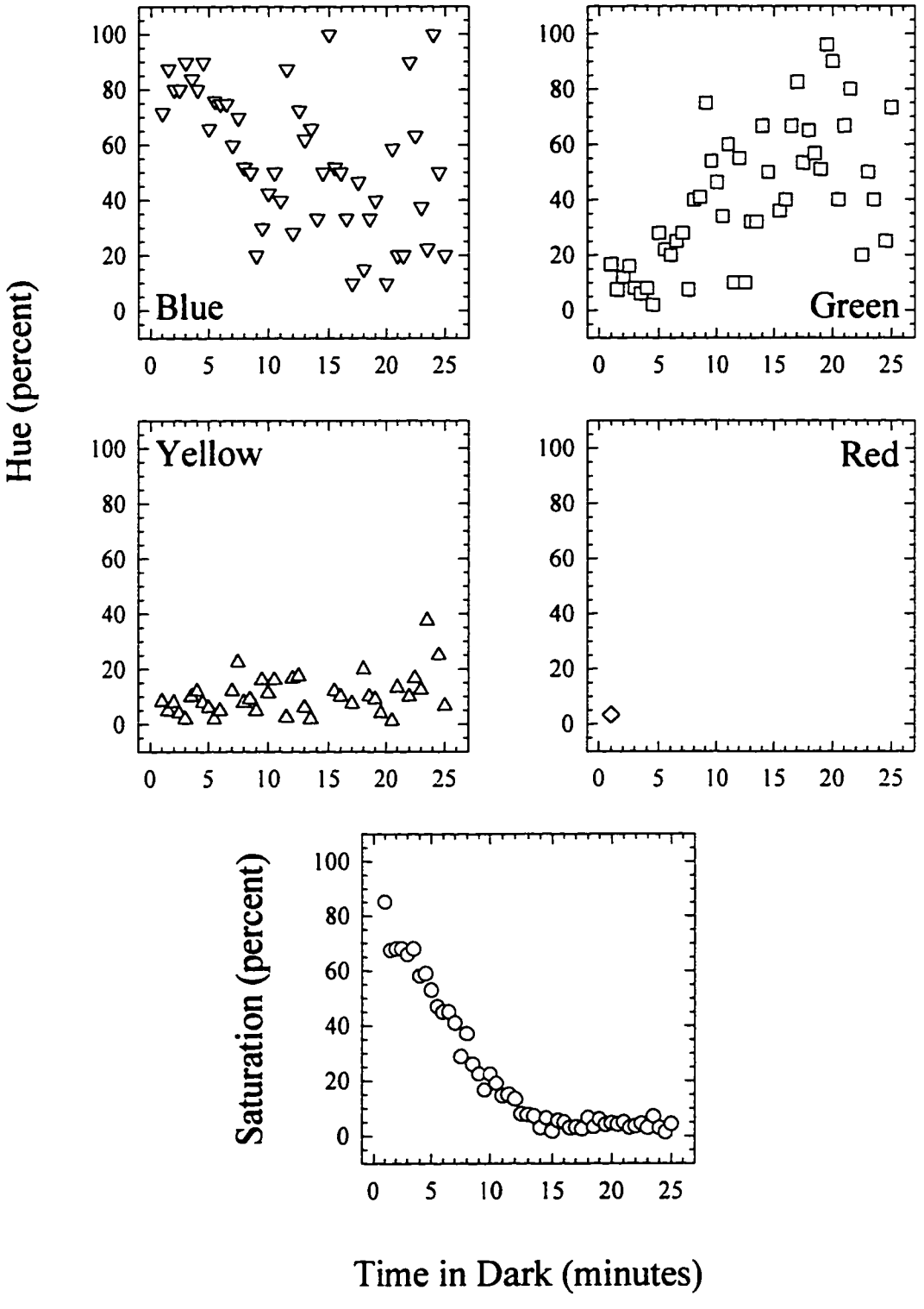

Figure 67. Hue and saturation scaling for observer MT for a 478 nm stimulus as a function of time in the dark following interocular preadaptation. The test stimulus was a 3^{o} circle presented for 100 ms every 5 s at 6^{o} in the right eye temporal field.

Figure 67. Hue and Saturation Scaling
MT 478 nm Interocular

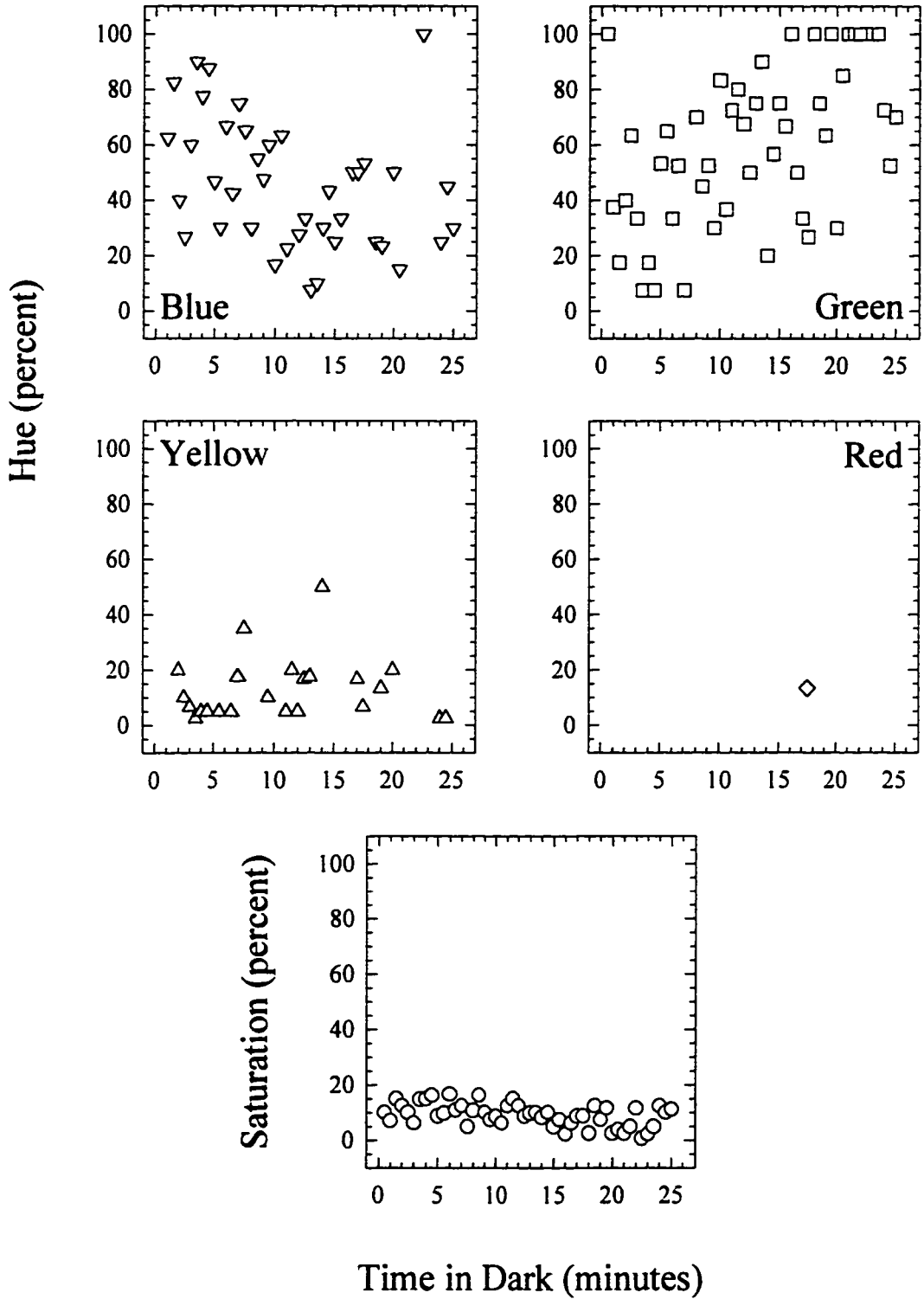

Figure 68. Hue and saturation scaling for observer MT for a 511 nm stimulus as a function of time in the dark following monocular preadaptation. The test stimulus was a 3^{o} circle presented for 100 ms every 5 s at 6^{o} in the right eye temporal field.

Figure 68. Hue and Saturation Scaling
MT 511 nm Monocular

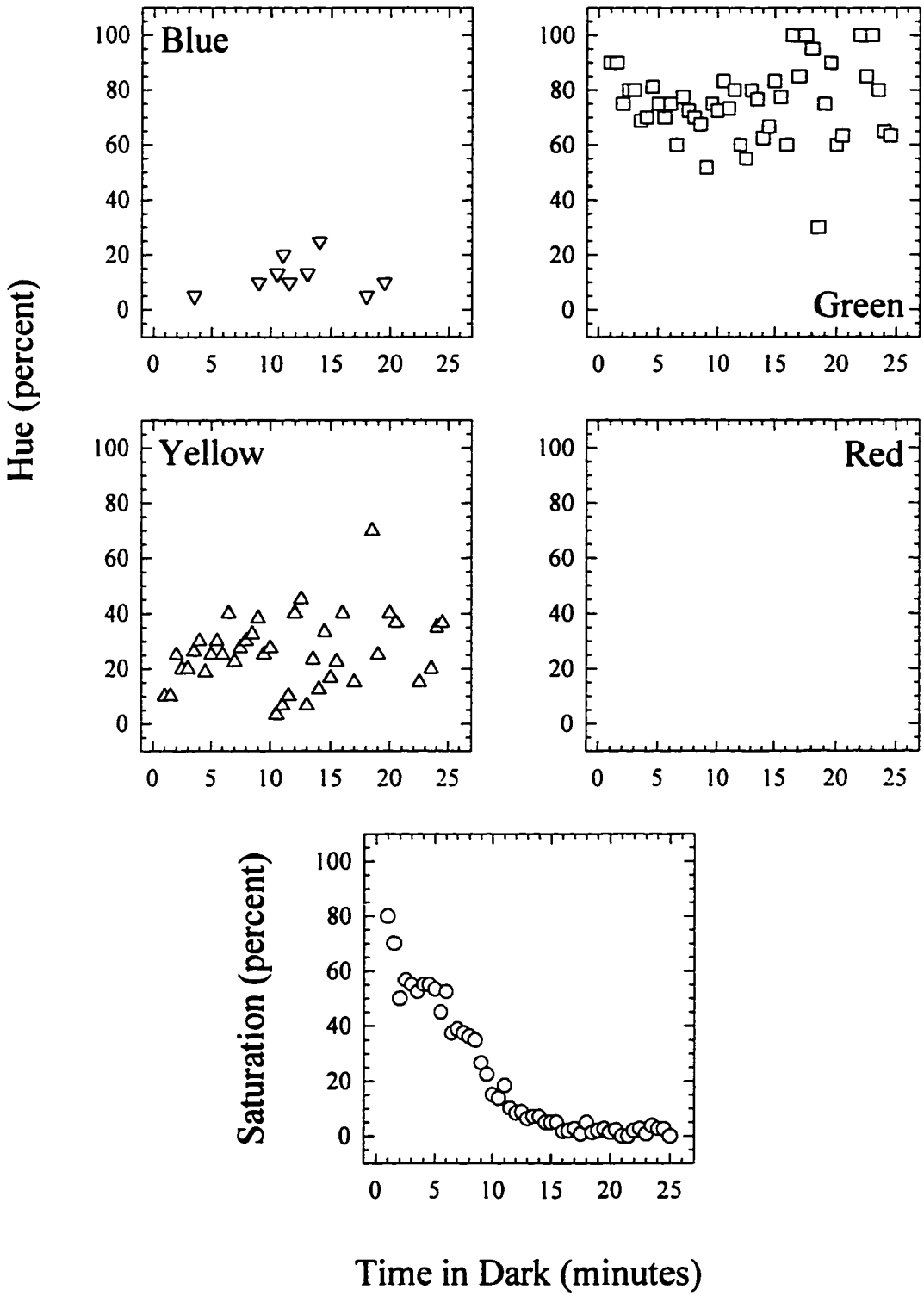

Figure 69. Hue and saturation scaling for observer MT for a 511 nm stimulus as a function of time in the dark following binocular preadaptation. The test stimulus was a 3^{o} circle presented for 100 ms every 5 s at 6^{o} in the right eye temporal field.

Figure 69. Hue and Saturation Scaling
MT 511 nm Binocular

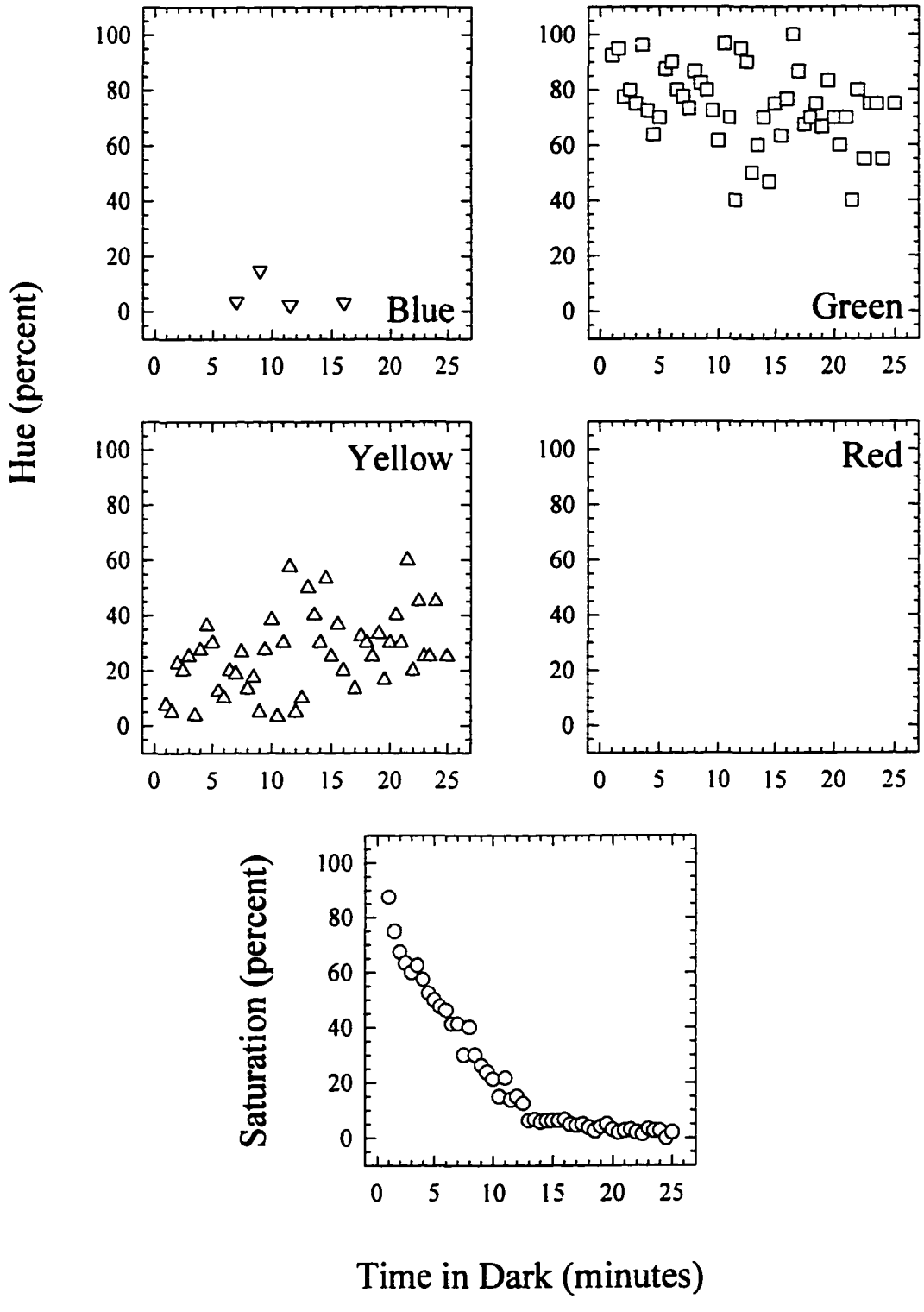

Figure 70. Hue and saturation scaling for observer MT for a 511 nm stimulus as a function of time in the dark following interocular preadaptation. The test stimulus was a 3^{o} circle presented for 100 ms every 5 s at 6^{o} in the right eye temporal field.

Figure 70. Hue and Saturation Scaling
MT 511 nm Interocular

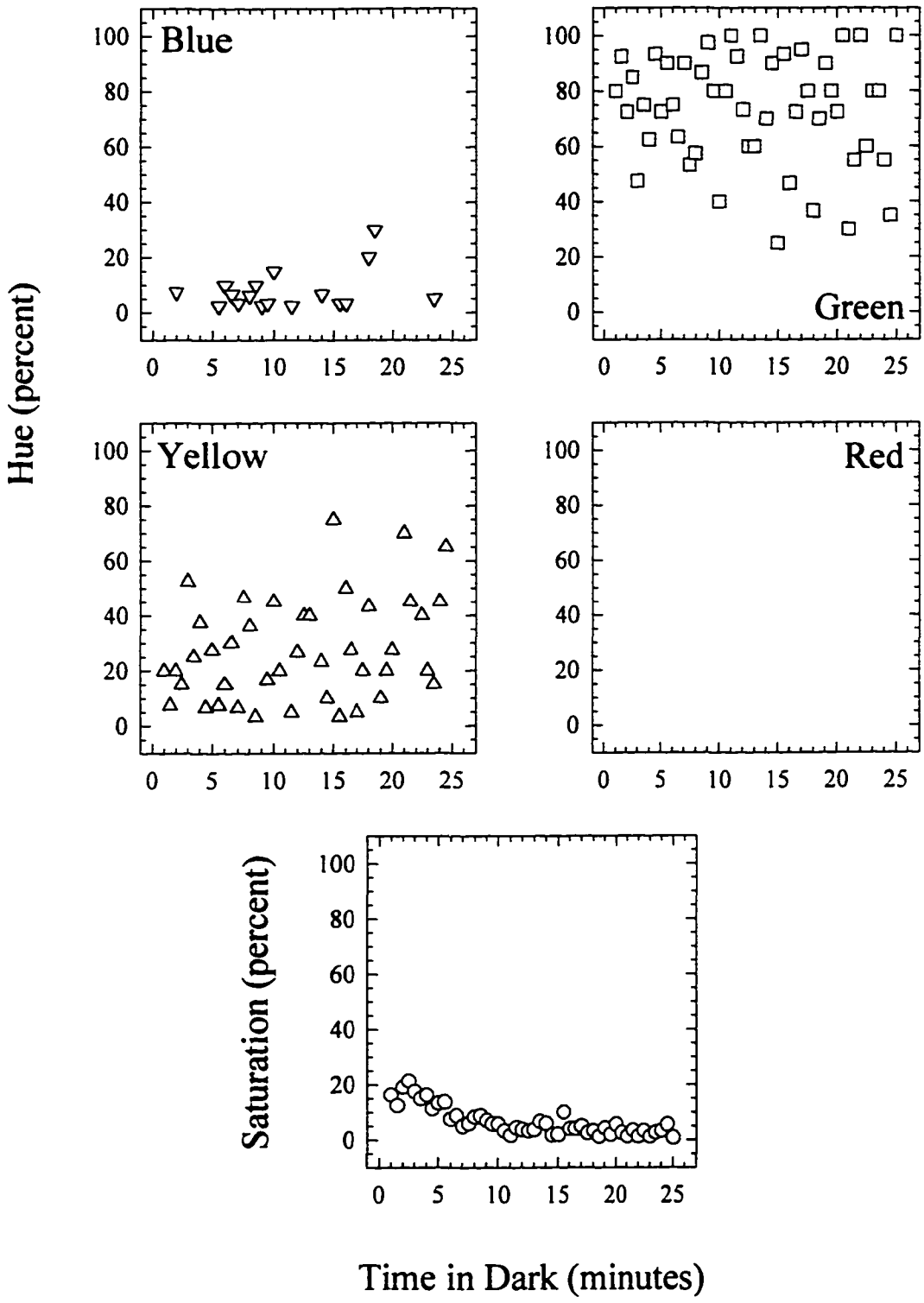

Figure 71. Hue and saturation scaling for observer MT for a 576 nm stimulus as a function of time in the dark following monocular preadaptation. The test stimulus was a 3^{o} circle presented for 100 ms every 5 s at 6^{o} in the right eye temporal field.

Figure 71. Hue and Saturation Scaling
MT 576 nm Monocular

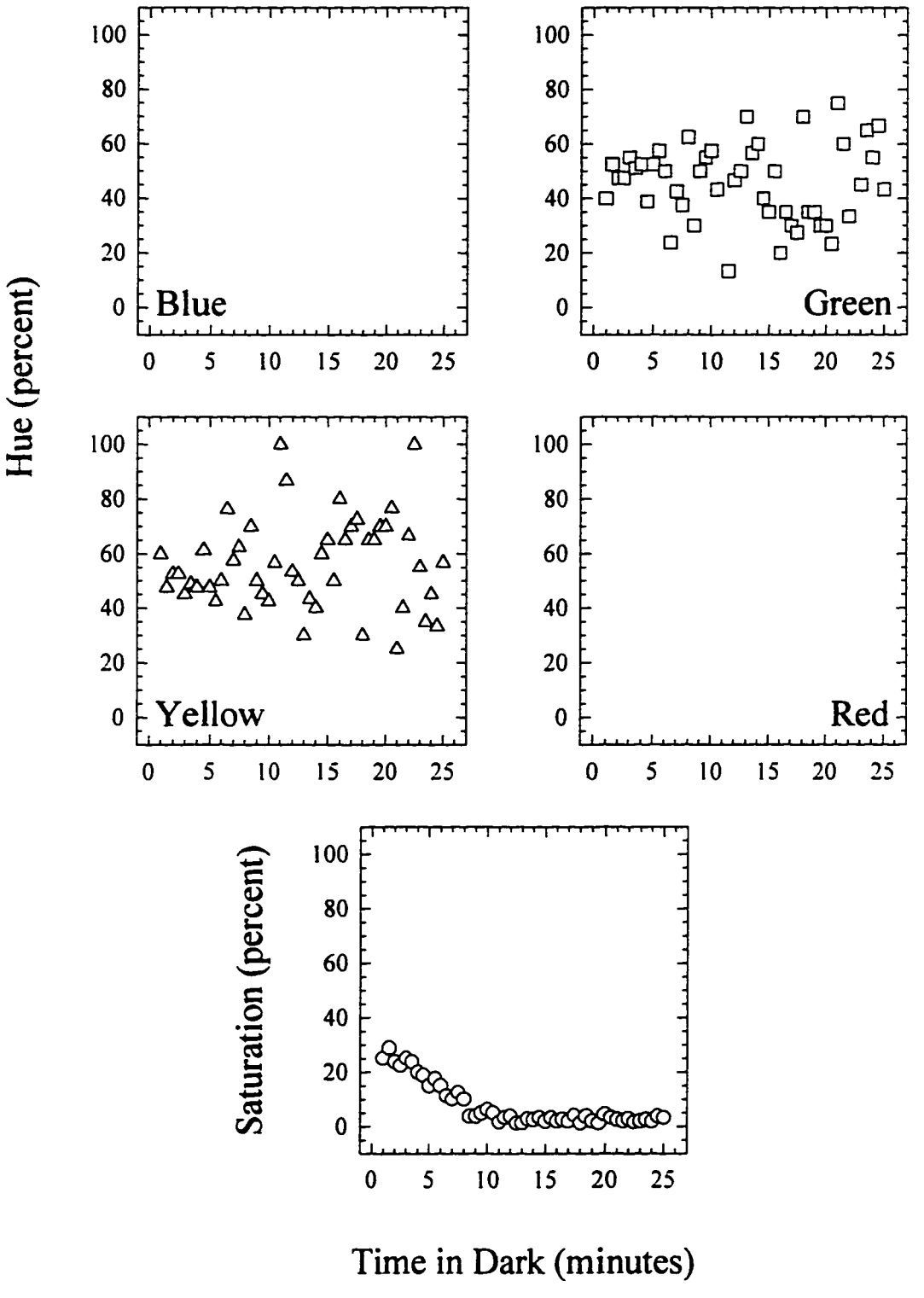

Figure 72. Hue and saturation scaling for observer MT for a 576 nm stimulus as a function of time in the dark following binocular preadaptation. The test stimulus was a 3^{o} circle presented for 100 ms every 5 s at 6^{o} in the right eye temporal field.

Figure 72. Hue and Saturation Scaling
MT 576 nm Binocular

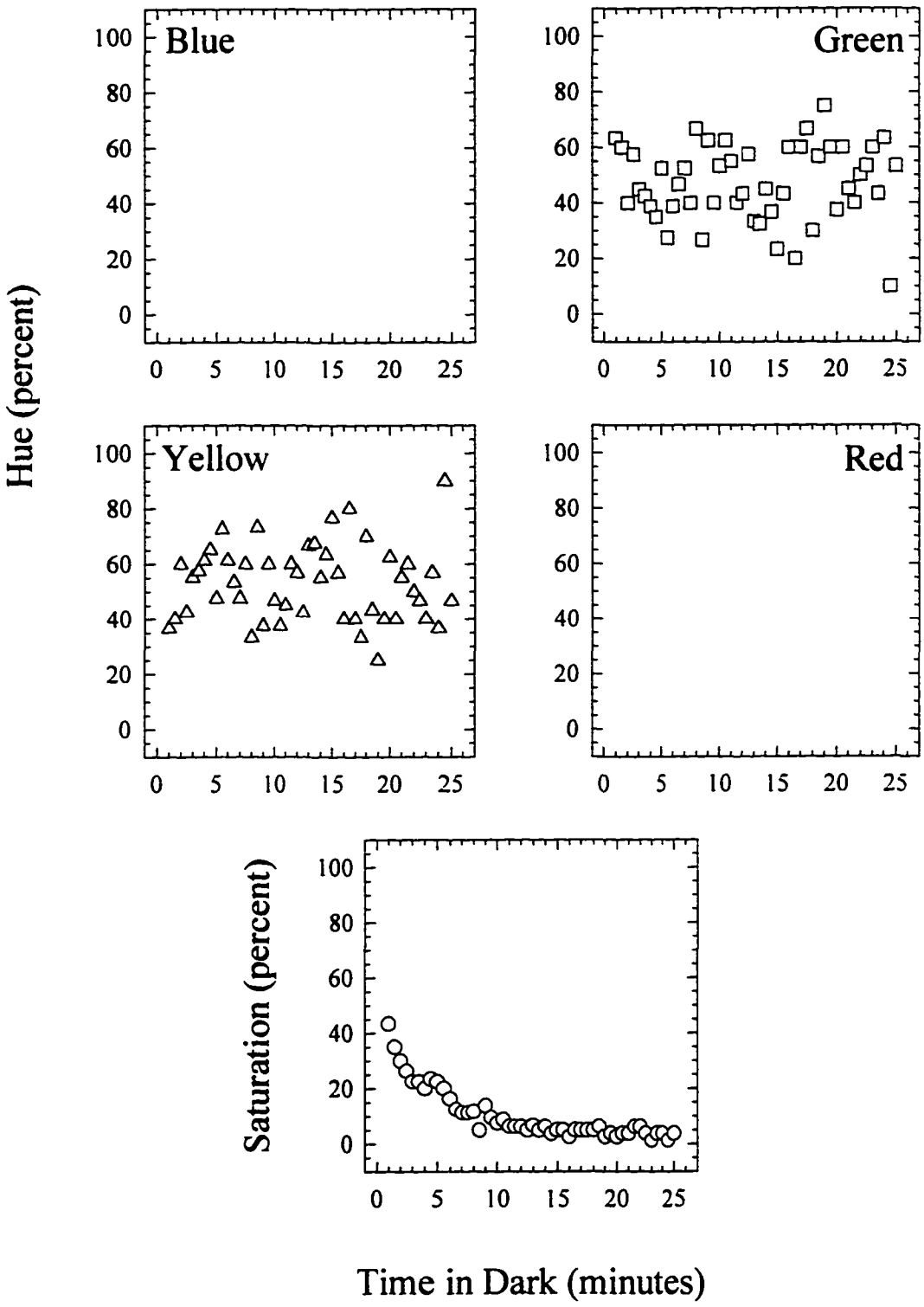

Figure 73. Hue and saturation scaling for observer MT for a 576 nm stimulus as a function of time in the dark following interocular preadaptation. The test stimulus was a 3^{o} circle presented for 100 ms every 5 s at 6^{o} in the right eye temporal field.

Figure 73. Hue and Saturation Scaling
MT 576 nm Interocular

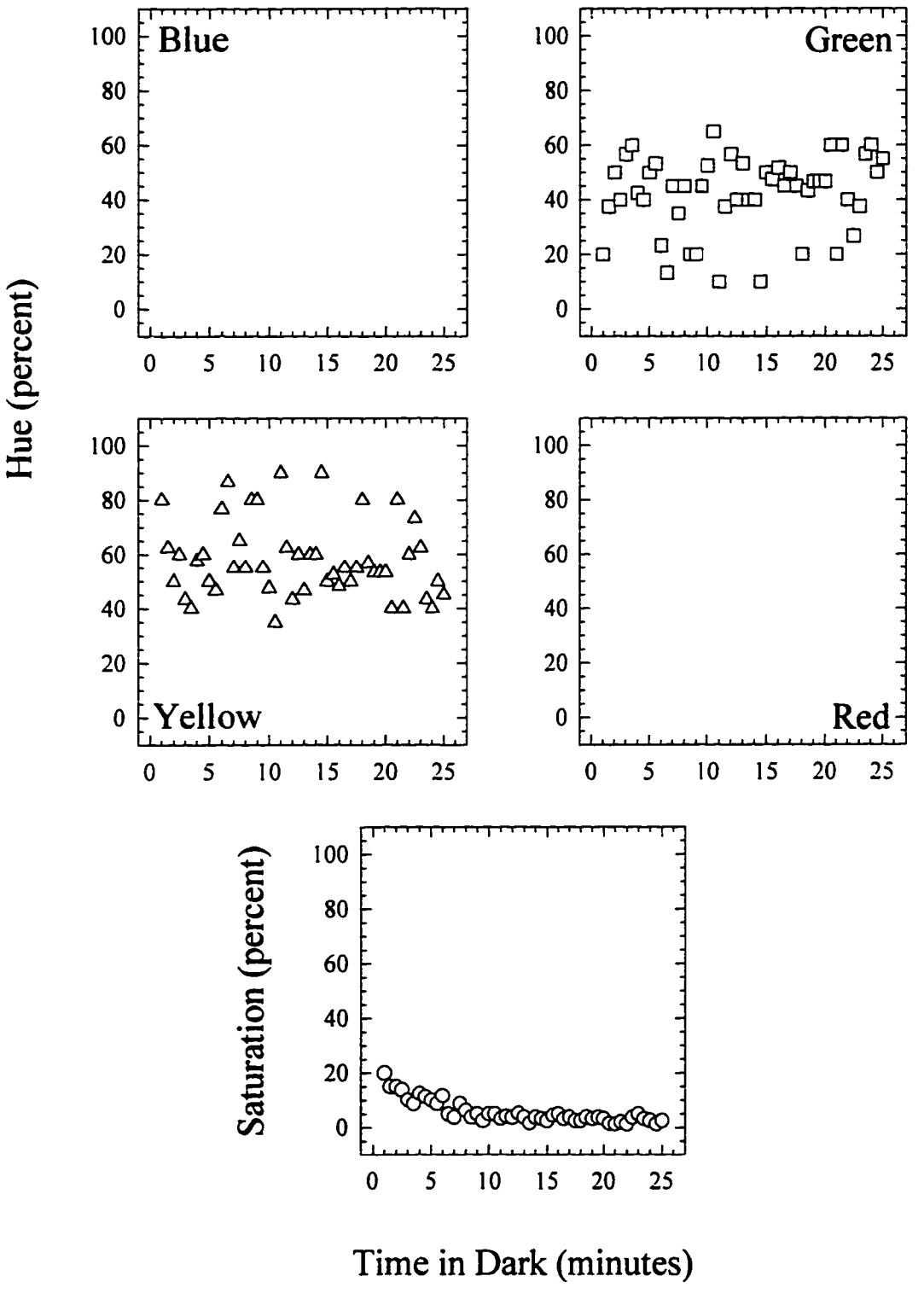

Figure 74. Hue and saturation scaling for observer MT for a 637 nm stimulus as a function of time in the dark following monocular preadaptation. The test stimulus was a 3^{o} circle presented for 100 ms every 5 s at 6^{o} in the right eye temporal field.

Figure 74. Hue and Saturation Scaling
MT 637 nm Monocular

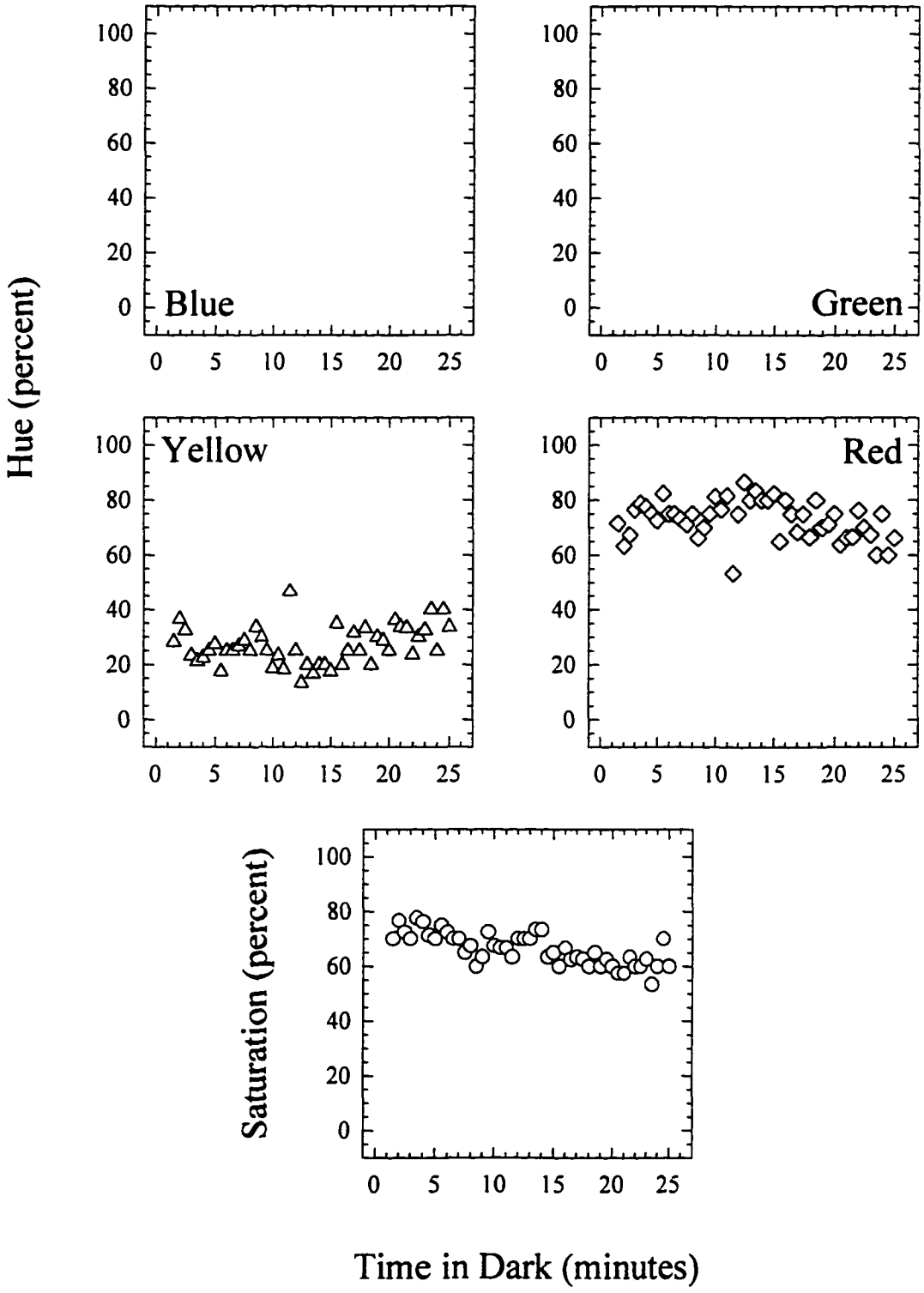

Figure 75. Hue and saturation scaling for observer MT for a 637 nm stimulus as a function of time in the dark following binocular preadaptation. The test stimulus was a 3^{o} circle presented for 100 ms every 5 s at 6^{o} in the right eye temporal field.

Figure 75. Hue and Saturation Scaling
MT 637 nm Binocular

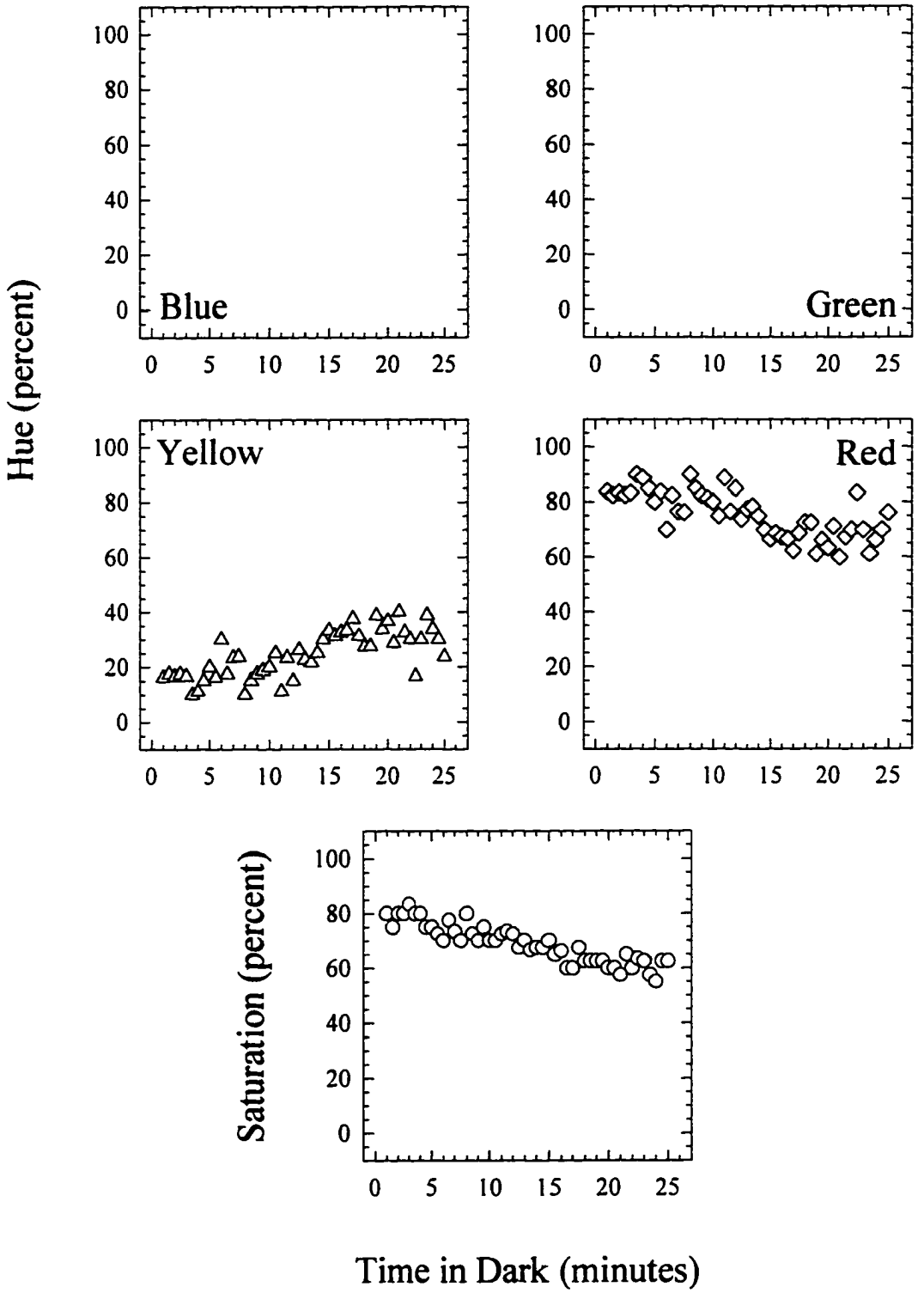

Figure 76. Hue and saturation scaling for observer MT for a 637 nm stimulus as a function of time in the dark following interocular preadaptation. The test stimulus was a 3^{o} circle presented for 100 ms every 5 s at 6^{o} in the right eye temporal field.

Figure 76. Hue and Saturation Scaling
MT 637 nm Interocular

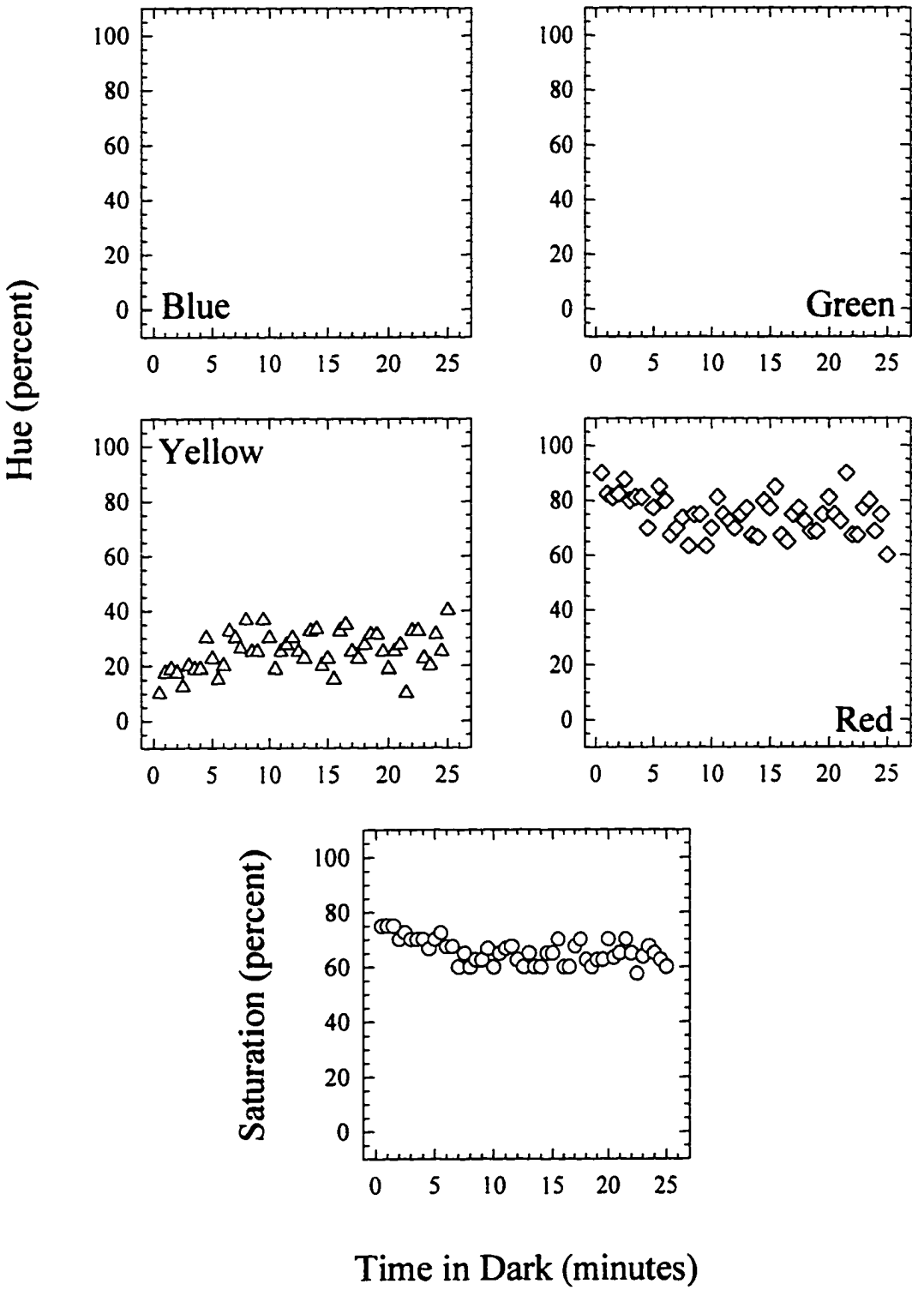

Figure 77. Hue and saturation scaling for observer AD for a 478 nm stimulus as a function of time in the dark following monocular preadaptation. The test stimulus was a 3^{o} circle presented for 100 ms every 5 s at 6^{o} in the right eye temporal field.

Figure 77. Hue and Saturation Scaling
AD 478 nm Monocular

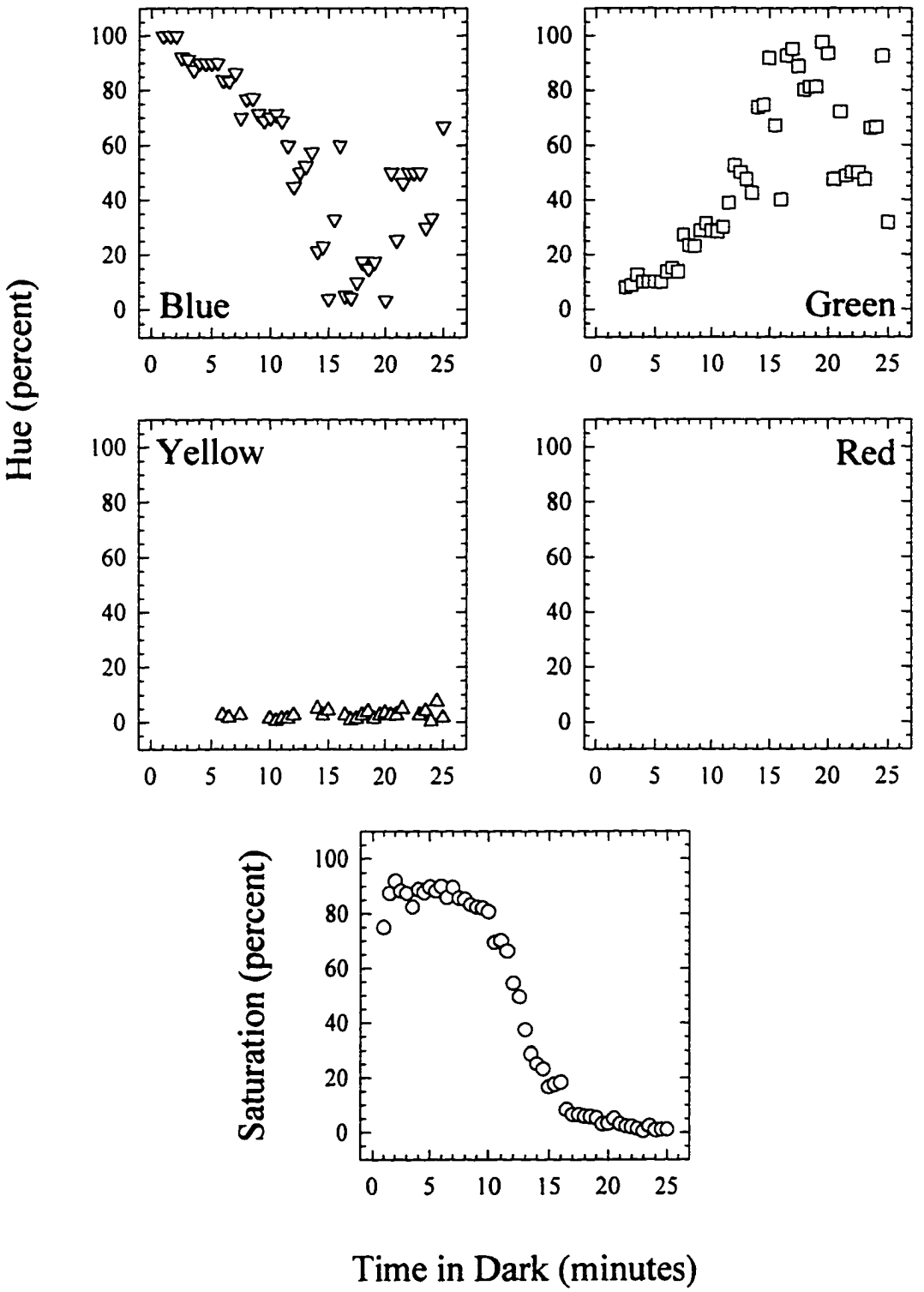

Figure 78. Hue and saturation scaling for observer AD for a 478 nm stimulus as a function of time in the dark following binocular preadaptation. The test stimulus was a 3^{o} circle presented for 100 ms every 5 s at 6^{o} in the right eye temporal field.

Figure 78. Hue and Saturation Scaling
AD 478 nm Binocular

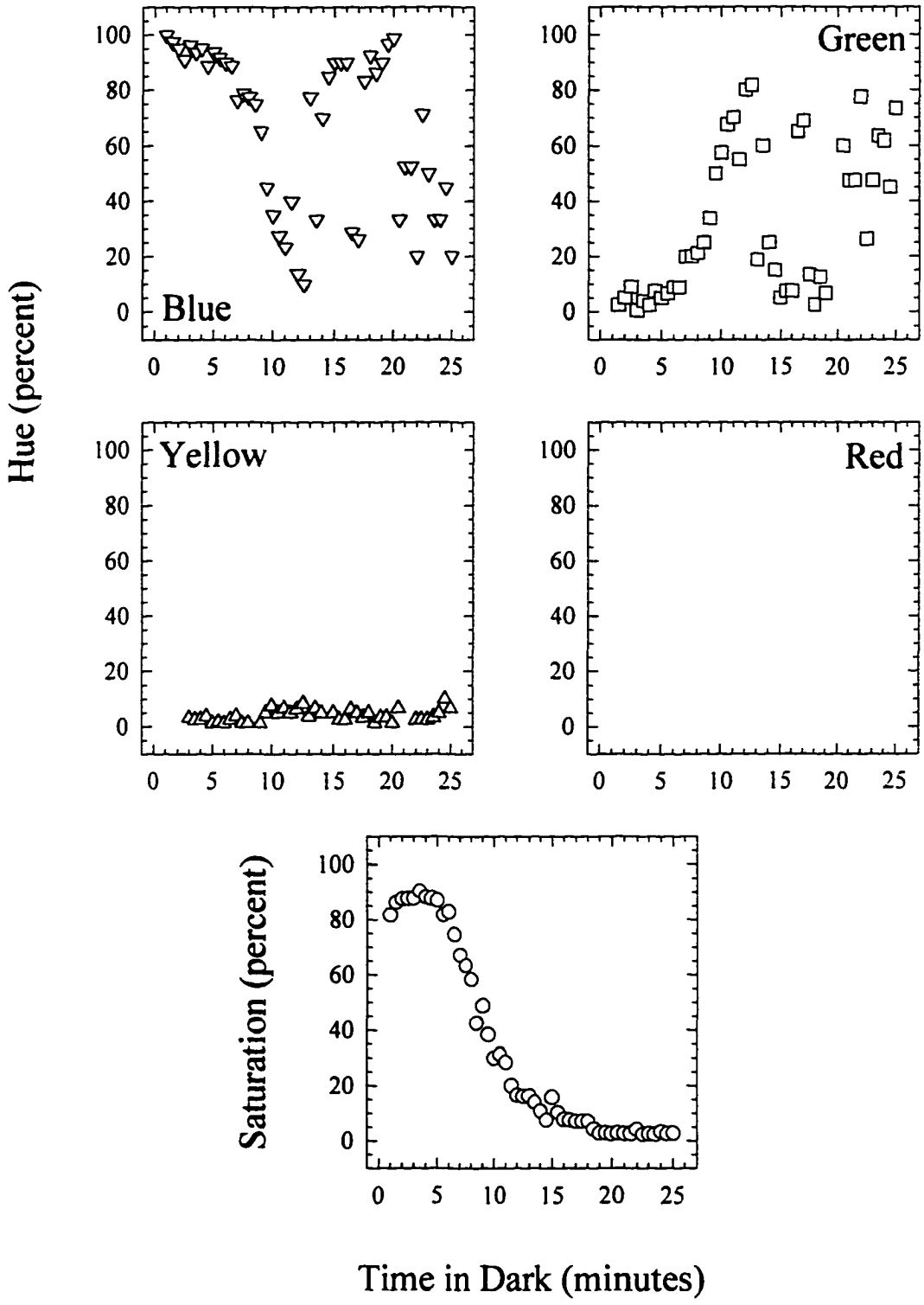

Figure 79. Hue and saturation scaling for observer AD for a 478 nm stimulus as a function of time in the dark following interocular preadaptation. The test stimulus was a 3^{o} circle presented for 100 ms every 5 s at 6^{o} in the right eye temporal field.

Figure 79. Hue and Saturation Scaling
AD 478 nm Interocular

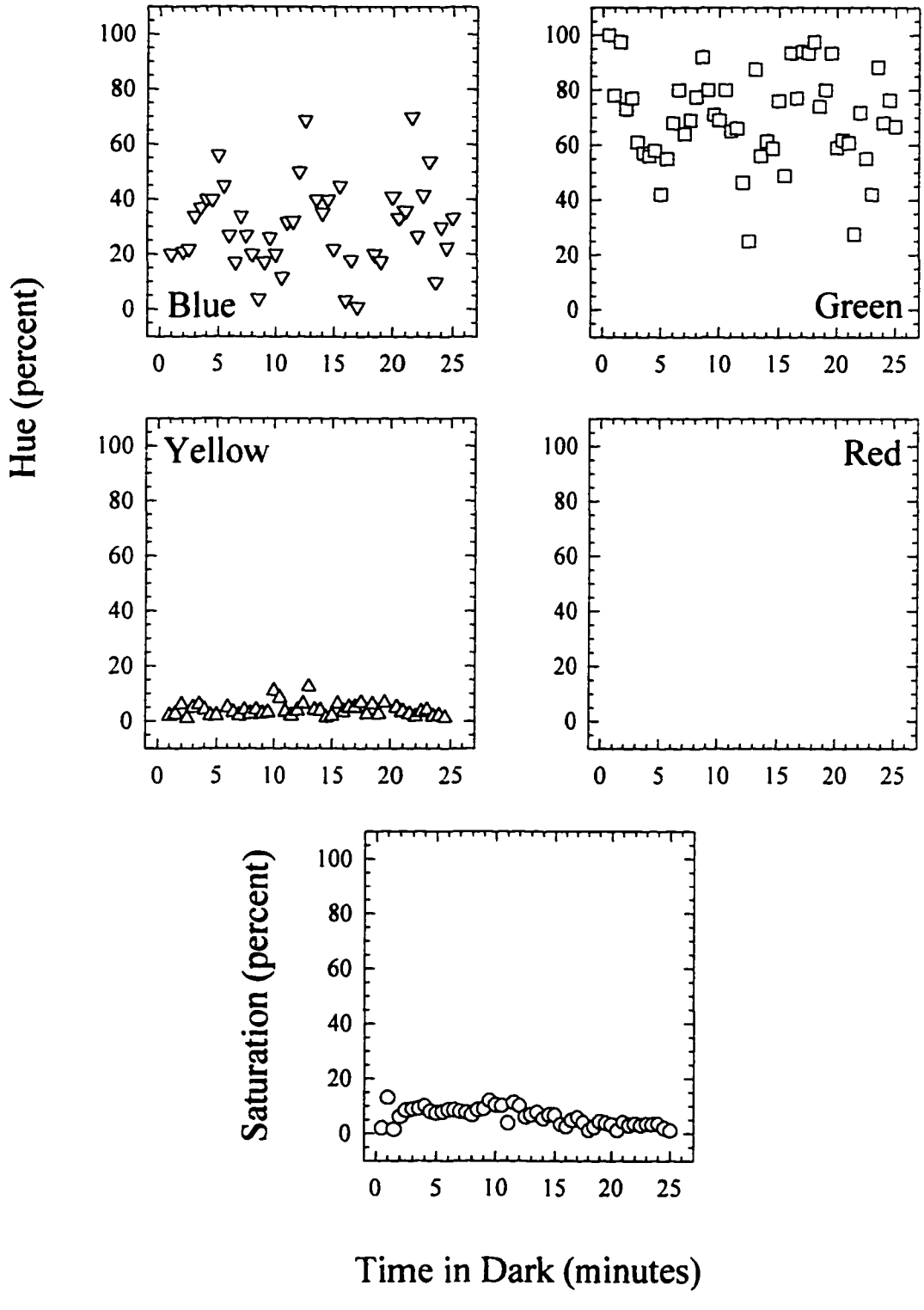

Figure 80. Hue and saturation scaling for observer AD for a 511 nm stimulus as a function of time in the dark following monocular preadaptation. The test stimulus was a 3^{o} circle presented for 100 ms every 5 s at 6^{o} in the right eye temporal field.

Figure 80. Hue and Saturation Scaling
AD 511 nm Monocular

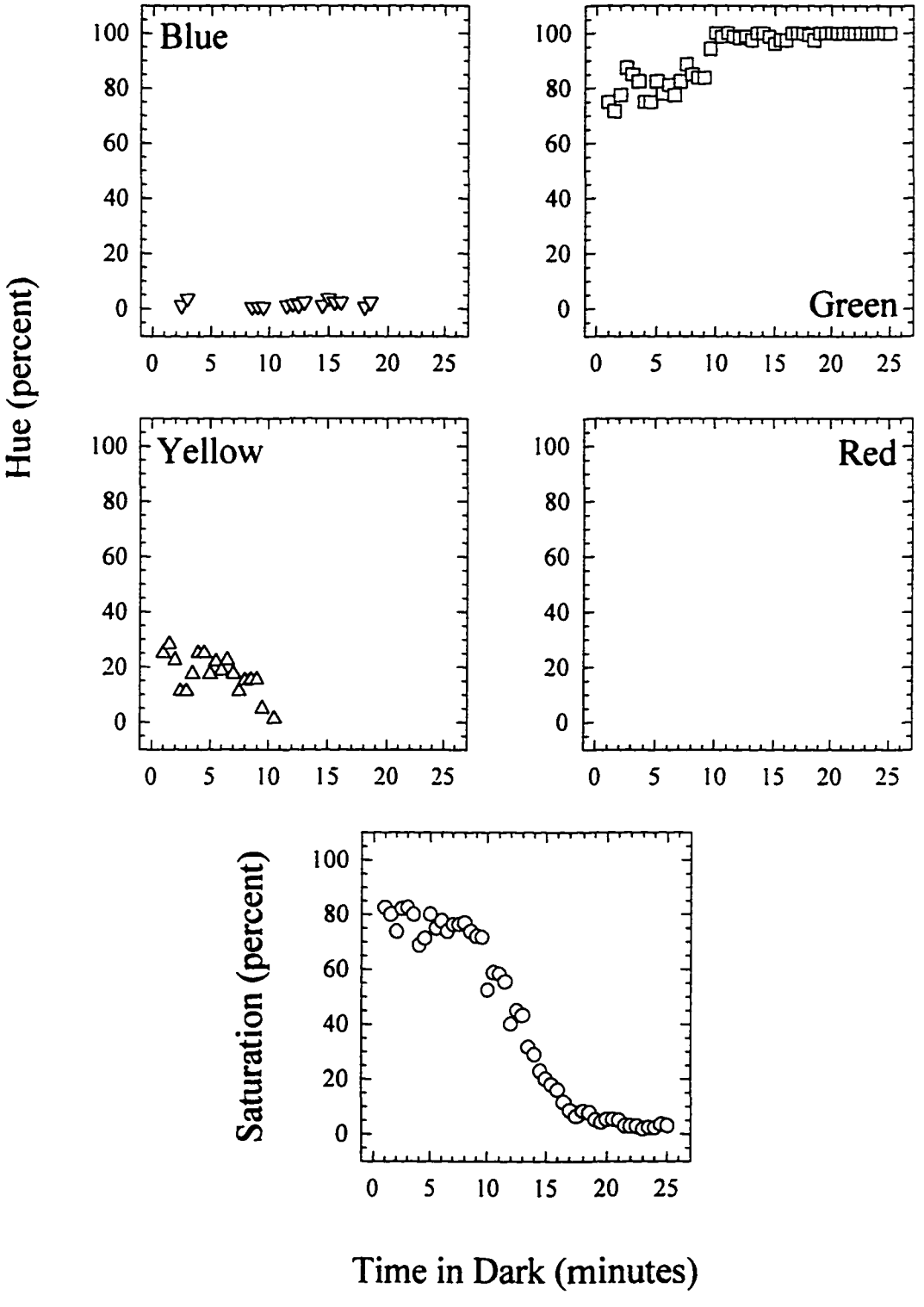

Figure 81. Hue and saturation scaling for observer AD for a 511 nm stimulus as a function of time in the dark following binocular preadaptation. The test stimulus was a 3^{o} circle presented for 100 ms every 5 s at 6^{o} in the right eye temporal field.

Figure 81. Hue and Saturation Scaling
AD 511 nm Binocular

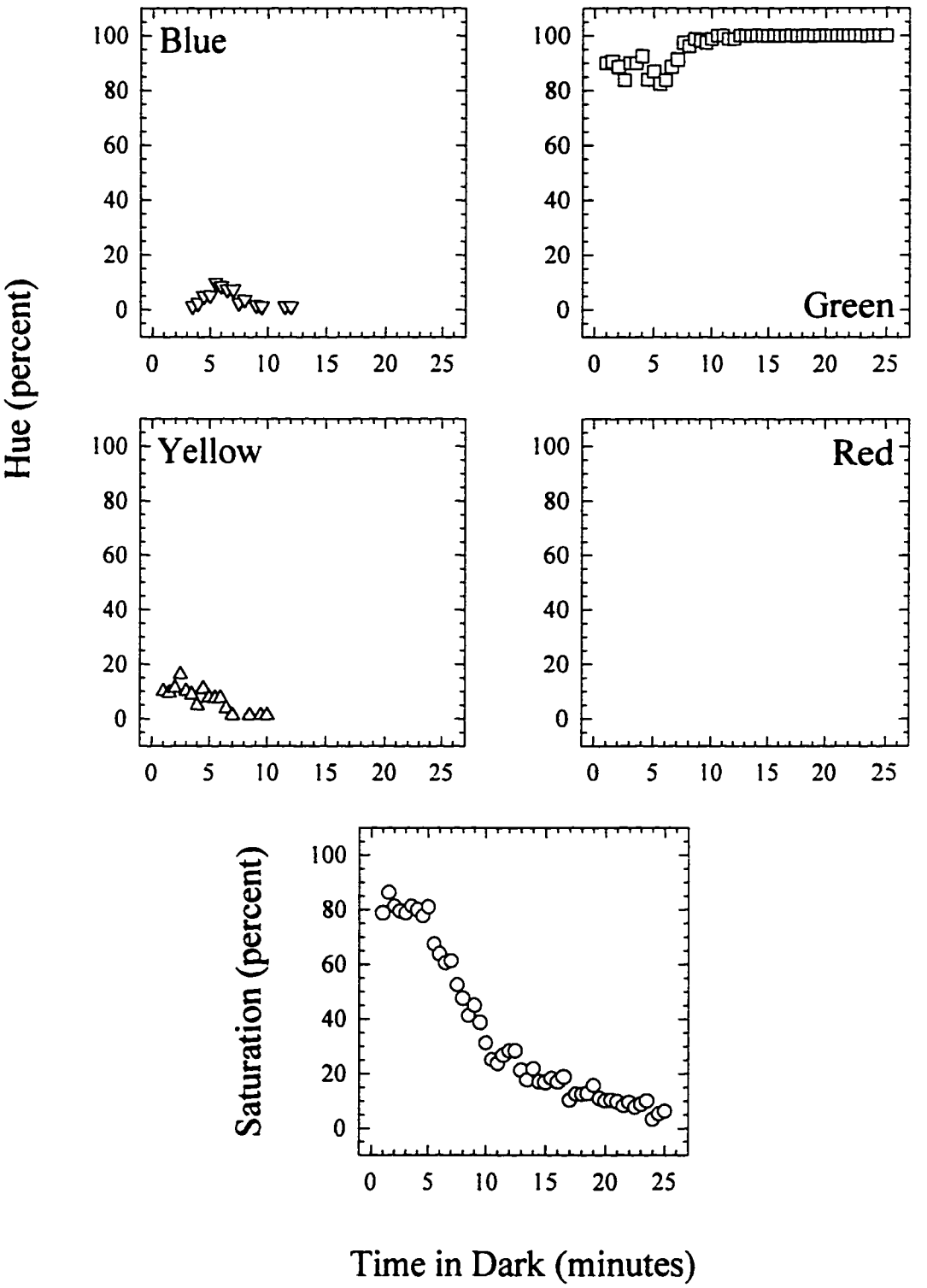

Figure 82. Hue and saturation scaling for observer AD for a 511 nm stimulus as a function of time in the dark following interocular preadaptation. The test stimulus was a 3^{o} circle presented for 100 ms every 5 s at 6^{o} in the right eye temporal field.

Figure 82. Hue and Saturation Scaling
AD 511 nm Interocular

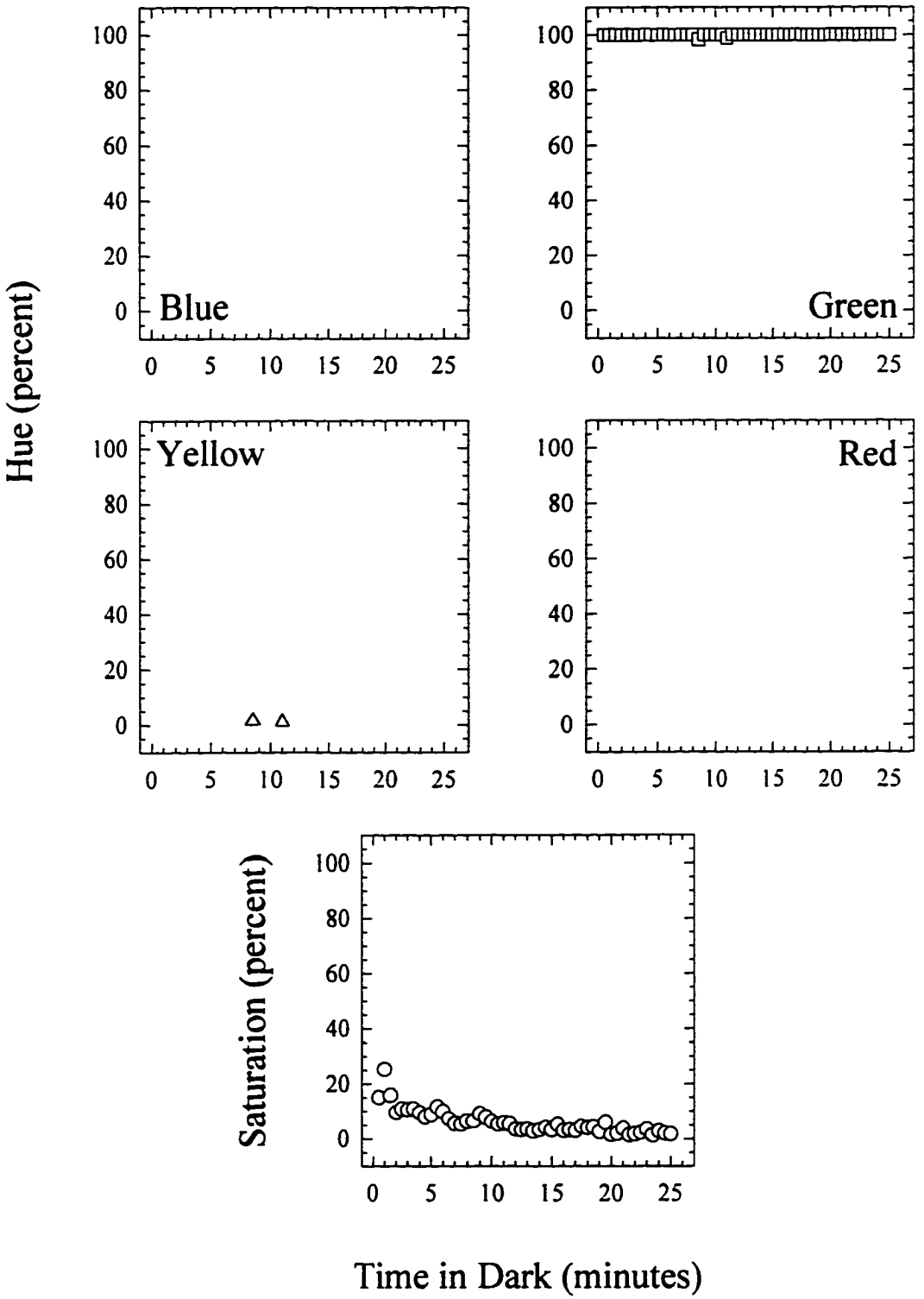

Figure 83. Hue and saturation scaling for observer AD for a 576 nm stimulus as a function of time in the dark following monocular preadaptation. The test stimulus was a 3^{o} circle presented for 100 ms every 5 s at 6^{o} in the right eye temporal field.

Figure 83. Hue and Saturation Scaling
AD 576 nm Monocular

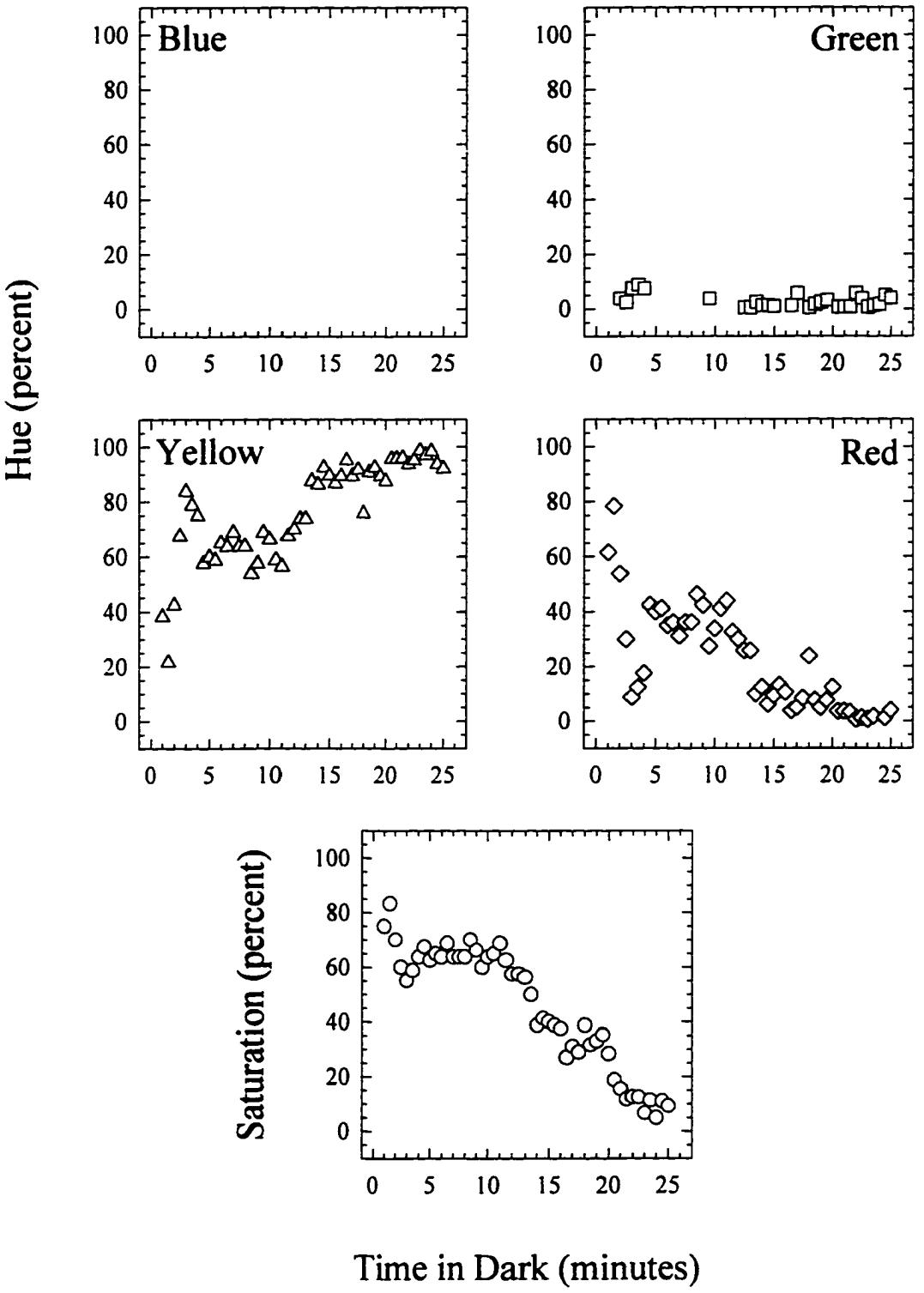

Figure 84. Hue and saturation scaling for observer AD for a 576 nm stimulus as a function of time in the dark following binocular preadaptation. The test stimulus was a 3^{o} circle presented for 100 ms every 5 s at 6^{o} in the right eye temporal field.

Figure 84. Hue and Saturation Scaling
AD 576 nm Binocular

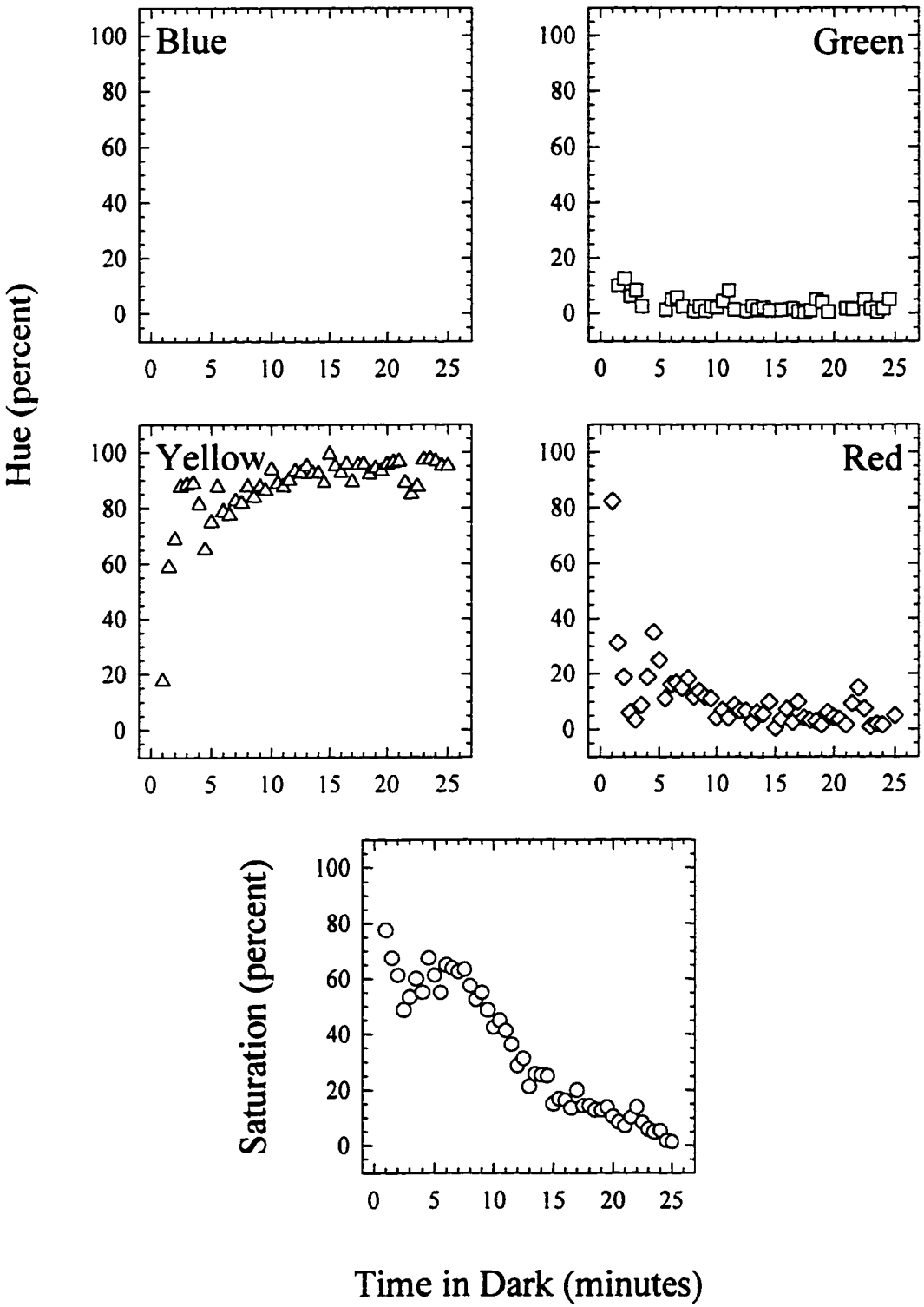

Figure 85. Hue and saturation scaling for observer AD for a 576 nm stimulus as a function of time in the dark following interocular preadaptation. The test stimulus was a 3^{o} circle presented for 100 ms every 5 s at 6^{o} in the right eye temporal field.

Figure 85. Hue and Saturation Scaling
AD 576 nm Interocular

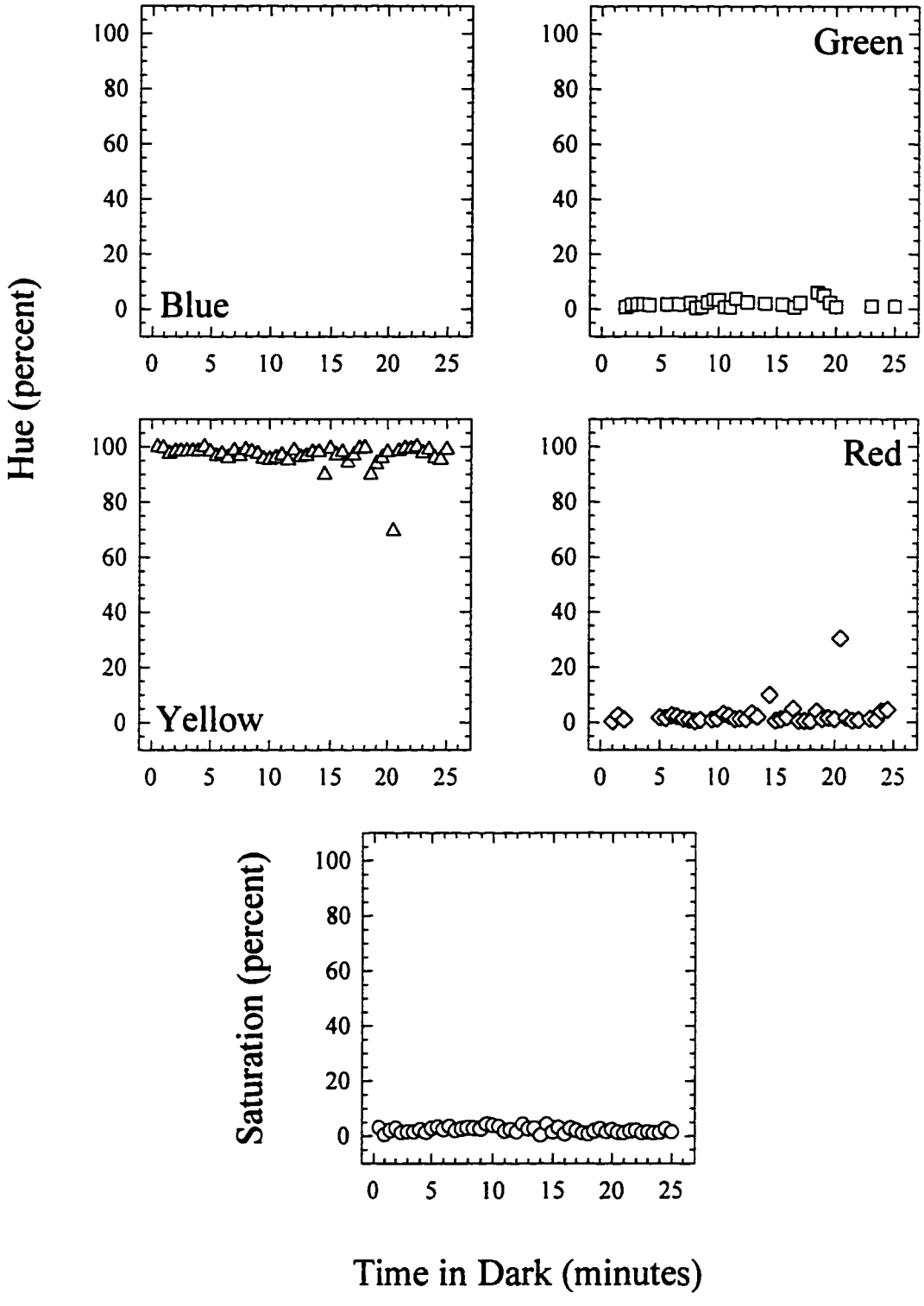

Figure 86. Hue and saturation scaling for observer AD for a 637 nm stimulus as a function of time in the dark following monocular preadaptation. The test stimulus was a 3^{o} circle presented for 100 ms every 5 s at 6^{o} in the right eye temporal field.

Figure 86. Hue and Saturation Scaling
AD 637 nm Monocular

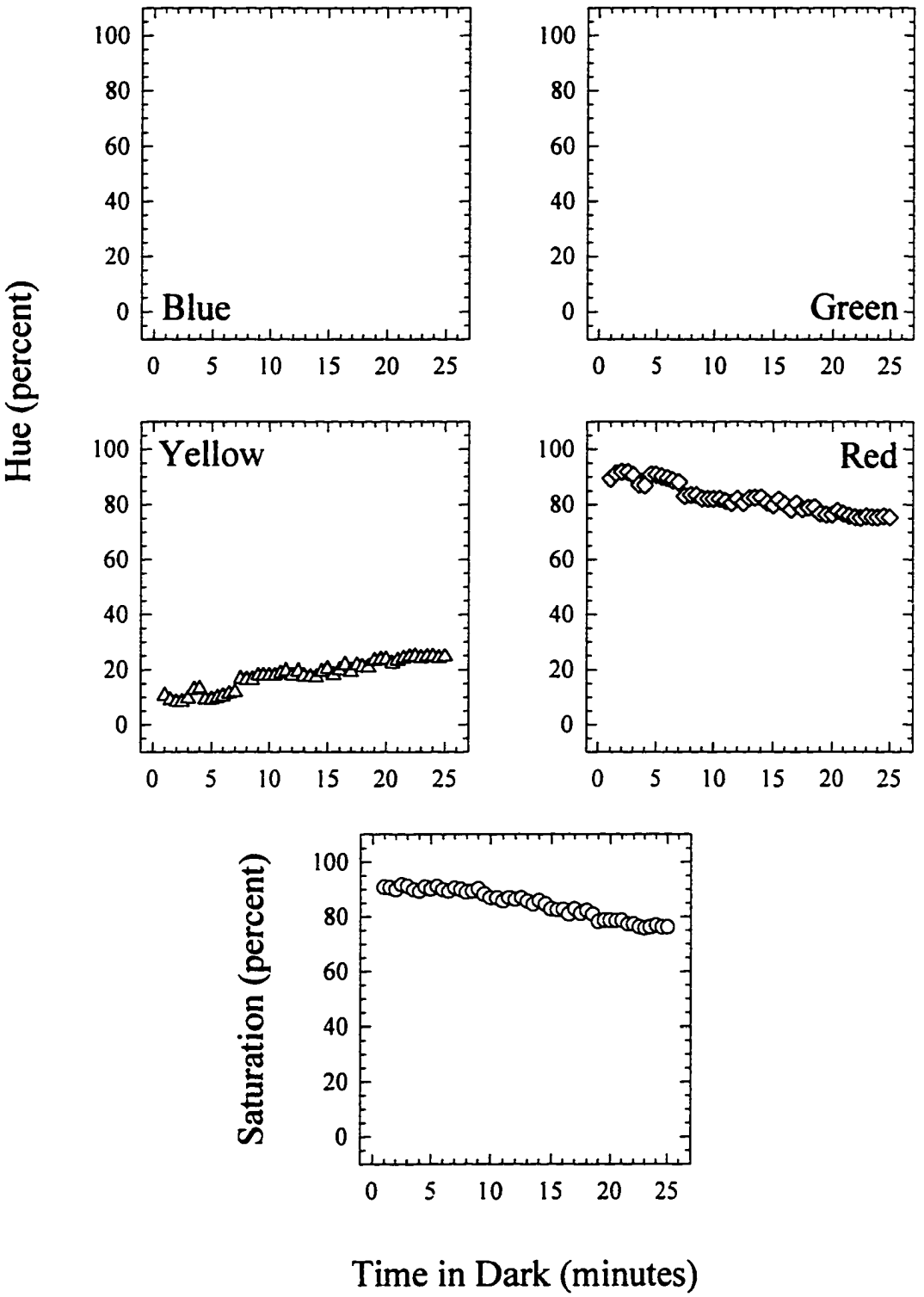

Figure 87. Hue and saturation scaling for observer AD for a 637 nm stimulus as a function of time in the dark following binocular preadaptation. The test stimulus was a 3^{o} circle presented for 100 ms every 5 s at 6^{o} in the right eye temporal field.

Figure 87. Hue and Saturation Scaling
AD 637 nm Binocular

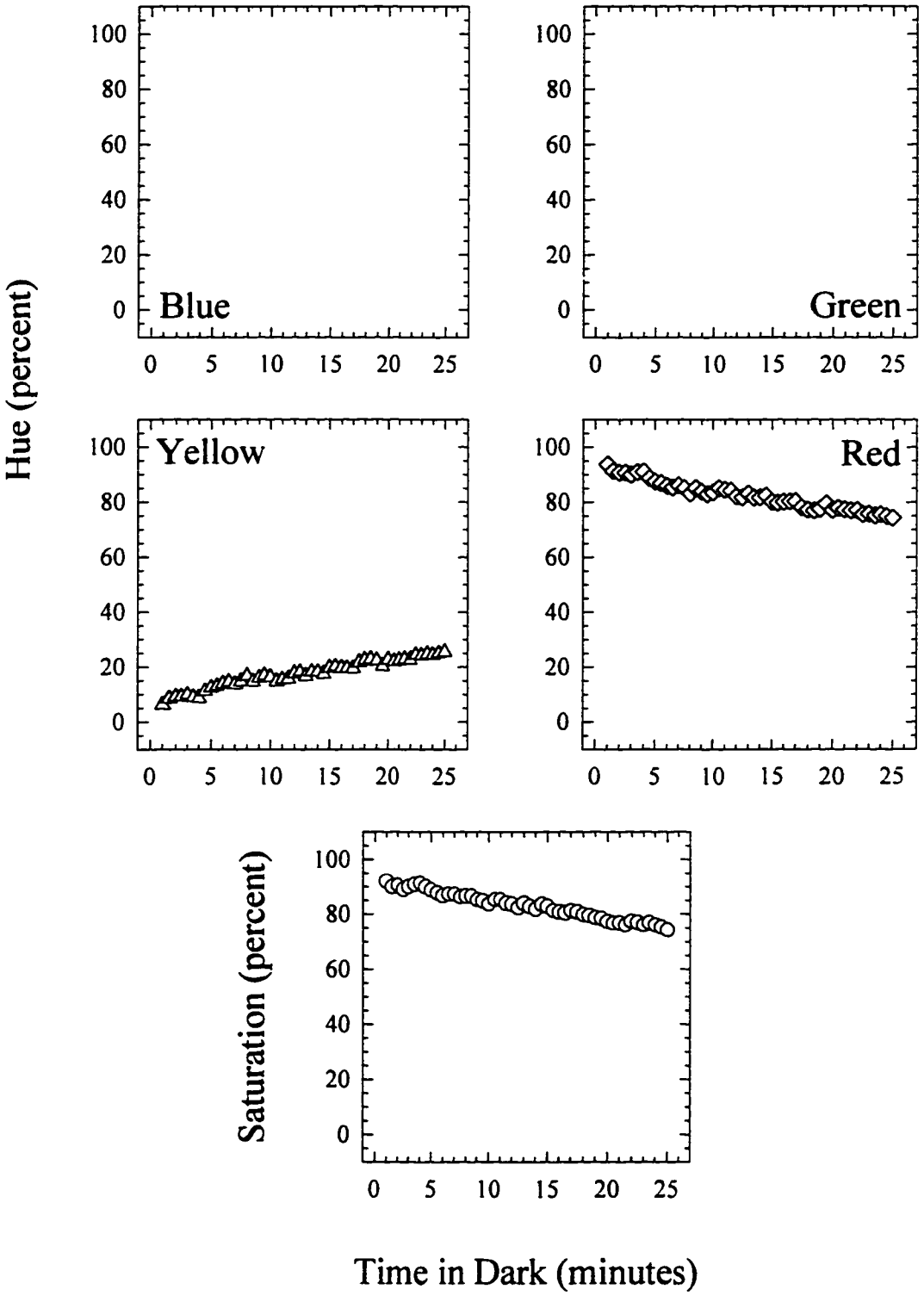

Figure 88. Hue and saturation scaling for observer AD for a 637 nm stimulus as a function of time in the dark following interocular preadaptation. The test stimulus was a 3^{o} circle presented for 100 ms every 5 s at 6^{o} in the right eye temporal field.

Figure 88. Hue and Saturation Scaling
AD 637 nm Interocular

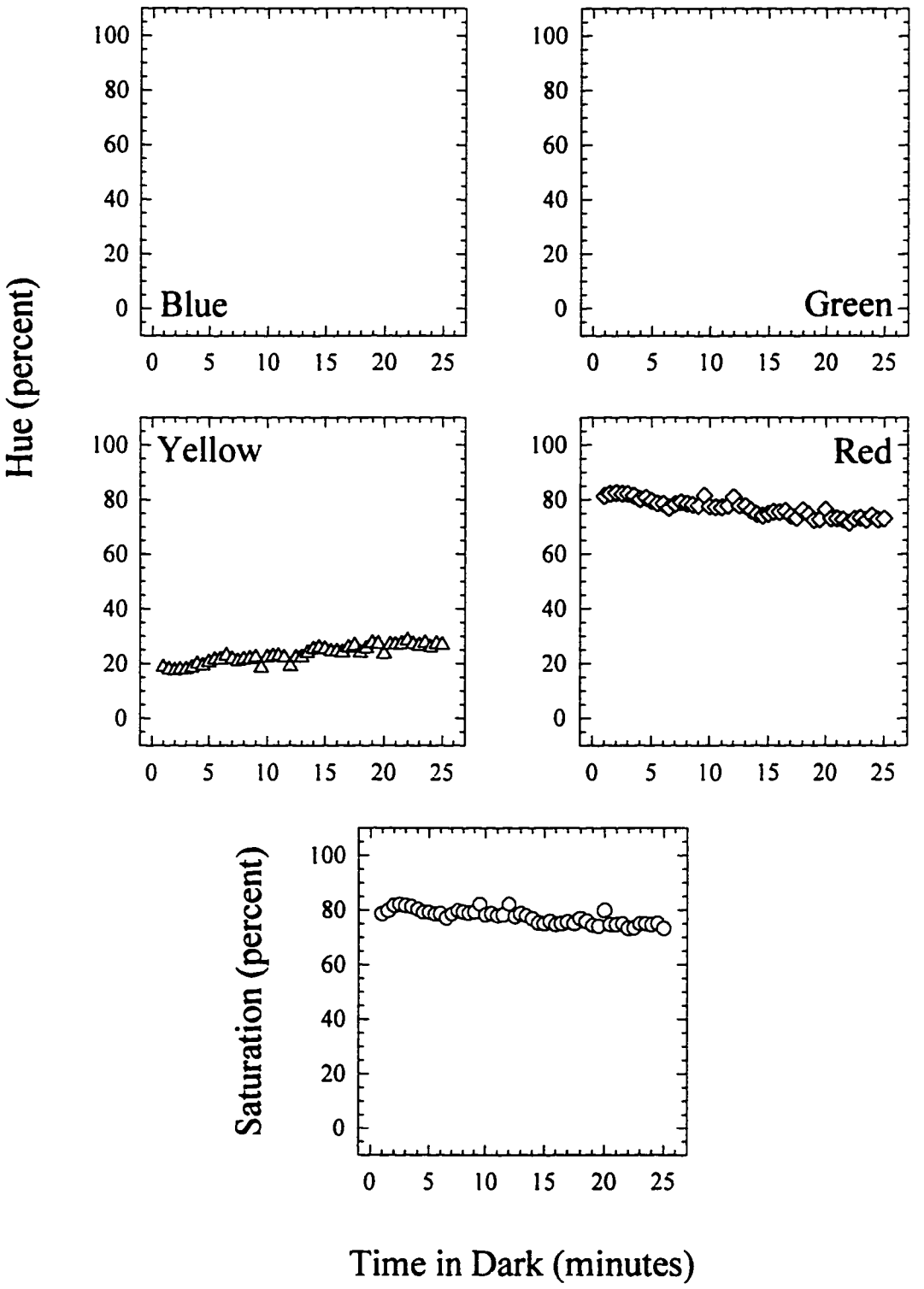

Bibliography

Abramov, I., & Gordon, J. (1994). Color appearance: On seeing red--or yellow, or green, or blue. Annual Review of Psychology, 45, 451-485.

Adelson, E. H. (1982). Saturation and adaptation in the rod system. Vision Research, 22, 1299-1312.

Aguilar, M., & Stiles, W. S. (1954). Saturation of the rod mechanism of the retina at high levels of stimulation. Optica Acta, 1, 59-65.

Alexander, K. R. & Fishman, G. A. (1984). Rod-cone interaction in flicker perimetry. British Journal of Ophthalmology, 68, 303-309.

Alexander, K. R., Fishman, G. A., & Derlacki, D. J. (1988). Mechanisms of rod-cone interaction: Evidence from congenital stationary nightblindness. Vision Research, 28, 575-583.

Ambler, B. A. (1974). Hue discrimination in peripheral vision under conditions of dark and light adaptation. Perception & Psychophysics, 15, 586-590.

Arden, G. B., & Frumkes, T. E. (1986). Stimulation of rods can increase cone flicker ERGs in man. Vision Research, 26, 711-721.

Auerbach, E., Dorrenhaus, A., & Cavonius, C. R. (1992). Changes in sensitivity of the dark-adapted eye during concurrent light adaptation of the other eye. Visual Neuroscience, 8, 359-363.

Battersby, W. S., & Wagman, I. H. (1962). Neural limitations of visual excitability: IV. Spatial determinants of retrochiasmal interaction. American Journal of Physiology, 203, 359-365.

Bauer, G. M., Frumkes, T. E., & Nygaard, R. W. (1983). The signal-to-noise characteristics of rod-cone interaction. Journal of Physiology, 337, 101-119.

Brill, M. H. (1990). Mesopic color matching: some theoretical issues. Journal of the Optical Society of America A, 7, 2048-2051.

Buck, S. L. (1996). Color pathways mediating simultaneous scotopic contrast. Manuscript submitted for publication.

Buck, S. L., & Knight, R. (1994). Partial additivity of rod signal with M- and L-cone signals in increment detection. Vision Research, 34, 2537-2545.

Buck, S. L., Peeples, D. R., & Makous, W. (1979). Spatial patterns of rod-cone interaction. Vision Research, 19, 775-782.

Coletta, N. J. & Adams, A. J. (1984). Rod-cone interaction in flicker detection. Vision Research, 24, 1333-1340.

Crawford, B. H. (1947). Visual adaptation in relation to brief conditioning stimuli. Proceedings of the Royal Society of London Series B, 134, 283-302.

Dacey, D. M., Lee, B. B., Stafford, D. K., Pokorny, J., & Smith, V. C. (1996). Horizontal cells of the primate retina: Cone specificity without spectral opponency. Science, 271, 656-659.

Daw, N. W., Jensen, R. J., & Brunken, W. J. (1990). Rod pathways in mammalian retinae. Trends in Neuroscience, 13, 110-115.

Denny, N., Frumkes, T. E., Barris, M. C., & Eysteinsson, T. (1991). Tonic interocular suppression and binocular summation in human vision. Journal of Physiology, 437, 449-460.

Denny, N., Frumkes, T. E., & Goldberg, S. H. (1990). Comparison of summatory and suppressive rod-cone interaction. Clinical Vision Science, 5, 27-36.

Deutman, A. F. (1977). Rod-cone dystrophy, primary hereditary, pigmentary retinopathy, retinitis pigmentosa. In A. E. Krill & D. B. Archer (Eds.), Krill's hereditary retinal and choroidal diseases Vol. II (pp. 479-576). New York: Harper and Row.

Drum, B. (1981). Brightness interactions between rods and cones. Perception & Psychophysics, 29, 505-510.

Edwards, D. P., Purpura, K. P., & Kaplan, E. (1995). Contrast sensitivity and spatial frequency response of primate cortical neurons in and around the cytochrome oxidase blobs. Vision Research, 35, 1501-1523.

Eysteinsson, T., Barris, M. C., Denny, N. & Frumkes, T. E. (1993). Tonic interocular suppression, binocular summation, and the visual evoked potential. Investigative Ophthalmology & Visual Science, 34, 2443-2448.

Frumkes, T. E. (1990). Classical and modern psychophysical studies of dark and light adaptation and their relationship to underlying retinal function. In K. N. Leibovic (Ed.), The science of vision (pp. 172-210). New York: Springer Verlag.

Frumkes, T. E. & Eysteinsson, T. (1988). The cellular basis for suppressive rod-cone interaction. Visual Neuroscience, 1, 263-273.

Frumkes, T. E., Lange, G., Naarendorp, F., & Eysteinsson, T. (1995). Suppressive rod-cone interactions: Underlying mechanisms and practical application. In B. Drum (Ed.), Colour Vision Deficiences XII (pp. 329-334). Dordrecht: Kluwer Academic Publishers.

Frumkes, T. E., Naarendorp, F., & Goldberg, S. H. (1988). Abnormalities in retinal neurocircuitry in protanopes: Evidence provided by psychophysical investigation of temporal-spatial interactions. Investigative Ophthalmology & Visual Science Supplement, 29, 163.

Frumkes, T. E., Sekuler, M. D., Barris, M. C., Reiss, E. H., Chalupa, L. M. (1973). Rod-cone interaction in human scoptopic vision--I. Temporal analysis. Vision Research, 13, 1269-1282.

Frumkes, T. E., & Temme, L. A. (1977). Rod-cone interaction in human scotopic vision--II Cones influence rod increment thresholds. Vision Research, 17, 673-679.

Goldberg, S. (1983). The effect of rod adaptation on cone-mediated flicker sensitivity. Unpublished doctoral dissertation, The City University of New York.

Goldberg, S. H., Frumkes, T. E., & Nygaard, R. W. (1983). Inhibitory influence of unstimulated rods in the human retina: Evidence provided by examining cone flicker. Science, 221, 180-182.

Gordon, I. E. (1989). Theories of visual perception. New York: Wiley.

Gordon, J., Abramov, I., & Chan, H. (1994). Describing color appearance: Hue and saturation scaling. Perception & Psychophysics, 56, 27-41.

Gouras, P., & Link, K. (1966). Rod and cone interaction in dark-adapted monkey ganglion cells. Journal of Physiology, 184, 499-510.

Graham, C. H., & Ratoosh, P. (1962). Notes on some interrelations of sensory psychology, perception, and behavior. In S. Koch (Ed.), Psychology: A study of a science: Vol. 4 (pp. 483-514). New York: McGraw-Hill.

Hecht, S. (1937). Rods, cones, and the chemical basis of vision. Physiological Reviews, 17, 239-290.

Hurvich, L. M., & Jameson, D. (1957). An opponent-process theory of color vision. Psychological Review, 64, 384-404.

Ikeda, M., & Urakubo, M. (1969). Rod-cone interrelation. Journal of the Optical Society of America, 59, 217-222.

Kaiser, P. K., & Boynton, R. M. (1996). Human color vision (2nd ed.). Washington, DC: Optical Society of America.

Kleinschmidt, J., & Dowling, J. E. (1975). Intracellular recordings from gecko photoreceptors during light and dark adaptation. Journal of General Physiology, 66, 617-648.

Kolb, H. (1994). The architecture of functional neural circuits in the vertebrate retina. Investigative Ophthalmology & Visual Science, 35, 2385-2404.

Kries, J. von, & Nagel, W. (1896). Ueber den einfluss von lichtstarke und adaptation auf das sehen des dichromaten (Grunblinden). Z. Psychol., 12, 1-38.

Lange, G., Denny, N., & Frumkes, T. E. (1997). Suppressive rod-cone interaction: Evidence for separate retinal (temporal) and extraretinal (spatial) mechanisms in achromatic vision. Manuscript submitted for publication.

Lansford, T. G., & Baker, H. D. (1969). Dark adaptation: An interocular light-adaptation effect. Science, 164, 1307-1309.

Lee, B. B. (1996). Receptive field structure in the primate retina. Vision Research, 36, 631-644.

Lembessis, E., Meaney, R., Moshe, D., & Frumkes, T. E. (1996). Interocular influences during dark adaptation. Investigative Ophthalmology & Visual Science Supplement, 37, 652.

Lie, I. (1963). Dark adaptation and the photochromatic interval. Documenta Ophthalmologica, 17, 411-510.

Livingstone, M. S., & Hubel, D. H. (1984). Anatomy and physiology of a color system in the primate visual cortex. Journal of Neuroscience, 4, 309-356.

Lythgoe, R. J., & Tansley, K. (1929). The relation of the critical frequency of flicker to the adaptation of the eye. Proceedings of the Royal Society of London Series B, 105, 60-92.

MacLeod, D. I. A. (1972). Rods cancel cones in flicker. Nature, 235, 173-174.

Makous, W., & Boothe, R. (1974). Cones block signals from rods. Vision Research, 14, 285-294.

Makous, W., Teller, D., & Boothe, R. (1976). Binocular interaction in the dark. Vision Research, 16, 473-476.

McKee, S. P., McCann, J. J., & Benton, J. L. (1977). Color vision from rod and long-wave cone interactions: Conditions in which rods contribute to multicolored images. Vision Research, 17, 175-185.

Merigan, W. H., & Maunsell, J. H. (1993). How parallel are the primate visual pathways? Annual Review of Neuroscience, 16, 369-402.

Montag, E. D. (1994). Surface color naming in dichromats. Vision Research, 34, 2137-2151.

Naarendorp, F., Denny, N., & Frumkes, T. E. (1988). Rod light and dark adaptation influence cone-mediated spatial acuity. Vision Research, 28, 67-74.

Naarendorp, F., & Frumkes, T. (1991). The influence of short-term adaptation of human rods and cones on cone-mediated grating visibility. Journal of Physiology, 432, 521-541.

Naarendorp, F., Rice, K. S., & Sieving, P. A. (1996). Summation of rod and s cone signals at threshold in human observers. Vision Research, 36, 2681-2688.

Nagy, A. L. (1980). Large-field substitution Rayleigh matches of dichromats. Journal of the Optical Society of America, 70, 778-784.

Nagy, A. L., & Wolf, S. (1993). Red-green color discrimination in peripheral vision. Vision Research, 33, 235-242.

Nygaard, R. W., & Frumkes, T. E. (1982). Calibration of the retinal illuminance provided by Maxwellian views. Vision Research, 22, 433-434.

Nygaard, R. W., & Frumkes, T. E. (1985). Frequency dependence in scotopic flicker sensitivity. Vision Research, 25, 115-127.

Palmer, D. A. (1976). Rod-cone mechanism underlying the Purkinje shift. Nature, 262, 601-603.

Paris, J. & Prestrude, A. M. (1975). On the mechanisms of the interocular light adaptation effect. Vision Research, 15, 595-603.

Peachey, N. S., Seiple, W. H., Auerbach, E., & Armington, J. C. (1987). Rod influence on thresholds using different detection criteria during dark adaptation. Acta Psychologica, 64, 261-270.

Pflug, R., Nelson, R., Ahnelt, P. K. (1990). Background-induced flicker enhancement in cat retinal horizontal cells. I. Temporal and spectral properties. Journal of Neurophysiology, 64, 313-325.

Pokorny, J., Smith, V. C., & Starr, S. J. (1976). Variability of color mixture data--II. The effect of viewing field size on the unit coordinates. Vision Research, 16, 1095-1098.

Polyak, S. L. (1941). The Retina. Chicago: University of Chicago Press.

Prestrude, A. M. (1976). The interocular light adaptation effect at varying retinal locations. Vision Research, 16, 1071-1075.

Prestrude, A. M., Watkins, L., & Watkins, J. (1978). Interocular light adaptation effect on the Lie "specific threshold." Vision Research, 18, 855-857.

Purpura, K., Kaplan, E., & Shapley, R. M. (1988). Background light and the contrast gain of primate P and M retinal ganglion cells. Proceedings of the National Academy of Sciences, 85 4534-4537.

Rodieck, R. W., & Rushton, W. A. H. (1976). Isolation of rod and cone contributions to cat ganglion cells by a method of light exchange. Journal of Physiology, 254, 759-773.

Sato, H., Katsuyama, N., Tamura, H., Hata, Y., & Tsumoto, T. (1994). Broad-tuned chromatic inputs to color-selective neurons in the monkey visual cortex. Journal of Neurophysiology, 72, 163-168.

Schneeweis, D. M., & Schnapf, J. L. (1995). Photovoltage of rods and cones in the macaque retina. Science, 268, 1053-1056.

Schultze, M. (1866). Zur anatomie und physiologie der Retina. Arch. Mikr. Anat. Entwicklungsmech., 2, 175-286.

Smith, V. C., & Pokorny, J. (1975). Spectral sensitivity of the foveal cone photopigments between 400 and 500 nm. Vision Research, 15, 161-171.

Smith, V. C., & Pokorny, J. (1977). Large-field trichromacy in protanopes and deuteranopes. Journal of the Optical Society of America, 67, 213-220.

Spillmann, L., & Conlon, J. E. (1972). Photochromatic interval during dark adaptation and as a function of background luminance. Journal of the Optical Society of America, 62, 182-185.

Stabell, B., & Stabell, U. (1976a). Effects of rod activity on color threshold. Vision Research, 16, 1105-1110.

Stabell, B., & Stabell, U. (1976b). Rod and cone contributions to peripheral colour vision. Vision Research, 16, 1099-1104.

Stabell, U., & Stabell, B. (1975). The effect of rod activity on colour matching functions. Vision Research, 15, 1119-1123.

Stabell, U., & Stabell, B. (1979). Change in hue with rod intrusion during dark-adaptation. Vision Research, 19, 1127-1131.

Stabell, U., & Stabell, B. (1994). Mechanisms of chromatic rod vision in scotopic illumination. Vision Research, 34, 1019-1027.

Stevens, S. S. (1951). Mathematics, measurement, and psychophysics. In S. S. Stevens (Ed.), Handbook of experimental psychology (pp. 1-49). New York: John Wiley.

Stevens, S. S. (1956). The direct estimation of sensory magnitudes--loudness. The American Journal of Psychology, 69, 1-25.

Stevens, S. S. (1958). Problems and methods of psychophysics. Psychological Bulletin, 55, 177-196.

Tootell, R. B. H., Silverman, M. S., Hamilton, S. L., De Valois, R. L., & Switkes, E. (1988). Functional anatomy of macaque striate cortex. III. Color. Journal of Neuroscience, 8, 1569-1593.

Trezona, P. W. (1970). Rod participation in the 'blue' mechanism and its effect on colour matching. Vision Research, 10, 317-332.

Trezona, P. W. (1973). The tetrachromatic colour match as a colorimetric technique. Vision Research, 13, 9-25.

Trezona, P. W. (1974). Additivity in the tetrachromatic colour matching system. Vision Research, 14, 1291-1303.

Ts'o, D. Y., & Gilbert, C. D. (1988). The organization of chromatic and spatial interactions in the primate striate cortex. Journal of Neuroscience, 8, 1712-1727.

van den Berg, T. J. T. P., & Spekreijse, H. (1977). Interaction between rod and cone signals studied with temporal sine wave stimulation. Journal of the Optical Society of America, 67, 1210-1217.

Vienot, F., & Chiron, A. (1992). Brightness matching and flicker photometric data obtained over the full mesopic range. Vision Research, 32, 533-540.

Vollaro, J., Lembessis, E., McMullen, C. A., & Frumkes, T. E. (1997). The influence of rod-adaptation on color-opponent mechanisms. Manuscript submitted for publication.

Watanabe, T., Mori, N., & Nakamura, F. (1992). A new superbright LED stimulator: Photodiode-feedback design for linearizing and stabilizing emitted light. Vision Research, 32, 953-961.

Whittle, P., & Challands, P. D. C. (1969). The effect of background luminance on the brightness of flashes. Vision Research, 9, 1095-1110.

Willmer, E. N. (1950). Low threshold rods and the perception of blue. Journal of Physiology, 111, 17P.

Wyszecki, G., & Stiles, W. S. (1967). Color science. New York: John Wiley.